



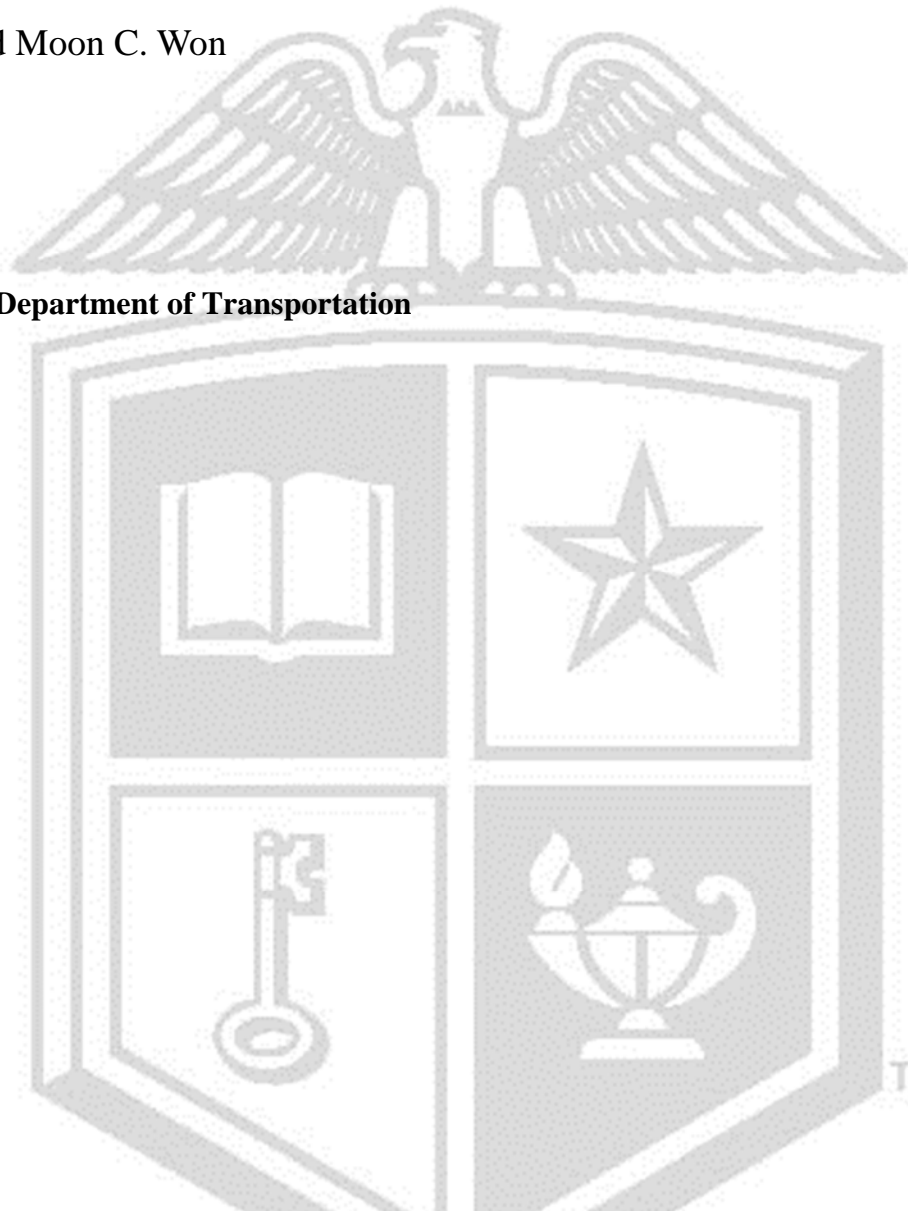
Texas Tech University
Multidisciplinary Research in Transportation

Proper Overlay Type and Designs for PCC Pavement

Pangil Choi, Hoonill Won, Fei Yu, and Moon C. Won

Performed in cooperation with the Texas Department of Transportation
and the Federal Highway Administration

Research Project 0-6910
Research Report 0-6910-R1
<http://www.techmrt.ttu.edu/reports.php>



| | | | |
|--|---|--|-----------|
| 1. Report No. FHWA/TX-18/0-6910-R1 | 2. Government Accession No.: | 3. Recipient's Catalog No.: | |
| 4. Title and Subtitle: Proper Overlay Type and Designs for PCC Pavement | | 5. Report Date: January 2018; Published October 2020 | |
| 7. Author(s): Pangil Choi, Hoonill Won, Fei Yu, and Moon C. Won | | 8. Performing Organization Report No. 0-6910-R1 | |
| 9. Performing Organization Name and Address: Texas Tech University College of Engineering Box 41023 Lubbock, Texas 79409-1023 | | 10. Work Unit No.(TRAIS): | |
| | | 11. Contract or Grant No.: Project 0-6910 | |
| 12. Sponsoring Agency Name and Address: Texas Department of Transportation Research and Technology Implementation Division P.O. Box 5080 Austin, TX 78763-5080 | | 13. Type of Report and Period Technical Report January 2016–January 2018 | |
| | | 14. Sponsoring Agency Code: | |
| 15. Supplementary Notes: Project performed in cooperation with Texas Department of Transportation and the Federal Highway Administration | | | |
| 16. Abstract: As of 2016, TxDOT managed a total of 16,327 lane miles of Portland cement concrete (PCC) pavement, which represents an important asset to TxDOT. As PCC pavements in Texas built in the 1960s through 1980s have already exceeded or are approaching the end of their design lives, many of these projects will require some form of rehabilitation. Considering the expected steady increase in truck traffic in the future, PCC overlays represent one of the best options for that rehabilitation. Currently, guidelines on PCC pavement overlays on PCC pavement focus on overlay slab thickness determination, but do not provide clear directions on (1) whether existing PCC pavement is a good candidate for concrete overlay, or (2) if the pavement is a good candidate, which overlay type—bonded concrete overlay (BCO) or unbonded concrete overlay (UBCO)—is appropriate. Sound guidelines are needed for the selection of an optimum overlay type, especially for continuously reinforced concrete pavement (CRCP) overlays, which could extend the performance period of structurally deficient PCC pavements in Texas at a reasonable cost. Three primary tasks conducted in this study were (1) the evaluations of PCC overlay performance of various BCO and UBCO projects built in Texas, (2) the development of BCO design procedures based on mechanistic-empirical principles, and (3) the development of threshold deflection values to determine whether existing pavements are good candidates for overlays. The structural behavior and performance of PCC overlays were investigated by deflection testing, bond strength testing, and material property evaluations. Three-dimensional finite element analyses were conducted to investigate structural responses of various PCC overlay systems under wheel and environmental loadings. Based on the analysis results and field performance of PCC overlays, a BCO design program was developed. For the UBCO system, detailed analyses were conducted to evaluate the soundness of the 1993 AASHTO design procedures. To facilitate the implementation of the research findings as well as to help TxDOT engineers select an optimum overlay type, the project team compiled the extensive information collected and made recommendations. | | | |
| 17. Key Words: CPCD, CRCP, BCO, overlay design | 18. Distribution Statement No Restrictions. This document is available to the public through the National Technical Information Service, Springfield, VA 22161, www.ntis.gov | | |
| 19. Security Classif. (of this report) Unclassified | 20. Security Classif. (of this page) Unclassified | 21. No. Of Pages | 22. Price |



TEXAS TECH UNIVERSITY

Multidisciplinary Research *in Transportation*[™]

Proper Overlay Type and Designs for PCC Pavement

Pangil Choi

Senior Research Associate, Ph.D.
Center for Multidisciplinary Research in Transportation
Texas Tech University

Hoonill Won

Post-doctoral Research Associate, Ph.D.
Center for Multidisciplinary Research in Transportation
Texas Tech University

Fei Yu

Graduate Research Assistant, M.S.
Center for Multidisciplinary Research in Transportation
Texas Tech University

Moon C. Won

Professor, P.E., Ph.D.
Civil, Environmental, and Construction Engineering
Texas Tech University

Project Number: 0-6910

Project Title: *Development of Proper Overlay Type and Designs for PCC Pavement*

Research Report Number: 0-6910-R1

Conducted for the Texas Department of Transportation

AUTHOR'S DISCLAIMER

The contents of this report reflect the views of the authors who are responsible for the facts and the accuracy of the data presented herein. The contents do not necessarily reflect the official view of policies of the Texas Department of Transportation or the Federal Highway Administration. This report does not constitute a standard, specification, or regulation.

PATENT DISCLAIMER

There was no invention or discovery conceived or first actually reduced to practice in the course of or under this contract, including any art, method, process, machine, manufacture, design or composition of matter, or any new useful improvement thereof, or any variety of plant which is or may be patentable under the patent laws of the United States of America or any foreign country.

ENGINEERING DISCLAIMER

Not intended for construction, bidding, or permit purposes.

TRADE NAMES AND MANUFACTURERS' NAMES

The United States Government and the State of Texas do not endorse products or manufacturers.

Trade or manufacturers' names appear herein solely because they are considered essential to the object of this report.

ACKNOWLEDGMENTS

This research study was sponsored by the Texas Department of Transportation in cooperation with the Federal Highway Administration. The support provided by the project team of this project—Mr. Andy Naranjo, Ms. Hua Chen, Mr. Ruben Carrasco, Mr. Wade Blackmon, and Mr. James Travis—is greatly appreciated.

Table of Contents

| | |
|---|------------|
| Chapter 1 Introduction..... | 1 |
| Chapter 2 Literature Review on PCC Overlays | 3 |
| 2.1. Introduction..... | 3 |
| 2.2 PCC Overlay Design Methods..... | 3 |
| 2.2.1 AASHTO 1993 PCC Overlay Design..... | 3 |
| 2.2.2 PCA Overlay Design..... | 9 |
| 2.2.3 COE Method | 14 |
| 2.2.4 UK PCC Overlay Design | 21 |
| 2.3. Previous Research for AC and PCC Overlays | 23 |
| Chapter 3 Performance Evaluation of PCC Overlays in Texas..... | 28 |
| 3.1. Introduction..... | 28 |
| 3.2. BCO Evaluations | 30 |
| 3.2.1 US 287 Bowie (PFC on CRCP BCO on CRCP)..... | 31 |
| 3.2.2 US 281 Wichita Falls (CRCP BCO on CRCP) | 41 |
| 3.2.3 US 75 Sherman (CRCP BCO on CPCD)..... | 54 |
| 3.2.4 Loop 610 South Houston (BCO on CRCP) | 63 |
| 3.3 UBCO Evaluations | 72 |
| 3.3.1 IH 35 Denton..... | 72 |
| 3.3.2 IH 35E Waxahachie (CPCD UBCO over CPCD)..... | 84 |
| Chapter 4 Analysis of Field Testing Results | 95 |
| 4.1 Introduction..... | 95 |
| 4.2 BCO | 95 |
| 4.2.1 BCO on CRCP | 95 |
| 4.2.2 CRCP BCO on CPCD | 111 |
| 4.3 UBCO | 121 |
| 4.3.1 Pavement Evaluation in UBCO Projects | 121 |
| 4.3.2 Evaluation of Current AASHTO UBCO Design Method | 124 |
| 4.3.4 Summary | 128 |
| Chapter 5 Development of CRCP BCO ME Design Program..... | 129 |
| 5.1 Introduction..... | 129 |
| 5.2 Distress Mechanisms in CRCP BCO on CRCP | 129 |

| | |
|---|------------|
| 5.2.1 Distress Development due to Delamination Caused by Large Deflections | 129 |
| 5.2.2 Distress Development along FDR Joints in Existing CRCP | 131 |
| 5.3 Distress Mechanisms in CRCP BCO on CPCD | 132 |
| 5.4 Determination of Deflection Threshold Values | 134 |
| 5.4.1 CRCP BCO on CRCP | 134 |
| 5.4.2 CRCP BCO on CPCD | 138 |
| 5.5 Mechanistic Modeling of CRCP BCO on CRCP | 141 |
| 5.5.1 Introduction | 141 |
| 5.5.2 Preliminary Analysis to Determine Geometric Configuration | 142 |
| 5.5.3 Development of Mechanistic Modeling for CRCP BCO on CRCP | 146 |
| 5.5.4 Numerical Results for CRCP BCO on CRCP | 150 |
| 5.6 Mechanistic Modeling of CRCP BCO on CPCD | 157 |
| 5.6.1 Development of mechanistic modeling for CRCP BCO on CPCD | 157 |
| 5.6.2 Numerical Results for CRCP BCO on CPCD | 160 |
| 5.7 CRCP BCO Mechanistic Empirical Design Program | 166 |
| 5.7.1 Development of TxBCO-ME program | 166 |
| 5.7.2 General Inputs | 167 |
| 5.7.3 Program Execution | 168 |
| Chapter 6 Development of PCC Overlay Design Standards and Specifications | 171 |
| 6.1 Introduction | 171 |
| 6.2 BCO | 171 |
| 6.2.1 Distress Repairs in the Existing Pavement | 172 |
| 6.2.2 Construction Variables related to Interface Bond | 173 |
| 6.2.3 Longitudinal Reinforcement Design | 178 |
| 6.2.4 Recommended Design Standards and Specifications | 179 |
| 6.3 UBCO | 180 |
| 6.3.1 Quality of HMA Interlayer | 180 |
| 6.3.2 Joint Mismatch | 182 |
| Chapter 7 Conclusions and Recommendations | 184 |
| References | 186 |
| Appendix A. SPECIAL SPECIFICATIONS FOR BCO | 191 |
| Appendix B. DESIGN STANDARDS FOR BCO | 198 |

List of Tables

| | |
|---|-----|
| Table 2.1 Durability adjustment factor (F_{dur}) | 5 |
| Table 2.2 Fatigue damage adjustment factor (F_{fat}) | 5 |
| Table 2.3 Number of punchouts in 2013 TxDOT PMIS (Punchouts > 5) | 6 |
| Table 2.4 Condition factor values (C) | 15 |
| Table 2.5 Summary of concrete overlay designs on concrete pavement (Ray 1967) | 21 |
| Table 2.6 Summary of UK concrete overlay on concrete pavement | 23 |
| Table 2.7 List of overlay design and implementation publications | 24 |
| | |
| Table 3.1 Pavement structure and details on field testing locations | 29 |
| Table 3.2 Pavement information for US 287 Bowie site | 31 |
| Table 3.3 Deflections at coring locations..... | 36 |
| Table 3.4 Material testing results for US 287 site..... | 40 |
| Table 3.5 Pavement information for US 281 Wichita Falls site | 41 |
| Table 3.6 Bond strength results for US 281 section..... | 53 |
| Table 3.7 Concrete properties in the US-281 section | 53 |
| Table 3.8 Pavement information for US 75 Sherman site..... | 55 |
| Table 3.9 Concrete properties in the US-75 section | 62 |
| Table 3.10 Pavement information for Loop 610 South site | 64 |
| Table 3.11 Bond strength testing results for Loop 610 South site | 70 |
| Table 3.12 Distresses and pavement score history (Loop 610 South L 36+0.0 ~ 36+0.3) | 72 |
| Table 3.13 Pavement information for IH 35 Denton site..... | 73 |
| Table 3.14 DCP testing results | 78 |
| Table 3.15 Laboratory testing results..... | 83 |
| Table 3.16 Pavement structure on IH 35E from LTPP database | 85 |
| Table 3.17 Pavement information for IH 35E site | 86 |
| Table 3.18 Laboratory testing | 93 |
| | |
| Table 4.1 Bond strength testing results | 105 |
| Table 4.2 BCO construction information..... | 106 |
| Table 4.3 Pavement information for IH 35 Denton and IH 35E Waxahachie..... | 122 |
| Table 4.4 Structure configurations of 3-D UBCO analysis | 127 |

| | |
|---|---------|
| Table 5.1 Values for normal stiffness and shear stiffness at each interface | 149 |
| Table 5.2 Variables for sensitivity analysis (CRCP BCO on CRCP)..... | 150 |
| Table 5.3 Analysis cases (CRCP BCO on CRCP) | 150 |
| Table 5.4 Variables for sensitivity analysis (CRCP BCO on CPCD) | 159 |
| Table 5.5 Analysis cases (CRCP BCO on CPCD) | 160 |
| Table 5.6 Vertical stresses table at interface (CRCP BCO on CPCD) | 166 |
| Table 6.1 Reinforcement requirements (TxDOT)..... | 180 |

List of Figures

| | |
|---|--------|
| Figure 2.1 F_{jc} adjustment factor (AASHTO 1993) | 4 |
| Figure 2.2 Structural capacity loss over time or traffic (AASHTO 1993)..... | 7 |
| Figure 2.3 Relationship between remaining life and condition factor (AASHTO 1993) | 8 |
| Figure 2.4 F_{jcu} adjustment factor for unbonded PCC overlays (AASHTO 1993) | 9 |
| Figure 2.5 Edge stresses for new and overlaid pavement in the PCA method design equivalency | 10 |
| Figure 2.6 Design chart for bonded overlay (Huang 1993) | 11 |
| Figure 2.7 Stress equivalent concept for UBCO (Tayabji and Okamoto 1985) | 12 |
| Figure 2.8 PCC overlay design chart for Case 1 condition of existing pavement (Huang 1993) | 13 |
| Figure 2.9 PCC overlay design chart for Case 2 condition of existing pavement (Huang 1993) | 13 |
| Figure 2.10 PCC overlay design chart for Case 3 condition of existing pavement (Huang 1993) | 14 |
| Figure 2.11 New single slab with thickness h_r combination of concrete overlay with thickness h_o and existing pavement h_e (Chou 1985)..... | 16 |
| Figure 2.12 Existing, overlay, and equivalent slab | 17 |
| Figure 2.13 Development of rigid overlay, partially bonded design criteria (Rollings 1988) | 19 |
| Figure 2.14 Design thickness for unreinforced concrete overlay (O’Flaherty 2002) | 22 |
| Figure 2.15 Design thickness for CRCP overlay (O’Flaherty 2002) | 22 |
| Figure 2.16 Design thickness for CRCP overlay | 23 |
| Figure 3.1 Overall testing location in Texas | 30 |
| Figure 3.2 Observed AC distresses | 32 |
| Figure 3.3 Test locations on US 287 | 32 |
| Figure 3.4 FWD testing result at poor section (with distresses) | 33 |
| Figure 3.5 FWD testing result at good section (without distresses) | 34 |
| Figure 3.6 Coring location near PFC distress | 35 |
| Figure 3.7 Punchout distress in the existing 8-in. CRCP (picture taken on December 3, 2010) | 36 |
| Figure 3.8 Coring operation..... | 37 |
| Figure 3.9 Concrete cores at P1 and P2 | 37 |
| Figure 3.10 Concrete cores at P3 and P4 | 38 |

| | |
|---|----|
| Figure 3.11 Concrete cores at good section (G1, G2, and G3) | 39 |
| Figure 3.12 Overall pavement condition at poor and good sections..... | 42 |
| Figure 3.13 Test locations on US 281 in Wichita Falls..... | 42 |
| Figure 3.14 FWD deflection on US 281 (poor section)..... | 43 |
| Figure 3.15 FWD deflection on US 281 (good section) | 43 |
| Figure 3.16 FWD deflection near the TCJ | 44 |
| Figure 3.17 MIRA image near the TCJ..... | 44 |
| Figure 3.18 MIRA image away from the TCJ | 45 |
| Figure 3.19 Horizontal cracks at the depth of longitudinal steel | 45 |
| Figure 3.20 DCP testing on US 281..... | 46 |
| Figure 3.21 DCP testing results | 47 |
| Figure 3.22 Modulus values at each layer | 47 |
| Figure 3.23 Core sampling..... | 48 |
| Figure 3.24 Concrete cores away from transverse crack and at transverse crack..... | 49 |
| Figure 3.25 Close-up view of G3 core taken at transverse crack | 50 |
| Figure 3.26 Bond strength testing procedure | 51 |
| Figure 3.27 Core sampling..... | 52 |
| Figure 3.28 MIRA images at transverse crack (C1 and C2) | 52 |
| Figure 3.29 Testing locations on US 75 | 57 |
| Figure 3.30 Number of distresses | 57 |
| Figure 3.31 Typical BCO distress on US 75 | 58 |
| Figure 3.32 Deflection comparisons between BCO and CPCD with BCO distresses..... | 59 |
| Figure 3.33 Distresses analysis in terms of deflection and existing CPCD condition (J-20 to J-80) | 60 |
| Figure 3.34 Distresses analysis in terms of deflection and existing CPCD condition (J-81 to J-120) | 61 |
| Figure 3.35 Plan view of experimental sections on Loop 610 South in Houston, showing details of design and layout..... | 63 |
| Figure 3.36 Testing location on Loop 610 South in Houston | 64 |
| Figure 3.37 Pavement condition on Loop 610 South | 65 |
| Figure 3.38 Distress map in experimental section on Loop 610 South in Houston | 66 |
| Figure 3.39 Testing location on Loop 610 South in Houston | 67 |
| Figure 3.40 Comparison for deflection between Dynaflect (1983) and FWD (2016)..... | 68 |

| | |
|--|----|
| Figure 3.41 Maximum normalized deflection vs. station number (Eagleson et al. 1982)..... | 69 |
| Figure 3.42 Average bond strength in each experimental section..... | 71 |
| Figure 3.43 Comparison with bond strength and deflection..... | 71 |
| Figure 3.44 Pavement score history on Loop 610 South site | 72 |
| Figure 3.45 Typical section on IH 35 in Denton..... | 73 |
| Figure 3.46 Testing locations on IH 35 NB | 74 |
| Figure 3.47 Pavement condition of poor and good sections..... | 75 |
| Figure 3.48 Distress comparisons between March 2012 and February 2016..... | 75 |
| Figure 3.49 FWD testing on IH 35 in Denton | 76 |
| Figure 3.50 LTE calculation at transverse contraction joint | 76 |
| Figure 3.51 Deflection comparison between joint and mid-slab on IH 35 in Denton County..... | 77 |
| Figure 3.52 LTE comparison between poor section and good section on IH 35 in Denton County..... | 77 |
| Figure 3.53 DCP testing on IH 35 in Denton County..... | 78 |
| Figure 3.54 Coring operation on IH 35 in Denton County | 79 |
| Figure 3.55 Coring locations for C-3, C-4, and C-5 around joint distress..... | 80 |
| Figure 3.56 MIRA testing result and core condition of C-1, C-2, and C-3 | 81 |
| Figure 3.57 MIRA testing result and core condition of C-4 and C-5 | 82 |
| Figure 3.58 Pavement score history on IH 35..... | 83 |
| Figure 3.59 Testing location in IH 35E in Ellis County..... | 86 |
| Figure 3.60 Condition of the pavement | 87 |
| Figure 3.61 Deflection comparison between joint and mid-slab | 88 |
| Figure 3.62 LTE comparison between good and poor sections | 89 |
| Figure 3.63 DCP testing results on IH 35E in Ellis County | 89 |
| Figure 3.64 Coring locations on IH 35E in Ellis County..... | 91 |
| Figure 3.65 Cores taken on IH 35E in Ellis County | 92 |
| Figure 3.66 Pavement score history on IH 35E | 93 |
| Figure 4.1 Deflection on old CRCP and average composite k-value prior to overlay (2010)..... | 97 |
| Figure 4.2 Representative distresses on old CRCP..... | 98 |
| Figure 4.3 FWD deflection with distresses on old CRCP | 98 |
| Figure 4.4 FWD deflection with distresses in old CRCP | 99 |

| | |
|--|-----|
| Figure 4.5 Distress comparison between old CRCP and BCO | 100 |
| Figure 4.6 Bond strength test locations on US 287 in Bowie (2012) | 101 |
| Figure 4.7 Bond strength test results for US 287 in Bowie | 102 |
| Figure 4.8 Bond strength testing on US 281 in Wichita Falls | 102 |
| Figure 4.9 Bond strength test results for US 281 in Wichita Falls (2016)..... | 103 |
| Figure 4.10 Bond strength test results for Loop 610 South in Houston (2016)..... | 103 |
| Figure 4.11 Bond strength distribution | 106 |
| Figure 4.12 BCO construction on US 287 in Bowie | 107 |
| Figure 4.13 BCO construction on US 281 in Wichita Falls..... | 108 |
| Figure 4.14 European recommendations for bond strength..... | 109 |
| Figure 4.15 Transition area on BCO on US 287 in Bowie | 110 |
| Figure 4.16 Distresses in TCJ on US 281 in Wichita Falls..... | 111 |
| Figure 4.17 FWD deflection on old CPCD..... | 112 |
| Figure 4.18 FWD deflection on old CPCD..... | 112 |
| Figure 4.19 Distress frequency based on range of joint numbers..... | 113 |
| Figure 4.20 FWD deflection and distress map from J-21 to J40 | 114 |
| Figure 4.21 Distress on J-31 | 114 |
| Figure 4.22 FWD deflection and distress map from J-41 to J-60..... | 114 |
| Figure 4.23 Construction joint at J-45 and distress on J-56..... | 115 |
| Figure 4.24 FWD deflection and distress map from J-61 to J-80..... | 115 |
| Figure 4.25 Distress on J-76 and J-80..... | 115 |
| Figure 4.26 FWD deflection and distress map from J-81 to J-100..... | 116 |
| Figure 4.27 Distress on J-86, J-92, J-93, and J-96..... | 116 |
| Figure 4.28 FWD deflection and distress map (previous condition) from J-101 to J-120 | 117 |
| Figure 4.29 Distress map on J-101 and J-120..... | 117 |
| Figure 4.30 Distress on J-101, J-102, J-104, J-106, J-107, J-110, and J-111..... | 118 |
| Figure 4.31 Distress on J-112, J-113, J-114, J-115, and J-115..... | 119 |
| Figure 4.32 Delamination propagation | 120 |
| Figure 4.33 Core with an attached non-woven fabric..... | 121 |
| Figure 4.34 Deflection @9,000lbs statewide deflection..... | 123 |
| Figure 4.35 Deteriorated AC interlayer in a good section of IH 35E | 123 |
| Figure 4.36 Cross section of slabs and their stress under load | 124 |
| Figure 4.37 Geometric configuration of CPCD UBCO on CPCD | 126 |

| | |
|---|-----|
| Figure 4.38 3-D finite element mesh model for UBCO pavement system..... | 126 |
| Figure 4.39 The stress ratio of UBCO for the case of k-value = 100 pci | 128 |
| Figure 5.1 Distress due to large deflection in existing CRCP (US 287 in Bowie) | 130 |
| Figure 5.2 Delamination and BCO distress (US 287 in Bowie) | 131 |
| Figure 5.3 Distress at FDR joint (US 287 in Bowie)..... | 132 |
| Figure 5.4 Distress in CRCP BCO on CPCD (US 75 in Sherman #1) | 133 |
| Figure 5.5 Distress in CRCP BCO on CPCD (US 75 in Sherman #2) | 134 |
| Figure 5.6 FWD deflection with distresses on the existing CRCP | 135 |
| Figure 5.7 Distress comparison between old CRCP and BCO | 137 |
| Figure 5.8 FWD deflection with distresses on old CRCP | 138 |
| Figure 5.9 Dry concrete in BCO that was removed and replaced | 139 |
| Figure 5.10 Deflection comparison between BCO and CPCD with BCO distresses | 140 |
| Figure 5.11 Deflection comparison between BCO and CPCD with BCO distresses | 141 |
| Figure 5.12 Geometric configuration for the existing CRCP and BCOs..... | 143 |
| Figure 5.13 Structural modeling and preliminary analysis results | 144 |
| Figure 5.14 Vertical stress distribution along path AA' | 145 |
| Figure 5.15 Vertical and principal stresses due to crack stiffness variation | 145 |
| Figure 5.16 CRCP BCO on CRCP configuration | 146 |
| Figure 5.17 Modeling of reinforcing steel and its interface with surrounding concrete..... | 147 |
| Figure 5.18 Finite element mesh model for CRCP BCO..... | 148 |
| Figure 5.19 Deformed shape and surface deflection | 152 |
| Figure 5.20 Vertical stress at interface (4B-8E)..... | 153 |
| Figure 5.21 Vertical stress at interface (4B-E10 and 4B-12E)..... | 154 |
| Figure 5.22 Deformed shape and vertical stress distribution in BCO #2 (4B-10E) | 155 |
| Figure 5.23 Effect of k-value variation on stress induced by the negative temperature loading (3B-10E) | 156 |
| Figure 5.24 CRCP BCO on CPCD configuration..... | 157 |
| Figure 5.25 Finite element mesh model for CRCP BCO on CPCD | 158 |
| Figure 5.26 Deformed shape and surface deflection | 162 |
| Figure 5.27 Effect of traffic loading on vertical stress at interface..... | 163 |
| Figure 5.28 Principal stress distribution (7-in. BCO+10-in. CPCD: 7B-10C) | 163 |
| Figure 5.29 Principal stress distribution at interface | 164 |

| | |
|--|-----|
| Figure 5.30 Vertical stress distribution at interface (7B-10C) | 165 |
| Figure 5.31 Overall algorithm of ME CRCP BCO design program | 167 |
| Figure 5.32 The interface of the CRCP BCO design program | 167 |
| Figure 5.33 The sub-windows of the interface for required inputs..... | 169 |
| Figure 5.34 Program result screen | 170 |
| | |
| Figure 6.1 Surface preparation of existing CRCP on the US-281 BCO project in Wichita Falls..... | 174 |
| Figure 6.2 Bond strength testing and concrete cores on US 281 | 175 |
| Figure 6.3 Bond strength testing and failure mode on US 281 in Wichita Falls | 175 |
| Figure 6.4 Close-up view of concrete core taken at transverse crack..... | 176 |
| Figure 6.5 Overall BCO condition on US 281 in Wichita Falls | 176 |
| Figure 6.6 Close-up view of surface texture after shot-blasting, US 287 BCO in Bowie | 178 |
| Figure 6.7 Bond strength and MIRA testing (interface failure)..... | 178 |
| Figure 6.8 Longitudinal rebar placement on US 281 in Wichita Falls | 179 |
| Figure 6.9 Longitudinal rebar placement on US 287 in Bowie | 180 |
| Figure 6.10 Deflection comparison between joint and mid-slab on IH 35E in Ellis County | 181 |
| Figure 6.11 Deteriorated AC interlayer in good and poor sections, IH 35E..... | 182 |
| Figure 6.12 Delamination and crack due to joint mismatch between existing CPCD and overlaid CPCD | 183 |

List of Acronyms

| | |
|--------|---|
| AASHTO | American Association of State Highway and Transportation of Officials |
| AC | asphalt concrete |
| BCO | bonded concrete overlay |
| COE | Corps of Engineers |
| COTE | coefficient of thermal expansion |
| CPCD | concrete pavement contraction design |
| CRCP | continuously reinforced concrete pavement |
| CSJ | control-section-job |
| DCP | dynamic cone penetrometer |
| ESAL | equivalent single axle load |
| FDR | full-depth repair |
| FWD | falling weight deflectometer |
| JPCP | jointed plain concrete pavement |
| JRCP | jointed reinforced concrete pavement |
| LTE | load transfer efficiency |
| LTPP | Long-Term Pavement Performance |
| ME | mechanistic-empirical |
| MEPDG | Mechanistic-Empirical Pavement Design Guide |
| PCA | Portland Cement Association |
| PCC | Portland cement concrete |
| PCCP | Portland cement concrete patch |
| PFC | permeable friction course |
| PMIS | Pavement Management Information System |
| TCJ | transverse construction joint |
| TPAD | Total Pavement Acceptance Device |
| TxDOT | Texas Department of Transportation |
| UBCO | unbonded concrete overlay |

Chapter 1 Introduction

As of 2016, the Texas Department of Transportation (TxDOT) managed a total of 16,327 lane miles of Portland cement concrete (PCC) pavement. Many miles of PCC pavement in Texas, especially those built in the 1960s through 1980, are approaching or already have exceeded the end of their design lives. In 1986, TxDOT changed the design period of PCC pavement from 20 to 30 years. PCC pavements designed or implemented prior to 1986 have insufficient slab thickness compared to current truck traffic volume. Those pavements require the rehabilitations such as overlay.

Currently three primary design guidelines or methods are used for PCC overlay in the US: the 1993 AASHTO design method, the Corps of Engineers design method, and the Portland Cement Association method. Those overlay design guidelines were developed with a focus on determination of the overlay slab thickness, but do not provide clear direction for a proper overlay type selection based on the structural condition of existing PCC pavement.

As a part of rehabilitation, the above-mentioned overlay methods have been applied to existing PCC pavements in Texas. The 20-plus TxDOT-built PCC overlays have varied substantially in performance: some have excellent performance and some failed within a few years after construction. This result indicates that either an inappropriate overlay type selection or an improper design/construction was applied.

Overlay behavior and performance vary depending on the combinations of existing pavement condition and overlay systems, as well as traffic and environmental conditions. There are three overlay systems used in Texas: (1) concrete pavement contraction design (CPCD) unbonded concrete overlay (UBCO) on CPCD, (2) bonded concrete overlay (BCO), with or without longitudinal reinforcement, on continuously reinforced concrete pavement (CRCP), and (3) CRCP BCO on CPCD. For CPCD UBCO on CPCD, two projects were evaluated, both of which have been open to traffic more than 25 years under heavy traffic. This system usually creates a thick pavement, due to the greater UBCO thickness required (as compared with BCO thickness and a 2-in. asphalt interlayer). CRCP forms more than 78% of PCC pavement lane miles of Texas. The cost of BCO is usually lower than that of UBCO mainly because of the BCO slab is thinner. On CRCP, the BCO slab thickness used in Texas varies from 2-in. to 8-in. TxDOT still has more than 3,700 lane miles of CPCD. Some of them are quite old and need rehabilitation. CRCP BCO on CPCD has rarely been used; the most widely used overlay type on CPCD is asphalt. However, asphalt overlay has reflection cracking issues and requires frequent maintenance and rehabilitations, especially under heavy truck traffic.

The primary objective of this project was to examine the threshold deflection values and develop guidelines to determine whether existing pavements are good candidates for overlays. First, the research team conducted a literature review of major PCC overlay design guidelines, both in the

US and worldwide, which is presented in Chapter 2. Chapter 3 discusses the evaluation of various PCC overlays on PCC pavements built in Texas, focusing on structural responses and performance, including visual survey, falling weight deflectometer (FWD) testing, dynamic cone penetrometer (DCP) testing, concrete coring, and laboratory testing. Chapter 4 presents in-depth discussions on field testing results. Chapter 5 relays a detailed structural analysis on CRCP BCO on CRCP and CRCP BCO on CPCD and discusses the development of a BCO mechanistic-empirical (ME) design program. Chapter 6 addresses the specifications and standards for concrete overlays. Chapter 7 summarizes conclusions and recommendations.

Chapter 2 Literature Review on PCC Overlays

2.1. Introduction

This chapter describes in-depth reviews of available publications on PCC overlays. The literature review revealed that almost all the publications on PCC overlays are focused on CPCD overlays on CPCD, and very little information is available on CRCP overlays. Considering the vast amount of CRCP lane miles in Texas that need overlays or will eventually need overlays, further efforts were made to collect information on CRCP overlays from publications both in the US and abroad.

Many miles of PCC pavement in Texas have reached the end of their design life. With many projects requiring overlay on PCC pavement, there is a need to develop overlay design procedures suited to each type of pavement. To develop rational overlay design procedures, which is one of the major objectives of this project, thorough review of the previously developed design procedures is needed. This chapter describes the existing PCC overlay design methods found in the literature review and identifies each method's limitations. As of now, three major PCC overlay design methods are available: the AASHTO design method, the Corps of Engineers design method, and the Portland Cement Association method. These design methods were developed with a focus on overlay slab thickness determination and do not provide clear directions to identify the type of overlay that is appropriate based on the structural condition of existing PCC pavements. The following sections describe the design concept of each method and discuss limitations. Note that, according to the literature review, most countries outside of the United States, with the exception of the United Kingdom, do not have an established method for PCC overlay design.

2.2 PCC Overlay Design Methods

2.2.1 AASHTO 1993 PCC Overlay Design

2.2.1.1 BCO Design

The American Association of State Highway and Transportation of Officials (AASHTO) pavement design method is one of the most widely used methods in the United States. The PCC overlay design procedures were illustrated in the AASHTO Guide for Design of Pavement Structure (AASHTO 1993). This method for new pavement designs was derived from the analysis of data obtained in the AASHO Road Test. The AASHTO PCC overlay design method uses one of two approaches—a visual survey of the existing pavement condition or the *remaining life* concept—to determine the effective thickness of the existing pavement.

1) Visual survey method

In this method, the condition of the existing pavement is evaluated visually, and the existing concrete slab thickness is converted to a new slab thickness that would have an identical structural capacity, called an *effective slab thickness*. The effective slab thickness (D_{eff}) is obtained in accordance with Eqn. 2.1.

$$D_{\text{eff}} = F_{jc} \times F_{dur} \times F_{fat} \times D \quad (\text{Eqn. 2.1})$$

where,

F_{jc} = joints and cracks adjustment factor

F_{dur} = durability adjustment factor

F_{fat} = fatigue damage adjustment factor

D = thickness of the existing concrete slab

Figure 2.1 shows the joints and cracks adjustment factor (F_{jc}) in the AASHTO 1993 PCC overlay design method. For example, when there are 60 deteriorated transverse joints and cracks per mile, 0.85 is selected for F_{jc} , which indicates the structural capacity of the concrete slab in this pavement is equivalent to 85% of the new concrete slab with the same thickness and slab support condition. However, no description of what constitutes deteriorated transverse joints and cracks is provided in this design method, nor how the function was developed.

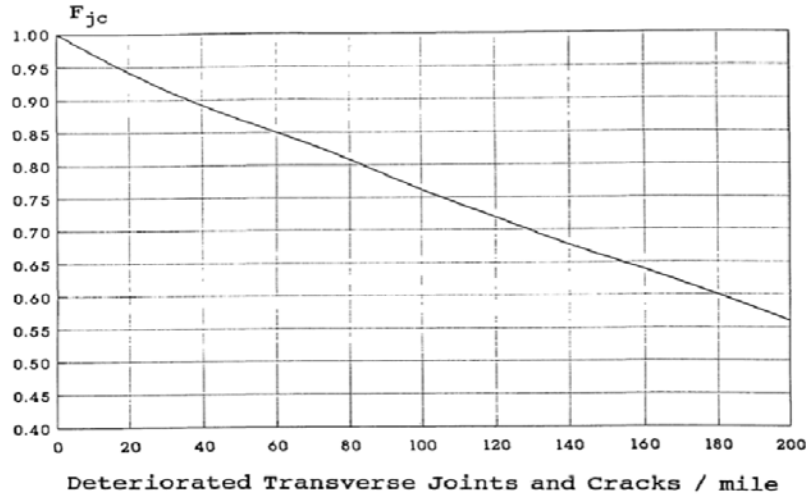


Figure 2.1 F_{jc} adjustment factor (AASHTO 1993)

This design guide states that the durability (F_{dur}) adjustment factor adjusts for an extra loss in present serviceability index when the existing slab has durability problems, such as “D” cracking or reactive aggregate distress. From the condition survey data, F_{dur} values are selected as shown in Table 2.1. The suggested factor could be conceptually agreeable; however, there is a risk of variability in the condition evaluations. The design guide does not provide descriptions or definitions of “substantial” and “extensive” cracking; nor does it define “some” and “severe” spalling.

Table 2.1 Durability adjustment factor (F_{dur})

| F_{dur} | Description |
|-------------|---|
| 1.00 | No sign of PCC durability problems |
| 0.96 – 0.99 | Durability cracking exists, but no spalling |
| 0.88 – 0.95 | Substantial cracking and some spalling exists |
| 0.80 – 0.88 | Extensive cracking and severe spalling exists |

Table 2.2 illustrates the determination of the fatigue adjustment factor (F_{fat}). The minimum value is suggested as 0.88, although the existing pavements could be severely deteriorated. From a practical standpoint, BCO is not recommended when the existing pavement has substantial structural deficiencies, as manifested by numerous punchouts in CRCP. In addition, BCO is not recommended if CPCD and jointed reinforced concrete pavement (JRCP) show a high level of structural distresses. The table also provided the adjustment factor for jointed plain concrete pavement (JPCP).

Table 2.2 Fatigue damage adjustment factor (F_{fat})

| F_{fat} | Description |
|-------------|---|
| 0.97 – 1.00 | Few transverse cracks/punchouts exist (none caused by “D” cracking or reactive aggregate distress) - JPCP: < 5% slabs are cracked - JRCP: < 25 working cracks per mile - CRCP: < 4 punchouts per mile |
| 0.94 – 0.96 | A significant number of transverse cracks/punchouts exist (none caused by “D” cracking or reactive aggregate distress) - JPCP: 5 – 15% slabs are cracked - JRCP: 25 – 75 working cracks per mile - CRCP: 4 – 12 punchouts per mile |
| 0.88 – 0.95 | Many transverse cracks/punchout exist (none caused by “D” cracking or reactive aggregate distress) - JPCP: > 15% slabs are cracked - JRCP: > 75 working cracks per mile - CRCP: > 12 punchouts per mile |

According to the 2013 TxDOT Pavement Management Information System (PMIS), there were 1,389 punchouts; 242 asphalt concrete (AC) patches; 9,136 Portland cement concrete patches (PCCPs); and 8,068 spallings on about 13,600 lane miles in CRCP. The average distress rate, excluding spallings, is about 0.79 each per lane mile. Table 2.3 illustrates the PMIS data, showing that the number of punchouts is greater than 5.0 per lane mile throughout Texas. Among 22 sections

with punchouts of 5 or more per lane mile, only 3 sections have the number of punchouts equal to or greater than 13 per lane mile. In the other sections, the fatigue damage factor for all CRCPs in Texas other than those 3 sections is greater than 0.94. This high fatigue damage factor implies that the effective thickness from fatigue damage is always greater than 94% of the existing CRCP thickness. In addition, according to the findings from the TxDOT rigid pavement database project (0-6274), only 14% of all the distresses recorded as punchout in the PMIS were true punchout distress due to structural deficiency of the pavement, while the other 86% were due to non-structural issues, such as poor joint construction or finishing operations (Choi et al. 2013). Accordingly, the minimum fatigue damage adjustment factor for all the CRCPs in Texas would be 0.97, i.e., the fatigue damage in the most deteriorated CRCP section in Texas is equivalent to 3% of the existing slab thickness. Thus, the effective thickness determination for fatigue damage does not appear to be reasonable.

Table 2.3 Number of punchouts in 2013 TxDOT PMIS (Punchouts > 5)

| DISTRICT | HIGHWAY | BEG_RM | END_RM | P_TYPE | P_CODE | Segment Length [mile] | No. of Lane | Lane Miles | SPL | PCH | ACP | PCCP | DISTRESS_SCORE | CONDITION_SCORE | RIDE_SCORE |
|----------|----------|--------|--------|--------|--------|-----------------------|-------------|-------------|-----------|------------|-----------|-------------|---------------------|-----------------|------------|
| 1 | US0075 R | 0000 | 1 0194 | 0 C | 01 | 0.6 | 2 | 1.2 | 2 | 6 | 9 | 5 | 8 | 0 | 0 |
| 5 | IH0027 R | 0012 | 0 0012 | 1 C | 01 | 0.5 | 2 | 1.0 | 1 | 6 | 0 | 24 | 10 | 10 | 3.2 |
| 5 | IH0027 R | 0021 | 0 0021 | 1 C | 01 | 0.5 | 2 | 1.0 | 0 | 5 | 0 | 20 | 12 | 12 | 3.1 |
| 5 | IH0027 R | 0053 | 0 0053 | 1 C | 01 | 0.5 | 2 | 1.0 | 11 | 6 | 0 | 17 | 11 | 11 | 3.5 |
| 12 | IH0045 L | 0011 | 0 0011 | 1 C | 01 | 0.5 | 3 | 1.5 | 0 | 13 | 2 | 13 | 5 | 5 | 4 |
| 12 | SL0008 L | 0696 | 0 0696 | 1 C | 01 | 0.5 | 3 | 1.5 | 0 | 10 | 0 | 0 | 24 | 14 | 2.5 |
| 12 | US0059 R | 0536 | 2 0538 | 0 C | 02 | 0.2 | 2 | 0.4 | 0 | 10 | 0 | 0 | 11 | 5 | 2.3 |
| 12 | IH0610 A | 0035 | 1 0036 | 0 C | 01 | 0.5 | 2 | 1.0 | 0 | 5 | 0 | 6 | 23 | 15 | 2.1 |
| 12 | IH0610 X | 0034 | 1 0035 | 0 C | 01 | 0.4 | 2 | 0.8 | 2 | 7 | 0 | 18 | 7 | 5 | 2.1 |
| 18 | IH0035ER | 0419 | 0 0419 | 1 C | 01 | 0.5 | 3 | 1.5 | 13 | 8 | 0 | 0 | 27 | 19 | 2.7 |
| 18 | IH0035ER | 0423 | 0 0423 | 1 C | 01 | 0.5 | 4 | 2.0 | 8 | 6 | 0 | 8 | 17 | 12 | 2.7 |
| 18 | IH0635 L | 0025 | 0 0025 | 1 C | 01 | 0.5 | 4 | 2.0 | 0 | 8 | 0 | 2 | 25 | 0 | 0 |
| 18 | IH0035ER | 0420 | 0 0420 | 1 C | 01 | 0.5 | 3 | 1.5 | 4 | 6 | 0 | 0 | 36 | 21 | 2.5 |
| 18 | SH0114 A | 0598 | 1 0598 | 1 C | 01 | 0.5 | 2 | 1.0 | 0 | 5 | 0 | 0 | 41 | 41 | 3.1 |
| 18 | SH0170 R | 0562 | 0 0562 | 1 C | 01 | 0.2 | 3 | 0.6 | 0 | 5 | 0 | 0 | 20 | 20 | 3.4 |
| 18 | SH0170 R | 0562 | 1 0562 | 1 C | 01 | 0.5 | 3 | 1.5 | 0 | 8 | 0 | 0 | 29 | 29 | 3.3 |
| 22 | IH0035 R | 0051 | 0 0051 | 1 C | 01 | 0.5 | 2 | 1.0 | 1 | 6 | 0 | 0 | 36 | 36 | 4 |
| 24 | IH0010 L | 0022 | 1 0023 | 0 C | 01 | 0.4 | 5 | 2.0 | 0 | 21 | 0 | 0 | 11 | 11 | 3.4 |
| 24 | IH0010 L | 0022 | 0 0022 | 1 C | 01 | 0.6 | 6 | 3.6 | 0 | 7 | 0 | 0 | 37 | 33 | 3 |
| 24 | IH0010 A | 0037 | 1 0038 | 0 C | 01 | 0.5 | 2 | 1.0 | 1 | 5 | 0 | 1 | 41 | 41 | 3.5 |
| 24 | IH0010 L | 0023 | 0 0023 | 1 C | 01 | 0.5 | 5 | 2.5 | 0 | 15 | 0 | 1 | 17 | 17 | 3.3 |
| 24 | IH0010 L | 0018 | 1 0019 | 0 C | 01 | 0.3 | 4 | 1.2 | 0 | 13 | 0 | 0 | 13 | 11 | 3 |
| | | | | | | | | 30.8 | 43 | 181 | 11 | 115 | | | |
| | | | | | | | | | | | | 307 | | | |
| | | | | | | | | | | | | 9.97 | | | |
| | | | | | | | | | | | | 1.42 | ea/lane mile | | |

SPL = spalling; PCH = punchout; ACP = asphalt concrete patch; PCCP = Portland cement concrete patch

2) Remaining life method

The other method to estimate the effective slab thickness of the existing pavement uses the remaining life of existing pavement. This method employs a condition factor, which will be discussed later, and the effective thickness is computed by Eqn. 2.2.

$$D_{\text{eff}} = CF \times D \quad (\text{Eqn. 2.2})$$

where,

CF = condition factor of existing pavement
 D = thickness of existing concrete slab

Figure 2.2 illustrates the structural capacity loss of a pavement system over time. To determine the remaining life of the existing pavement, the values for two variables need to be determined: the actual amount of traffic the pavement has carried to date (N_p) and the total amount of traffic the pavement could be expected to carry to “failure” ($N_{1.5}$) (when serviceability equals 1.5, to be consistent with the AASHTO Road Test equations). Both traffic amounts (total traffic to date and total traffic to failure) should be expressed in 18-kip equivalent single axle loads (ESAL). Once both traffic numbers are determined, the remaining life of the pavement can be determined by Eqn. 2.3.

$$RL = 100 \left[1 - \left(\frac{N_p}{N_{1.5}} \right) \right] \quad (\text{Eqn. 2.3})$$

where,

RL = remaining life (percent)

N_p = total traffic to date, 18-kip ESAL

$N_{1.5}$ = total traffic to pavement failure ($P_t = 1.5$), 18-kip ESAL

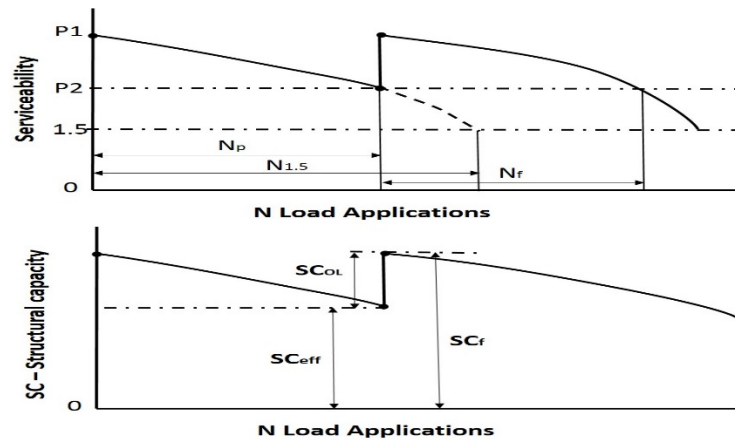


Figure 2.2 Structural capacity loss over time or traffic (AASHTO 1993)

Once the remaining life is determined, the condition factor is estimated from Figure 2.3, which illustrates the relationship between remaining life and condition factor. It should be noted that this remaining life concept does not directly consider the structural condition of the existing pavement. According to Eqn. 2.3, if the cumulative traffic exceeds the design traffic, the remaining life becomes negative. In Texas, many CRCP projects that might require overlays actually have exceeded their design lives in terms of time as well as traffic, which will result in an effective slab thickness of about half of the existing slab thickness.

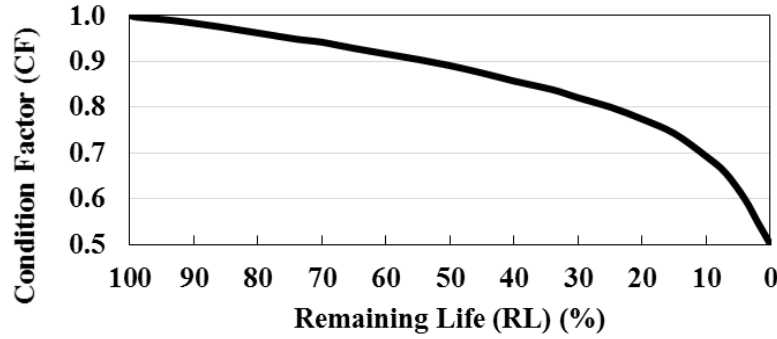


Figure 2.3 Relationship between remaining life and condition factor (AASHTO 1993)

It is observed that, depending on which method is used (condition survey or remaining life method), quite different effective slab thicknesses could result, decreasing accuracy in identifying for CRCPs in Texas that might require bonded overlays in the near future. Therefore, a more reasonable method to determine effective slab thickness is needed to deliver consistent results.

2.2.1.2 UBCO Design

For UBCO design, the effective thickness of existing pavement (D_{eff}) is determined by Eqn. 2.4.

$$D_{\text{eff}} = F_{\text{jcu}} \times D \quad (\text{Eqn. 2.4})$$

where,

F_{jcu} = joints and cracks adjustment factor for UBCOs

D = existing PCC slab thickness, inches

F_{jcu} is determined from the number of deteriorated transverse joints and cracks per mile as shown in the graph in Figure 2.4. The design guide states that since field surveys of unbonded jointed concrete overlays have shown very little evidence of reflection cracking or other problems caused by the existing slab, the F_{dur} and F_{fat} are not needed for UBCO design.

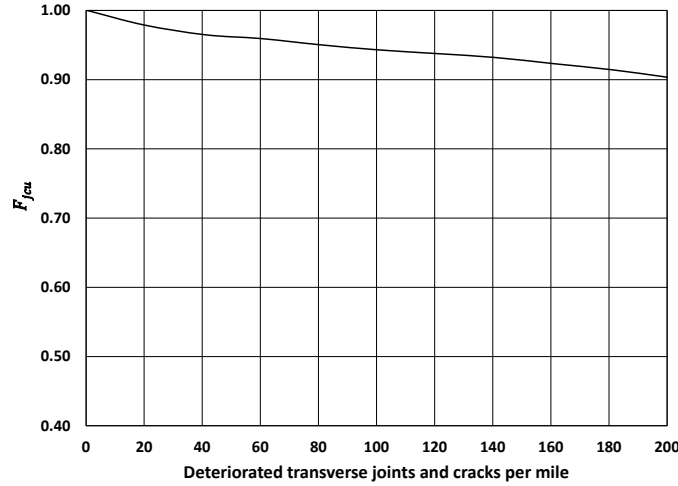


Figure 2.4 F_{jcu} adjustment factor for unbonded PCC overlays (AASHTO 1993)

2.2.1.3 Slab Thickness Determination

The suggested typical range of bonded overlay thickness is around two to six inches, and a thickness of three to four inches has been successfully and typically used for highway pavement overlays (Smith et al. 2002). For UBCO, the required thickness is typically greater than that for bonded overlay. The slab thickness for overlays is determined from Eqn. 2.5.

$$D_{ol}^n = D_f^n - D_{eff}^n \quad (\text{Eqn. 2.5})$$

where,

D_{ol} = required thickness of PCC overlay, inches

D_f = slab thickness to carry future traffic, inches

D_{eff} = effective thickness of existing slab, inches

$n = 1$ for BCO,

$n = 2$ for UBCO

2.2.2 PCA Overlay Design

The Portland Cement Association (PCA) PCC overlay design was developed from the mechanistic analysis of pavement systems obtained from the finite element computer program JSLAB. The method consists of designing an overlay system that is structurally equivalent to a new full-depth pavement placed on the same subbase and subgrade—which is conceptually the same as the AASHTO design method. Unlike the Corps of Engineers procedure that will be discussed later, this method uses an evaluation of the existing pavement by means of condition surveys, deflection tests, and in-situ testing, to consider its condition in the design. The design basis is the analysis of the stresses at the edge of the pavement (Tayabji and Okamoto 1985). For bonded overlay, the critical stress condition employed in this method is the concrete edge stress at the bottom of the new CRCP (σ_n) and at the bottom of the existing pavement (σ_e), as shown in Figure 2.5. The development of BCO design assumes that BCO will eventually fail due to the fatigue damage at

the bottom of the existing concrete slab. This premise also assumes that the bond between existing concrete and overlaid slabs will be maintained throughout the BCO performance period.

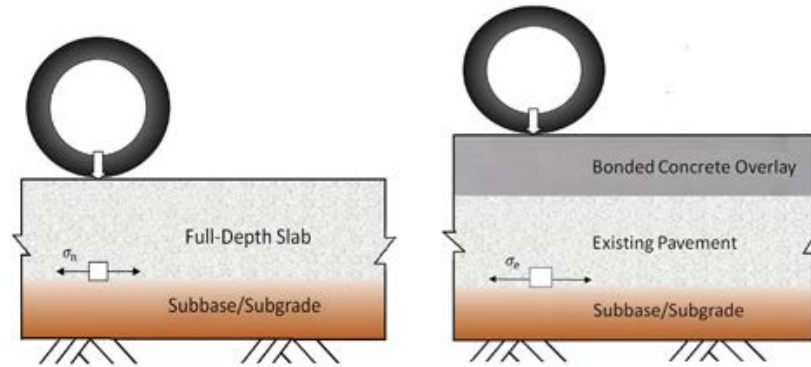


Figure 2.5 Edge stresses for new and overlaid pavement in the PCA method design equivalency

Since the concrete strengths are different in the existing and overlaid concrete slabs, the selection of the overlay slab thickness is based on the ratio of concrete stress at edge condition to concrete strength, as shown in **Eqn. 2.6**.

$$\frac{\sigma_n}{S_{cn}} \geq \frac{\sigma_e}{S_{ce}} \quad (\text{Eqn. 2.6})$$

where,

- σ_n = critical edge stress in the new pavement
- S_{cn} = modulus of rupture of the new concrete
- σ_e = critical edge stress in the existing pavement
- S_{ce} = modulus of rupture of the existing concrete

The design chart for the BCO thickness design thus developed is shown in **Figure 2.6**.

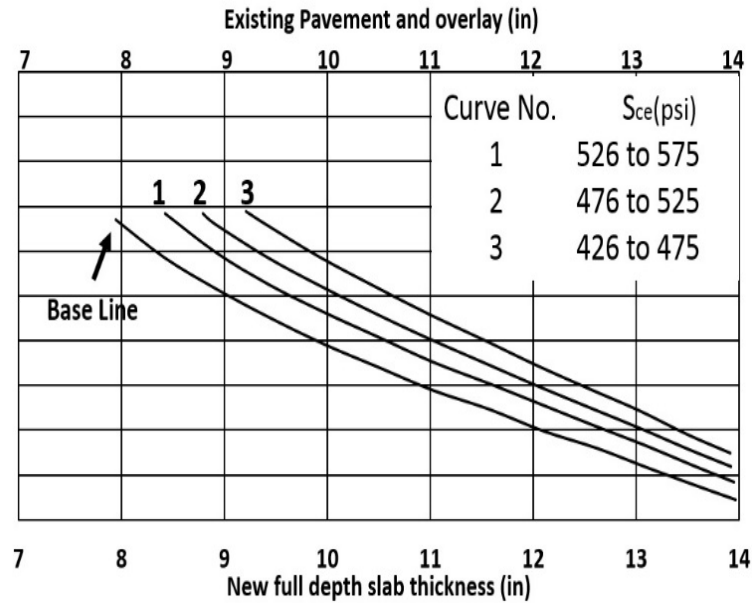


Figure 2.6 Design chart for bonded overlay (Huang 1993)

In the design chart, three different curves (representing different moduli of rupture of the existing concrete) are shown. Curve 1 is applicable for modulus of rupture from 526 to 575 psi, curve 2 from 476 to 525 psi, and curve 3 from 426 to 475 psi. Given the thickness of the full-depth pavement and the curve number, the combined thickness of the existing pavement and the overlay can be read from the chart. The difference between the combined thickness and the thickness of the existing pavement is the overlay thickness required.

The chart cannot be applied if the modulus of rupture in the existing pavement is lower than 426 psi or higher than 575 psi. When the modulus of rupture is lower than 425 psi, it would be better to apply an unbonded overlay rather than bonded. When the modulus of rupture of the existing concrete is greater than 575 psi, the existing pavement is considered as good as the new pavement.

Even though the BCO design method described above appears to be technically sound, its application to actual projects could pose a challenge, since accurately estimating the modulus of rupture in the existing concrete slab would be quite difficult. Test specimens could be obtained by cutting concrete blocks from the existing concrete slabs; however, this operation is quite time-consuming and almost impossible for CRCP due to the longitudinal steel. Modulus of rupture could be estimated from the compressive strength of concrete cores taken from the existing slabs, but large scatters were observed between compressive strength and modulus of rupture. The values thus obtained by conversion of compressive strength to modulus of rupture may not be accurate enough for the overlay slab thickness design.

For UBCO design, PCA employs a concept of structural equivalence between UBCO and full-depth slabs, the same concept used for BCO designs, except for the location of stress in the overlaid

slab. In UBCO, the critical stress is at the bottom of the overlaid slab, while it was at the bottom of the existing slab in BCO. The critical stress condition in UBCO is also at edge condition as in BCO. The premise made in UBCO design is that UBCO will fail due to the fatigue damage at the bottom of the overlaid slab, as shown in Figure 2.7 (Tayabji and Okamoto 1985).

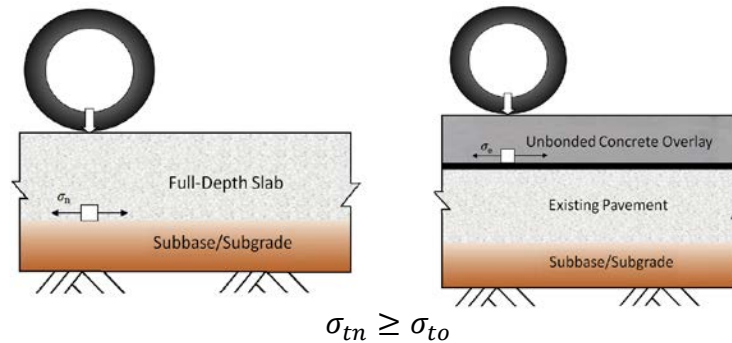


Figure 2.7 Stress equivalent concept for UBCO (Tayabji and Okamoto 1985)

The stress data used to prepare the design charts for the determination of UBCO thickness were developed by using the program JSLAB. These charts are applicable to existing concrete pavements that have effective modulus of elasticity values ranging from about 3,000,000 to about 4,000,000 psi. Design charts are presented for three cases of existing pavement condition.

Case 1: This case is applied when the existing pavement exhibits a large amount of mid-slab and corner cracking with poor load transfer at joints and cracks, as well as to badly D-cracked pavements, unless falling weight deflectometer (FWD) load testing indicates that the load transfer across joints and cracks is adequate; in that case, Case 2 should be used.

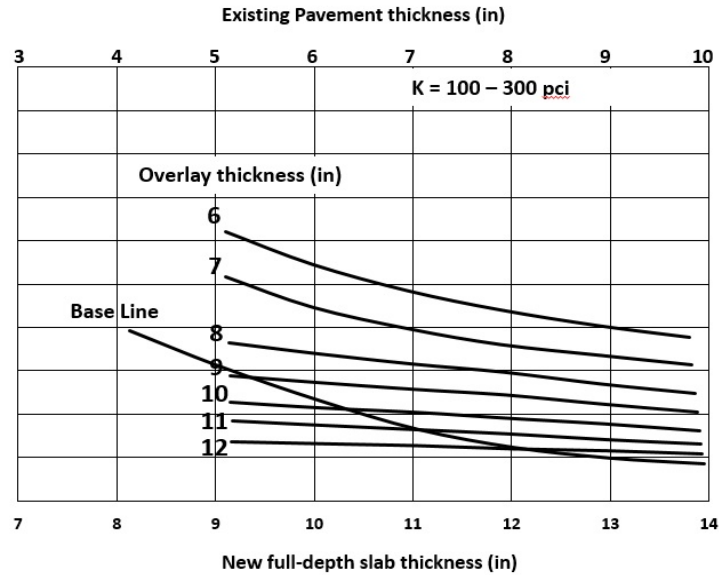


Figure 2.8 PCC overlay design chart for Case 1 condition of existing pavement (Huang 1993)

Given the thicknesses of the full-depth pavement and existing pavement, the overlay thickness can be estimated from the graph shown in Figure 2.8.

Case 2: When the existing pavement exhibits a small amount of mid-slab and corner cracking or exhibits reasonably good load transfer at the joints and cracks, Case 2 is applied. As in Case 1, with the thicknesses of the full-depth pavement and existing pavement, the overlay thickness can be estimated from the graph shown in Figure 2.9.

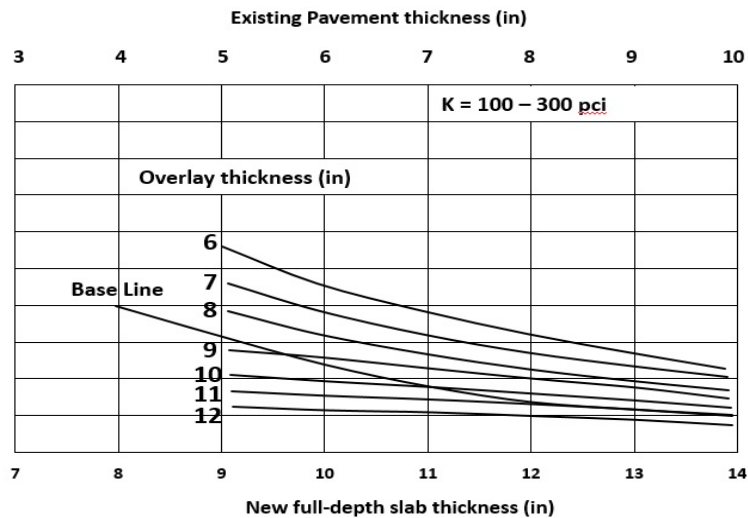


Figure 2.9 PCC overlay design chart for Case 2 condition of existing pavement (Huang 1993)

Case 3: When the existing pavement exhibits a small amount of mid-slab cracking and good load transfer at the cracks and joints, this case is applied. In this case, with the thicknesses of the full-depth pavement and existing pavement, the overlay thickness is determined from the graph shown in **Figure 2.10**.

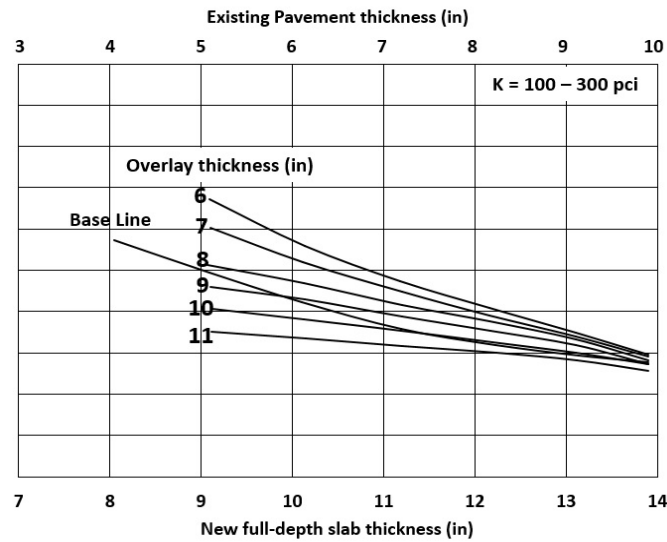


Figure 2.10 PCC overlay design chart for Case 3 condition of existing pavement (Huang 1993)

2.2.3 COE Method

The Corps of Engineers (COE) design method was originally developed for the design of PCC overlays on plain concrete airport pavements using the concept of effective thickness approach. The three types of concrete overlays considered in the COE method are as follows (Chou 1983):

- Bonded: This requires careful surface preparation to ensure that full bond is achieved.
- Partially bonded: The concrete overlay is placed directly on the existing concrete with little surface preparation other than minor cleaning.
- Unbonded: In this overlay type, a leveling course of AC is placed between the concrete slabs to prevent bonding.

2.2.3.1 Determination of Concrete Overlay Thickness

The required thickness h_o of concrete overlay can be determined using **Eqn. 2.7**:

$$h_o^n = h_r^n - Ch_e^n \quad (\text{Eqn. 2.7})$$

where,

h_o = required overlay thickness

h_r = required full-depth concrete slab thickness for the design loading

h_e = existing pavement thickness

C = a condition factor, which depends on the structural integrity of the existing pavement

n = a power dependent on the bond condition between the existing pavement and concrete overlay

$n = 1.0$ for fully bonded overlays

$n = 1.4$ for partially bonded overlays

$n = 2.0$ for unbonded overlays

The suggested condition factor values are shown in **Table 2.4** (Chou 1985).

Table 2.4 Condition factor values (C)

| C | Base pavement condition |
|----------|--|
| 1.0 | Existing pavement is in good structural condition with little or no structural cracking. |
| 0.75 | Existing pavement has some initial structural cracking but little progressive distress such as spalling and multiple cracks. |
| 0.35 | Existing pavement is badly cracked and may show multiple instances of cracking, shattered slabs, spalling, and faulting. |

Figure 2.11 shows an overlay slab with a thickness h_o placed on top of the existing slab with a thickness h_e , as well as a pavement system with a structurally equivalent capacity. In other words, the pavement system with a slab thickness h_r is structurally equivalent to the overlaid pavement system.

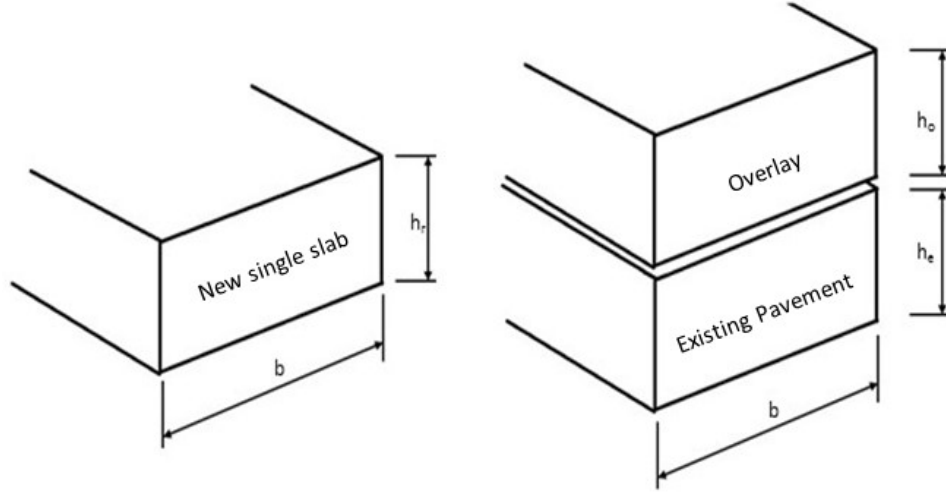


Figure 2.11 New single slab with thickness h_r combination of concrete overlay with thickness h_o and existing pavement h_e (Chou 1985)

Accordingly, for the unbonded case, the moment in the equivalent slab is the sum of the moments in the top and bottom slabs in the overlaid system, as shown in Eqn. 2.8.

$$M_r = M_o + M_e \quad (\text{Eqn. 2.8})$$

Eqn. 2.8 can be re-written as shown in Eqn. 2.9,

$$\frac{\sigma_r I_r}{\frac{h_r}{2}} = \frac{\sigma_o I_o}{\frac{h_o}{2}} + \frac{\sigma_e I_e}{\frac{h_e}{2}} \quad (\text{Eqn. 2.9})$$

where I is the moment inertia of the cross section with respect to the neutral axis of the slab and is equal to $bh^3/12$. σ_r , σ_o and σ_e are concrete stresses due to wheel loading at the bottom of full-depth, overlaid, and existing concrete slabs. Eqn. 2.9 can be rewritten as shown in Eqn. 2.10,

$$\sigma_r h_r^2 = \sigma_o h_o^2 + \sigma_e h_e^2 \quad (\text{Eqn. 2.10})$$

Here, there are four unknown variables and only one equation. To determine the overlay thickness, the values of the other three variables— σ_r , σ_o and σ_e —need to be known or assumed. With the assumption of $\sigma_r = \sigma_o = \sigma_e$, the UBCO thickness can be determined from Eqn. 2.11.

$$h_o^2 = h_r^2 - Ch_e^2 \quad (\text{Eqn. 2.11})$$

Eqn. 2.11 is quite similar to the AASHTO design equation for UBCO. The assumption of $\sigma_r = \sigma_o = \sigma_e$ is quite convenient for the overlay thickness determination, as there is no clear description or justifications for this assumption. Intuitively, however, the assumption of $\sigma_r = \sigma_o = \sigma_e$ is not correct, and the research team of this research study confirmed the unreasonableness of this assumption with finite element method analysis.

The Rollings (1988) report explains the relationship among the three concrete stresses for the

development of the overlay slab thickness determination. Simple beam theory was used to derive equations for unbonded overlays and an equivalent slab similar to the COE overlay design equation given earlier. An overlay slab and an existing slab can be considered to be structurally identical to an equivalent slab, as shown in **Figure 2.12**. If a thin slice of unit width b from this equivalent slab is subjected to a moment M_r , the curvature of the beam becomes as shown in **Eqn. 2.12**:

$$\frac{1}{\rho_r} = \frac{M_r}{E_r I_r} \quad (\text{Eqn. 2.12})$$

where,

ρ_r = radius of curvature
 M_r = moment
 E_r = modulus of elasticity
 I_r = moment of inertia

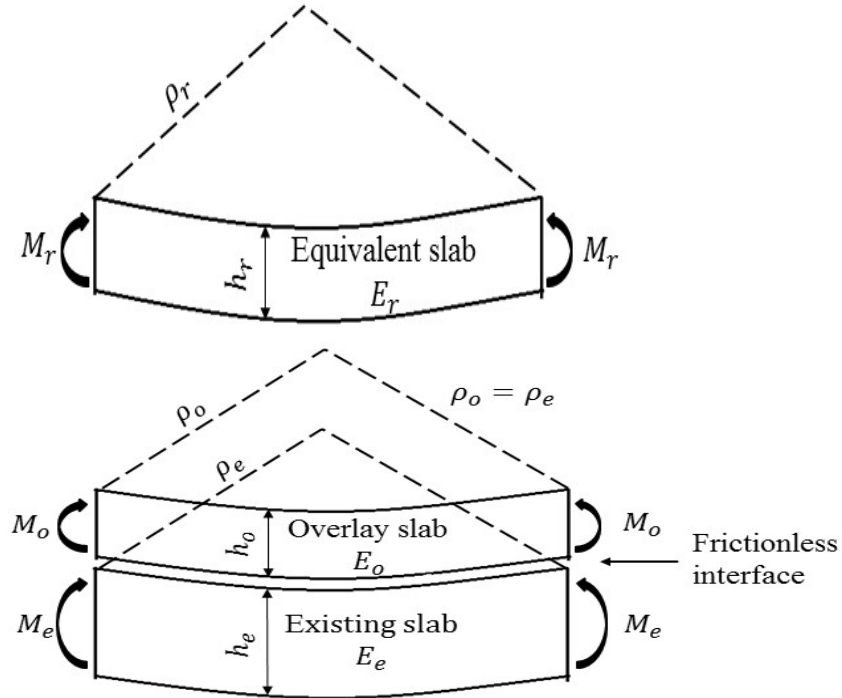


Figure 2.12 Existing, overlay, and equivalent slab

If the overlay and existing slab are subject to an equivalent moment such that $M_r = M_o + M_e$, compatibility requires the radius of curvature of the existing and the overlay slabs to be equal so that **Eqn. 2.13** should hold true.

$$\frac{1}{\rho} = \frac{M_o}{E_o I_o} = \frac{M_e}{E_e I_e} \quad (\text{Eqn. 2.13})$$

There are three potential ways of defining an equivalent slab: (a) the equivalent slab must have the same rigidity as the overlay and existing slab, $E_r I_r = E_o I_o + E_e I_e$, (b) the tensile stress in the

equivalent slab (σ_r) must be equal to the tensile stress in the existing slab (σ_e), or (c) the tensile stress in the equivalent slab (σ_r) must be equal to the tensile stress in the overlay (σ_o) (Rollings 1988).

2.2.3.2 BCO ($n=1$)

In BCO, the exponent in Eqn. 2.7 is set at 1.0, and the resulting design equation for BCO is as shown in Eqn. 2.14.

$$h_o = h_r - Ch_e \quad (\text{Eqn. 2.14})$$

Bonded overlays are designed with the assumption that the existing slab is in generally good condition and the overlay is bonded to the existing rigid pavement; the two are expected to behave as a monolithic slab. The structural capacity remaining in the existing substrate is fully utilized. As such, it is accounted for in the design equations, which contributes to reducing the thickness of the overlay required. This is only attainable if the bond between overlay and existing slabs is achieved and maintained throughout the performance period.

2.2.3.3 Partially Bonded Concrete Overlay ($n=1.4$)

For partially bonded overlays, the use of $n=1.4$ was based on the results of the COE's full-scale traffic tests (Rollings 1988), shown in Figure 2.13.

The Introduction of the Full-Scale Overlay Test Pavements (Rollings 1988) states:

“Since 1944 the Corps of Engineers' investigational program for the design and construction of military airfield pavements has included full-scale traffic tests of all types of conventional pavement sections. The traffic loadings used have been those of the main gear of the operational aircraft in use or anticipated by the U. S. Air Force. These tests have included traffic loading of overlay pavement sections. The first overlay traffic tests were made with a 60,000 lb single wheel loading at Lockbourne AFB near Columbus, Ohio in 1944. During 1954 and 1955, tests were made with a 100,000 lb twin wheel loading at the Sharonville, Ohio test site of the Corps of Engineers' Ohio River Division Laboratories. Later, during 1958 and 1959, at this same site, traffic tests of overlay pavement sections were made with 325,000 and 275,000 lb twin-tandem wheel gear loadings. These are the details of the pavement sections and the significant physical properties of the concrete and subgrades pertinent to these tests.”

In the analysis of the data from testing, the “C” factor of 0.75 is used for computing the equivalent single slab thickness h_r , for partial bond case:

$$h_r = \sqrt[1.4]{h_o^{1.4} + 0.75h_e^{1.4}} \quad (\text{Eqn. 2.15})$$

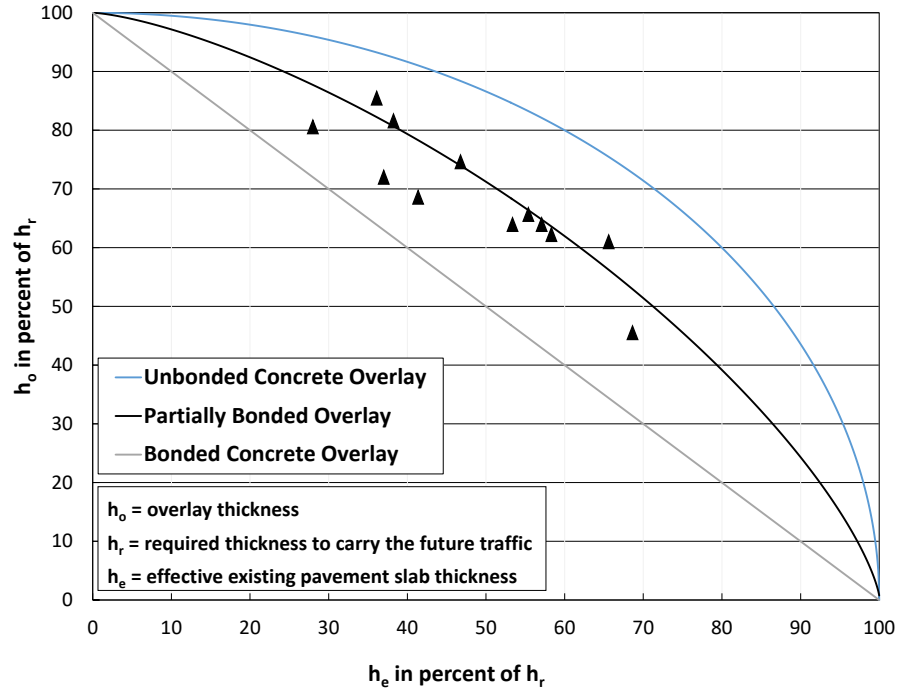


Figure 2.13 Development of rigid overlay, partially bonded design criteria (Rollings 1988)

The repair recommendation for partially bonded rigid overlays of rigid pavements generally follows the same recommendation as those for the BCOs, except that only high severity cracks and shattered slabs need to be replaced prior to the overlay. All joints with deteriorated distress should be also replaced.

2.2.3.4 UBCO ($n=2$)

The original source showing the use of the exponent $n=2.0$ in the equation for unbonded concrete cannot be traced. The earliest literature found concerning the applicability of the equation for unbonded overlays was a publication of the American Concrete Institute. It states, “It is not known by whom or when the suggestion was first made for use of the formula which assumed that the structural capacity of two slabs, one superimposed on the other, is equivalent to that of a single slab the square of whose thickness is equal to the sum of the squares of the two slabs” (Chou 1985). Eqn. 2.16 provides the equation under discussion.

$$h_1^2 = h_0^2 - Ch_2^2 \quad (\text{Eqn. 2.16})$$

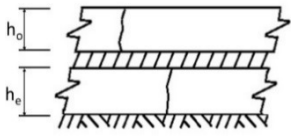
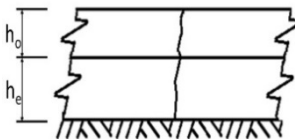
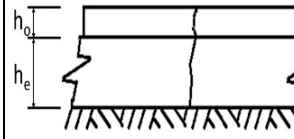
The following statements are directly quoted from the American Concrete Institute publication concerning the applicability of Eqn. 2.16 for unbonded overlays (Chou 1985):

“Until recently there has been no comprehensive analysis of stresses involved in multiple layers of concrete pavements similar to the Westergaard and Pickett studies of stresses in a single slab. It is not known by whom or when the suggestion was first made for use of the formula which assumed that the structural capacity of two slabs, one superimposed

on the other, is equivalent to that of a single slab the square of whose thickness is equal to the sum of the squares of the two slabs. This formula came into use with the full understanding that it was not technically accurate. It may be approximately correct under the conditions that (1) the two slabs have the same stiffness, and (2) that there is no friction between them. Since it is most unlikely that the two slabs will be of the same stiffness, it is to be expected that one will be stressed more than the other. This is offset by the fact that, normally, considerable friction will exist between the two slabs which will cause them to act to some degree as an integral unit and thus reduce the stresses below what they would be if the two acted separately with no friction between them."

Table 2.5 summarizes the overlay designs as well as information on the condition of the pavements appropriate for each overlay type.

Table 2.5 Summary of concrete overlay designs on concrete pavement (Ray 1967)

| Type of overlay | | Unbonded overlay | Partially bonded overlay | Bonded overlay |
|--|---------------------------------------|---|---|---|
| | |  |  |  |
| Procedure | | Clean surface debris and excess joint seal, place separate AC, place overlay concrete | Clean surface debris and excess joint seal and remove rubber place overlay concrete | Scarify all loose concrete, clean joints and acid, place bonding grout and overlay concrete |
| Matching of joints in overlay pavement | | Not necessary | Required | Required |
| Formula for computing thickness of overlay | | $h_o = \sqrt[2]{h_r^2 - Ch_e^2}$ | $h_o = \sqrt[1.4]{h_r^{1.4} - Ch_e^{1.4}}$ | $h_o = h_r - h_e$ |
| Minimum thickness (inch) | | 6 | 5 | 1 |
| Structural condition of existing pavement | No structural defects $C=1.0$ | Yes | Yes | Yes |
| | Limited structural defects $C=0.7$ | Yes | Only if defects can be repaired | Only if defects can be repaired |
| | Severe structural defects $C=0.3$ | Yes | No | No |

h_o = required overlay thickness

h_r = required thickness for the design loading

h_e = existing pavement thickness

C = condition factor of the existing pavement

One of the major drawbacks in the COE design method is that it defines pavement failure as cracking or structural breakup. This definition may be valid for jointed concrete pavement, but not for CRCP, where transverse cracking develops and does not necessarily constitute pavement distress.

2.2.4 UK PCC Overlay Design

The RILEM state-of-the-art report, “Bonded Cement-Based Material Overlays for the Repair, the Lining or the Strengthening of Slabs or Pavements” (Bissonnette et al. 2015), discusses the European Standard dedicated to repair systems and strengthening pavement systems with overlays. The United Kingdom (UK) permits the concrete overlay design options as shown in Table 2.6, and

presents a design method that uses overlay design charts that determine the thickness for unreinforced concrete pavement, JRCP, and CRCP, as shown in Figures 2.14, 2.15, and 2.16 (O'Flaherty 2002) respectively.

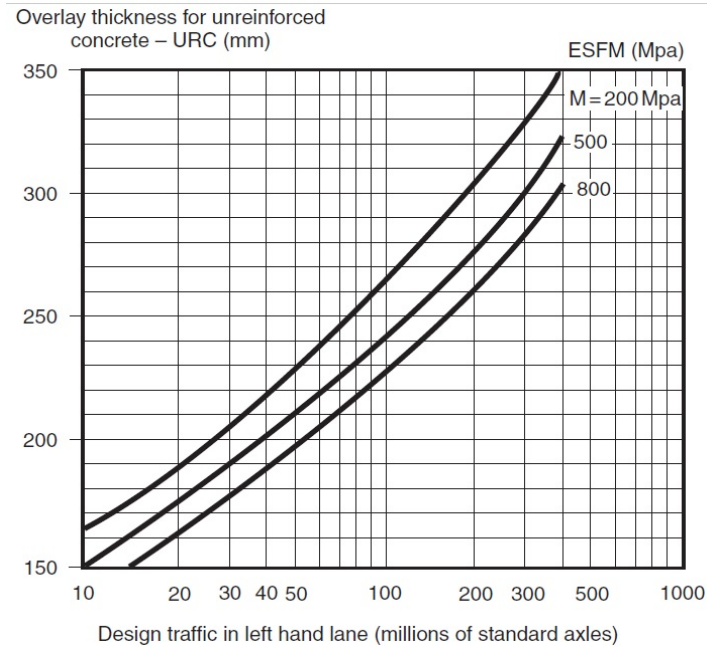


Figure 2.14 Design thickness for unreinforced concrete overlay (O'Flaherty 2002)

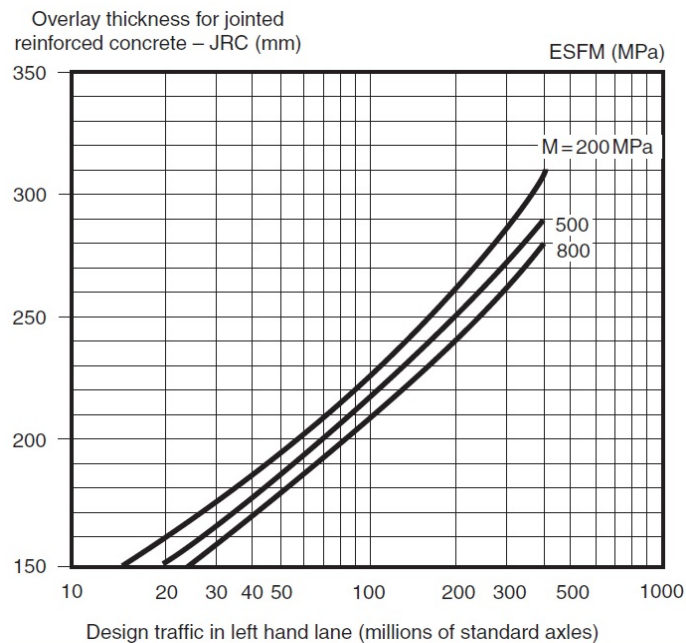


Figure 2.15 Design thickness for CRCP overlay (O'Flaherty 2002)

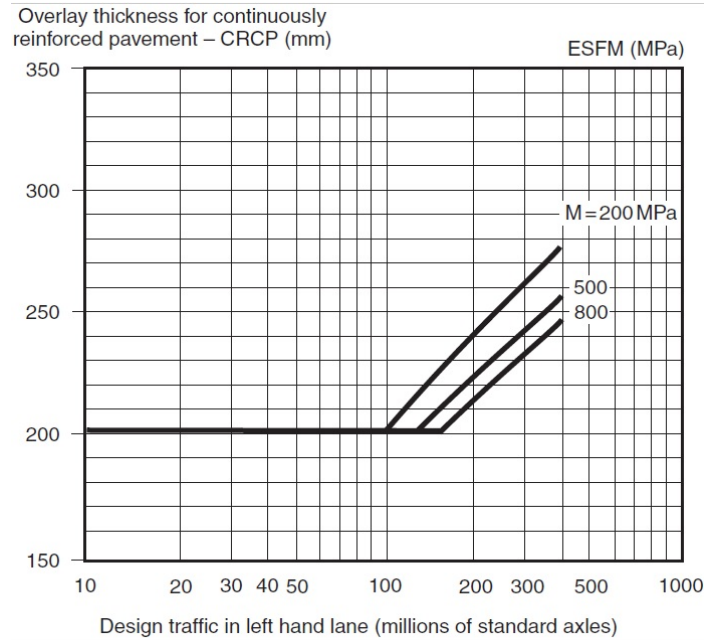


Figure 2.16 Design thickness for CRCP overlay

The ESFM (equivalent surface foundation modulus) is a measure of the strength of the existing road structure and is defined as the modulus of a uniform elastic foundation that would give the same deflection under the same wheel load as that of the existing structure. The ESFM can be evaluated from the results of FWD deflection tests (O'Flaherty 2002).

Table 2.6 Summary of UK concrete overlay on concrete pavement

| | | Existing pavement | | |
|---|------|--------------------------------|------------|------|
| | | Flexible or flexible composite | URC or JRC | CRCP |
| Overlay | URC | 2 | 3 | 1 |
| | JRC | 2 | 3 | 1 |
| | CRCP | 1 | 4 | 1 |
| Notes: | | | | |
| 1. Acceptable and no surface treatment other than remedial works is normally necessary. | | | | |
| 2. Separation membrane required. | | | | |
| 3. No treatment other than remedial works is normally necessary, but joints should occur above one another. | | | | |
| 4. This combination not normally appropriate. | | | | |
| 5. URC = Unreinforced concrete | | | | |
| JRC = Jointed reinforced concrete CRCP = Continuously reinforced concrete pavement | | | | |

2.3. Previous Research for AC and PCC Overlays

Table 2.7 shows all the publications for AC and PCC overlay design methods, including

implementation projects. As this table illustrates, the majority of publications are for the AC overlay practices, with a few publications on the PCC overlay practices. Notably, there are no good CRCP overlay design methods for CRCP.

Most countries adopted the AASHTO 93 design method and some of them have their own methods for overlay design. For example, Ireland (K. Maji 2014) and Australia (Jameson 2013) have a granular overlay designs for pavement, while the UK's overlay design methods for concrete pavement use the determination of thickness charts, as discussed earlier.

Table 2.7 List of overlay design and implementation publications

| (Author year) | Title | Type of overlay | | | | Note |
|---|---|-----------------|-----|------|------|-----------------------|
| | | AC | PCC | | | |
| | | | BCO | UBCO | PBCO | |
| (Circular 2009) | Airport pavement design and evaluation | ○ | ○ | ○ | | FAA |
| (Lahitou et al. 2008) | Debonding in BCOs over CRCPs | | ○ | | | COE/ PCA AASHTO |
| (The U.S. Army Corps of Engineers 1984) | Engineering and design airfield rigid pavement mobilization construction | | ○ | ○ | ○ | COE |
| (Roesler and Hiller 2013) | CRCP: design using the AASHTOWARE pavement ME design procedure | | | ○ | | AASHTO |
| (Cable et al. 2005) | Design and construction procedures for concrete overlay and widening of existing pavements | | ○ | | | ACPA/ PCA |
| (Mu and Vandebossche 2011) | Development of design guide for thin and ultra-thin concrete overlays of existing asphalt pavements, Task 2: Review and selection of structural response and performance models | | ○ | | | UWT |
| (Rasmussen et al. 2011) | CRCP design and construction guideline | | | ○ | | AASHTO |

Table 2.7 List of overlay design and implementation publications (continued)

| (Author year) | Title | Type of overlay | | | | Note |
|------------------------------------|---|-----------------|-----|------|------|-----------------------|
| | | AC | PCC | | | |
| | | | BCO | UBCO | PBCO | |
| (Packard and Association 1973) | Design of concrete airport pavement | | ○ | ○ | ○ | COE |
| (Eichhorn et al. 1986) | Development of an improved overlay design procedure for Oregon | ○ | ○ | ○ | | AASHTO |
| (Delatte 2014) | Concrete pavement design, construction, and performance | | ○ | ○ | ○ | PCA/ FAA AASHTO |
| (Delatte et al. 1998) | Investigating performance of BCOs | | ○ | | | |
| (Lee et al. 2014) | Comparison of performance of overlay pavements constructed on deteriorated concrete pavements using LTPP database | | ○ | | | AASHTO |
| (Ballarini and Liao 2012) | Mechanistic Modeling of Unbonded Concrete Overlay Pavements | | | ○ | | MEPDG/ COE/ PCA |
| (Li et al. 2011) | Use of the 1993 AASHTO Guide, MEPDG and Historical performance to update the WSDOT Pavement Design Catalog | ○ | | | | AASHTO |
| (Chojnacki 2000) | Evaluation of fiber-reinforced unbonded overlay | | | ○ | | |
| (Voigt et al. 1989) | Rehabilitation of concrete pavements Volume II - Overlay rehabilitation techniques | | ○ | | | AASHTO |
| (Delatte et al. 1996) | Partial construction report of a BCO on IH-10, El Paso, and guide for expedited BCO design and construction | | ○ | × | | |
| (Tayabji et al. 2009) | New applications for thin concrete overlays: three case studies | | ○ | ○ | | |
| (Lundy et al. 1991) | Delamination of BCOs at early ages | | ○ | ○ | ○ | COE/ AASHTO |
| (Treviño et al. 2000) | Full-scale BCO on IH-30 in Ft. Worth, Texas | | ○ | | | AASHTO |
| (Lance Huddleston and Fowler 1995) | Effects of early traffic loading on a BCO | | ○ | | | AASHTO |

Table 2.7 List of overlay design and implementation publications (continued)

| (Author year) | Title | Type of overlay | | | | Note |
|---|---|-----------------|-----|------|------|------------------------------|
| | | AC | PCC | | | |
| | | | BCO | UBCO | PBCO | |
| (McCullough and Fowler 1994) | BCO project selection, design, and construction | | ○ | | | AASHTO |
| (McCullough and Rasmussen 1999) | Fast-track paving: concrete temperature control and traffic opening criteria for BCOs, Vol. 1: Final report | | ○ | | | |
| (Fick and Harrington 2012) | Concrete overlay field application program final report: Volume I | | ○ | ○ | | AASHTO |
| (McGhee 1994) | Portland cement concrete resurfacing | | ○ | ○ | | |
| (Fick and Harrington 2015 (Revised Feb 2016)) | Guide specification for concrete overlays | | ○ | ○ | | MEPDG |
| (O'Flaherty 2002) | Highways; the location, design, construction, and maintenance of pavements | ○ | ○ | ○ | ○ | UK |
| (Jameson 2013) | Technical basis of Austroads guide to pavement technology: part 2: pavement structural design | | | | | Granular overlay / Australia |
| (Molenaar 1983) | Structural performance and design of flexible road constructions and AC overlays | ○ | | | | |
| (New Zealand 2000) | New Zealand supplement to the document, Pavement Design–A guide to the structural design of road pavements | ○ | | | | |
| (K.Maji 2014) | Guidelines on the depth of overlay to be used on rural regional and local roads | | | | | Granular overlay /Ireland |
| (Jundhare et al. 2012) | Ultra-Thin Whitetopping in India: State-of-Practice | | ○ | | | UTW |

Table 2.7 List of overlay design and implementation publications (continued)

| (Author year) | Title | Type of overlay | | | | Note |
|--------------------------|--|-----------------|-----|------|------|---------------------------------|
| | | AC | PCC | | | |
| | | | BCO | UBCO | PBCO | |
| (Harrington et al. 2014) | Preservation and Rehabilitation of Urban Concrete Pavements Using Thin Concrete Overlays: Solutions for Joint Deterioration in Cold Weather States | | ○ | | | MEPDG |
| (Hall et al. 2001) | Rehabilitation strategies for highway pavements | ○ | ○ | ○ | | AASHTO |
| (Daleiden et al. 1994) | Evaluation of the AASHTO design equations and recommended improvements | | ○ | ○ | | AASHTO |
| (Bagate et al. 1987) | A mechanistic design for thin-bonded concrete overlay pavements | | ○ | ○ | ○ | AASHTO PCA/ COE |
| (Lahitou et al. 2008) | Debonding in BCOs over CRCPs | | ○ | | | AASHTO PCA/ COE/ MEPDG |

Notes:

AASHTO: American Association of State Highway and Transportation of Officials “Guide for Design of Pavement Structures” design method

COE: Corps of Engineers design method

PCA: Portland Cement Association design method

UTW: Ultra-Thin Whitetopping

FAA: Federal Aviation Administration

MEPDG: Mechanistic-Empirical Pavement Design Guide

Chapter 3 Performance Evaluation of PCC Overlays in Texas

3.1. Introduction

This chapter discusses the field testing conducted in this project on the structural responses and performance of various PCC overlays on PCC pavement in Texas, along with preliminary findings, including material properties evaluated. More detailed information on the analysis of the field-testing results is presented in Chapter 4.

As of 2016, TxDOT manages a total of 16,327 lane miles of PCC pavement, which represents an important asset to TxDOT. As PCC pavements in Texas built in the 1960s through 1980s have already exceeded or are approaching the end of their design lives, many of these projects will require some form of rehabilitation. This is especially true for the projects built prior to 1986, when TxDOT changed the pavement design period from 20 to 30 years, as those projects have already exceeded their design lives.

As of the writing of this report, there are more than 20 PCC overlay projects in Texas and the performance of those overlay projects has varied substantially. Some have shown excellent performance, while some failed within a few years after construction, which indicates that either no proper overlay type selection procedure was followed, or key elements of design/materials selection/construction were not adequately applied. In this study, six overlay projects were selected for field evaluations: (1) US 287 in Bowie, (2) US 281 in Wichita Falls, (3) US 75 in Sherman, (4) Loop 610 South in Houston, (5) IH 35 in Denton, and (6) IH 35E in Waxahachie. Detailed information on each project is shown in **Table 3.1**. The CSJ (control-section-job) numbers are for overlay construction, and net length is the length of each project evaluated, not the overlay project length. Among the six projects, four are BCO and two are UBCO.

Table 3.1 Pavement structure and details on field testing locations

| No. | CSJ | Hwy | Net Length [mile] | RM [Beg] | RM [End] | TxDOT District | County | Date of Completion [Existing] | Date of Completion [Overlay] | Existing Pavement Type | Overlay Pavement Type | Thickness [in.] | Base Type |
|-----|-------------|--------|-------------------|--------------|--------------|----------------|----------|-------------------------------|------------------------------|------------------------|------------------------|--|--------------------------------------|
| 1 | 0013-05-017 | US 287 | 0.7 | 220 +0.80 | 220 +1.50 | Wichita | Montague | 08/30/1972 | 11/00/2012 | CRCP | CRCP | 4-BCO 8-Existing | 4-in. ASPH STAB |
| 2 | 0249-01-012 | US 281 | 0.2 | 194 +0.30 | 194 +0.40 | Wichita | Wichita | 00/00/1969 | 06/19/2002 | CRCP | CRCP | 4-BCO 8-Existing | - |
| 3 | 6182-92-001 | US 75 | 0.4 | 202 +0.90 | 202 +1.30 | Paris | Grayson | 00/00/1984 | 06/15/2010 | CPCD | CRCP | 7-BCO 10-Existing | 6-in. Flexible |
| 4 | 0000-00-000 | LP 610 | 0.17 | 36 +0.15 | 36 +0.32 | Houston | Harris | 00/00/1970 | 07/22/1983 | CRCP | Plain/CRCP/ Fibrous | 2-3 var.-BCO 8-Existing | 6-in. CSB |
| 5 | 0195-02-035 | IH 35 | 0.1 | 475 +0.69 | 475 +0.80 | Dallas | Denton | 00/00/1960 | 00/00/1987 | CPCD | CPCD | 11-UBCO ACP Level Up 10-Existing | 6-in. Roadbed Treatment (TY-B) |
| 6 | 0048-04-050 | IH 35E | 0.1 | 406 +0.60 | 406 +0.70 | Dallas | Ellis | 11/04/1959 | 10/22/1990 | CPCD | CPCD | 10-UBCO ACP Level Up 10-Existing | - |

The objectives of the field evaluations were to assess the performance of PCC overlays and obtain information on structural responses and material properties that will help improve PCC overlay design, materials selection, and construction practices. Field testing included deflection testing with an FWD, testing on concrete integrity with MIRA (an ultrasonic shear-wave tomography tool), dynamic cone penetrometer (DCP) testing, bond strength testing, and coring. Laboratory evaluations included materials testing for concrete dynamic modulus of elasticity and coefficient of thermal expansion (CoTE). Compressive strength was not evaluated, since compressive strength testing destroys the specimens and strength is usually not an issue in concrete pavements in Texas. The specimens are kept in the laboratory for any additional testing that might be needed in the future. Figure 3.1 shows the field-testing locations of the PCC overlay projects that included both BCO and UBCO. The GPS coordinates indicate representative locations of the field testing, and those for the beginning and ending locations of field testing are presented in the subsequent sections in this chapter.

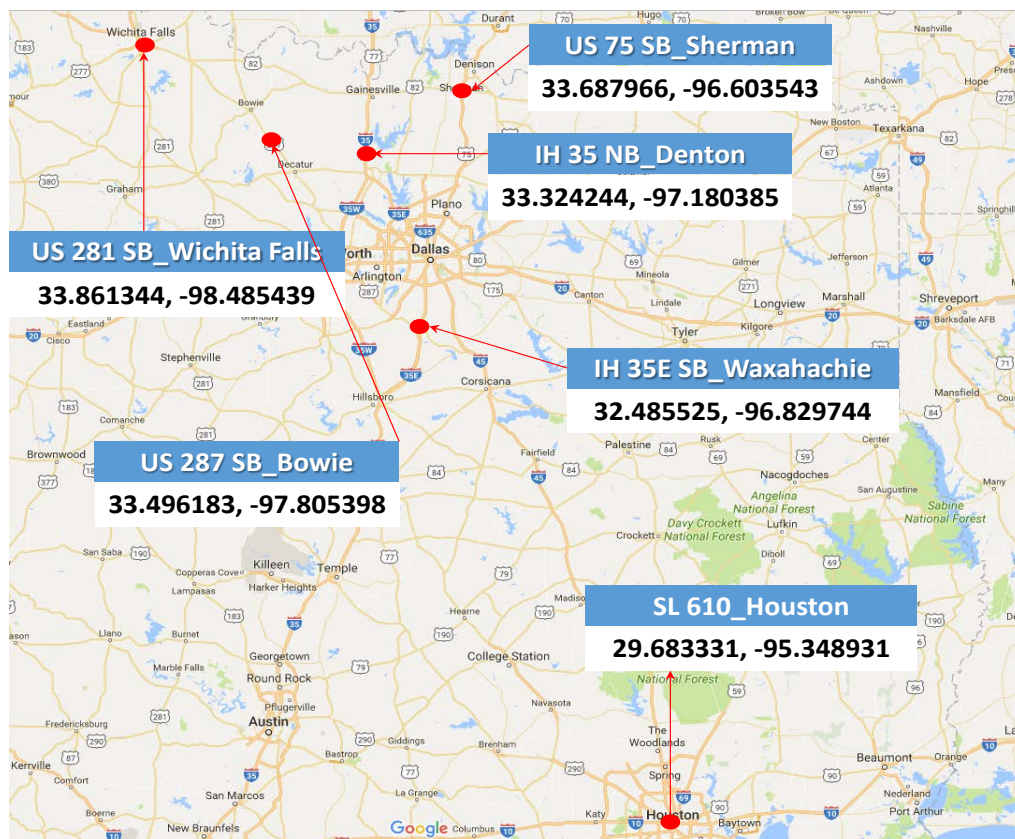


Figure 3.1 Overall testing location in Texas

3.2. BCO Evaluations

Four BCO projects were evaluated: two 4-in. BCO over 8-in. CRCP, one 2- and 3-in. BCO on 8-in. CRCP, and one 7-in. BCO over 10-in. CPCD.

3.2.1 US 287 Bowie (PFC on CRCP BCO on CRCP)

3.2.1.1 Pavement Information

The first testing location to discuss is US 287 in Bowie, from reference marker 220+0.8 to 220+1.5. The 8-in. existing CRCP was built in August 1972 and a 4-in. CRCP BCO was placed in November 2012. The existing 8-in. CRCP provided 40 years of service, twice the design life of 20 years. For 4-in. BCO, #6 transverse bars were placed at 4-ft spacing on top of the existing 8-in. CRCP, and #6 longitudinal steel was placed at 10-in. spacing, which is 1.10% longitudinal steel ratio of 4-in. slab thickness. The details about pavement attributes and the test location are shown in [Table 3.2](#).

Table 3.2 Pavement information for US 287 Bowie site

| Attribute | Information | Special Note |
|------------------------------|---|--|
| CSJ | 0013-05-017 | - |
| County | Montague | - |
| TxDOT District | Wichita Falls | - |
| Reference Marker | 220+0.8 – 220+1.5 (0.7 miles) | Southbound |
| GPS Coordinates | 33.490194, -97.801175 ~ 33.482514, -97.79545 | - |
| Construction Year (existing) | Aug. 1972 | - |
| Construction Year (BCO) | Nov. 2012 | - |
| Pavement Type | 1-in. PFC Overlay + 4-in. CRCP BCO | 1-in. permeable friction course (PFC) placed in April, 2014 |
| Slab Thickness | 4-in. CRCP BCO + 8-in. CRCP | - |
| Shoulder Type | Asphalt Shoulder | - |
| Base Type | 4-in. Asphalt Stabilized Base | - |
| Subgrade Type | APPR 4-in. FND, CRSE | - |
| Drainage Type | Open Ditch | - |
| Con. Pavement Details | CPCR (b) - 67 (1) | - |

3.2.1.2 Visual Survey

After the completion of the 4-in. CRCP BCO in November 2012, distresses in the form of segmentation of concrete slabs in 4-in. BCO started showing up, and to prevent further deteriorations, a 1-in. permeable friction course (PFC) layer was placed in April 2014. Prior to field testing, a visual condition survey was conducted to identify major distress types and to select locations for in-depth evaluations. The major distress types observed at this location were those in the PFC layer that reflected from the distresses in the 4-in. BCO. [Figure 3.2](#) shows the surface conditions of the PFC layer that reflected from the distresses in the 4-in. BCO. Most PFC distresses were observed at the repair joint areas in the existing 8-in. CRCP, which reflected to the 4-in. BCO, where large deflections were measured. As will be discussed later, full debonding between the BCO and CRCP was identified where PFC distresses were observed. Based on the visual survey results, two sections were selected for further evaluations: one with distresses (poor) and the other without distresses (good), as shown in [Figure 3.3](#).



(a) Reflected distress from the existing punchout on 8-in. CRCP



(b) Reflected distress at repair joint in BCO

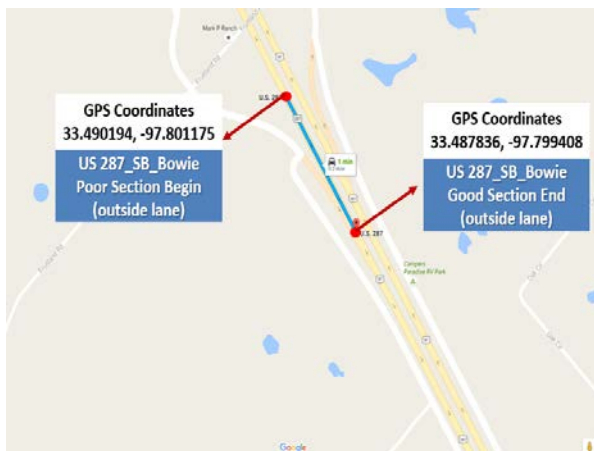


(c) Surface condition due to BCO distress #1

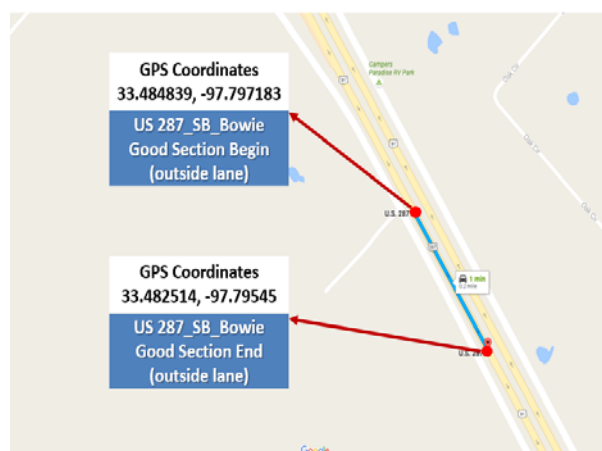


(d) Surface condition due to BCO distress #2

Figure 3.2 Observed AC distresses



(a) With distresses (poor section)



(b) Without distresses (good section)

Figure 3.3 Test locations on US 287

3.2.1.3 Deflection Testing with FWD

To identify factors responsible for PCC overlay performance, FWD testing was conducted and concrete material properties such as the dynamic modulus of elasticity and CoTE were evaluated in the laboratory.

FWD testing was conducted at 10-ft intervals over approximately 1,000-ft for each section. **Figures 3.4 and 3.5** show deflections measured in poor and good sections, respectively. It is observed that overall deflections and their variability were larger in the poor section than in the good section. In the poor section, deflections greater than 7 mils were recorded at two locations, which coincided with PFC distress locations, whereas the deflections in the good section were smaller and more uniform. It appears that delamination or debonding at the poor section was also responsible for larger deflections. Field testing was conducted in 2010 on the existing 8-in. CRCP prior to the overlay, which included Total Pavement Acceptance Device (TPAD) testing, DCP testing, and deflection testing with FWD. Also, bond strength testing was conducted in November 2012, prior to the opening of the 4-in. BCO to traffic. Those field-testing results are discussed in Chapter 4.

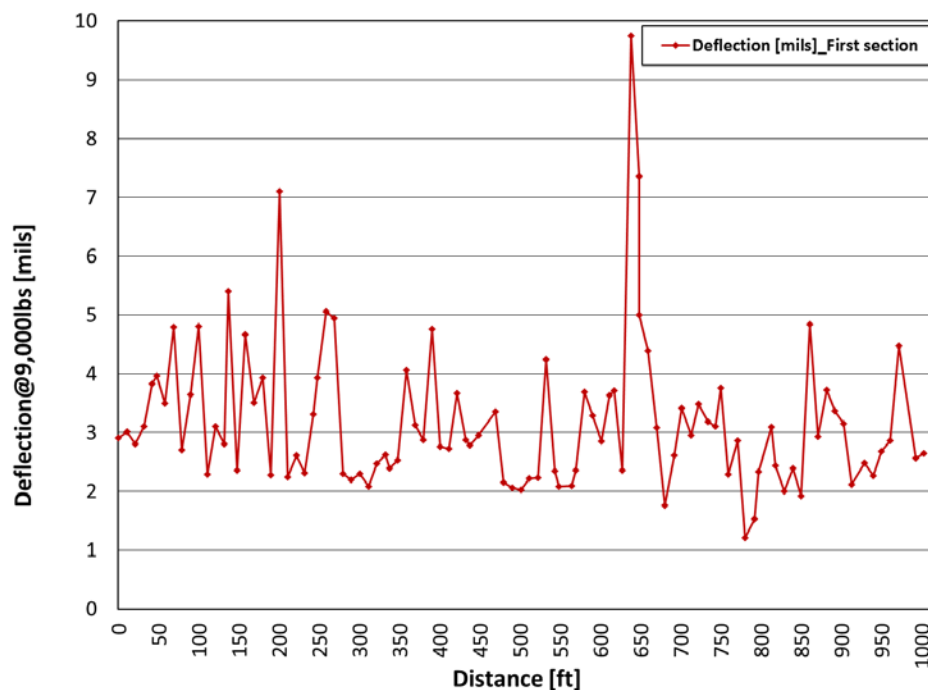


Figure 3.4 FWD testing result at poor section (with distresses)

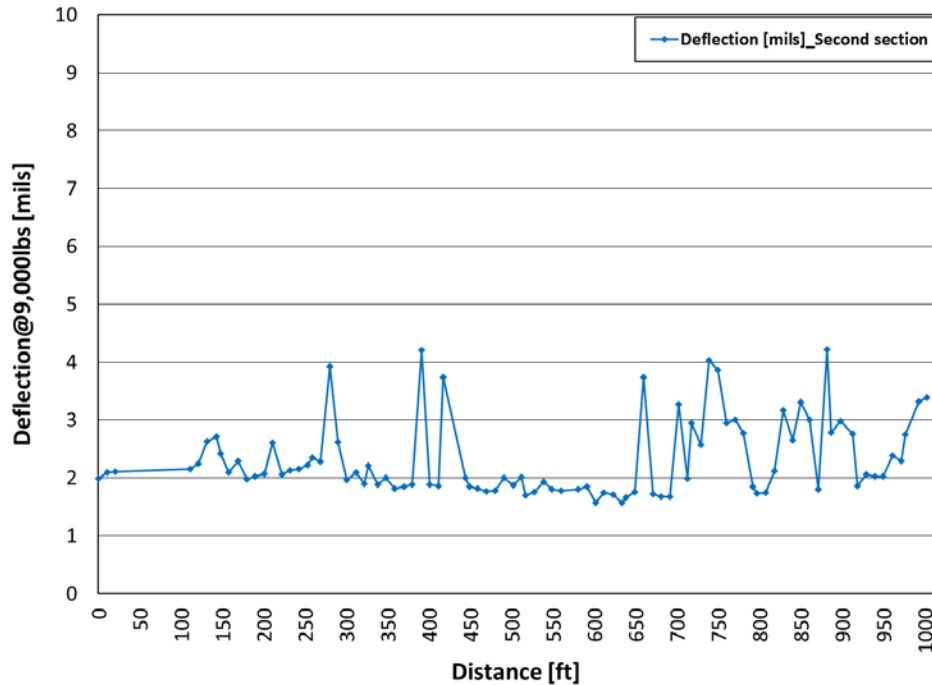


Figure 3.5 FWD testing result at good section (without distresses)

3.2.1.4 Concrete Coring

As discussed earlier, FWD testing was conducted at two locations, one with distresses on PFC overlay (poor section) and the other without distresses (good section). Four cores were taken at the poor section (P1, P2, P3, and P4) and three cores at the good section (G1, G2, and G2) based on the measured deflection and pavement distress.

Figure 3.6 shows coring locations for P1 and P2. Two cores were taken upstream and downstream of a distress area. There was a punchout distress on 8-in. CRCP at this location as shown in Figure 3.7, and the personnel of TxDOT's Wichita Falls District repaired this section by full-depth repair (FDR) method before the BCO construction. However, repaired punchout still reflected through the BCO and PFC overlay, which indicates that FDR in the existing CRCP was not able to completely restore the structural condition of the pavement. Quite often FDR just replaces distressed concrete with new concrete, without restoring slab support. The poor slab support must have caused the punchout distress in the first place. Table 3.3 illustrates the measured deflections on PFC overlay at each coring location. The average deflection at the poor section was 3.62 mils compared with 2.21 mils at the good section. Even without detailed statistical analysis, this difference clearly indicates the effects of overlaid slab deflections on the performance of BCO. Figure 3.8 shows the coring operation. As Figures 3.9 and 3.10 show, debonding failures occurred at all coring locations in the poor section. On the other hand, good bonding was observed at all coring locations in the good section, as shown in Figure 3.11. This strong correlation between bonding condition and the overlay pavement deflections and performance is interesting and

valuable information. First, it appears that debonding was caused by poor slab support or discontinuities along FDR boundaries and resulting large slab deflections, even after FDR. Small deflections in the good section appear to be due to adequate slab support, which is also responsible for good bonding. Figure 3.11-(e) shows a core taken at the good section. It shows a good bonding, even though the core was taken at a transverse crack in the existing 8-in. CRCP, which indicates that transverse cracks in CRCP do not necessarily cause debonding.



Figure 3.6 Coring location near PFC distress



Figure 3.7 Punchout distress in the existing 8-in. CRCP (picture taken on December 3, 2010)

Table 3.3 Deflections at coring locations

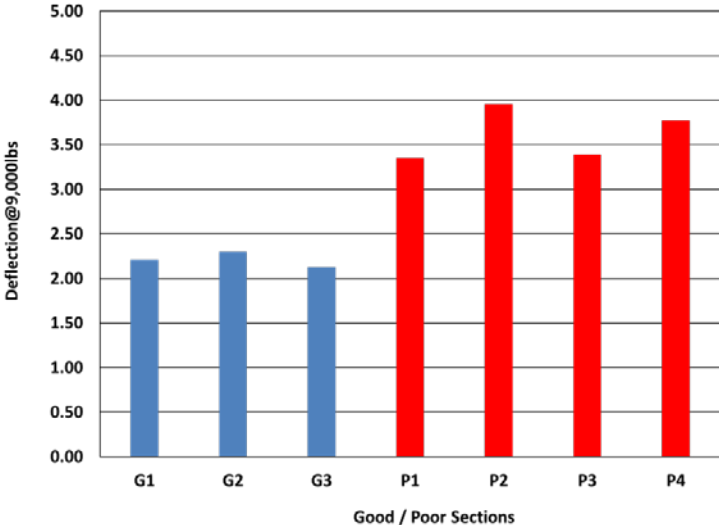
| Cores | Deflection [mils] |  <table><caption>Data for Figure 3.3 Bar Chart</caption><thead><tr><th>Section</th><th>Deflection @ 9,000 lbs (mils)</th></tr></thead><tbody><tr><td>G1</td><td>2.21</td></tr><tr><td>G2</td><td>2.30</td></tr><tr><td>G3</td><td>2.13</td></tr><tr><td>P1</td><td>3.35</td></tr><tr><td>P2</td><td>3.95</td></tr><tr><td>P3</td><td>3.39</td></tr><tr><td>P4</td><td>3.77</td></tr></tbody></table> | Section | Deflection @ 9,000 lbs (mils) | G1 | 2.21 | G2 | 2.30 | G3 | 2.13 | P1 | 3.35 | P2 | 3.95 | P3 | 3.39 | P4 | 3.77 |
|---------|-------------------------------|--|---------|-------------------------------|----|------|----|------|----|------|----|------|----|------|----|------|----|------|
| Section | Deflection @ 9,000 lbs (mils) | | | | | | | | | | | | | | | | | |
| G1 | 2.21 | | | | | | | | | | | | | | | | | |
| G2 | 2.30 | | | | | | | | | | | | | | | | | |
| G3 | 2.13 | | | | | | | | | | | | | | | | | |
| P1 | 3.35 | | | | | | | | | | | | | | | | | |
| P2 | 3.95 | | | | | | | | | | | | | | | | | |
| P3 | 3.39 | | | | | | | | | | | | | | | | | |
| P4 | 3.77 | | | | | | | | | | | | | | | | | |
| P1 | 3.35 | | | | | | | | | | | | | | | | | |
| P2 | 3.95 | | | | | | | | | | | | | | | | | |
| P3 | 3.39 | | | | | | | | | | | | | | | | | |
| P4 | 3.77 | | | | | | | | | | | | | | | | | |
| G1 | 2.21 | | | | | | | | | | | | | | | | | |
| G2 | 2.30 | | | | | | | | | | | | | | | | | |
| G3 | 2.13 | | | | | | | | | | | | | | | | | |



Figure 3.8 Coring operation



a. P1 core (debonding)



b. P2 core (debonding)

Figure 3.9 Concrete cores at P1 and P2



a. Coring location for P3



b. P3 core (debonding)



c. Coring location for P4



d. P4 core (debonding)

Figure 3.10 Concrete cores at P3 and P4



a. Coring location for G1



b. G1 core (good bonding)



c. Coring location for G2



d. G2 core (good bonding)



e. G3 core (good bonding)



f. Close-up view of G3 core

Figure 3.11 Concrete cores at good section (G1, G2, and G3)

3.2.1.5 Laboratory Testing

Laboratory testing was conducted to evaluate material properties of the existing 8-in. concrete slab, which included CoTE and dynamic modulus using cores taken from the field. The results of concrete properties are summarized in [Table 3.4](#), as well as thickness information for each layer. Concrete overlay thickness is a little thicker than the design thickness of 4.0-in., and the existing CRCP thicknesses were measured at about 8.0-in. It shows that the thicknesses of concrete layers (old CRCP and BCO) were greater in the poor section than in the good section—a strong indication that the performance at this location was not necessarily related to concrete slab thicknesses. Rather, as discussed previously, the support condition under the existing 8-in. CRCP appears to be the major factor determining pavement performance.

The average CoTE value of the concrete cores was evaluated to 2.7 microstrain/°F, which is quite low. Also, the average dynamic modulus was estimated to 5.8 x10⁶ psi. The values obtained for these two properties are within reasonable ranges and thus are not considered to have contributed to the distresses at this location.

Table 3.4 Material testing results for US 287 site

| TxDOT District | Highway | Specimen ID | RM | Core Size [in.] | | | | CoTE [x10 ⁻⁶ /°F] | Dynamic Modulus [x10 ⁶ psi] |
|----------------|---------|-------------|----------|-----------------|-----|-----|----------------|------------------------------|--|
| | | | | Thickness [in.] | | | Diameter [in.] | | |
| | | | | CRCP | BCO | PFC | | | |
| Wichita Falls | US 287 | G1 | 220+1.30 | 7.5 | 4.3 | 1.2 | 3.967 | 2.41 | 5.34 |
| | | G2 | 220+1.31 | 7.9 | 4.4 | 1.2 | 3.965 | 3.14 | 6.27 |
| | | G3 | 220+1.32 | 7.9 | 4.0 | 1.1 | 3.963 | - | - |
| | | P1 | 220+0.96 | 8 | 4.6 | 1.1 | 3.960 | 2.46 | 5.90 |
| | | P2 | 220+0.96 | 8 | 4.5 | 1.0 | 3.961 | 2.62 | 5.56 |
| | | P3 | 220+0.98 | 8 | 5.9 | 1.1 | 3.963 | - | - |
| | | P4 | 220+1.00 | 7.7 | 5.2 | 1.1 | 3.963 | - | - |

3.2.1.7 Summary

Field evaluations were conducted on US 287 in Bowie with FWD testing and concrete coring. Two sections with and without distresses were selected based on visual survey results. The findings from field testing are as follows:

- 1) Distresses on the PFC overlay in the form of reflective or localized cracking were observed in a number of locations.
- 2) Sections with and without distresses on the PFC layer (designated as poor and good sections, respectively) were selected and the deflections and concrete condition of the two sections compared. Deflections in the good section were smaller and more uniform than those in the poor section. Also, debonding between old 8-in. CRCP and 4-in. BCO

was observed in the poor section, while none in the good section. It appears that poor slab support under old 8-in. CRCP and potential discontinuities at FDR boundaries resulted in debonding and distresses in the poor section.

- 3) Slab thicknesses were within the range of the design values. Slab thicknesses in old CRCP and BCO in the poor section were actually greater than those in the good section, indicating that deficient slab thicknesses were not the primary cause of the distresses observed.

3.2.2 US 281 Wichita Falls (CRCP BCO on CRCP)

3.2.2.1 Pavement Information

A section of US 281 in Wichita Falls, from reference marker 194+0.3 to 194+0.4, was selected as a testing location. The 8-in. existing CRCP was built in 1969 and the 4-in. CRCP BCO was constructed in June 2002, after 33 years of service. For 4-in. BCO, #6 transverse bars were placed at 1.5-ft spacing on top of the existing 8-in. CRCP, and #6 longitudinal steel was placed at 8-in. spacing, which is a 1.375% longitudinal steel ratio for 4-in. slab thickness. Considering the design life of 8-in. CRCP section was 20 years, the pavement outperformed the intended design by 13 years. The details about pavement and location attributes are shown in [Table 3.5](#).

Table 3.5 Pavement information for US 281 Wichita Falls site

| Attribute | Information | Special Note |
|------------------------------|--|--------------|
| CSJ | 0249-01-012 | - |
| County | Wichita | - |
| TxDOT District | Wichita Falls | - |
| Reference Marker | 194+0.3 – 194+0.4 (0.2 miles) | Southbound |
| GPS Coordinates | 33.861528, -98.485403 ~ 33.857958, -98.485439 | - |
| Construction Year (existing) | 1969 | - |
| Construction Year (BCO) | June, 2002 | - |
| Pavement Type | CRCP BCO | - |
| Slab Thickness | 4-in. BCO + 8-in. CRCP | - |
| Shoulder Type | Tied concrete | - |
| Base Type | Treated soil | - |
| Subgrade Type | - | - |
| Drainage Type | Open Ditch | - |
| Con. Pavement Details | - | - |

3.2.2.2 Visual Survey

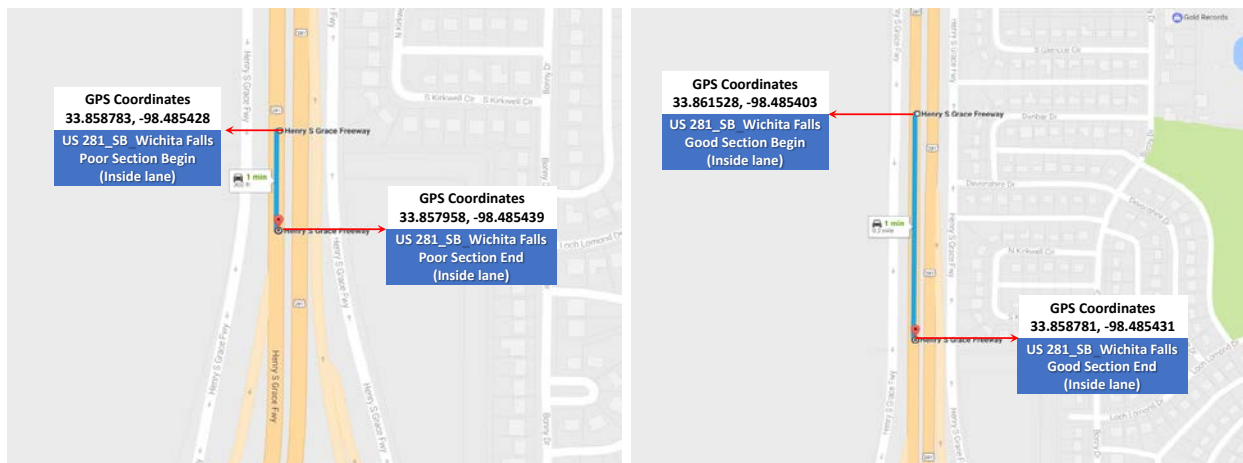
The overall BCO condition on US 281 was good, without any distresses except at a transverse construction joint (TCJ) area. Based on the visual survey results, two sections were selected as good and poor sections, as with the US-287 test section in Bowie. **Figure 3.12-(a)** shows a distress near a TCJ at the poor section and **Figure 3.12-(b)** provides an overall view of the good section selected. **Figure 3.13** shows the testing location on US 281 in Wichita Falls.



(a) Distress at construction joint (poor section)

(b) Overall view (good section)

Figure 3.12 Overall pavement condition at poor and good sections



(a) With distress (poor section)

(b) Without distress (good section)

Figure 3.13 Test locations on US 281 in Wichita Falls

3.2.2.3 Structural Evaluations

1) FWD Testing

FWD testing was conducted at 10-ft intervals at both good and poor sections and at 1-ft intervals near the TCJ in the poor section. **Figures 3.14 and 3.15** show FWD testing results at the poor and

good sections, respectively. Average deflections were measured at 3.2 mils at the good section and 3.9 mils at the poor section. Deflections near the TCJ (at about 105-ft) were larger than those further away from the TCJ. To identify the cause(s) for the large deflection at the TCJ, in-depth evaluations—including coring, DCP testing, and the MIRA testing—were conducted, which will be discussed later. It should be noted that the TCJ here is in the 4-in. BCO, and does not necessarily affect the TCJ in the existing 8-in. CRCP. It was quite difficult to determine whether the TCJ in BCO matched the TCJ in the existing CRCP. However, it is most likely that the TCJ in BCO was placed to facilitate the construction of BCO, not to match the existing TCJ in the existing CRCP. The distress observed near the TCJ was due to materials/construction-related issues during BCO construction.

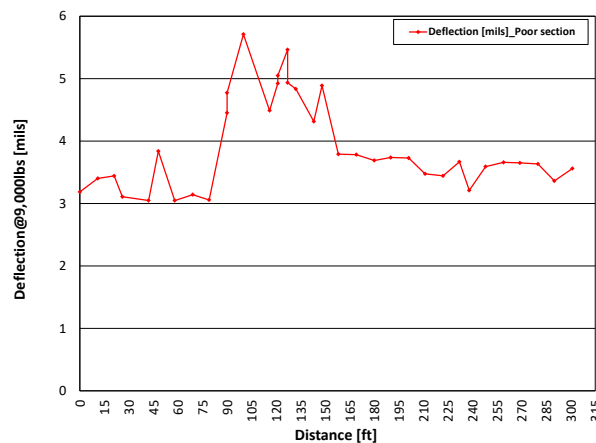


Figure 3.14 FWD deflection on US 281 (poor section)

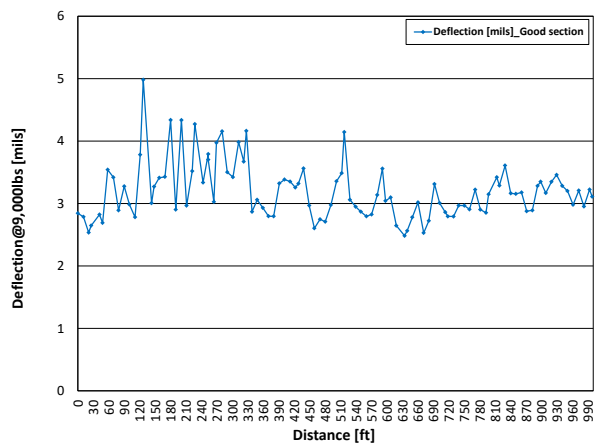


Figure 3.15 FWD deflection on US 281 (good section)

2) In-depth Evaluations of Distress at TCJ

FWD testing was conducted at 1-ft intervals from 8-ft away on one side of the TCJ and 10-ft away from the other side of the TCJ, and testing results are illustrated in [Figure 3.16](#). Deflection increases toward the TCJ (Testing Points 10 and 11) as clearly demonstrated in [Figure 3.16](#).

MIRA testing was also conducted at every FWD testing location, and delamination was detected near the TCJ at the overlay interface (4-in. depth from the top) and within the existing CRCP (8-in depth from the top) as shown in [Figure 3.17](#). This delamination indicates that there was an existing horizontal crack within the existing 8-in. CRCP. On the other hand, delamination and horizontal crack disappeared away from the TCJ, as shown in [Figure 3.18](#). [Figure 3.19](#) shows slabs removed at this location during FDRs, and horizontal cracks were observed. In Texas, horizontal cracks at the depth of longitudinal steel and resulting distresses such as slab segmentation are the primary distress type in CRCP. Punchout due to closely spaced transverse cracks and cantilever action is rarely observed.

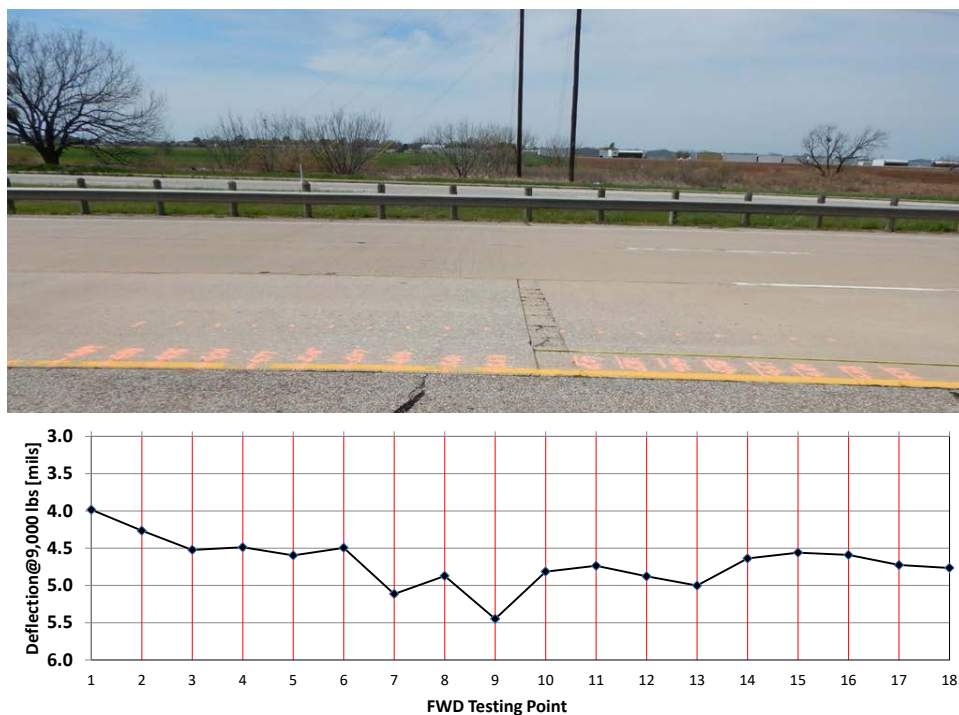


Figure 3.16 FWD deflection near the TCJ

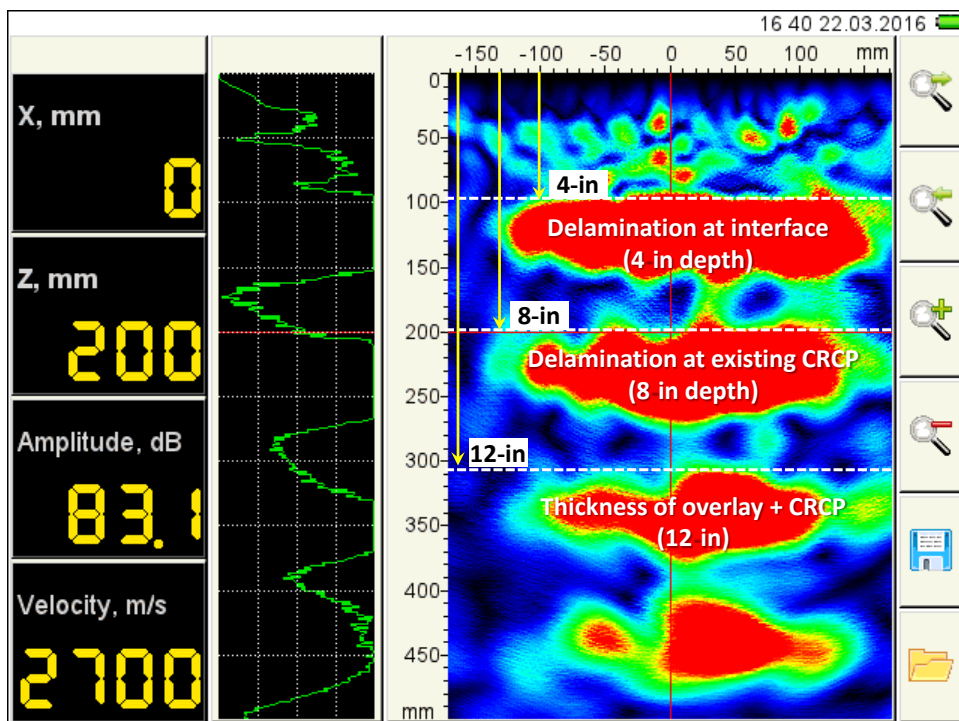


Figure 3.17 MIRA image near the TCJ

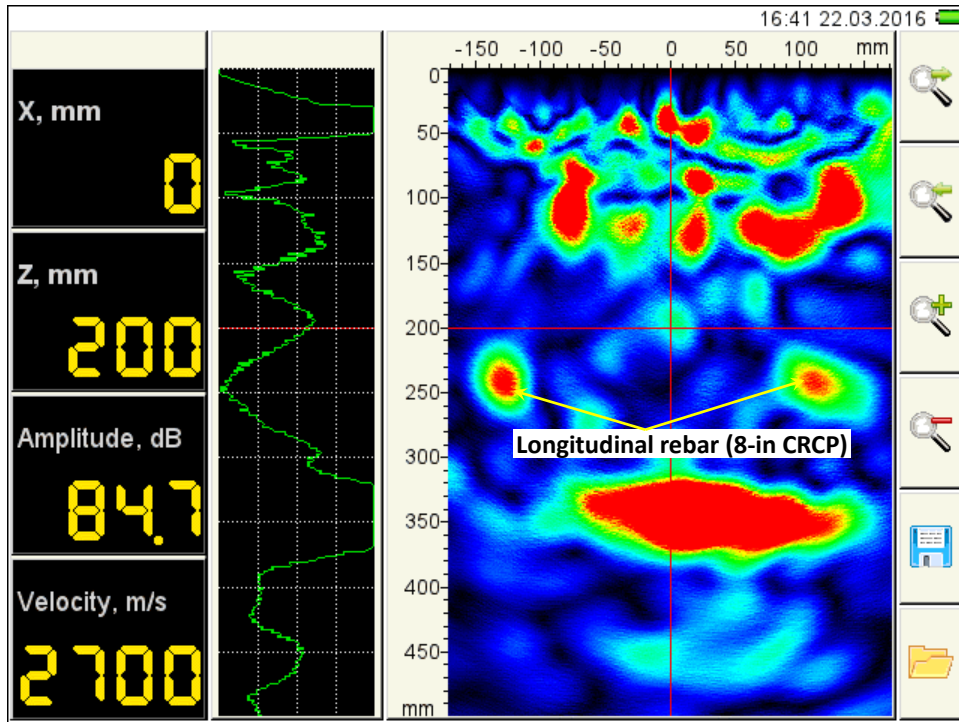


Figure 3.18 MIRA image away from the TCJ



Figure 3.19 Horizontal cracks at the depth of longitudinal steel

3) DCP Testing

To evaluate the support and base conditions, DCP testing was conducted at nine locations: five locations in the good section, and four locations in the poor section near the TCJ. **Figure 3.20**

shows DCP testing in the field.

Testing results are illustrated in **Figures 3.21 and 3.22**. The variability in the modulus values of 6-in. base layer estimated from DCP data is rather large, ranging from 27 ksi to 81 ksi, while subgrade modulus is relatively uniform, at about 8,000 psi. These modulus values are somewhat lower than the average values obtained in Texas. On the other hand, the performance of this BCO project has been quite satisfactory for the last 14 years. Although accurate truck traffic information was not available at this location, little truck traffic was observed during field testing. It appears that the level of slab support provided by subgrade and base at this location has been adequate for the traffic load experienced. In contrast, it appears that the truck traffic level at the US-287 section in Bowie was much higher, which might explain the multiple pavement distresses at that location.



Figure 3.20 DCP testing on US 281

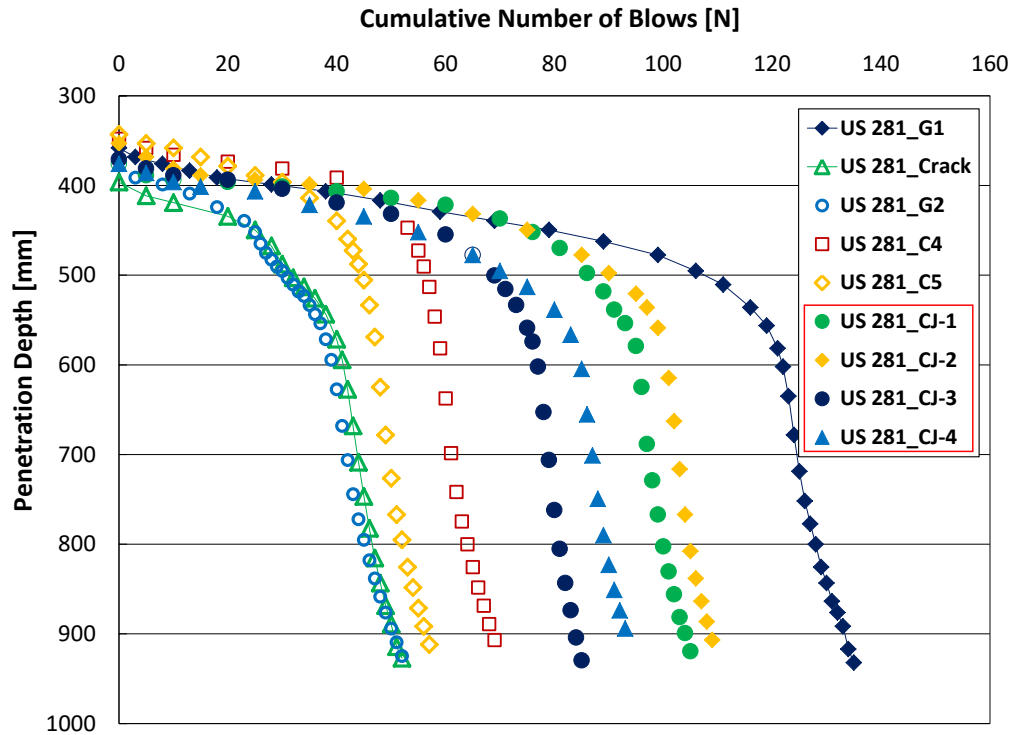


Figure 3.21 DCP testing results

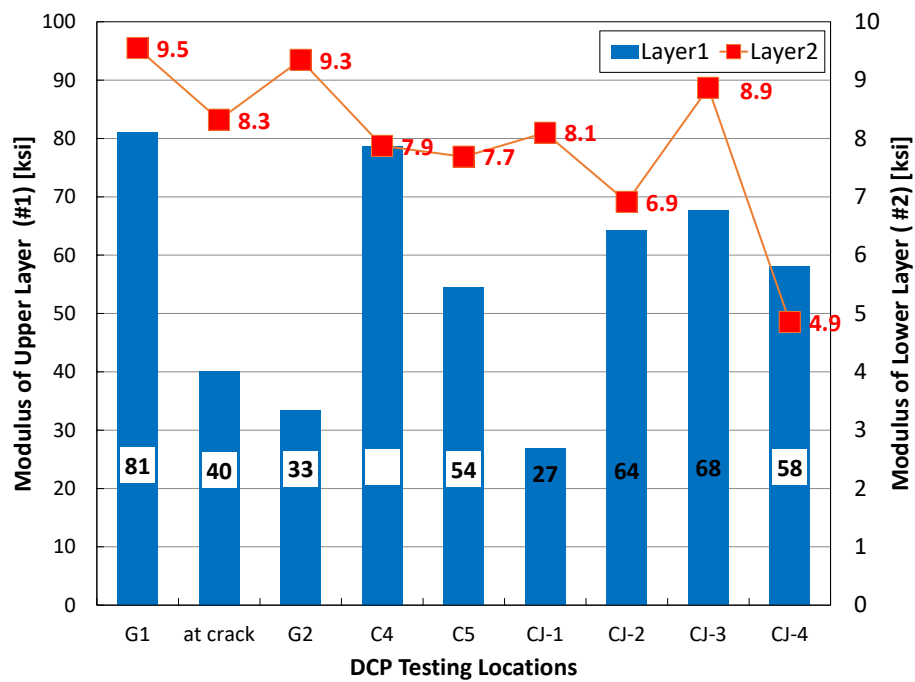


Figure 3.22 Modulus values at each layer

3.2.2.4 Concrete Coring

Three cores were taken at the good section. As shown in Figure 3.23, two cores were taken from a transverse crack and the third was taken right at the transverse crack in the BCO. The core at the

transverse crack was taken to determine whether the transverse crack in BCO was a full-depth crack and whether the reinforcement placed at the bottom of 4-in. BCO was able to hold the crack tight.

Figure 3.24 illustrates the condition of concrete cores at each location, along with deflection at 9,000 pounds measured from FWD testing. As shown in this figure, good bonding was observed at the interface both at the crack and away from the crack. **Figure 3.25** shows a close-up view of the core taken at the transverse crack. This figure illustrates that the transverse crack did not progress toward the pavement bottom, but rather stopped at the mid-depth in the BCO. It shows that the placement of longitudinal steel near the bottom of 4-in. BCO, along with the use of crushed limestone as coarse aggregate (which provides a low CoTE), adequately restrained concrete volume changes due to temperature and moisture variations.

Bond strength testing results at these locations are discussed in the next section.

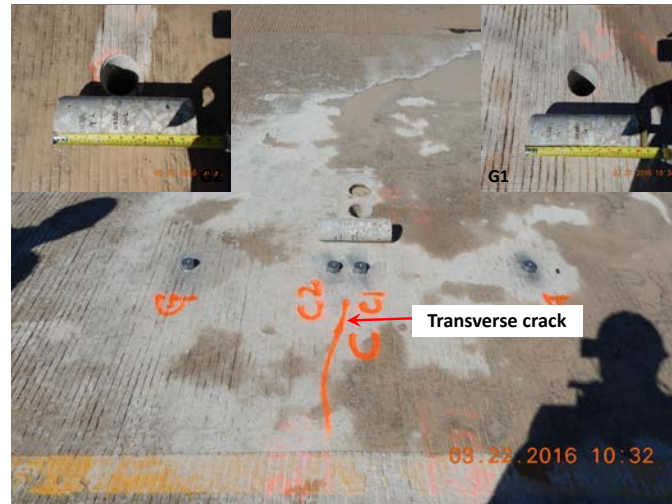


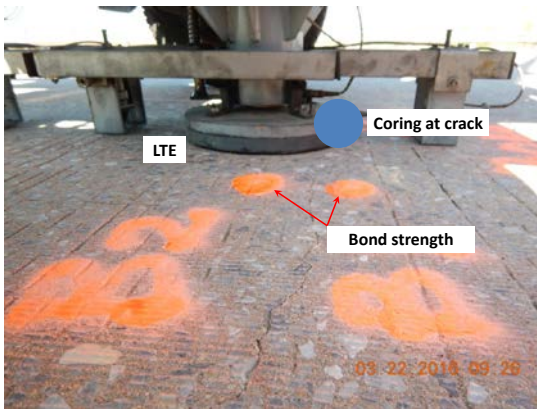
Figure 3.23 Core sampling



a. G-1: away from transverse crack
(deflection @ 9,000 lbs: 3.5 mils)



b. G-2: away from transverse crack
(deflection @ 9,000 lbs: 3.2 mils)



c. G-3: at transverse crack
(deflection @ 9,000 lbs: 4.0 mils)



d. G-3 core at transverse crack

Figure 3.24 Concrete cores away from transverse crack and at transverse crack



Figure 3.25 Close-up view of G3 core taken at transverse crack

3.2.2.5 Bond Strength Testing

Bond strength testing was conducted in accordance with ASTM C1583/C1583M (Standard Test Method for Tensile Strength of Concrete Surfaces and the Bond Strength or Tensile Strength of Concrete Repair and Overlay Materials by Direct Tension (Pull-off Method)). **Figure 3.26** shows a bond strength testing procedure, following these steps in the field:

- Step 1 – **Figure 3.26-(a)**: Selection of coring location and coring
- Step 2 – **Figure 3.26-(b)**: Surface grinding and cleaning to provide good bonding between disc and concrete
- Step 3 – **Figure 3.26-(c)**: Application of rapid-setting epoxy
- Step 4 – **Figure 3.26-(d)**: Testing device setup (load speed and horizontal level of device)
- Step 5 – **Figure 3.26-(e)**: Pull-off testing
- Step 6 – **Figure 3.26-(f)**: Investigation of failure mode

Locations for bond strength testing were selected on the basis of deflection, as well as whether transverse cracks existed. **Figure 3.27** shows bond strength testing results with a deflection value at each location. MIRA testing was also conducted before bond strength testing. C1 and C2 in **Figure 3.27** are located near a transverse crack in the overlay pavement. **Figures 3.28-(a) and (b)** show MIRA images at the locations C1 and C2. The reinforcements in the BCO and existing 8-in. CRCP are shown and no delamination observed at the interface between 4-in. BCO and 8-in. existing CRCP.



a. Coring



b. Surface grinding



c. Rapid setting epoxy



d. Device setup



e. Testing



f. Failure mode determination

Figure 3.26 Bond strength testing procedure

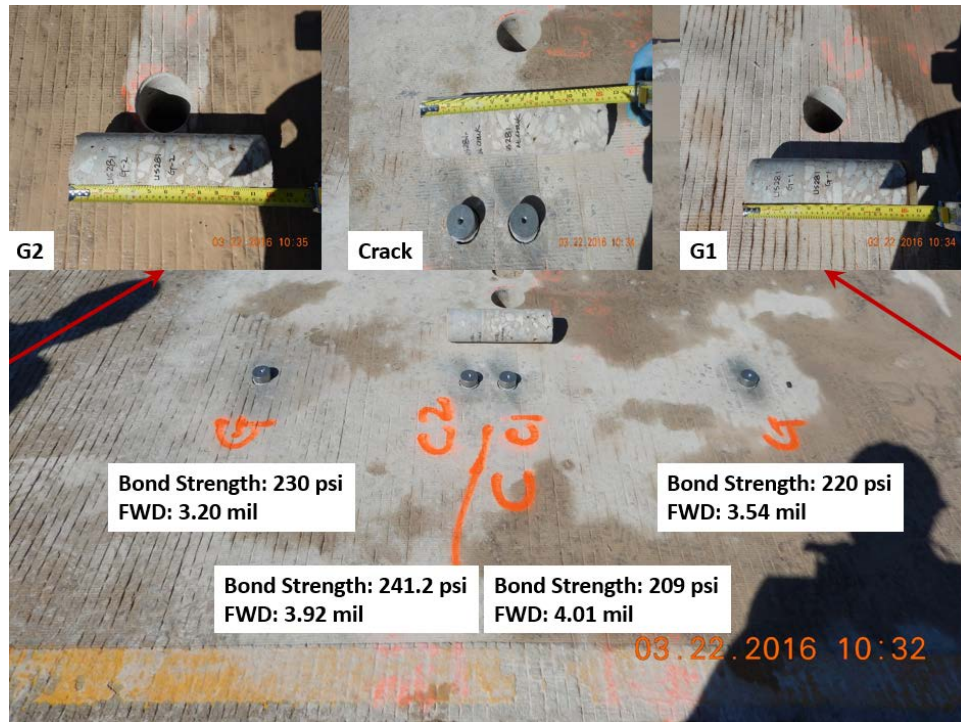


Figure 3.27 Core sampling

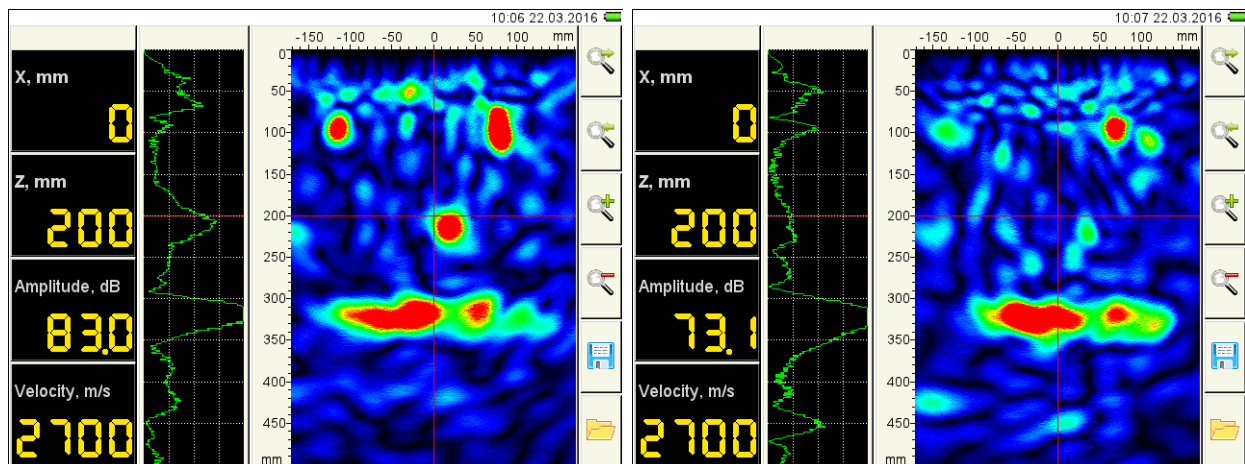


Figure 3.28 MIRA images at transverse crack (C1 and C2)

Bond strength testing results including failure modes are summarized in [Table 3.6](#). At nine testing locations, failure planes were within the overlay layer in two locations, and within the 8-in. CRCP in five locations. No failures occurred at the interface between 4-in. BCO and 8-in. CRCP, which implies good interface bonding. In the other two locations, failure occurred at the interface between testing disk and the top of the BCO, which implies that the testing preparation was not properly done. In the good section, bond strength values were larger than 200 psi, regardless of the locations

of failure plane. On the other hand, bond strength at the poor section was low. Recall that the poor section was near the distressed area at the TCJ, and horizontal cracking was observed within the 8-in. CRCP. It is interesting to note that the bond strength values where the failure plane was within the 8-in. CRCP were much larger in the good section than in the poor section. It appears that the concrete in the existing 8-in. CRCP in the poor section was damaged, resulting in lower bond strengths.

Table 3.6 Bond strength results for US 281 section

| Testing Date | TxDOT District | County | Specimen Name | | Deflection @9,000 lbs [mils] | Bond Strength [psi] | Failure Mode |
|--------------|----------------|---------|---------------|-----|------------------------------|---------------------|--------------|
| 3/22/ 2016 | Wichita Falls | Wichita | Good Section | G1 | 3.5 | 220 | within BCO |
| | | | | G2 | 3.2 | 230 | within CRCP |
| | | | | C1 | 4.0 | 209 | within CRCP |
| | | | | C2 | 3.9 | 241 | within BCO |
| | | | | C5 | 4.5 | 254 | within CRCP |
| | | | Poor Section | P8 | 5.7 | 143 | within CRCP |
| | | | | P9 | - | 126 | within CRCP |
| | | | | P10 | - | 143 | Disk failure |
| | | | | P11 | 4.0 | 205 | Disk failure |
| | | | | | | | |

3.2.2.6 Concrete Material Properties

Cores taken from the field were tested in the laboratory for CoTE and dynamic modulus. The concrete properties are summarized in **Table 3.7**. The average CoTE value of concrete cores was evaluated at 3.0 microstrain/°F. Also, the average dynamic modulus was measured at 5.7 x10⁶ psi. These values are within reasonable range, and contributed to the excellent performance of this BCO.

Table 3.7 Concrete properties in the US-281 section

| TxDOT District | County | Specimen Name | RM | Size [in.] | | | Weight [lbs] | CoTE [x10 ⁻⁶ /°F] | Dynamic Modulus [x10 ⁶ psi] |
|----------------|---------|---------------|----------|------------|-----|----------|--------------|------------------------------|--|
| | | | | Thickness | | Diameter | | | |
| | | | | Existing | BCO | | | | |
| Wichita | Wichita | G1 | 194+0.35 | 8.0 | 4.2 | 3.970 | - | - | - |
| | | At crack | 194+0.35 | 8.4 | 4.1 | 3.966 | 7.277 | 3.01 | 5.6 |
| | | G2 | 194+0.35 | 8.0 | 4.0 | 3.973 | 7.332 | 3.00 | 5.8 |

3.2.2.8 Summary

Field evaluations were conducted on US 281 in Wichita Falls with FWD testing, concrete coring, DCP testing, bond strength testing, and MIRA testing. Two test sections were selected for testing: one with distresses (near the TCJ) and the other without distresses. The findings from field testing are as follows:

- 1) Overall performance of this section has been excellent. The only distress observed was at the TCJ in BCO.
- 2) Slab support condition at this location as evaluated by DCP was somewhat inferior to typical sections in Texas. Truck traffic in this section appears to be low, which might explain the satisfactory performance of this section with the given slab support condition.
- 3) A transverse crack in BCO did not go through the BCO slab depth; rather, it stopped within 2-in. of the concrete surface. Longitudinal reinforcement, along with the low CoTE of the concrete in BCO, was able to properly restrain concrete volume changes due to temperature and moisture variations.
- 4) Failure planes in the bond strength testing were all within the 4-in. BCO or 8-in. CRCP, not at the interface between the two slabs. Also, bond strength values in the good section were all above 200 psi, while most of the bond strength values in the poor section were below 200 psi.
- 5) Relatively large deflections were measured near the TCJ where delamination at the interface between BCO and existing CRCP was observed, as was horizontal cracking at the mid-depth of the 8.0-in. existing CRCP. It appears that the larger deflections were caused by the delamination in the concrete slabs.

3.2.3 US 75 Sherman (CRCP BCO on CPCD)

3.2.3.1 Pavement Information

US 75 in Sherman, from reference marker 202+0.9 to 202+1.3 is a unique site, as 7-in. bonded CRCP was placed on severely deteriorated 10-in. jointed plain concrete pavement (CPCD). The CPCD was placed in 1984 on top of a 6-in. flexible base and the 7-in. CRCP BCO was placed in 2010. The condition of CPCD in Sherman was quite poor, with severe pumping, slab settlement, and slab cracking observed. However, faulting was not an issue, since dowels were placed at transverse contraction joints. Even with continuous repairs and maintenance, the performance of this CPCD project has deteriorated, and it was decided to employ a different rehabilitation strategy; 7-in. CRCP BCO was selected as a potential rehabilitation method. CPCD condition was evaluated in Sherman and the location with the most distresses was selected for 7-in. CRCP BCO. The most distressed CPCD area for BCO was selected with an eye to determine whether this overlay system works in this area; if so, the same overlay system should work in the other areas in Sherman. Accordingly, this section is a test site to evaluate the feasibility of 7-in. CRCP overlay on

extensively deteriorated CPCD. The length of the test section was 0.4 miles. The steel design for 7-in. CRCP BCO consisted of #6 longitudinal steel at 8-in. spacing, placed at 4-in. from the BCO surface, and #6 bars at 3-ft spacing for transverse steel just below the longitudinal steel. The longitudinal steel ratio was 0.79% of the 7-in. BCO cross-sectional area. More detailed information on this project can be found in the research project report 5-4893 (Ryu et al 2011). The details about pavement and location attributes are shown in Table 3.8.

Table 3.8 Pavement information for US 75 Sherman site

| Attribute | Information | Special Note |
|------------------------------|--|--------------|
| CSJ | 6182-92-001 | - |
| County | Grayson | - |
| TxDOT District | Paris | - |
| Reference Marker | 202+0.9 – 202+1.3 (0.4 miles) | Southbound |
| GPS Coordinates | 33.687144, -96.604206 ~ 33.682528, -96.607286 | - |
| Construction Year (existing) | 1984 | - |
| Construction Year (BCO) | June, 2010 | - |
| Pavement Type | CRCP BCO over CPCD | - |
| Slab Thickness | 7-in. CRCP BCO + 10-in. CPCD | - |
| Shoulder Type | Tied-Concrete Shoulder | - |
| Base Type | 6-in. Flexible Base | - |
| Subgrade Type | Lime Treated Subgrade | - |
| Drainage Type | Open Ditch | - |
| Con. Pavement Details | - | - |

3.2.3.2 Visual Survey

Prior to BCO construction, detailed information was collected in this section, which included a distress map and deflection data at three locations in each slab (upstream, mid-slab, and downstream, along 3-ft from outside longitudinal joint) in the outside lane in the existing 10-in. CPCD. The information on the CPCD prior to BCO was utilized to analyze the current pavement condition and to develop any correlations between CPCD condition and CRCP BCO performance. Figure 3.29 shows the test location.

There were 22 distresses observed in CRCP BCO, all of which were in the outside lane. There were no distresses in the inside lane. All 22 distresses occurred at the locations of transverse contraction joints in the existing CPCD. In all, 148 transverse contraction joints were found in CPCD under 7-in. CRCP BCO, which indicates about 15% distress ratio at the joints.

Interestingly, only one distress was observed in the section placed on the first day of outside lane

construction, and the remainder of the distresses were observed in the section placed on the second day of the outside lane construction. At this location, 7-in. CRCP was placed in the inside lane and inside shoulder first. Then the inside lane was opened to traffic, and 7-in. CRCP overlay was placed in the outside lane and outside shoulder. The direction of the construction for both lanes was from north to south. The construction of the inside lane and shoulder went quite smoothly, with no issues. However, during the construction of the outside lane and shoulder, concrete delivered to the jobsite was quite dry and the finishing operation was quite difficult. Some of the concrete had to be removed, and replaced with new concrete, which will be further discussed in Chapter 4. **Figure 3.30** illustrates the number of distresses observed during the visual survey. The embedded figure in **Figure 3.30** also shows a CPCD distress map from slab number-101 (J-101) to slab number-120 (J-120), which was developed during the CPCD condition survey prior to BCO construction. Because the majority of the distresses in BCO were in the section placed on the second day of the outside lane construction and the quite poor condition of CPCD in that area, it appears that either construction quality issues and/or the poor condition of CPCD contributed to the distress development. **Figure 3.31** illustrates a typical distress observed; it appears to have reflected from the existing CPCD joints. It should also be noted that 2-ft wide non-woven fabric was placed along the transverse joints throughout the lane width. The objective was to minimize the detrimental effect of large deflections in existing CPCD on 7-in. BCO performance, since deflections measured on CPCD prior to the BCO construction were more than 20 mils at a number of locations. At that time, it was construed that placing 7-in. CRCP BCO directly on CPCD with such large deflections might result in severe distresses and placing non-woven fabric was expected to alleviate the detrimental effect of large deflections in CPCD on 7-in. CRCP BCO performance. It turned out that this was not the case, because some of the distresses with similar condition shown in **Figure 3.31** were repaired as early as 2012 by removing both the concrete in the 7-in. BCO and non-woven fabric, followed by placing new concrete. These repairs performed very well, indicating that the use of non-woven fabric was not needed, and also the poor quality of the construction of the outside lane might have contributed to the distresses in the 7-in. BCO.

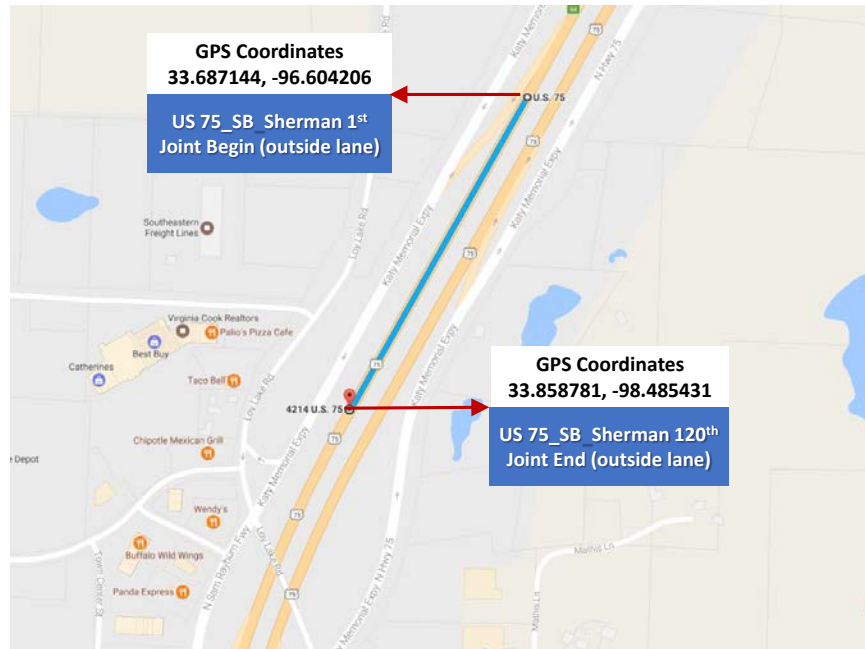


Figure 3.29 Testing locations on US 75

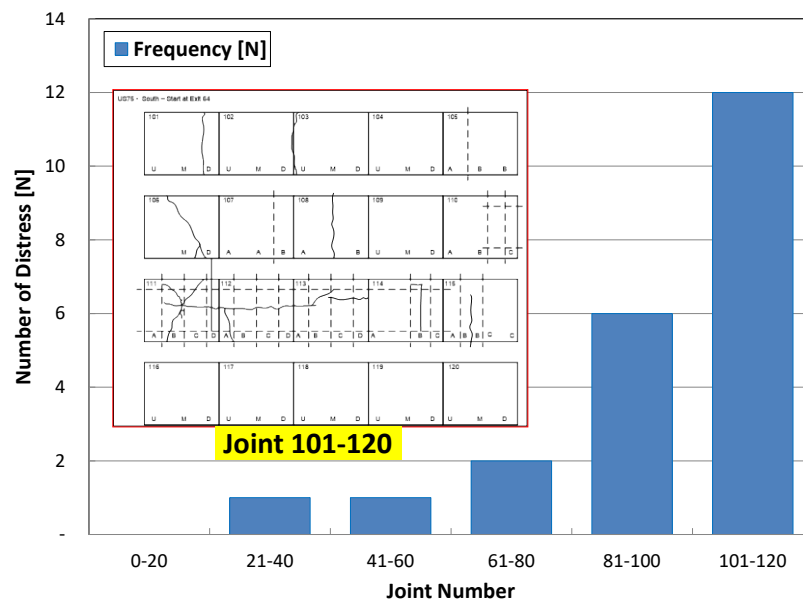
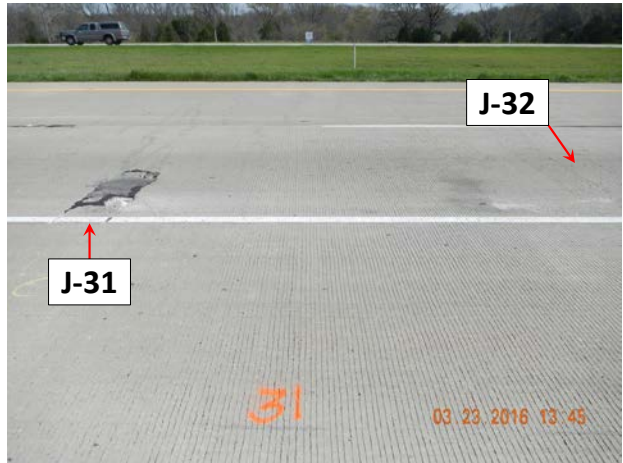


Figure 3.30 Number of distresses



a. Distress at Joint #31 (J-31)



b. TCJ (J-45)



c. Distress at J-71



d. Distress at J-80

Figure 3.31 Typical BCO distress on US 75

3.2.3.3 Falling Weight Deflectometer

FWD testing was conducted on BCO every 15-ft for the length of the site. The 7-in. CRCP BCO started at the mid-slab between the 15-ft joint spacing of the existing CPCD. **Figure 3.32** shows a comparison between deflections on CPCD and on CRCP. The overall deflection after the BCO was placed decreased substantially; however, BCO distresses were observed at the locations of relatively large deflections on CPCD. FWD testing on CRCP BCO stopped at Joint #97 since traffic control had to be lifted. In **Figure 3.32**, black squares indicate the locations of distress and green squares the locations of PCCPs. On the other hand, although deflections on CPCD were relatively small from J-90 to J-110, distresses and PCCPs were observed. Detailed information on distresses in terms of deflection and existing CPCD distress are illustrated in **Figures 3.33 and 3.34**. In these figures, black squares denote BCO distress and black circles indicate areas with large deflections in BCO. Also, green squares indicate PCCPs, and cross-hatched areas with red and green denote distress and repairs in BCO, respectively. Figure 3.33 indicates that areas with large

deflections in CPCD did not necessarily experienced distresses in BCO; however, deflections in CPCD where distresses developed in BCO were above a certain value. It appears that large deflections in CPCD are not a sufficient condition, but rather a necessary condition for distresses in BCO. This finding is a little different from the findings at US 287 in Bowie, where large deflections in 8-in. existing CRCP were close to sufficient condition for 4-in. BCO. The difference appears to be the thickness of CRCP BCO—7-in. at this location versus 4-in. at the US-287 site in Bowie. Figure 3.34 illustrates the same information from Joint 81 to Joint 120, where deflections in CPCD were quite small, while a number of distresses and PCCPs were observed in BCO. It is not clear whether BCO construction practice or other conditions, such as poor-quality repairs of CPCD, were responsible for the large frequency of distresses and PCCPs in this area.

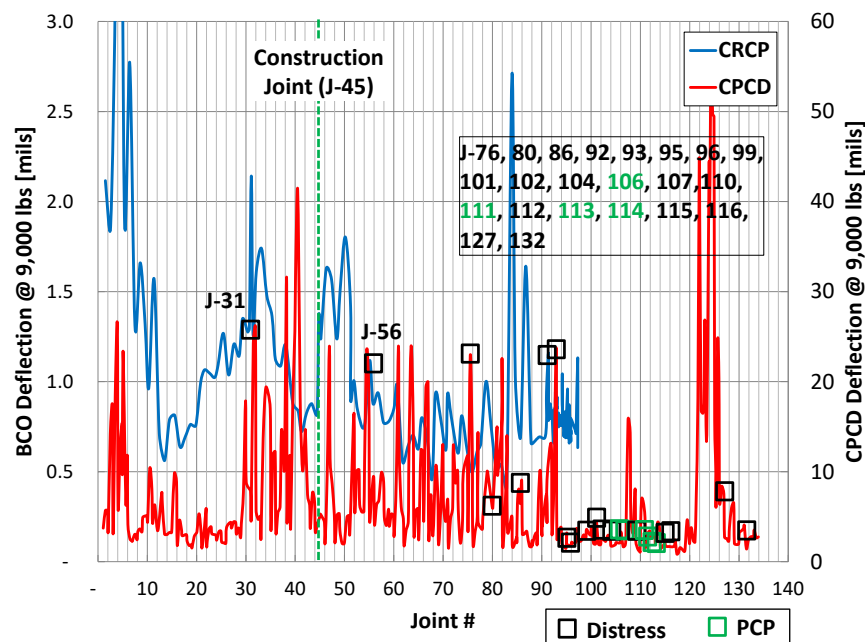
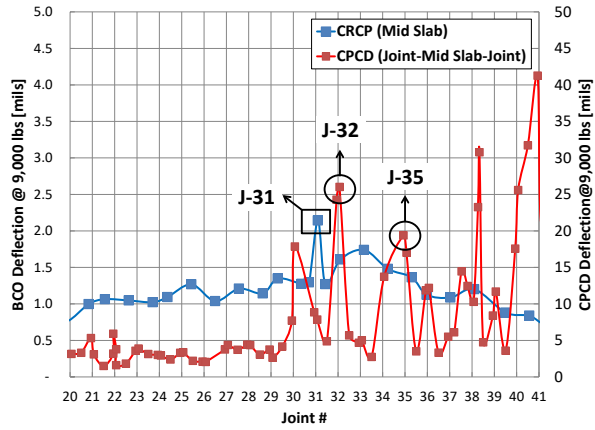
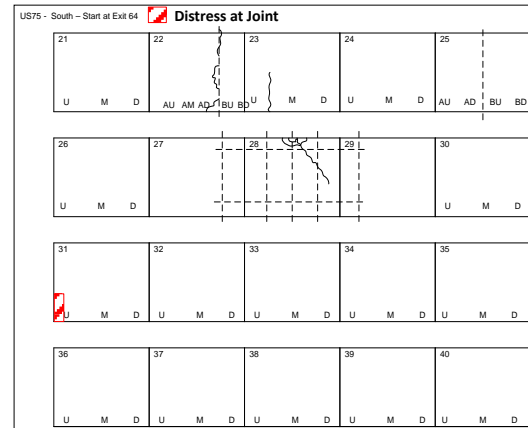


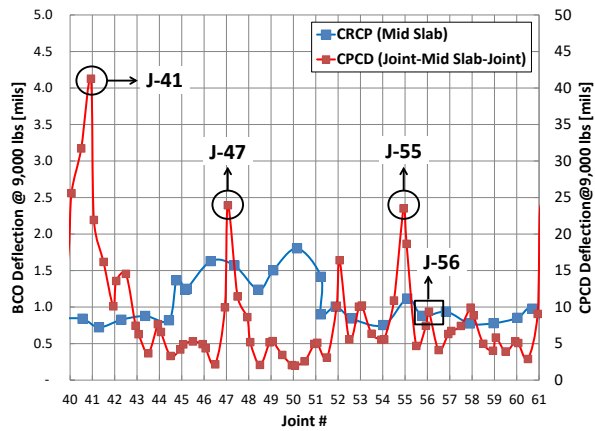
Figure 3.32 Deflection comparisons between BCO and CPCD with BCO distresses



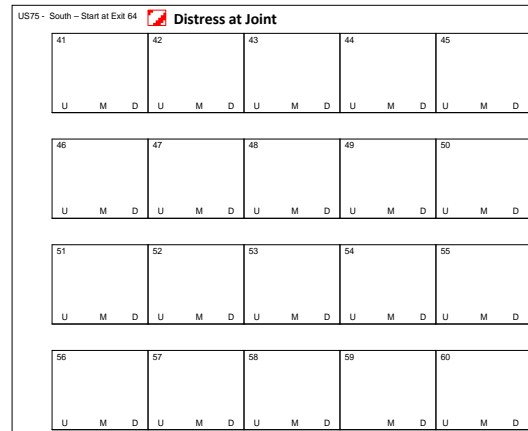
a. Deflection vs BCO distress (J-21 to J-40)



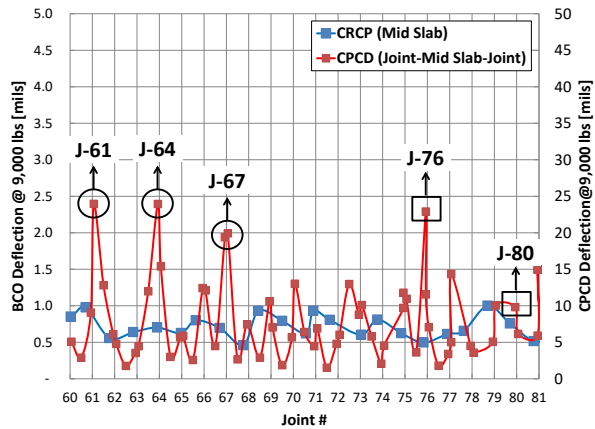
b. Distress map (J-21 to J-40)



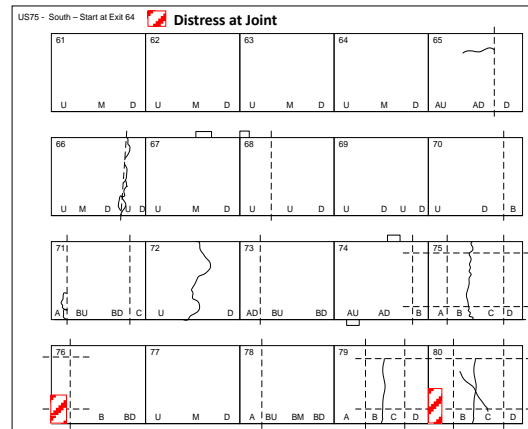
c. Deflection vs BCO distress (J-41 to J-60)



d. Distress map (J-41 to J-60)

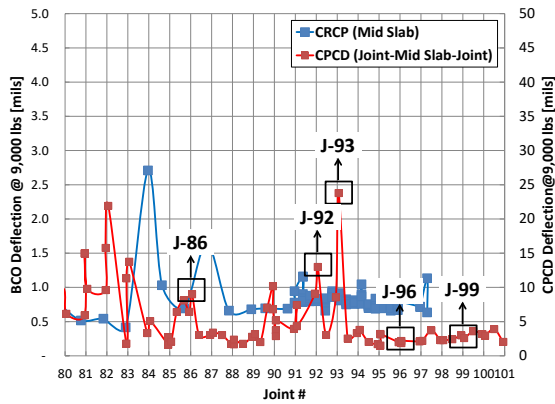


e. Deflection vs BCO distress (J-61 to J-80)

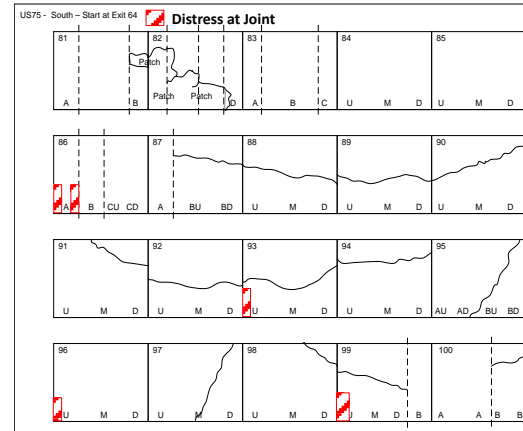


f. Distress map (J-61 to J-80)

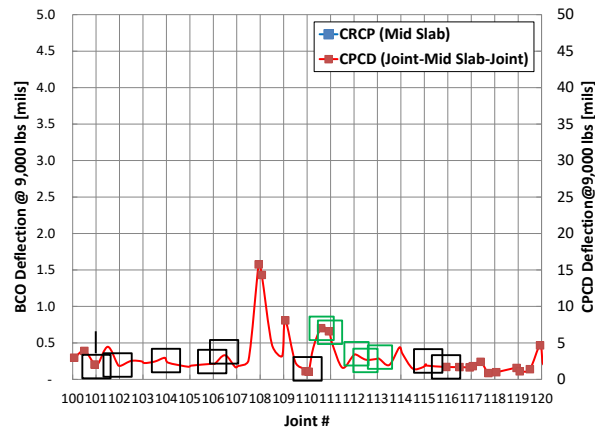
Figure 3.33 Distresses analysis in terms of deflection and existing CPCD condition (J-20 to J-80)



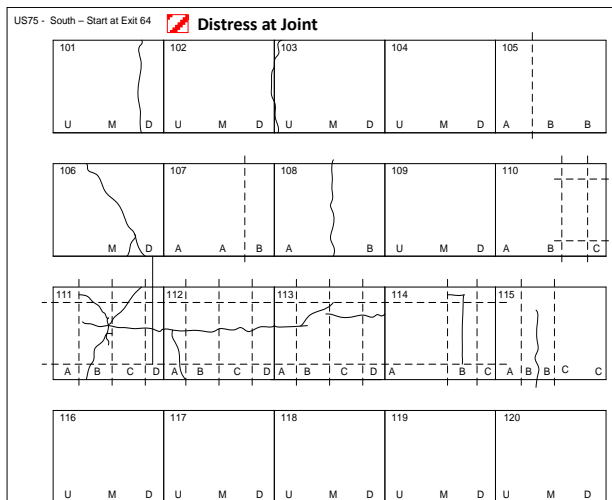
a. Deflection vs BCO distress (J-81 through J-100)



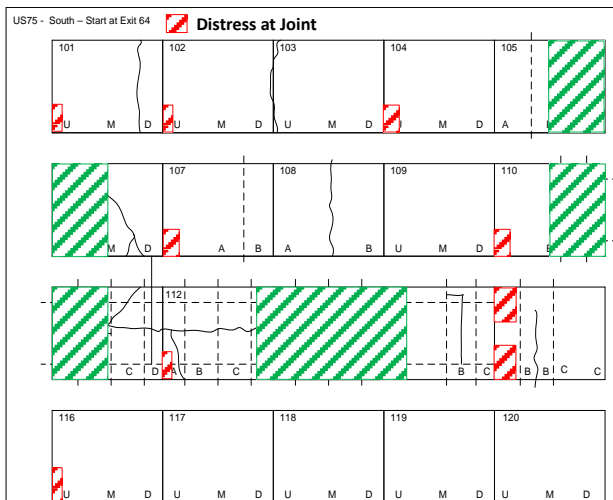
b. CPCD distress map and BCO distress (J-81 through J-100)



c. Deflection vs BCO distress (J-101 through J-120)



d. CPCD distress map (J-81 through J-100)



e. BCO distress map (J-81 through J-100)

Figure 3.34 Distresses analysis in terms of deflection and existing CPCD condition (J-81 to J-120)

3.2.3.4 Concrete Material Properties

Due to the issues with the coring machine during field testing, only one solid concrete core was taken in the BCO. Neither bond strength testing nor DCP testing was conducted.

Table 3.9 shows a dynamic modulus of elasticity value measured from one core obtained. The dynamic modulus value is within a reasonable range. The length of the specimen after end treatments was not adequate for CoTE testing.

Table 3.9 Concrete properties in the US-75 section

| Date | TxDOT District | County | Specimen Name | RM | Size [in.] | | | Weight [lbs] | Dynamic Modulus [x10 ⁶ psi] |
|-----------|----------------|---------|---------------|---------|------------|---------|----------|--------------|--|
| | | | | | Thickness | | Diameter | | |
| | | | | | Existing | Overlay | | | |
| 3/23/2016 | Paris | Grayson | C4 (ND) | 202+1.2 | - | 7.0 | 3.651 | 6.186 | 5.1 |

3.2.3.5 Summary

Visual survey and field testing were conducted to evaluate the BCO condition on US 75. The surveyed distress results in the BCO were compared with slab deflections, distresses, and condition in CPCD prior to BCO. The findings are summarized as follows:

- 1) Although accurate traffic information is not available, truck traffic at this location is clearly quite high.
- 2) No distresses were observed in the inside lane, and all 22 distresses developed in the outside lane. All 22 distresses were at the locations of existing transverse contraction or repair joints in CPCD. Since there were 148 transverse contraction joints in the entire section, the distress ratio is about 15%.
- 3) Only one distress was observed in the section placed on the first day of the outside lane construction, and all remaining distresses were observed on the second day of the outside lane construction. The CPCD condition at the location of the second day construction was quite poor. Accordingly, it appears that either construction quality issues and/or the poor condition of CPCD contributed to the distress development.
- 4) In some areas, no good correlation was observed between deflections on existing CPCD measured prior to BCO and distresses in BCO. Also, it appears that large deflections in CPCD are a necessary condition for distresses in BCO, but not necessarily a sufficient condition.

3.2.4 Loop 610 South Houston (BCO on CRCP)

3.2.4.1 Pavement Information

In 1984, BCO test sections were placed on Loop 610 South, with the primary objective of evaluating various treatments for bonding effectiveness as well as for reinforcement types. The test sections are located on Loop 610 South in TxDOT's Houston District, from reference marker 36+0.15 to 36+0.32. The 8-in. existing CRCP was built in 1970s and the 2-in. to 3-in. BCOs were placed in 1984. In December 1984, Bagate evaluated the effects of interface condition on thin bonded PCC overlays (Bagate et al. 1985). The interface conditions included in the evaluations were dry surface and cement grout with Daraweld-C pre-surface treatment. One year after the construction of BCOs, in November 1985, Kailasanathan conducted deflection testing on individual experimental sections, which were 2-in. plain concrete (160 ft), 2-in. reinforced concrete (200 ft), 3-in. reinforced concrete (180 ft), 3-in. fibrous concrete (180 ft), and 2-in. fibrous concrete pavement, as shown in Figure 3.35. Accordingly, the BCO applied at this location is not CRCP BCO. The Lane-Wells Dynaflect device was used throughout that study to measure pavement deflections (Kailasanathan et al. 1984). Since deflection testing on BCO was conducted with FWD in this study, in order to assess the variations in deflections and possibly structural capacity of the pavement section over more than 30 years, correlations between Dynaflect and FWD need to be quantified. Detailed data analysis is discussed in Chapter 4.

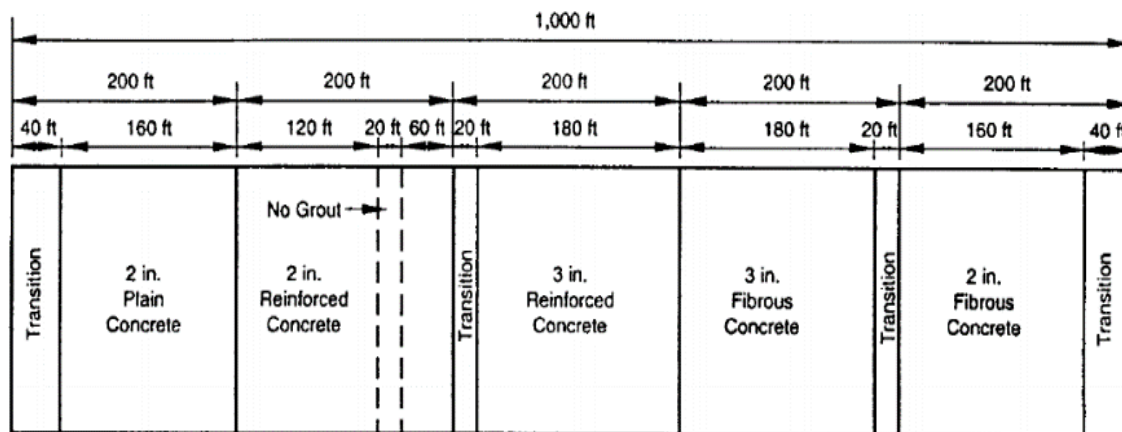


Figure 3.35 Plan view of experimental sections on Loop 610 South in Houston, showing details of design and layout

The details about pavement and location attributes are shown in Table 3.10. Figure 3.36 shows the testing section on Loop 610 South in Houston.

Table 3.10 Pavement information for Loop 610 South site

| Attribute | Information | Special Note |
|------------------------------|--|---|
| CSJ | XXXX-XX-XXX | - |
| County | Harris | - |
| TxDOT District | Houston | - |
| Reference Marker | 36+0.15 – 36+0.32 (0.17 miles) | - |
| GPS Coordinates | 29.682852, -95.349579 ~ 29.681808, -95.352103 | Eastbound |
| Construction Year (existing) | 1970's | - |
| Construction Year (BCO) | 1984 | - |
| Pavement Type | BCO over CRCP | Plain / Reinforced / Fibrous Concrete Pavement |
| Slab Thickness | 2~3-in. var. BCO + 8-in. CRCP | - |
| Shoulder Type | Tied-Concrete Shoulder | - |
| Base Type | 6-in. Cement Treated Subbase | - |
| Subgrade Type | Asphalt Shoulder | - |
| Drainage Type | Open Ditch | - |
| Con. Pavement Details | - | - |

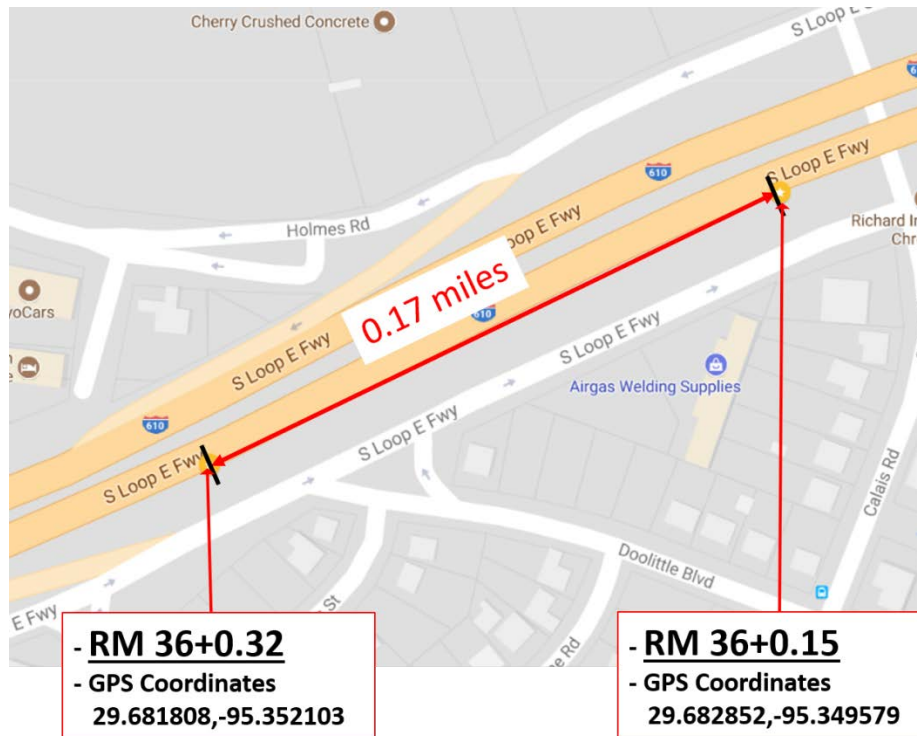


Figure 3.36 Testing location on Loop 610 South in Houston

3.2.4.2 Visual Survey

Figure 3.37-(a) provides an overall view of the section. Several PCCPs were placed at the longitudinal joints (Figure 3.37-(b)), and a Fibrecrete patch was also observed, as shown in Figure 3.37-(c). PCCPs at the outside lane were also observed (Figure 3.37-(d)). Bond strength testing was conducted near the PCCP after FWD testing. A detailed distress map was developed, as shown in Figure 3.38.



a. Overall view



b. PCCPs at longitudinal joint



c. Fibrecrete patch



d. PCCP at outside lane

Figure 3.37 Pavement condition on Loop 610 South

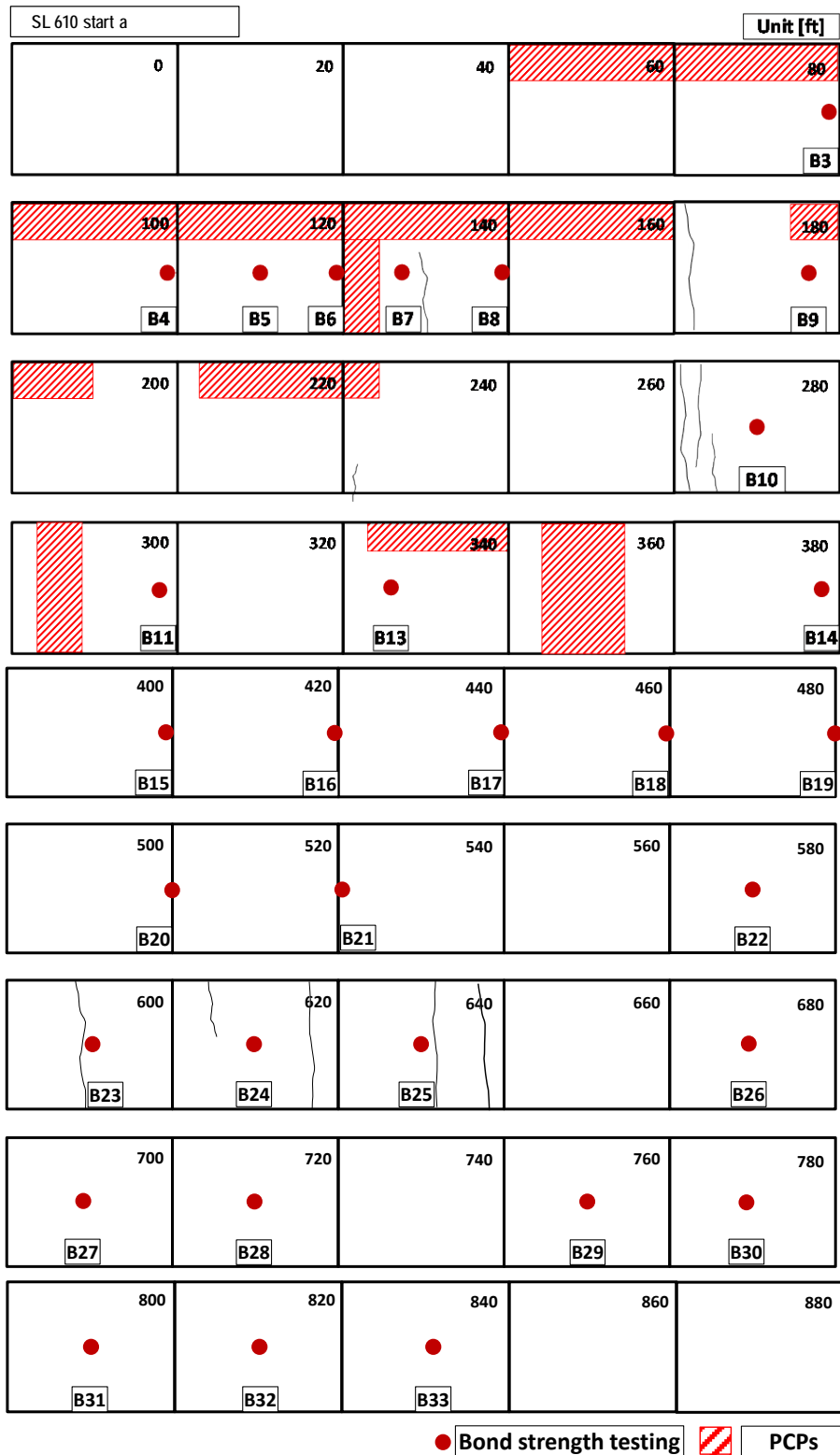


Figure 3.38 Distress map in experimental section on Loop 610 South in Houston

3.2.4.3 FWD testing

FWD testing was conducted in each experimental section with 10-ft spacing. **Figure 3.39** shows the results of FWD testing. The graph shows overall deflections in 2-in. and 3-in. fibrous concrete pavements are lower than those in 2-in. reinforced concrete and 2-in. plain concrete. Since thicknesses are different and slab support condition is not known, the information may not be interpreted as the effect of reinforcement type on slab deflections. Also, the previous Dynaflect data, which was gathered in 1983, was analyzed and compared with the current FWD data. According to a report from Center for Transportation Research (**Bagate et al. 1985**), five series of deflection testing were conducted on Loop 610 South in Houston: (1) May 11, 1983 before overlay, (2) September 8, 1983 first survey immediately after overlay, (3) February 15–16, 1984 second survey after overlay, (4) November 7–8, 1984 third survey after overlay, and (5) May 7–8, 1985 fourth and final survey after overlay. **Figure 3.40** shows the comparison between Dynaflect conducted immediately after overlay in 1983 September and FWD testing conducted in 2016. The deflections were normalized at 1,000 lbs loading. Detailed comparisons with mechanistic implications will be discussed in Chapter 4.

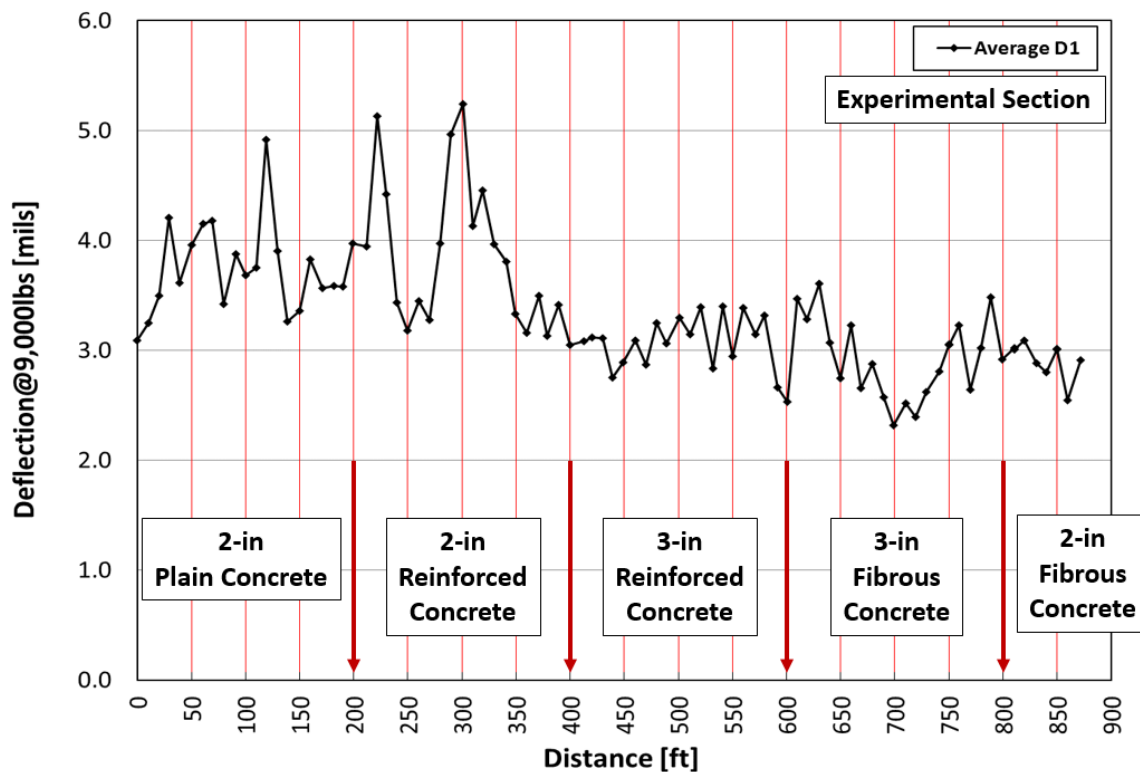


Figure 3.39 Testing location on Loop 610 South in Houston

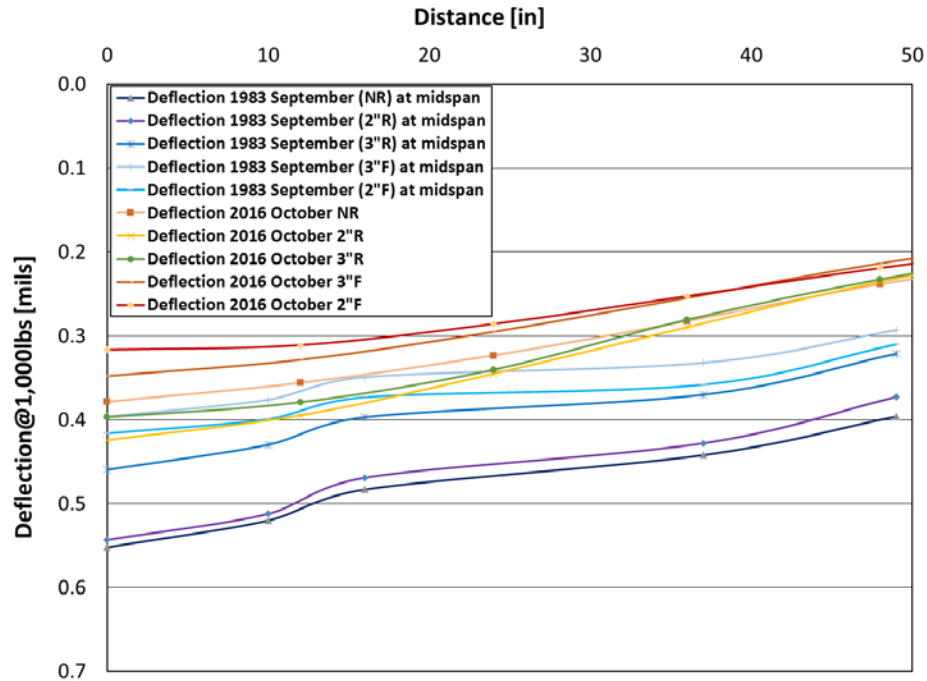


Figure 3.40 Comparison for deflection between Dynaflect (1983) and FWD (2016)

Effort was made to identify a correlation between the deflections from Dynaflect and FWD. However, only few reports available about this correlation. [Figure 3.41](#) shows the comparison of the deflections between Dynaflect and FWD at the same locations on 8-in. CRCP on IH 10 ([Eagleson et al. 1982](#)). A reasonable correlation is observed between Dynaflect and FWD deflections, even though some discrepancies are observed. For example, the deflection at station number 231.00 for Dynaflect testing is lower than that for FWD testing, but at the station number 233.00 it is the other way around.

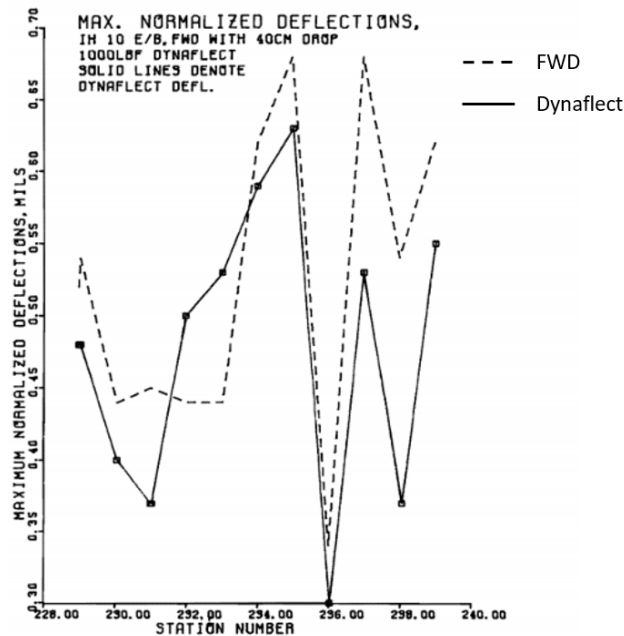


Figure 3.41 Maximum normalized deflection vs. station number (Eagleson et al. 1982)

3.2.4.4 Bond Strength Testing

In all, 33 bond strength tests were conducted. Among those, disk failures occurred at four locations due to poor surface treatment, and coring issues prevented bond testing at two locations. The results are shown in [Table 3.11](#). It is observed that the bond strength at this location is much higher than the values observed at the US-281 BCO site in Wichita Falls. Recall that this section was under heavy traffic for more than 30 years. Detailed analysis of the testing results, along with technical implications on TxDOT implementations, will be presented in Chapter 4.

Table 3.11 Bond strength testing results for Loop 610 South site

| No. | Date | TxDOT District | County | Highway | Core # | FWD DMI [ft] | Bond Strength [psi] | Deflection @ 9000 lbs [mils] | Failure Mode |
|-----|------------|----------------|--------|---------|--------|--------------|---------------------|------------------------------|---------------------------|
| 1 | 10/27/2016 | Houston | Harris | SL 610 | B1 | - | 475 | - | OF |
| 2 | | | | | B2 | - | 303 | - | DF |
| 3 | | | | | B3 | - | 605 | 3.56 | EF |
| 4 | | | | | B4 | - | 149 | 3.78 | OF |
| 5 | | | | | B5 | - | 216 | 3.94 | EF |
| 6 | | | | | B6 | - | 573 | 5.16 | OF |
| 7 | | | | | B7 | - | 591 | 4.02 | DF |
| 8 | | | | | B8 | - | 493 | 3.32 | OF |
| 9 | | | | | B9 | - | 589 | 3.76 | EF |
| 10 | | | | | B10 | - | 266 | 3.34 | EF |
| 11 | | | | | B11 | - | - | - | Coring |
| 12 | | | | | B12 | - | - | - | Coring (Pull out by hand) |
| 13 | | | | | B13 | - | 90 | - | DF |
| 14 | | | | | B14 | 378.8 | 553 | 3.23 | DF |
| 15 | | | | | B15 | 399.9 | 364 | 3.13 | EF |
| 16 | | | | | B16 | 420.2 | 264 | 3.25 | OF |
| 17 | | | | | B17 | 439.1 | 575 | 3.76 | EF |
| 18 | | | | | B18 | 459.8 | 470 | 3.16 | EF |
| 19 | | | | | B19 | 480.1 | 344 | 3.31 | EF |
| 20 | | | | | B20 | 500.8 | 332 | 3.24 | OF |
| 21 | | | | | B21 | 521 | 167 | 3.41 | EF |
| 22 | | | | | B22 | 570.6 | 506 | 3.19 | OF |
| 23 | | | | | B23 | 592.1 | 216 | 2.61 | OF |
| 24 | | | | | B24 | 610 | 122 | 3.51 | EF |
| 25 | | | | | B25 | 630.1 | 238 | 3.69 | EF |
| 26 | | | | | B26 | 669.3 | 186 | 2.76 | OF |
| 27 | | | | | B27 | 689.5 | 429 | 2.62 | EF |
| 28 | | | | | B28 | 710.2 | 243 | 2.43 | OF |
| 29 | | | | | B29 | 749.9 | 169 | 3.09 | EF |
| 30 | | | | | B30 | 769.7 | 284 | 2.70 | EF |
| 31 | | | | | B31 | 789.1 | 449 | 3.53 | EF |
| 32 | | | | | B32 | 810.6 | 422 | 3.02 | OF |
| 33 | | | | | B33 | 830.9 | 332 | 2.78 | OF |

Figure 3.42 summarizes the bond strength information in each experimental section. A possible correlation between bond strength and deflections on BCO was investigated and its results are shown in Figure 3.43. There is no clear trend, which implies that, as long as bond strength is sufficient to prevent debonding, slab deflections are dependent on other factors, such as slab support and/or thicknesses of the layers.

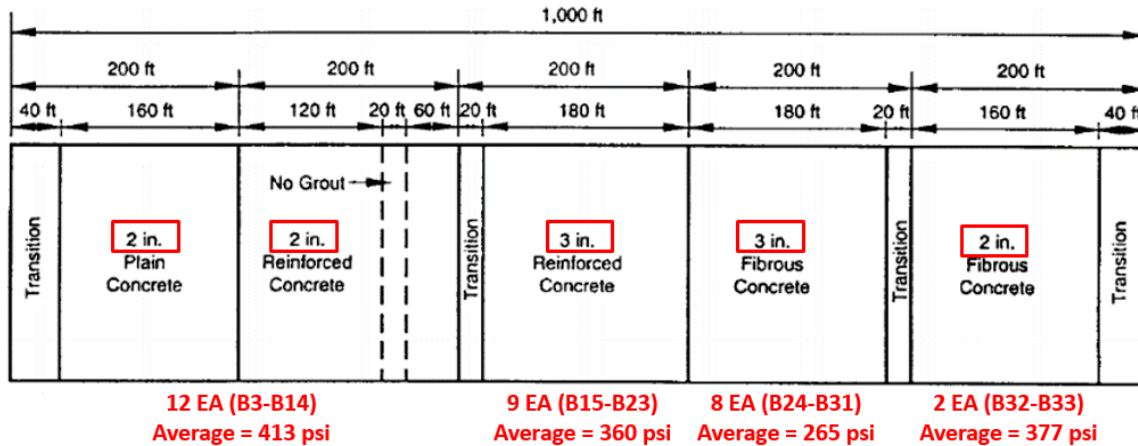


Figure 3.42 Average bond strength in each experimental section

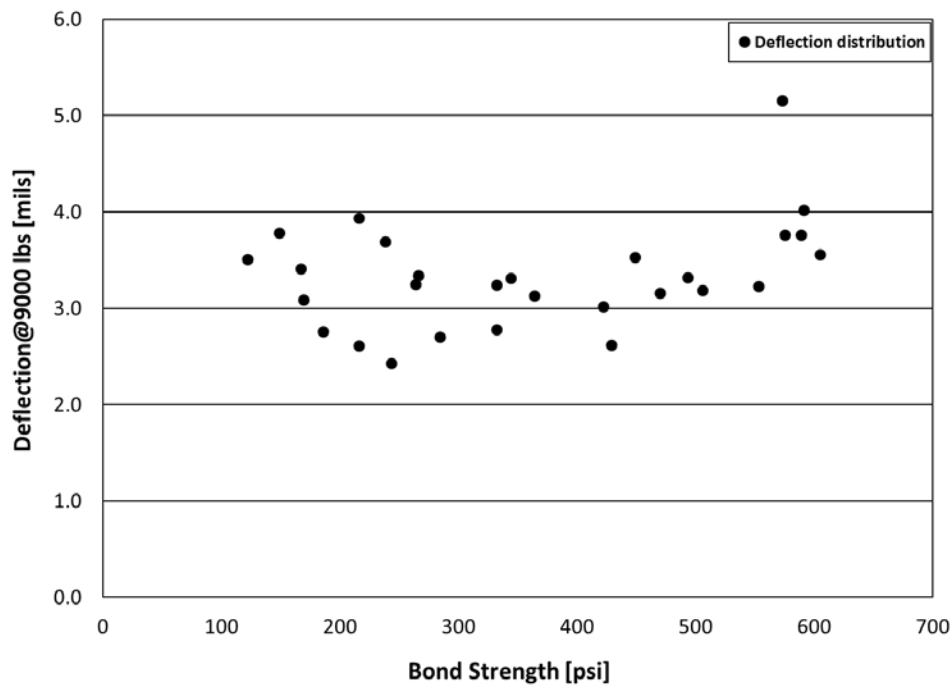


Figure 3.43 Comparison with bond strength and deflection

3.2.4.5 Pavement Score Evaluation

The pavement score history was investigated, including distress, condition, and ride score, as shown in [Figure 3.44](#). The distress and ride scores went down abruptly at 2004 and 2005, and then went up after 2010, only to go down again in 2011. This trend can be explained by the way TxDOT PMIS calculates distress and condition scores. In the TxDOT PMIS rating system, concrete patches reduce the distress and condition scores. [Table 3.12](#) shows the information on concrete patches from 2013 to 2015. The number of concrete patches went up from 1 in 2013 to 9 in 2014, which resulted in a substantial decrease in distress and condition scores. From 2014 to 2015, the number

of patches went down from 9 to 2, and both the distress and condition scores went up.

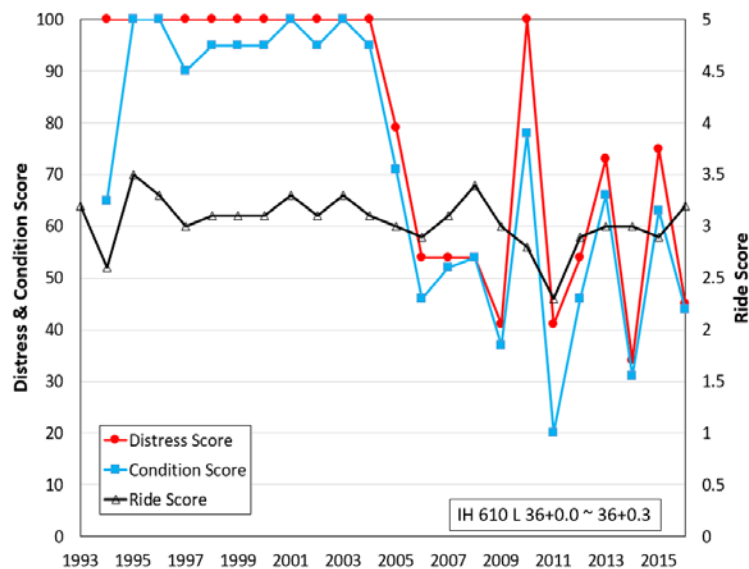


Figure 3.44 Pavement score history on Loop 610 South site

Table 3.12 Distresses and pavement score history (Loop 610 South L 36+0.0 ~ 36+0.3)

| | 2013 PMIS | 2014 PMIS | 2015 PMIS |
|-----------------------------|-----------|-----------|-----------|
| CRCP_PCC_PATCHES_QTY | 1 | 9 | 2 |
| Distress Score | 73 | 34 | 75 |
| Condition Score | 66 | 31 | 63 |
| Ride Score | 3 | 3 | 2.9 |

3.2.4.6 Summary

FWD and bond strength testing were conducted on Loop 610 South in Houston (CRCP BCO on CRCP). Since extensive testing was conducted prior to, during, and after BCO—and available documentation describes prior work and the values obtained for various testing efforts—this location represents one of the most valuable BCO sites. Detailed data analysis will be presented in Chapter 4.

3.3 UBCO Evaluations

3.3.1 IH 35 Denton

3.3.1.1 Pavement Information

A section of IH 35, from reference marker 475+0.69 to 475+0.80, was selected as a test location. The 10-in. existing CPCD was built in 1960 and the 11-in. CPCD BCO was placed on the top of the existing CPCD in 1987, with a 2-in. asphalt level up course in between. This CPCD UBCO

section has provided good performance for the last 30 years with almost no distresses. The details about pavement and location attributes are shown in Table 3.13. A typical section and testing location are depicted in Figures 3.45 and 3.46, respectively.

Table 3.13 Pavement information for IH 35 Denton site

| Attribute | Information | Special Note |
|------------------------------|--|--------------------|
| CSJ | 0195-02-035 (UBCO) | 0195-02-016 (CPCD) |
| County | Denton | - |
| TxDOT District | Dallas | - |
| Reference Marker | 475+0.69 – 475+0.80 (0.1 miles) | - |
| GPS Coordinates | 33.324297, -97.180361 ~ 33.325947, -97.180461 | - |
| Construction Year (existing) | 1960 | - |
| Construction Year (UBCO) | 1987 | - |
| Pavement Type | CPCD UBCO over CPCD | - |
| Slab Thickness | 11-in. CPCD UBCO + 10-in. CPCD | 2-in. ACP Level Up |
| Shoulder Type | - | - |
| Base Type | 6-in. Roadbed Treatment (TY-B) | - |
| Subgrade Type | Tied-Concrete Shoulder | - |
| Drainage Type | Open Ditch | - |
| Coarse Aggregate Type | - | - |
| Con. Pavement Details | - | - |

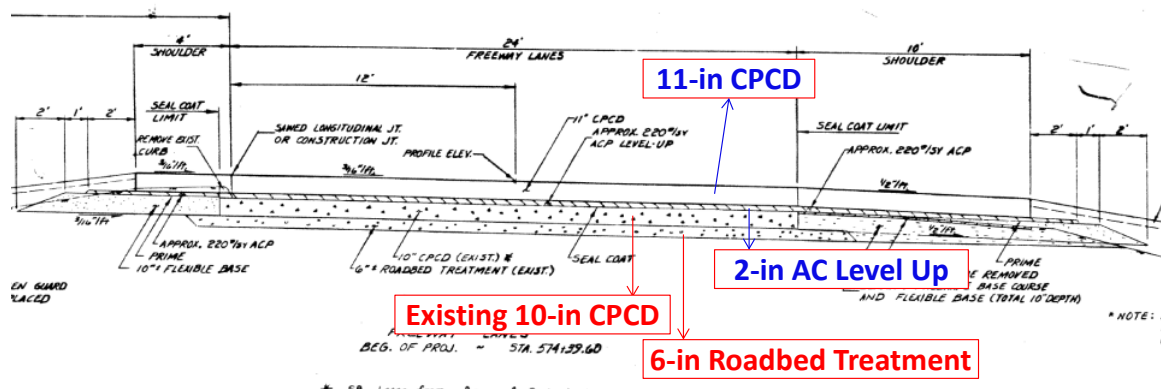


Figure 3.45 Typical section on IH 35 in Denton

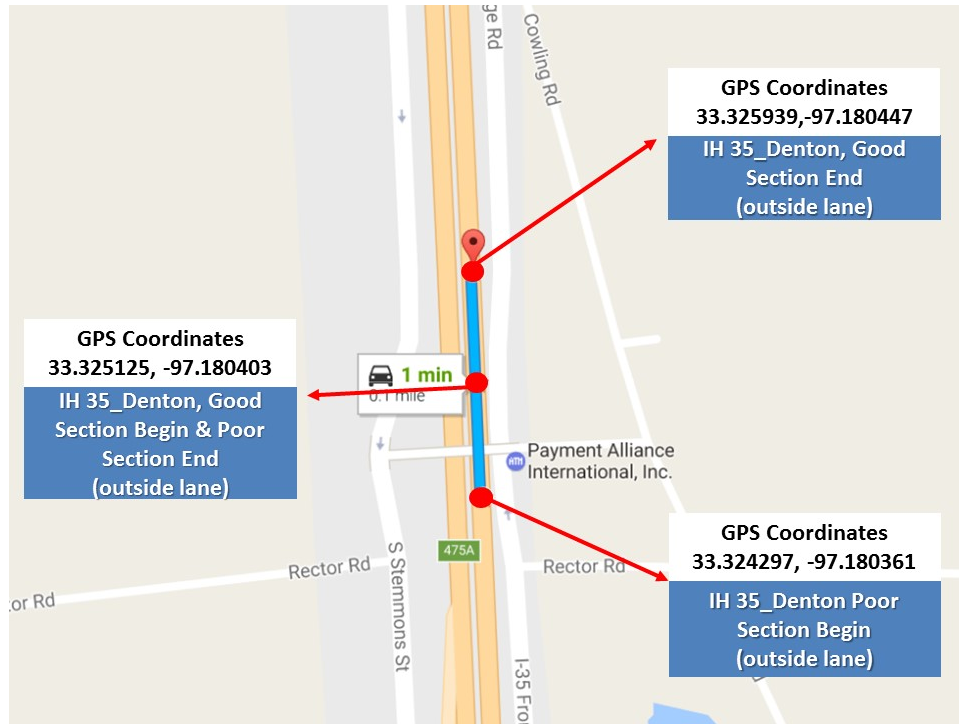


Figure 3.46 Testing locations on IH 35 NB

3.3.1.2 Visual Survey

A visual survey was conducted on February 26, 2016, to select locations for field testing and evaluation. Based on the pavement condition, two sections were selected: one section with distresses (poor section) and the other without distresses (good section), as shown in **Figure 3.47**. The only distress type observed in this UBCO project was an asphalt patch under the wheel path at transverse contraction joints, as shown in **Figure 3.47-(a)**.

The performance of this UBCO section was monitored under the TxDOT research project 0-6274 (rigid pavement database), and the condition of this distress was evaluated on March 23, 2012. **Figures 3.48-(a) and (b)** illustrate the comparisons of the distresses at the same joint. They show a minute progress in the distress over a 4-year timeframe, and additional asphalt patching material was placed.

To evaluate the condition of this pavement, field testing was conducted using FWD and DCP.



a. Poor section



b. Good section

Figure 3.47 Pavement condition of poor and good sections



a. Picture taken on March 23, 2012



b. Picture taken on February 26, 2016

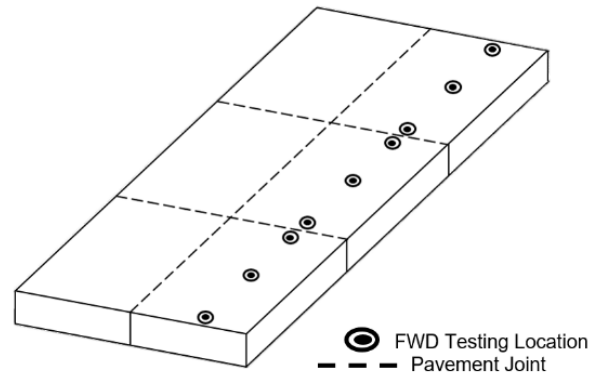
Figure 3.48 Distress comparisons between March 2012 and February 2016

3.3.1.3 FWD testing

FWD testing was conducted on March 24, 2016, as shown in [Figure 3.49-\(a\)](#). In order to compare the deflections between the mid-slab and transverse contraction joint, FWD testing was conducted at three different locations for each slab: at the upstream, mid-slab, and downstream of the slab, as depicted in [Figure 3.49-\(b\)](#). Load transfer efficiency (LTE) was also estimated at each transverse contraction joint by a ratio of d_u to d_l , as shown in [Figure 3.50](#). The mid-slab deflection was compared with deflections at the joint.



a. FWD testing on IH 35



b. FWD drop locations

Figure 3.49 FWD testing on IH 35 in Denton

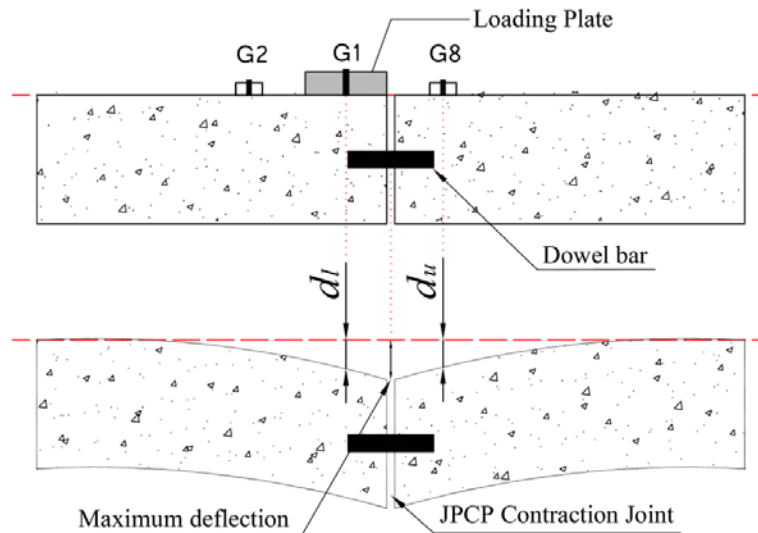


Figure 3.50 LTE calculation at transverse contraction joint

Figures 3.51-(a) and (b) illustrate deflection comparisons at transverse contraction joints and at mid-slab for the poor and the good sections. It is observed that the overall deflections are quite small, indicating that the structural capacity of this UBCO system is quite adequate. It is also observed that the mid-slab deflections were a little lower than those at the joints in the poor section, as shown in Figure 3.51-(a). The average deflections at the joint and mid-slab were 0.91 and 0.85, respectively. On the other hand, in the good section, there was no significant difference in deflections at joint and mid-slab. The average deflections at joint and mid-slab were 0.78 and 0.76, respectively. Also, the average deflection at the good section was slightly lower than that at the poor section. These results illustrate that joint behavior at the poor section was a little more active compared that in the good section. However, it should be recognized that the criterion used for the

selection of “good” and “poor” sections was asphalt patching, as shown in [Figure 3.48](#). It is not clear whether the increased deflections at joints in the poor section caused those distresses. It might have. However, there are CPCD sections in Texas with deflections at transverse contraction joints greater than the values obtained in the poor section, but with no distresses observed. Accordingly, it can be postulated that these distresses could have been due to materials/construction quality issues. [Figure 3.52](#) compares the LTE between the poor section and good sections; no significant difference was identified between the two sections. It is also observed that LTE values remained quite high after almost 30 years under heavy traffic.

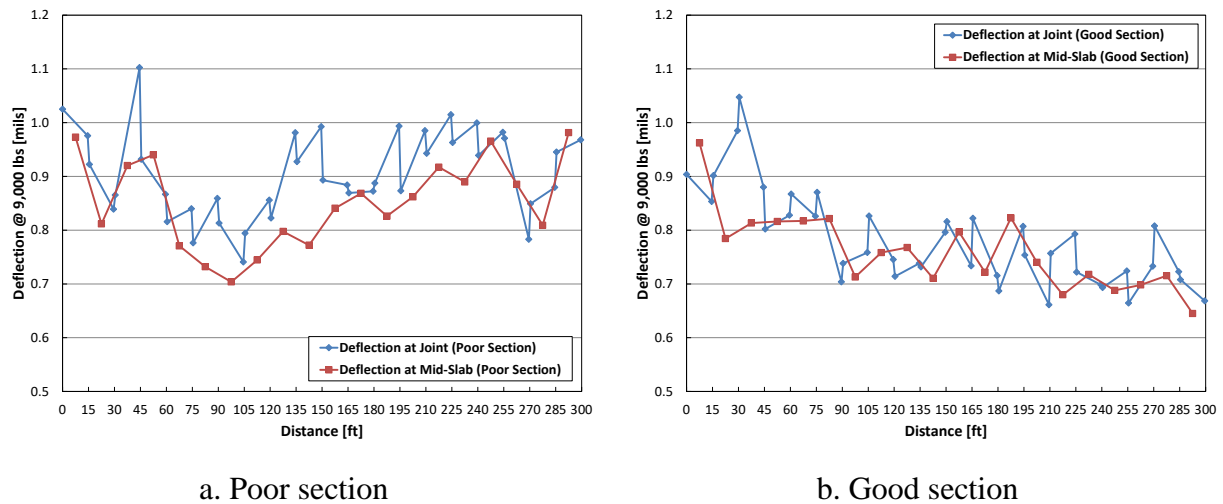


Figure 3.51 Deflection comparison between joint and mid-slab on IH 35 in Denton County

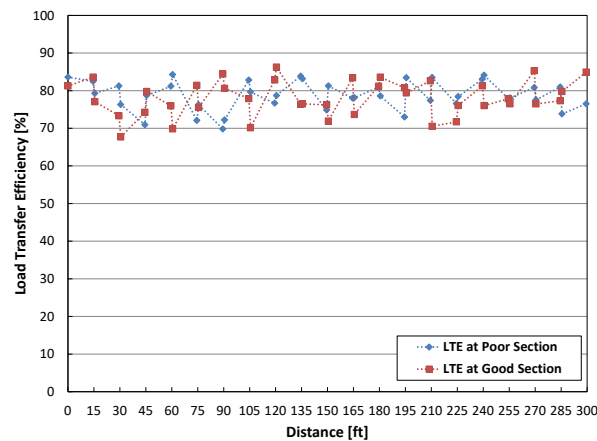


Figure 3.52 LTE comparison between poor section and good section on IH 35 in Denton County

3.3.1.4 DCP Testing

DCP testing was conducted at good and poor sections to compare base support characteristics. [Figure 3.53-\(a\)](#) shows DCP testing operation near the distress at this location. [Figure 3.53-\(b\)](#)

presents DCP testing results. The testing was conducted up to 27-in. and 29-in. depths from the pavement surface, which is 4-in. or 6-in. underneath the existing 10-in. CPCD slab, respectively. As shown in the testing results, the condition of subgrade was quite poor, while the pavement provided good structural performance in terms of low deflections. Satisfactory structural performance of this pavement system in the presence of poor support conditions should not be interpreted as an indication that poor support condition is acceptable. Rather, the good structural capacity of this pavement system is thanks to the 23-in. pavement system (11-in. concrete, 2-in. AC layer, and 10-in. concrete slab). A very thick slab system could overcome the deficiencies in the slab support, even though the system will cost much more to build.

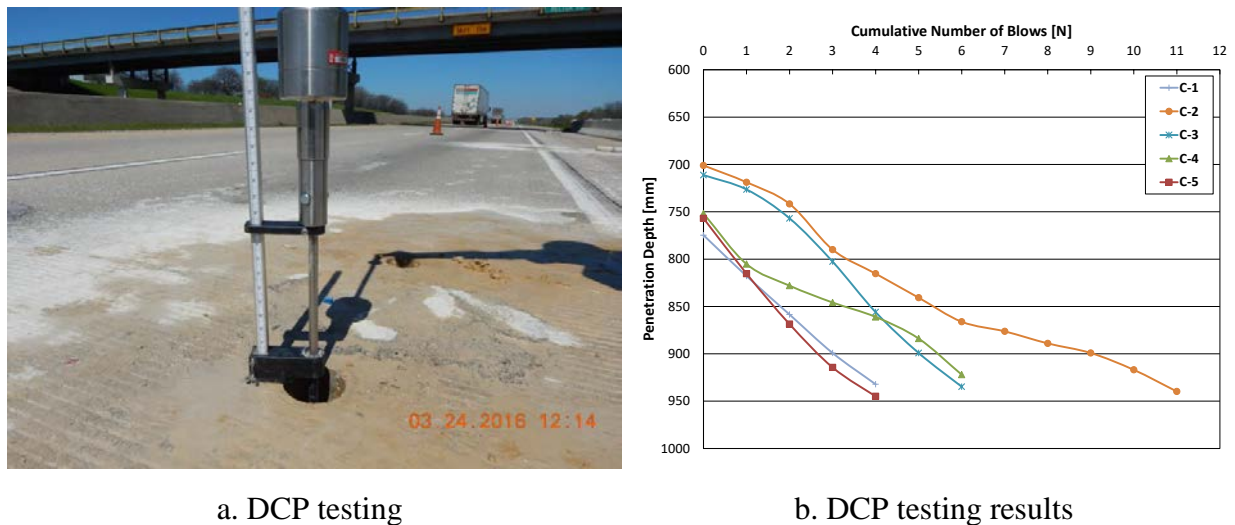


Figure 3.53 DCP testing on IH 35 in Denton County

Table 3.14 DCP testing results

| Coring | Reference Marker | Thickness [in.] | | | Testing Depth [in.] | mm/blow | CBR | Modulus [ksi] |
|--------|------------------|-----------------|-----|---------------|---------------------|---------|------|---------------|
| | | UBCO | AC | Existing CPCD | | | | |
| C-1 | 475B+0.27 | 10.0 | 2.0 | 11.0 | 30.5 | 39.62 | 4.74 | 6.9 |
| C-2 | 475B+0.27 | 10.0 | 2.0 | 11.0 | 27.6 | 21.73 | 9.29 | 10.6 |
| C-3 | 475B+0.28 | 10.0 | 2.0 | 11.0 | 28.0 | 39.82 | 4.71 | 6.9 |
| C-4 | 475B+0.28 | 10.5 | 2.0 | 11.0 | 29.6 | 25.04 | 7.92 | 9.6 |
| C-5 | 475B+0.29 | 10.8 | 2.0 | 11.0 | 29.8 | 47.50 | 3.87 | 6.1 |

3.3.1.5 Concrete Coring

Locations for coring were selected after the MIRA testing. Five cores were taken at distressed areas. **Figure 3.54** shows the coring operation. The CPCD overlay thicknesses, AC level-up layer,

and existing CPCD were in compliance with the design thicknesses. **Figure 3.55** illustrates coring locations for C-3, C-4, and C-5 for in-depth evaluation of distress at the transverse contraction joint. While coring operation was underway, it was observed that for all five cores, the AC interlayers came out in a fully-bonded condition to the overlaid CPCD; this is illustrated in **Figures 3.56 and 3.57**. The quality of asphalt material was quite solid without deterioration. This finding implies that the UBCO system behaves as a partially-bonded condition rather than a fully-unbonded condition, and should be considered for the UBCO thickness design.

Figure 3.57-(a) illustrates the MIRA testing result at Location C-4 (see **Figure 3.55**), showing a delamination at 3.5-in. depth from the pavement surface. The core taken at this location clearly shows that there is delamination at 3.5-in. depth as shown in **Figure 3.57-(b)**. It appears that delamination occurred first at transverse contraction joints and repeated wheel loading applications resulted in the distress observed. At this point, the exact mechanism of initial delamination at the joints is not known. On the other hand, at the same joint with distresses under wheel path, delamination was not detected by MIRA between wheel paths, which contravenes the assumption of delamination first, followed by the distress. Further investigations will be needed to accurately identify the mechanisms of the distress observed at this location.



Figure 3.54 Coring operation on IH 35 in Denton County

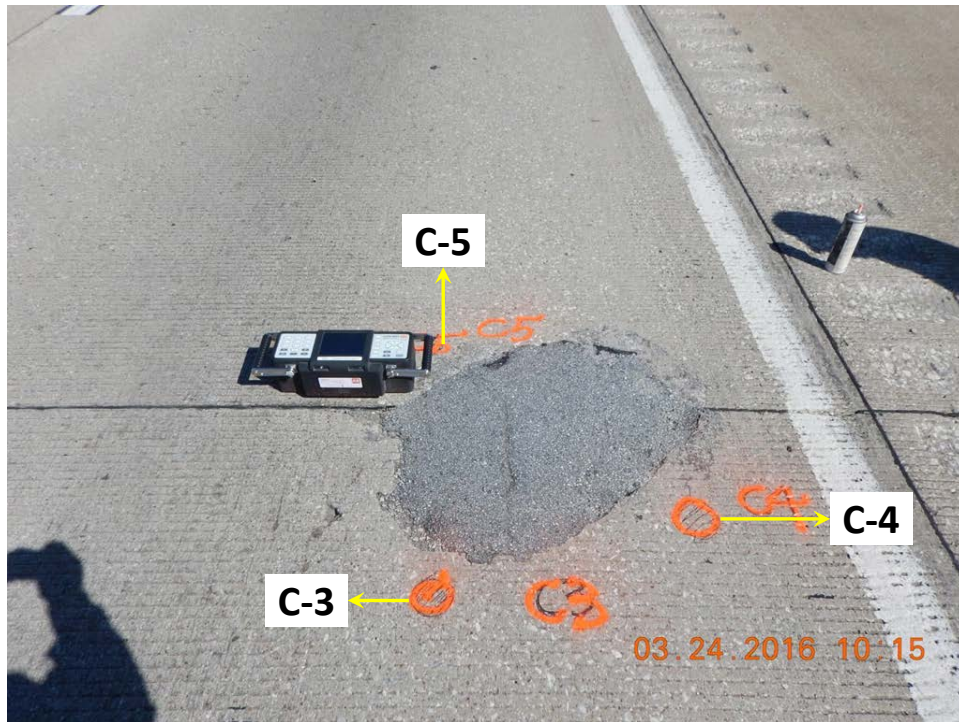
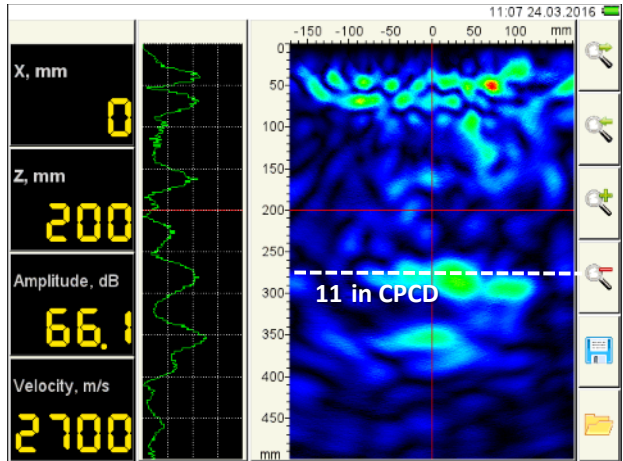


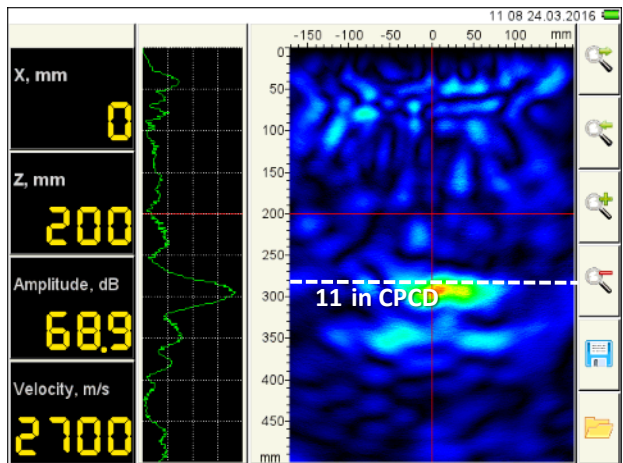
Figure 3.55 Coring locations for C-3, C-4, and C-5 around joint distress



a. MIRA image at C-1



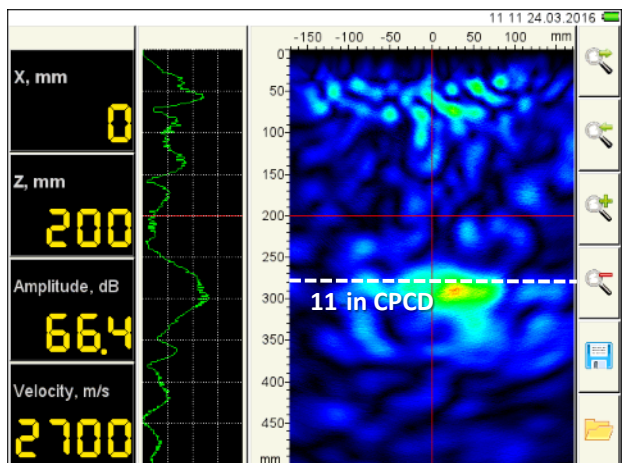
b. C-1 core (1.0 mil@9,000 lbs)



c. MIRA image at C-2



d. C-2 core (0.9 mils@9,000 lbs)

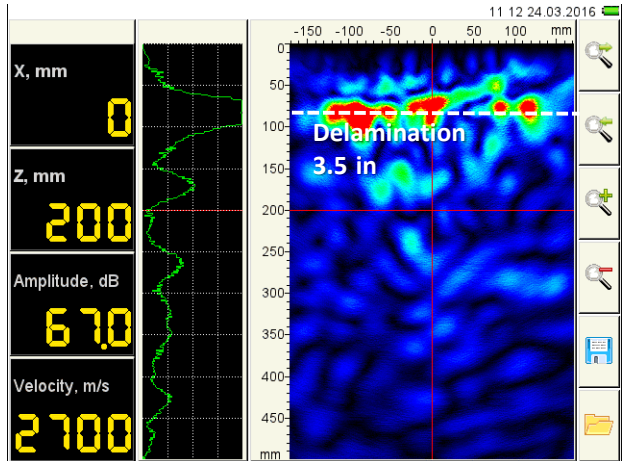


e. MIRA image at C-3



f. C-3 core (1.1 mils@9,000 lbs)

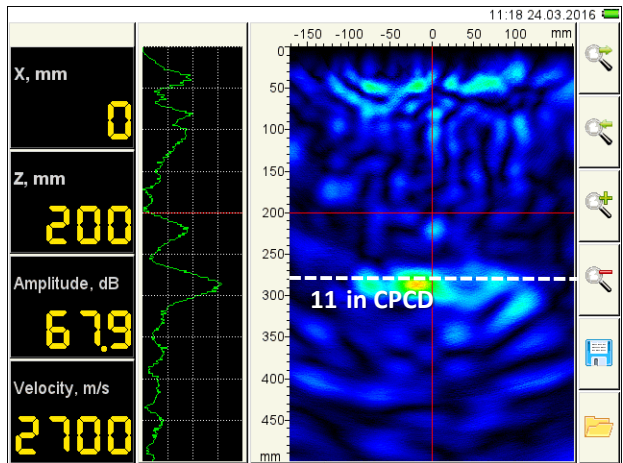
Figure 3.56 MIRA testing result and core condition of C-1, C-2, and C-3



a. MIRA image at C-4



b. C-4 core (0.9 mils@9,000 lbs)



c. MIRA image at C-5



d. C-5 core (0.9 mils@9,000 lbs)

Figure 3.57 MIRA testing result and core condition of C-4 and C-5

3.3.1.6 Concrete Material Properties

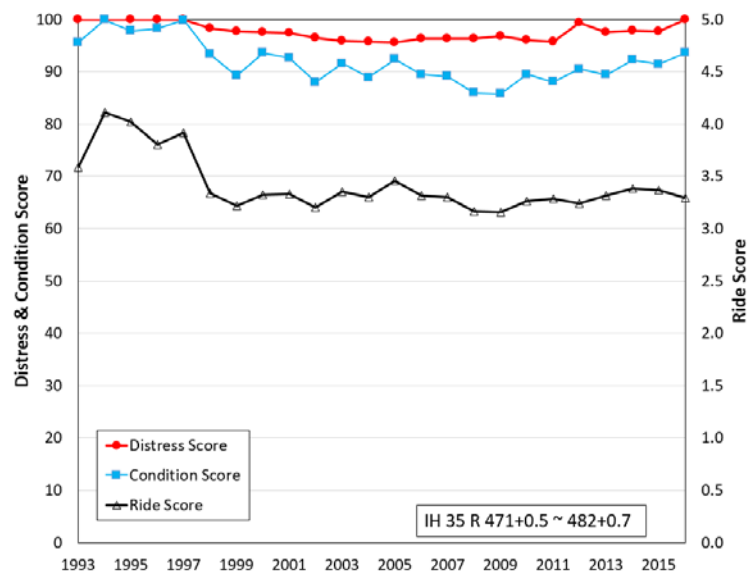
Concrete specimens obtained from the coring were evaluated for elastic modulus and CoTE. The testing results are presented in [Table 3.15](#). The elastic modulus of concrete overlay was about 5.1×10^6 psi, and that for the existing concrete was 4.8×10^6 psi. The CoTE values of the overlay concrete and existing concrete were small, at $3.5 \times 10^{-6}/^{\circ}\text{F}$, and $3.2 \times 10^{-6}/^{\circ}\text{F}$, respectively.

Table 3.15 Laboratory testing results

| TxDOT District | Highway | Specimen Name | Reference Marker | Elastic Modulus ×106 [psi] | | CoTE [×10 ⁻⁶ /°F] | |
|----------------|----------|---------------|------------------|-------------------------------|----------|---------------------------------|----------|
| | | | | Overlay | Existing | Overlay | Existing |
| Dallas | IH 35 NB | C1 | 475+0.69 | 5.0 | 4.5 | 3.4 | - |
| | | C2 | 475+0.69 | 4.9 | 5.3 | 3.6 | - |
| | | C3 | 475+0.70 | 5.4 | - | - | 3.2 |

3.3.1.7 Pavement Score Evaluation

Figure 3.58 shows the pavement score history at this location. The distress and condition scores were greater than 90 in 2016, which means that the pavement condition can be classified as “very good,” but the 2016 ride score was 3.3, which indicates that the pavement condition is classified as “good.” During the pavement survey in the tested overlay section, a few asphalt patches were observed under the wheel path at the transverse contraction joint; otherwise there were no other distresses.

**Figure 3.58 Pavement score history on IH 35**

3.3.1.8 Summary

Field evaluation was conducted to collect the information on UBCO section on IH 35 in Denton County, in TxDOT’s Dallas District. The findings from the field evaluations are summarized as follows:

- 1) The overall pavement condition was quite good, but distresses were observed at transverse contraction joints under the wheel paths. Delamination at the depth of about

3.5-in. was observed near distresses. At this point, the correct mechanism of the distresses observed in this section is not known.

- 2) According to the deflection data from FWD testing, there is no significant difference between the poor section and the good section as defined by the presence of distresses at transverse contraction joints, which means the structure capacities in two sections are quite similar.
- 3) Although slab support condition is poor, the pavement performance has been quite satisfactory. However, satisfactory structural performance of this pavement system despite the poor support condition should not be interpreted to be that a poor support condition is acceptable. Rather, the good structural capacity of this pavement system is thanks to the total 23-in. pavement system (11-in. concrete, 2-in. asphalt mixture, and 10-in. concrete slab).
- 4) AC materials in the interlayers came out fully bonded to the overlaid CPCD during the concrete coring operation, which might indicate that this UBCO behaves as partially-bonded rather than fully-unbonded as assumed in the UBCO design.

3.3.2 IH 35E Waxahachie (CPCD UBCO over CPCD)

3.3.2.1 Pavement Information

This section on IH 35E in Ellis County (in TxDOT's Dallas District) consists of 10-in. CPCD UBCO with 1.6-in. AC level-up on 10-in. CPCD. The original 10-in. CPCD was completed in November 1959, and the 10-in. CPCD UBCO was placed in October 1990. The performance of this pavement has been excellent, with almost no distresses.

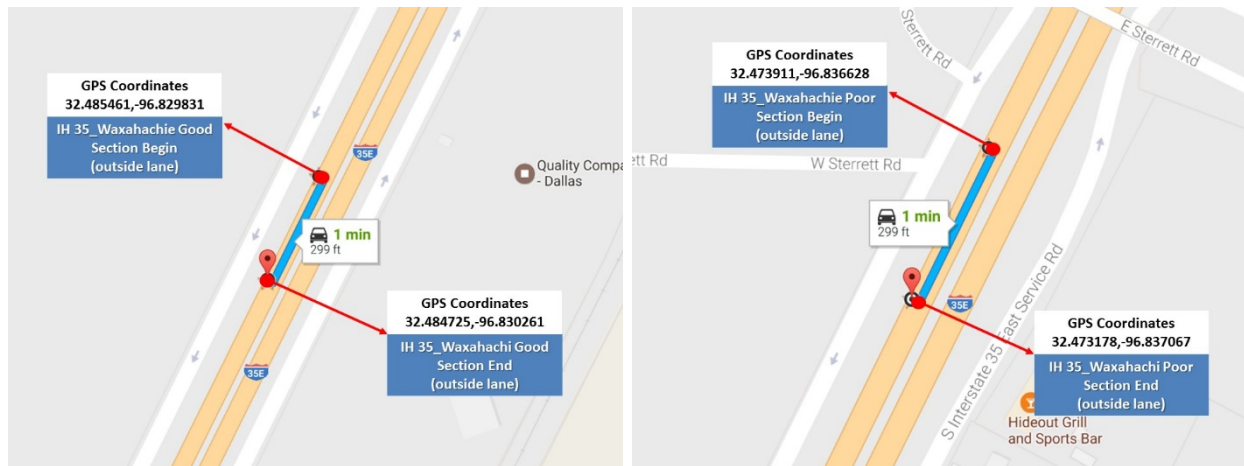
Part of this section was included in the Long-Term Pavement Performance (LTPP) program that was initiated in 1989. **Table 3.16** delineates the types of information collected under the LTPP program. **Table 3.17** summarizes the pavement and location attributes. **Figure 3.59** shows the locations of the pavement evaluated in this research study, which is from reference marker 406+0.60 to 406+0.70.

Table 3.16 Pavement structure on IH 35E from LTPP database

| LTPP Section M&R History | | | | Layer Information | | | |
|--------------------------|---|---------------------|--|-------------------|--------------------------------|-----------------|---|
| Experiment Number | Construction Number (CN) and Max Later Number | CN Event (M&R Date) | CN Event (Code and Description) | Layer Number | Layer Type | Thickness [in.] | Material Code Description |
| GPS-9 | CN1 (Layer Max=5) | Sep-1989 | Date test section initially accepted for study into LTPP program | 1 | Subgrade (untreated) | 67 | 107-Fine-Grained Soils: Clay with Sand |
| | | | | 2 | Unbonded (granular) base | 7.8 | 309-Fine-Grained Soils |
| | | | | 3 | Portland cement concrete layer | 9.9 | 4-Portland Cement Concrete (JPCP) |
| | | | | 4 | Asphalt concrete layer | 1.4 | 78-Dense Graded Asphalt Concrete Interlayer |
| | | | | 5 | Portland cement concrete layer | 10.3 | 4-Portland Cement Concrete (JPCP) |

Table 3.17 Pavement information for IH 35E site

| Attribute | Information | Special Note |
|------------------------------|--|---------------------|
| CSJ | 0067-06-034 | - |
| County | Ellis | - |
| TxDOT District | Dallas | - |
| Reference Marker | 407+0.5 – 406+0.7 (0.1 miles) | - |
| GPS Coordinates | 33.485486, -96.829769 ~ 32.472033, -96.837739 | - |
| Construction Year (existing) | 1960 | - |
| Construction Year (UBCO) | Oct 1990 | - |
| Pavement Type | CPCD UBCO | - |
| Slab Thickness | 10-in. CPCD UBCO + 1.6-in. AC Level Up + 10-in. CPCD | 1.6-in. AC Level Up |
| Shoulder Type | Tied-Concrete Shoulder | - |
| Base Type | 7.8-in. Unbonded Granular Base | - |
| Subgrade Type | Untreated | - |
| Drainage Type | Open Ditch | - |
| Coarse Aggregate Type | - | - |
| Con. Pavement Details | - | - |



a. First section

b. Second section

Figure 3.59 Testing location in IH 35E in Ellis County

3.3.2.2 Visual Survey

Visual survey was conducted on February 27, 2016. Two sections (good and poor) were selected based on visual pavement condition evaluations. Even though the sections were divided into good and poor sections, distress level in the poor section was quite low. Field evaluations including FWD testing, MIRA testing, and DCP testing were conducted on March 29, 2016. Under a heavy traffic volume at this location, the overall pavement condition was quite satisfactory, with the exception of intermittently observed minor distresses at transverse contraction joints. **Figure 3.60** shows the pavement condition at good and poor sections. In the poor section, a distress resembling distresses in CRCP at TCJs is observed.



a. Good section



b. Distress at the good section



c. Poor section



d. Distress in poor section

Figure 3.60 Condition of the pavement

3.3.2.3 FWD Testing

FWD testing was conducted over 600-ft of pavement, with 300-ft for each section. The testing protocol was the same as at IH 35 in Denton County. The deflections measured at the joints were

used to estimate LTE.

Figure 3.61 shows the deflection comparison between the transverse contraction joint and mid-slab at each section. At both sections, the mid-slab deflections were a little lower than those at the joints, which is as expected. The average deflections at joint and mid-slab were 2.07 and 1.70 mils, respectively, in the good section. In the poor section, the average deflections at joint and mid-slab were 0.81 and 0.71 mils, respectively. The average deflection at the good section is larger than that at the poor section. It should be noted that the criteria for good and poor section selection was surface distress, which was not necessarily caused by structural deficiency. As will be discussed later, the larger deflections in the good section were due to the condition of AC interlayer. Coring and DCP testing were performed to determine the causes for the deflection differences between the two sections.

Figure 3.62 shows the LTE comparison between the good section and poor section, and the average LTE at the good and poor sections were 83% and 74%, respectively.

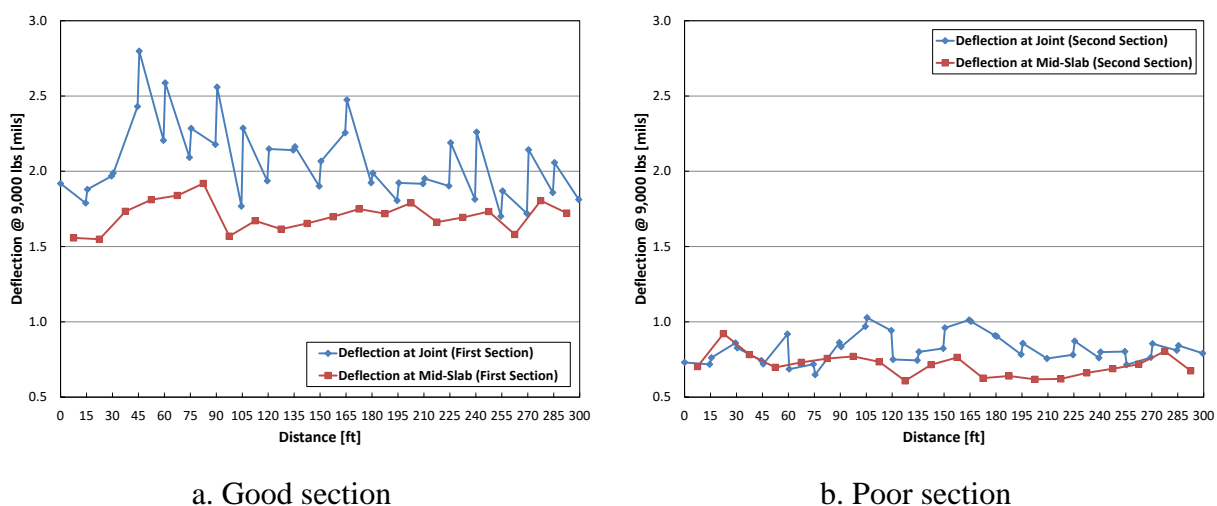


Figure 3.61 Deflection comparison between joint and mid-slab

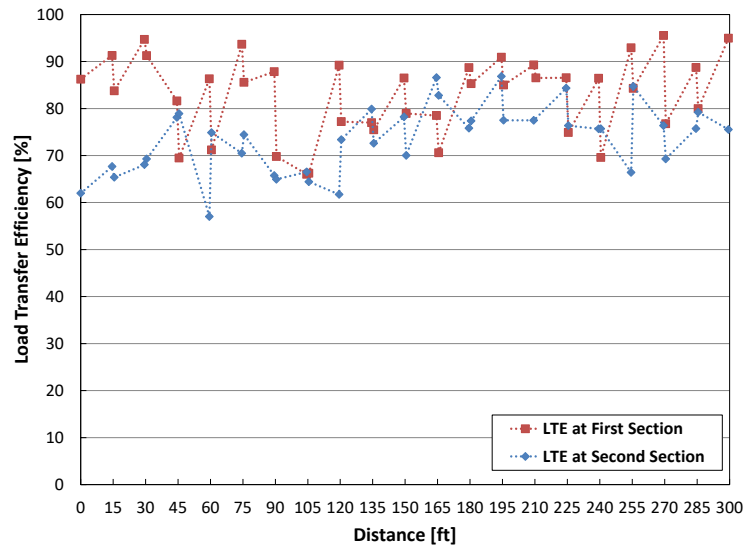


Figure 3.62 LTE comparison between good and poor sections

3.3.2.4 DCP Testing

DCP testing was performed at seven locations with three locations in the good section and four at the poor section.

Test results show that the modulus values of the layer under the old CPCD slab at the poor section are lower than those at the good section, as shown in [Figure 3.63](#). However, deflection results showed the poor section had smaller deflections than did the good section, which is somewhat contradictory to the expected result.

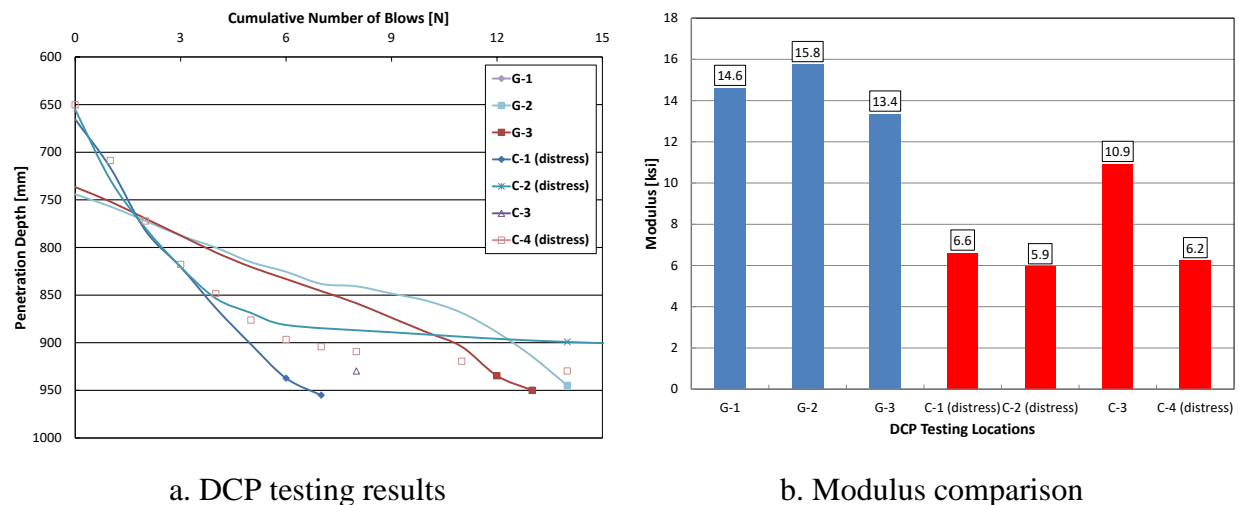


Figure 3.63 DCP testing results on IH 35E in Ellis County

3.3.2.5 Concrete Coring

Three cores were taken in the good section, and four cores in the poor section. [Figure 3.64](#)

illustrates the locations of coring. **Figure 3.65** shows the condition of the cores.

As shown in **Figures 3.65-(a) and (b)**, the asphalt interlayer was severely deteriorated, resulting in large deflections. In contrast, a small deflection was measured at the poor section because the asphalt interlayer was in good condition, as shown in **Figures 3.65-(c), (d), (e), and (f)**. Accordingly, it is determined that the main reason for the discrepancy between deflections and base modulus was the quality of the asphalt interlayer. In other words, larger deflections in the good section were due to deteriorated AC interlayer.

Figure 3.65-(d) shows the core taken directly on top of a crack at the outside wheel path of the outside lane, and illustrates that the transverse contraction joint in the overlaid CPCD was mismatched with the old CPCD joint along the crack. As shown in the picture, this distress also included delamination at 3.0-in. or 3.5-in. depth from the pavement surface. The distress here suggests that during UBCO construction of CPCD, matching new joint locations with those in old joints is important, unless joints are mismatched intentionally, which will be further discussed in the next chapter.



a. Coring location for G-1

b. Coring locations for G-2 and G-3



c. Coring location for C-1



d. Coring location for C-2



e. Coring locations for C-3 and C-4

Figure 3.64 Coring locations on IH 35E in Ellis County



a. G-1 core condition at the good section



b. G-3 core condition at the good section



c. C-1 core condition at the poor section



d. C-2 core condition at the poor section



e. C-3 core condition at the poor section



f. C-4 core condition at the poor section

Figure 3.65 Cores taken on IH 35E in Ellis County

3.3.2.6 Concrete Material Properties

Table 3.18 presents concrete material properties evaluated in this investigation. The elastic modulus and CoTE of overlaid concrete and the existing concrete were evaluated; the average elastic modulus of the overlay was 5.2×10^6 psi, and that for the existing concrete was 5.7×10^6 psi. In the concrete pavement research community, it has been a well-accepted concept that concrete modulus decreases over time due to repeated wheel applications. Various methods for the prediction of remaining life of concrete pavements have been proposed based on this idea that ‘wheel loading applications decrease concrete modulus due to fatigue damage.’ The information obtained here does not necessarily support that concept. Average CoTE values obtained were $2.7 \times 10^{-6}/^{\circ}\text{F}$ for overlaid concrete and $3.8 \times 10^{-6}/^{\circ}\text{F}$ for the existing concrete. The testing results and thickness information from the cores are summarized in **Table 3.18**.

Table 3.18 Laboratory testing

| TxDOT District | Highway | RM | Specimen Name | Thickness [in.] | | | Elastic Modulus [$\times 10^6$ psi] | | CoTE [$\times 10^{-6}/^{\circ}\text{F}$] | |
|----------------|-----------|----------|---------------|-----------------|---------------|---------------|--------------------------------------|----------|--|----------|
| | | | | Overlay | AC Interlayer | Existing CPCD | Overlay | Existing | Overlay | Existing |
| | | | | | | | | | | |
| Dallas | IH 35E SB | 407+0.58 | G1 | 10.0 | 1.5 | 10.0 | 4.7 | 6.0 | 2.7 | - |
| | | 407+0.57 | G2 | 10.0 | 1.5 | 10.5 | 5.2 | 5.6 | - | 3.8 |
| | | 407+0.57 | G3 | 9.8 | 1.5 | 9.3 | 5.2 | 5.9 | - | - |
| | | 406+0.71 | C1 | 10.0 | 1.5 | 9.0 | 5.2 | 5.6 | - | 3.9 |
| | | 406+0.72 | C2 | 10.0 | 1.5 | 9.5 | 5.2 | 5.6 | - | - |
| | | 406+0.69 | C3 | 10.0 | 1.5 | 9.5 | 5.3 | 5.4 | 2.7 | 3.6 |
| | | 406+0.69 | C4 | 10.0 | 1.5 | 10.0 | 5.4 | - | 2.6 | - |

3.3.2.7 Pavement Score Evaluation

Figure 3.66 shows the pavement score history, including condition, distress, and ride scores, for the UBCO section on IH 35E. Based on the TxDOT PMIS, the IH 35E UBCO section can be classified as in “very good” condition.

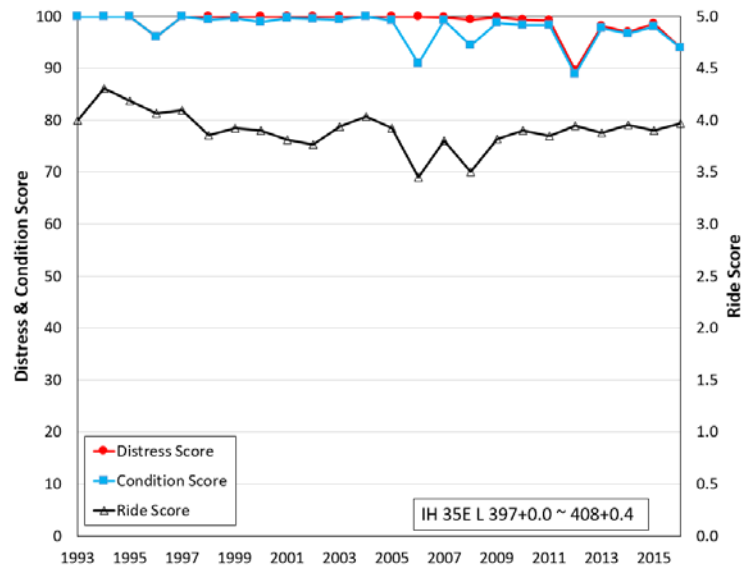


Figure 3.66 Pavement score history on IH 35E

3.3.2.8 Summary

Various testing was conducted to evaluate pavement condition in the CPCD UBCO system on IH 35E in Ellis County, within TxDOT’s Dallas District. The findings are summarized as follows:

- 1) The pavement performance in this section has been excellent, with few minor distresses observed.
- 2) Deflections in the section with better base modulus were larger than those in the section with lower base modulus. The reason for this discrepancy between slab support and deflections was the condition of asphalt interlayer. Even though no distresses have been developed in the section with deteriorated asphalt interlayer, in the long run, larger deflections could compromise the performance of UBCO. Construction specifications for UBCO should include the durability of the asphalt interlayer.
- 3) One distress observed in this section was due to slight mismatching of transverse contraction joints in UBCO and in the existing CPCD.

Chapter 4 Analysis of Field Testing Results

4.1 Introduction

Structural responses and performance of PCC overlay vary depending on the combinations of existing pavement condition and overlay systems, as well as traffic and environmental conditions, which makes the selection of an optimum overlay type and designs a challenge. Testing results discussed in Chapter 3 present a valuable data set that could be quite useful for the development of guidelines on PCC overlay type selection and design. Some of the information discussed in Chapter 3 is presented in this chapter to facilitate the discussion. Only three PCC overlay systems have been used in Texas: (1) BCO on CRCP, (2) CRCP BCO on CPCD, and (3) CPCD UBCO on CPCD. Accordingly, field testing and data analysis have been conducted on those three systems. For BCO on CRCP and CRCP BCO on CPCD, field testing was conducted in four projects: US 287 in Bowie (Wichita Falls District), US 281 in Wichita Falls (Wichita Falls District), US 75 in Sherman (Paris District), and Loop 610 South in Houston (Houston District). For CPCD UBCO on CPCD, field testing and data analysis were conducted on two projects: IH 35 in Denton and IH 35E in Waxahachie, both in the Dallas District. Details of these projects such as pavement structures and when they were built were discussed in the previous chapter.

4.2 BCO

In general, BCOs are applied to existing pavements that are in a relatively good condition. CRCP BCO is expected to have the greatest potential use in the future at TxDOT. As of 2016, CRCP constitutes more than 78% of the total PCC pavement lane miles in Texas, and the cost of BCO is usually lower than UBCO, primarily because BCO requires smaller slab thicknesses and does not involve the asphalt materials needed for UBCO. The study team analyzed data collected from field testing by visual survey or non-destructive testing (such as FWD, DCP, and MIRA), or via other testing methods, including bond strength testing and concrete material testing with cores. Some of this testing was conducted in previous studies. The analysis was aimed at identifying the following information:

- a) Minimum structural requirements of existing PCC pavement for BCOs
- b) Existing PCC pavement characteristics affecting BCO performance
- c) Minimum bond strength required for satisfactory BCO pavement performance
- d) Evaluation of conservatism in the current AASHTO UBCO design procedures
- e) Construction aspects of BCO and UBCO for better performance

4.2.1 BCO on CRCP

This section discusses the field-testing data obtained in Chapter 3 from US 287 in Bowie, US 281

in Wichita Falls, and Loop 610 South in Houston. As discussed earlier, these sections have been in service for 4 years to 33 years, which should provide valuable information on both short-term and long-term performance of BCOs on CRCP.

4.2.1.1 Modulus of Subgrade Reaction under Old CRCP Prior to Overlay

Findings from the TxDOT rigid pavement database project (0-6274) clearly indicate the importance of slab support on the performance of PCC pavement. It could be quite interesting to find out whether PCC pavements with poor slab support could be rehabilitated with bonded PCC overlay, as numerous PCC pavement projects in Texas used non-stabilized base with rather poor performance. In the US-287 project, FWD testing was conducted in December 2010 on 8-in. CRCP to evaluate slab support condition. The length of the evaluation was 1,000 ft, and the deflections are shown in [Figure 4.1](#). The dynamic modulus of subgrade reaction (k-value) was back-calculated with the Westergaard deflection equation to arrive at the interior loading condition:

$$k = \left(\frac{P}{8d_0l_k^2}\right)\left\{1 + \left(\frac{1}{2\pi}\right)\left[\ln\left(\frac{a}{2l_k}\right) - 0.673\right]\left(\frac{a}{l_k}\right)^2\right\} \quad (\text{Eqn. 4.1})$$

where,

k = dynamic modulus of subgrade reaction (k-value, psi/in.)

P = FWD loading (lbs)

d_0 = deflection under the loading plate (in.)

a = radius of loading plate (in.); 5.9-in.

l_k = radius of relative stiffness from AREA method (in.); $\left[\frac{\ln\left(\frac{36-AREA}{1812.279133}\right)}{-2.559340}\right]^{4.387009}$

$AREA = 6 \times \left[1 + 2 \times \left(\frac{d_1}{d_0}\right) + 2 \times \left(\frac{d_2}{d_0}\right) + \frac{d_3}{d_0}\right]$

d_i = in order of d_0 , d_1 , d_2 and d_3 ; deflection under the loading plate, deflections at 12-in., 24-in., and 36-in. from the center of the loading plate, respectively

The static modulus of subgrade reaction is generally obtained by dividing dynamic k-values by 2; in this case, the static modulus was derived from only 7 data points and the correlation between dynamic and static k-values was quite poor ([Darter et al. 1995](#)). In this chapter, back-calculated dynamic k-values are reported without the conversion to static k-values. The average dynamic k-value for 1000-ft section was 195 psi/in. If this value is converted to a static k-value, it would be less than 100 psi/in., which is quite small, especially considering 300 psi/in. is the default static k-value in PCC pavement designs at TxDOT. This indicates quite poor slab support condition at this location.

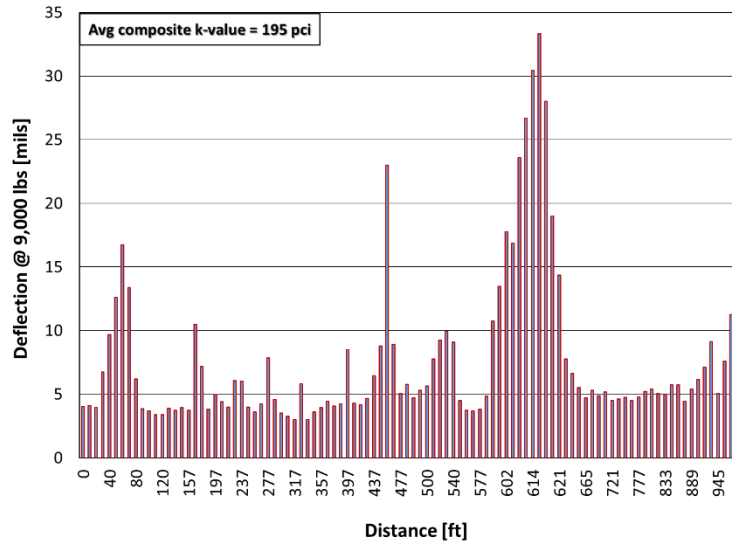


Figure 4.1 Deflection on old CRCP and average composite k-value prior to overlay (2010)

4.2.1.2 Comparison between Deflections in Existing Pavement and Distresses in BCO

On US 287 in Bowie, distresses appeared in existing CRCP at several locations, in the form of punchouts and half-moon-shaped longitudinal cracks. Also evident were transverse cracks with large crack widths and concrete chipping. FWD deflections in these locations were much higher than at other locations. It would be of great importance to identify whether these distresses with high deflections will reflect through to BCO and cause distresses in BCO. **Figure 4.2** shows typical distresses in the existing CRCP, and the FWD deflections near those distress locations are shown in **Figure 4.3**.



a. Chipping at transverse crack in old CRCP

b. FDR in old CRCP



c. Diagonal cracking in old CRCP

d. Severely distressed CRCP

Figure 4.2 Representative distresses on old CRCP

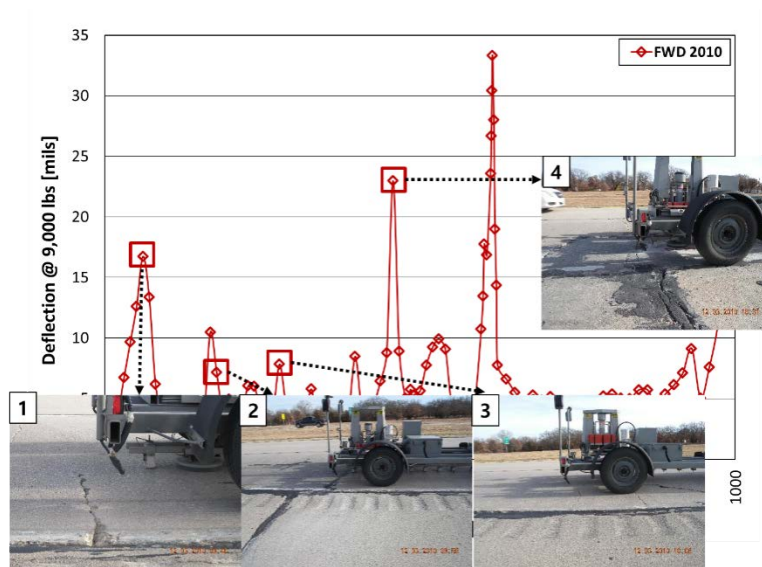


Figure 4.3 FWD deflection with distresses on old CRCP

There were distresses in BCO where deflections in the old CRCP were larger than 20 mils. It should be noted that, prior to BCO construction, severe distresses in the existing 8-in. CRCP in those areas were repaired with FDRs.

Since the locations of distresses in the existing CRCP prior to BCO construction were accurately recorded with GPS, it was feasible to determine whether those distresses reflected through BCO and caused distresses in BCO. **Figure 4.4** shows the relationship between distresses in BCO and deflections in the existing CRCP. Red squares indicate distresses in BCO in the form of slab segmentation caused by delamination, while green dots indicate a lack of distresses in BCO. It shows a rather good correlation between deflections in the existing CRCP and distresses in BCO. This implies that FDRs done prior to BCO failed to restore the structural capacity of the existing CRCP, primarily because the distresses in the existing CRCP were due to deficient slab support—and the FDRs did not restore slab support. Instead, FDRs just replaced fragmented concrete with new concrete.

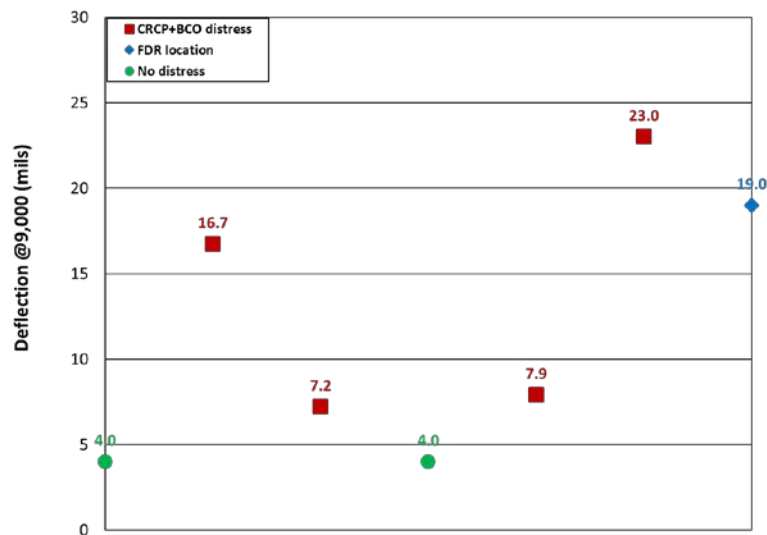


Figure 4.4 FWD deflection with distresses in old CRCP

Figure 4.5 shows comparisons between FWD deflections on existing CRCP measured in 2010 and distresses in BCO. It is interesting to note that the distresses in BCO are of similar shapes to those in the existing CRCP, even though some of these distresses were repaired prior to BCO placement.

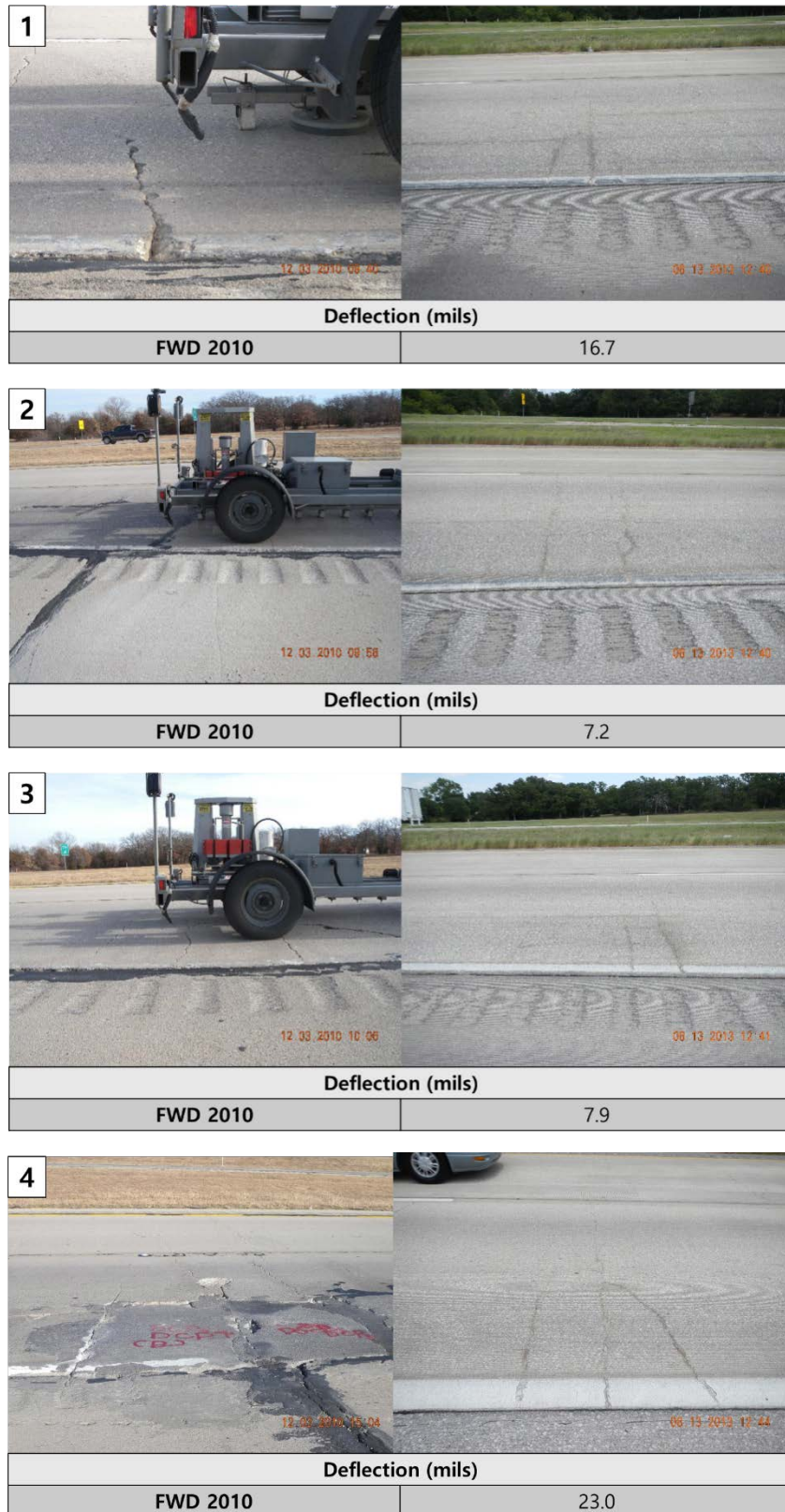


Figure 4.5 Distress comparison between old CRCP and BCO

4.2.1.3 Threshold Deflection Value in Existing CRCP for BCO

Since there is a decent correlation between deflections in the existing CRCP and BCO performance, even though the number of data points is quite limited, it would be possible to determine a threshold deflection value in the existing CRCP that could be used as a selection criterion for the feasibility of 4-in. BCO on 8-in. CRCP. From the information in Figure 4.4, a threshold value between 5 and 7 mils appears to be reasonable for 4-in. BCO on 8-in. CRCP. It is to be noted that this value is valid only for 4-in. BCO on 8-in. CRCP with comparable truck traffic. If a 5-in. BCO is to be placed, a larger threshold value could be selected. To develop more generalized threshold values for various BCO thicknesses and existing CRCP conditions, theoretical modeling and analysis need to be conducted. To develop a mechanistic-empirical (ME) BCO design procedure, which is one of the objectives of this research study, mechanistic analysis was conducted on various BCO on CRCP systems and the results are presented in Chapter 5.

4.2.1.4 Bond Strength Evaluations and Minimum Required Bond Strength

The importance of bond strength on BCO performance has been well demonstrated. To evaluate the effect of bond strength on BCO performance, bond strength testing was conducted on all BCO on CRCP projects. Figure 4.6 and Figure 4.7 show the locations of bond strength testing in US 287 in Bowie and bond strength testing results, respectively. More detailed discussions on bond strength testing results are presented later. Bond strength varied from 117 psi to 241 psi.

Figure 4.8 shows bond strength testing in US 281 in Wichita Falls, and Figure 4.9 shows the testing results. Bond strength varied from 126 psi to 254 psi.

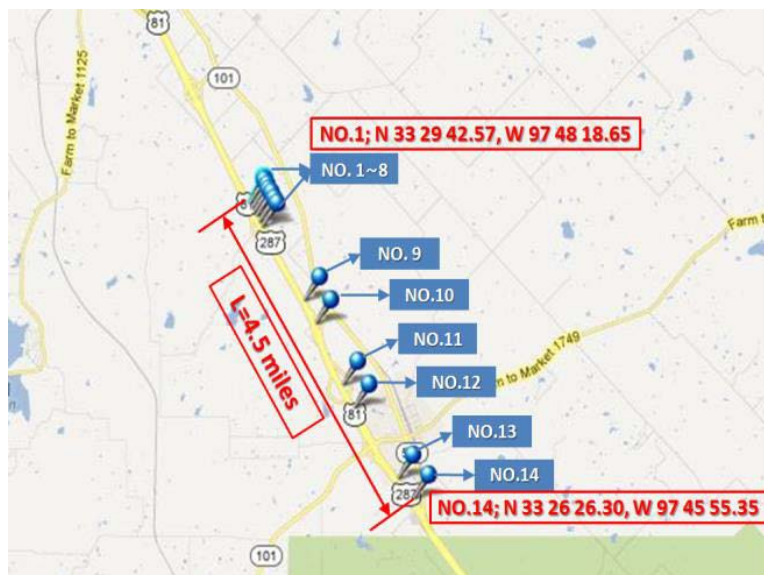


Figure 4.6 Bond strength test locations on US 287 in Bowie (2012)

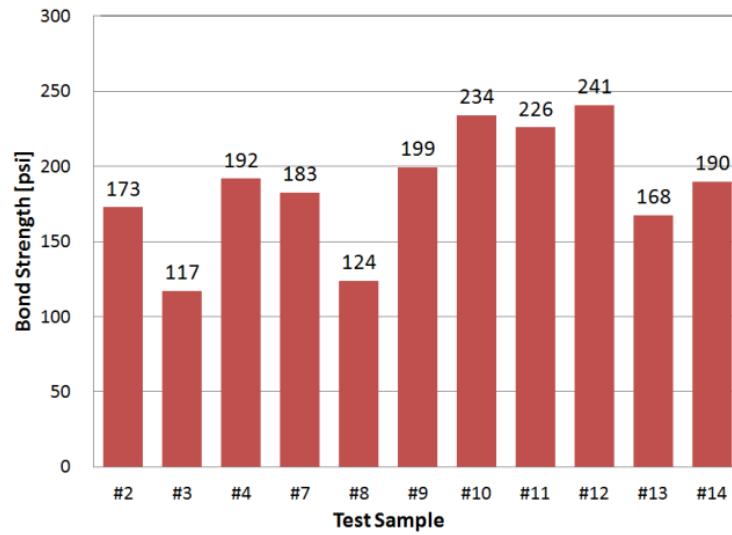


Figure 4.7 Bond strength test results for US 287 in Bowie



Figure 4.8 Bond strength testing on US 281 in Wichita Falls

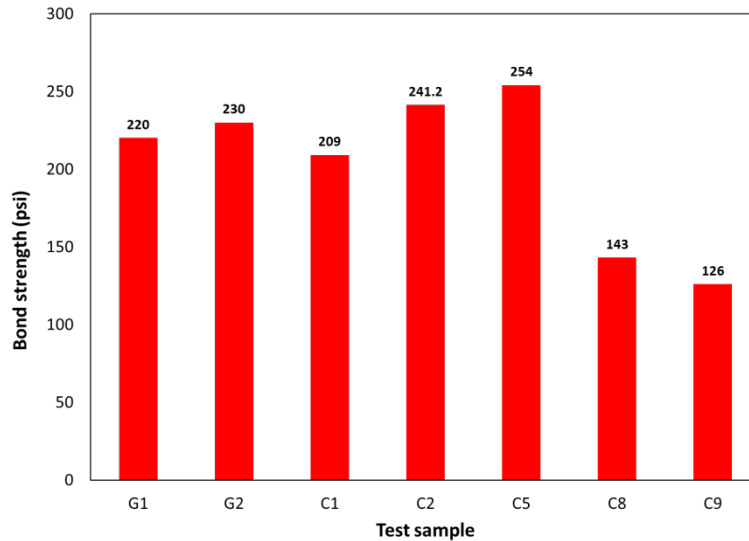


Figure 4.9 Bond strength test results for US 281 in Wichita Falls (2016)

Figure 4.10 shows bond strength testing results from Loop 610 South in Houston. Five different slab thickness and reinforcement type combinations were used at this location: (1) 2-in. plain (B3 to B6); (2) 2-in. reinforced with welded wire fabric (B7 to B14); (3) 3-in. reinforced with welded wire fabric (B15 to B23); (4) 3-in. with fibers (B24 to B31); and (5) 2-in. with fibers (B32 to B33). B1 and B2 were at a transition zone. Also, issues arose with the coring operation at B11 and B12, and bond strength testing was not conducted at these two locations.

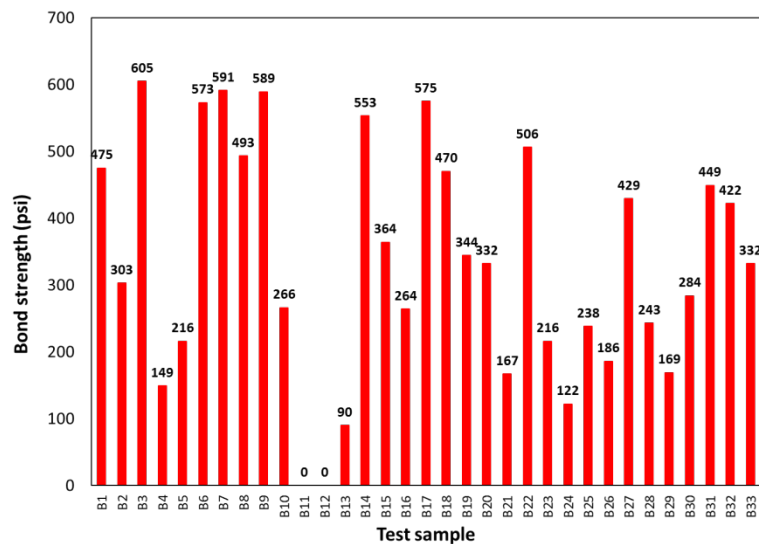


Figure 4.10 Bond strength test results for Loop 610 South in Houston (2016)

Table 4.1 summarizes the overall testing results from the three projects with failure mode. The average bond strength values were 186 psi in US 287, 197 psi in US 281, and 355 psi in Loop 610 South. It is noted that average bond strength on Loop 610 South was much greater than the

strengths measured in the other projects, possibly because of the use of cement grout. Table 4.1 uses several abbreviations for failure mode: IF denotes a failure at the interface between overlay and existing concrete slabs, OF a failure in the overlay, BF a failure in existing concrete slab, and DF a disk failure, which is a failure between aluminum disk and the top of the BCO. “Coring” indicates a problem with coring operations and no bond strength was obtained at those locations.

The table indicates that on US 287 in Bowie, all the failures or separations in the bond testing occurred at the interface, which implies poor surface preparation or other construction and materials issues. On US 281, there were no failures at the interface; more failures developed in the existing CRCP than in the overlaid concrete. On Loop 610 South, there was no interface failure, and an almost equal number of failures occurred in the existing CRCP and overlay. It should be noted that when the failures in the bond strength testing occur in the existing CRCP or within the overlay, the strength being measured is actually the direct tensile strength of the concrete in that layer. It is interesting to note that on US 281, tensile strengths of concrete in the existing CRCP were quite low, while those on Loop 610 South were quite high. Since no interface failures were observed on US 281 and Loop 610 South, surface preparation and BCO construction practices in those two projects appear to have been quite satisfactory, while those in US 287 appear to be of poor quality. This set of data presents quite valuable information, and further analysis and interpretations will be conducted. **Figure 4.11** shows the bond strength distributions at all three projects. As discussed earlier, the bond strength values at Loop 610 South in Houston (actually the concrete tensile strength) are much higher than those in the other two projects. Note that on Loop 610 South in Houston, plain concrete, reinforced concrete, and fibrous concrete are designated as NC, RC, and FC, respectively.

Table 4.2 provides information on types of surface treatment and pre-surface treatment information (if available) along with the average bond strength.

Table 4.1 Bond strength testing results

| No. | Bond strength (psi) | | | Failure mode | | |
|-----|---------------------|--------|----------|--------------|--------|----------|
| | US 287 | US 281 | Loop 610 | US 287 | US 281 | Loop 610 |
| 1 | - | 220 | 475 | IF | OF | OF |
| 2 | 173 | 230 | 303 | IF | BF | DF |
| 3 | 117 | 209 | 605 | IF | BF | BF |
| 4 | 192 | 241 | 149 | IF | OF | OF |
| 5 | - | 254 | 216 | IF | BF | BF |
| 6 | - | 143 | 573 | IF | BF | OF |
| 7 | 183 | 126 | 591 | IF | BF | DF |
| 8 | 124 | 143 | 493 | IF | DF | OF |
| 9 | 199 | 205 | 589 | IF | DF | BF |
| 10 | 234 | - | 266 | IF | - | BF |
| 11 | 226 | - | - | IF | - | Coring |
| 12 | 241 | - | - | IF | - | Coring |
| 13 | 168 | - | 90 | IF | - | DF |
| 14 | 190 | - | 553 | IF | - | DF |
| 15 | - | - | 364 | - | - | BF |
| 16 | - | - | 264 | - | - | OF |
| 17 | - | - | 575 | - | - | BF |
| 18 | - | - | 470 | - | - | BF |
| 19 | - | - | 344 | - | - | BF |
| 20 | - | - | 332 | - | - | OF |
| 21 | - | - | 167 | - | - | BF |
| 22 | - | - | 506 | - | - | OF |
| 23 | - | - | 216 | - | - | OF |
| 24 | - | - | 122 | - | - | BF |
| 25 | - | - | 238 | - | - | BF |
| 26 | - | - | 186 | - | - | OF |
| 27 | - | - | 429 | - | - | BF |
| 28 | - | - | 243 | - | - | OF |
| 29 | - | - | 169 | - | - | BF |
| 30 | - | - | 284 | - | - | BF |
| 31 | - | - | 449 | - | - | BF |
| 32 | - | - | 422 | - | - | OF |
| 33 | - | - | 332 | - | - | OF |

IF = interface failure, OF = overlay failure, BF = failure in existing concrete slab, DF = disk failure, coring = problem with coring operations. See text preceding this table for more detailed description of these terms.

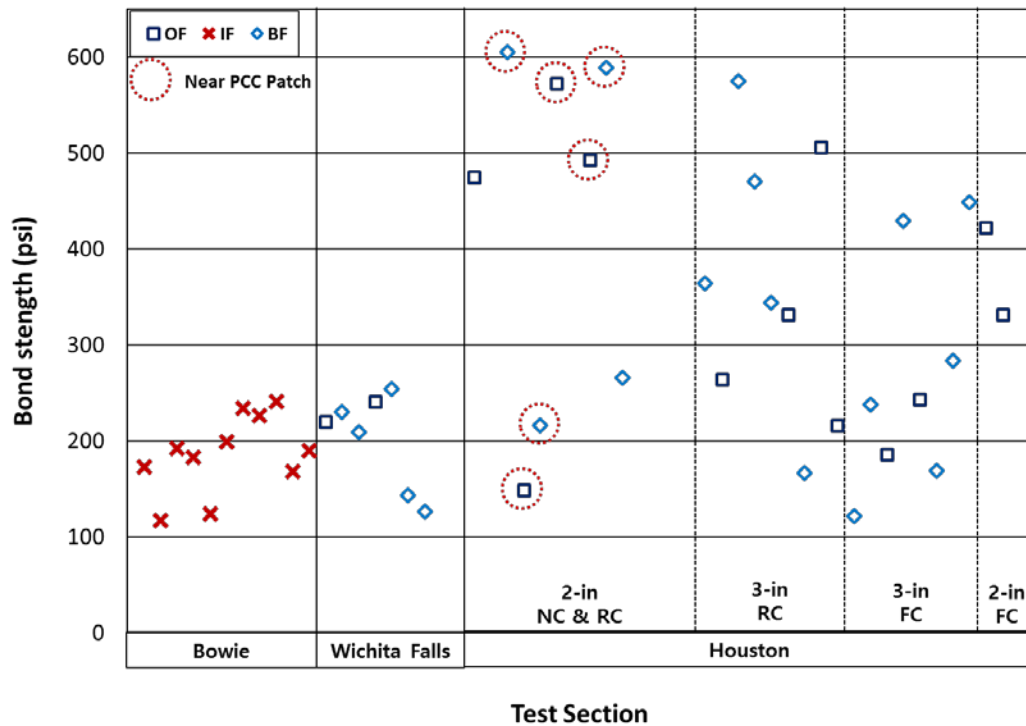


Figure 4.11 Bond strength distribution

Table 4.2 BCO construction information

| Attributes | US 287 Bowie | US 281 Wichita Falls | LP 610 Houston |
|-----------------------------------|-------------------------------------|-------------------------------------|---|
| Reference marker | 220+0.8 – 220+1.5 | 194+0.3 – 194+0.4 | 36+0.15 – 36+0.32 |
| Existing pavement thickness (in.) | 8 | 8 | 8 |
| Existing pavement type | CRCP | CRCP | CRCP |
| Surface preparation | - | - | Roto milling (1/4-in.) |
| Surface treatment | Shot-blast Pressure air cleaning | Shot-blast Pressure air cleaning | Sand blast Pressure air cleaning |
| Bond agents | - | - | w/c (0.62) grout broomed with plasticizer |
| Average bond strength (psi) | 186 | 197 | 355 |

Figures 4.12 and 4.13 illustrate BCO construction at US 287 and US 281, respectively.



Figure 4.12 BCO construction on US 287 in Bowie



Figure 4.13 BCO construction on US 281 in Wichita Falls

Bond strength is essential to achieving good performance in PCC overlays, because a good bond is needed for composite actions of the overlay and existing slabs in order to reduce the stress levels in the concrete due to both environmental and wheel loading applications. If stresses are excessive at the interface between overlay and existing slabs, two types of bond failures could occur: tensile failure (Mode I failure) and shear failure (Mode II failure). In BCO pavement system, it is well understood that primary debonding at the interface follows Mode I failure (Medina-Chavez et al. 2008). That is one of the reasons why pull-out testing is used for the evaluation of bond strength in BCO. Even though it is agreed that tensile bond strength is a good indicator to ensure monolithic behavior of a BCO system, different values have been suggested for an acceptable bond strength. Efforts were made to investigate how the acceptable bond strength values were derived. Bond strength requirements in the US, Europe, and Japan are discussed.

4.2.1.5 Review of Bond Strength Requirement

1) Bond strength requirements and recommendations in the US

The American Concrete Pavement Association (ACPA 1990) states that achieving good bond is a

key to long-term performance of BCO pavements. The bond strength of 200 psi is sufficient to withstand shear stresses and ensure a good bond. This number was determined in the laboratory (Felt 1956). Laboratory testing confirmed that laminated or bonded beams with a bond strength in the neighborhood of 200 psi behaved as if they were monolithic.

Delatte and Sehdev suggested that an acceptable bond strength at 28 days could be 130 psi, while a value of 200 psi was mentioned as an acceptable value (Delatte and Sehdev 2003). Gillette determined that a bond strength of 200 psi is adequate and any loss of bonding usually occurs soon after construction (Gillette 1965). Furthermore, he concluded that little or no growth in the debonded area occurred over time or under traffic loading.

There are other research papers on bond strength; however, the recommended values cited are from the information discussed above.

In summary, it appears that 200 psi at 28 days is the most recommended value in the US, even though a lower value was also suggested. This lack of a well-established bond strength requirement is due to the difficulty of obtaining field data on good-performing and poor-performing BCOs where bond strength was the only determining factor.

2) Bond strength requirements and recommendations in Europe

European Standard prEN 4504-3 requires 290 psi for bond strength in BCOs. It also requires that no single bond strength testing value should be less than 75% of the required 290 psi, which is about 220 psi, as shown in Figure 4.14. Compared with the requirements in the US, European requirements are quite stringent.

European Recommendation (European Standards)

| Property | Test method | Requirement | Comments |
|------------------------------|------------------------------------|------------------------------|--|
| Bond tensile strength | EN 1542 (Pull-off test) | 2.0 Mpa (290 psi) | Mean Value No single value less than 75% of minimum requirement |

Figure 4.14 European recommendations for bond strength

3) Bond strength requirements and recommendations in Japan

The Japan Highway Research Foundation (1995) developed the “Design and Execution Manual for Bonded Concrete Overlays,” which states that tensile bond strength of 145 psi at the interface between overlay and substrate slabs is adequate to ensure good bond. This value was derived from an experimental research study. This value is about half of the required value in Europe and lower than the value recommended in the US.

4.2.1.6 Performance at Transition Areas

During the field evaluations of BCO performance, it was observed that distresses were more prevalent in areas with discontinuities, such as transition areas between asphalt pavement and BCO, near the bridge expansion joints, or at longitudinal/transverse construction joints. **Figure 4.15** shows transition area conditions in the western end of the US-287 section in Bowie. This distress is confined to the outside lane, which implies that heavy truck wheel loading might have increased stress levels at the interface beyond the bond strength in this area. **Figure 4.16** shows distresses in a TCJ area on US 281 in Wichita Falls. As discussed in Chapter 3, severe delaminations were observed in this area. It appears that warping and curling of concrete caused initial delamination, which developed into fragmentation of overlay concrete. This indicates more stringent quality control or modifications in design may be needed at transverse or longitudinal construction joints, such as better curing.



Figure 4.15 Transition area on BCO on US 287 in Bowie



Figure 4.16 Distresses in TCJ on US 281 in Wichita Falls

4.2.2 CRCP BCO on CPCD

4.2.2.1 Deflection on Old CPCD and CRCP BCO

As discussed earlier, a CPCD section on US 75 in Sherman—10-in. CPCD on 6-in. flexible base—experienced severe distresses in the form of slab cracking and settlement, which degraded ride quality. A primary cause for the poor performance was low quality material in the base layer as well as poor drainage condition. To extend the pavement life of this section, in 2010 a 7-in. CRCP BCO was placed on the CPCD. To develop a BCO design, the structural condition of the section was evaluated, which included FWD testing at upstream, mid-slab, and downstream of each slab. **Figure 4.17** presents deflection on the 10-in. existing CPCD along the section. It shows large deflections, some more than 50 mils, and numerous instances of more than 20 mils, which indicates quite poor slab support condition at those locations. These large deflections were at transverse contraction joints, near cracks, or repair joints. In addition, a detailed distress map was developed at that time, and the information from the distress map was used to determine the effect of distresses in CPCD on CRCP BCO condition. **Figure 4.18** shows deflections on CPCD and BCO condition. It shows that, in general, distresses in BCO coincide with large deflections in CPCD, although there are exceptions. The numbers in the insert indicate joint numbers where distresses (black) or repaired areas (green) in BCO exist. It is interesting to note that deflections on CPCD at joint numbers 95 or larger were quite small, while there were a number of distresses or repairs made in those areas, which implies potential construction issues during BCO placement. During the design of 7-in. CRCP, a major concern was whether these large deflections could induce distresses at those locations. To retard the reflection cracking from transverse contraction joints, a decision was made to place non-woven fabric on top of transverse contraction joints. The width of the fabric was 2-ft (1-ft at each side of the joint) from one edge of the pavement to the other edge

(Ryu et al. 2011). One of the challenges at this location was heavy truck traffic. There is no WIM station near this project and, accordingly, detailed traffic information is not available. However, no distresses were observed in the inside lanes, while distresses developed in the outside lane. This indirectly indicates the effects of heavy truck traffic in this section of highway.

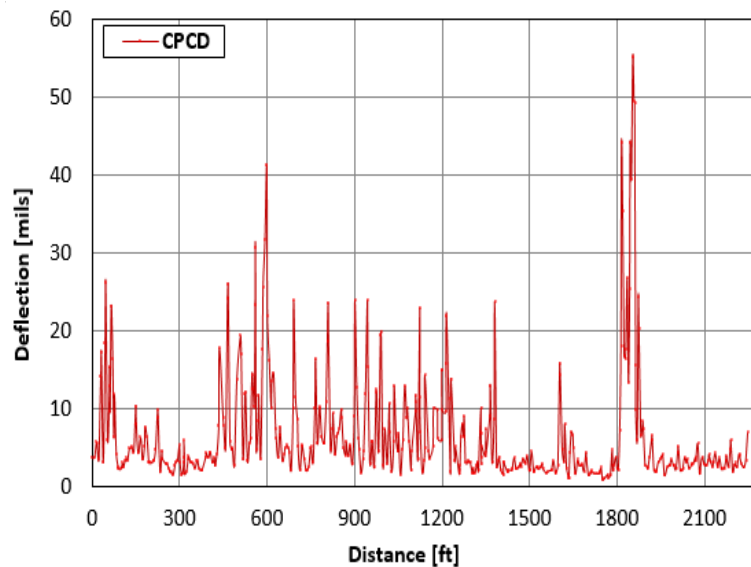


Figure 4.17 FWD deflection on old CPCD

Figure 4.18 shows the deflection comparison between CPCD and CRCP.

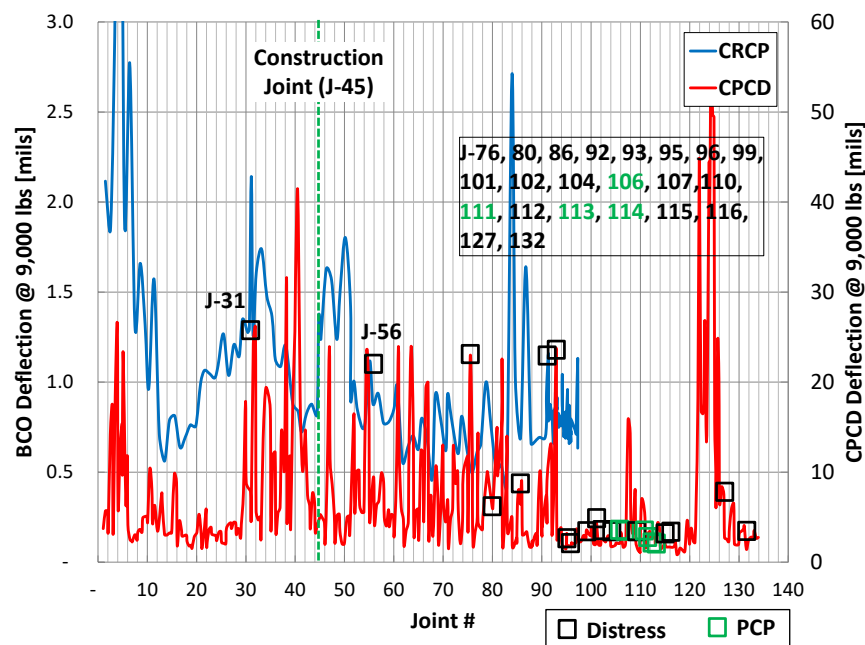


Figure 4.18 FWD deflection on old CPCD

4.2.2.2 Distress Distribution along the Project

Figure 4.19 shows distress frequency on CPCD prior to overlay in terms of the range of joint numbers. It shows that more distresses existed at slabs with large joint numbers. Figures 4.20–4.31 present FWD deflection on CPCD and CRCP BCO, a distress map of CPCD, and photographs of distresses on CRCP BCO. The information is presented for a group of 20 joints, from Joint 21 to Joint 40. The objective of this illustration is to present all the information together so that any obvious correlations could be easily detected.

Based on the information presented, the following statements could be made:

- 1) Most of the distresses on CRCP BCO were at transverse contraction joints in the existing CPCD.
- 2) In general, large deflections on CPCD at transverse contraction joints increased the potential for distresses in CRCP BCO.
- 3) However, in slabs with Joint No. 95 or above where the deflections on CPCD were small, the frequency of distresses on CRCP BCO was quite high. This appears to illustrate the construction quality issues.
- 4) Overall, joint deflections at 9,000 lbs loading of less than 8 mils on CPCD could be a good threshold value for the feasibility of CRCP BCO.

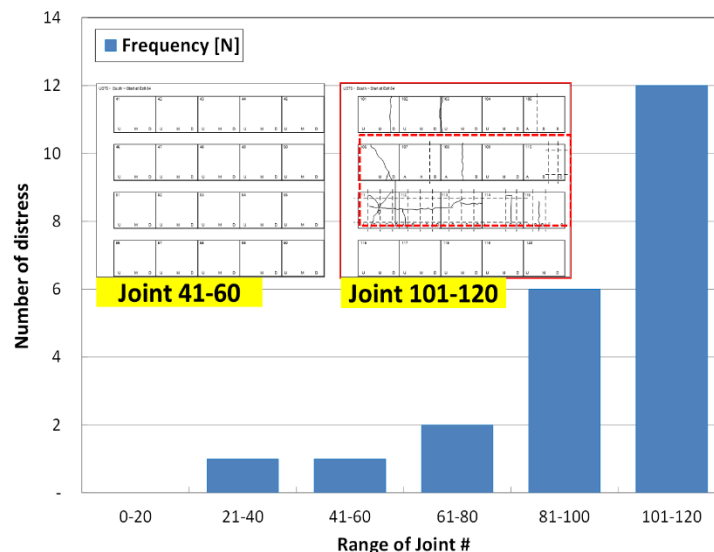


Figure 4.19 Distress frequency based on range of joint numbers

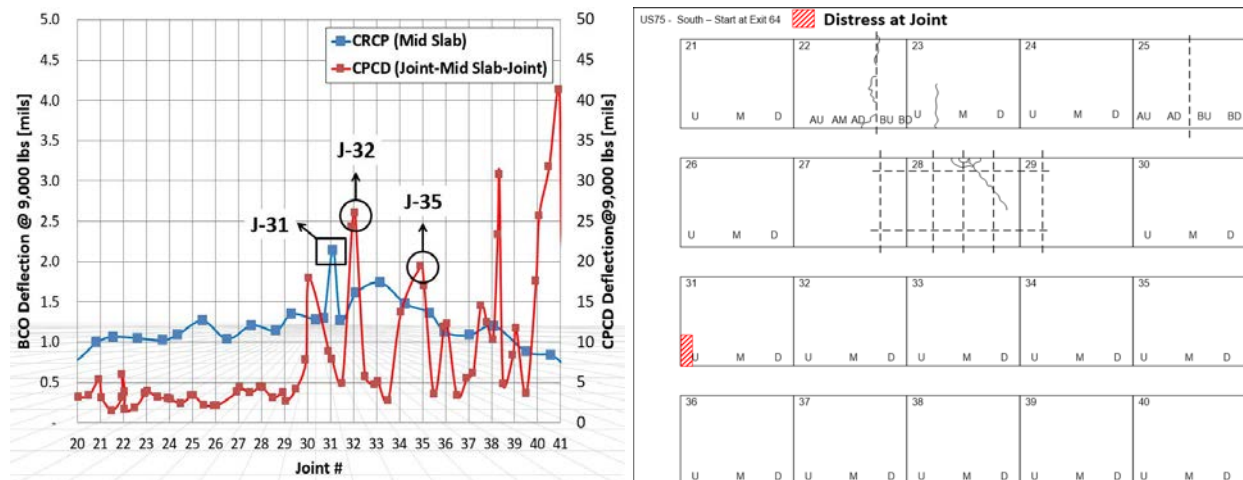


Figure 4.20 FWD deflection and distress map from J-21 to J40

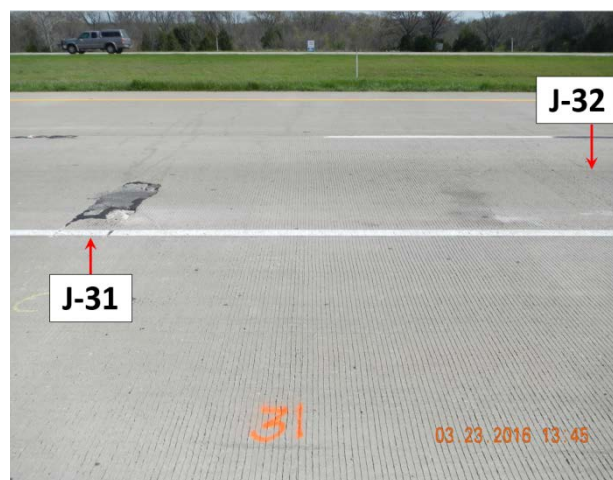


Figure 4.21 Distress on J-31

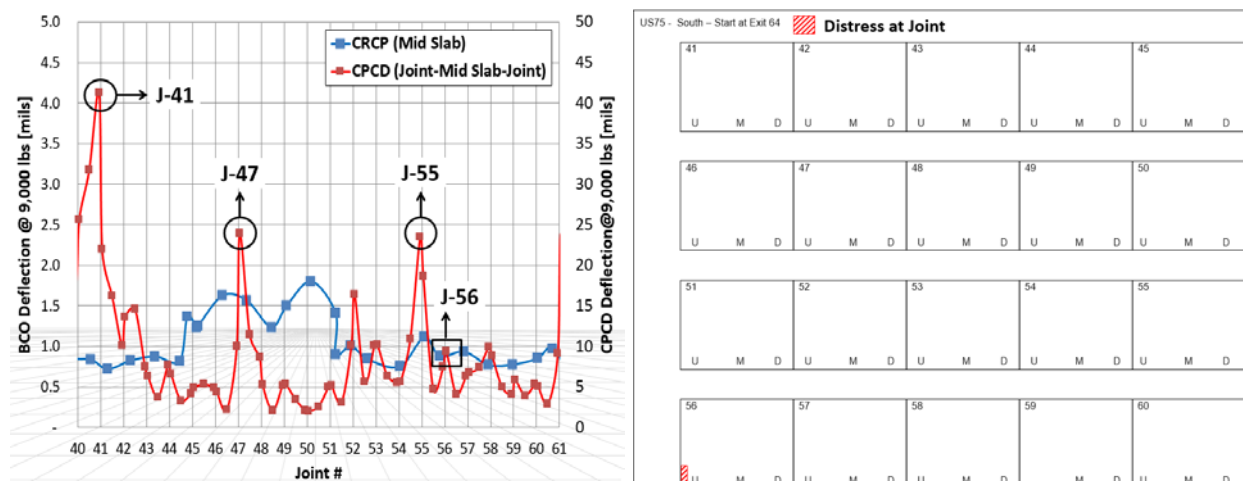


Figure 4.22 FWD deflection and distress map from J-41 to J-60



Figure 4.23 Construction joint at J-45 and distress on J-56

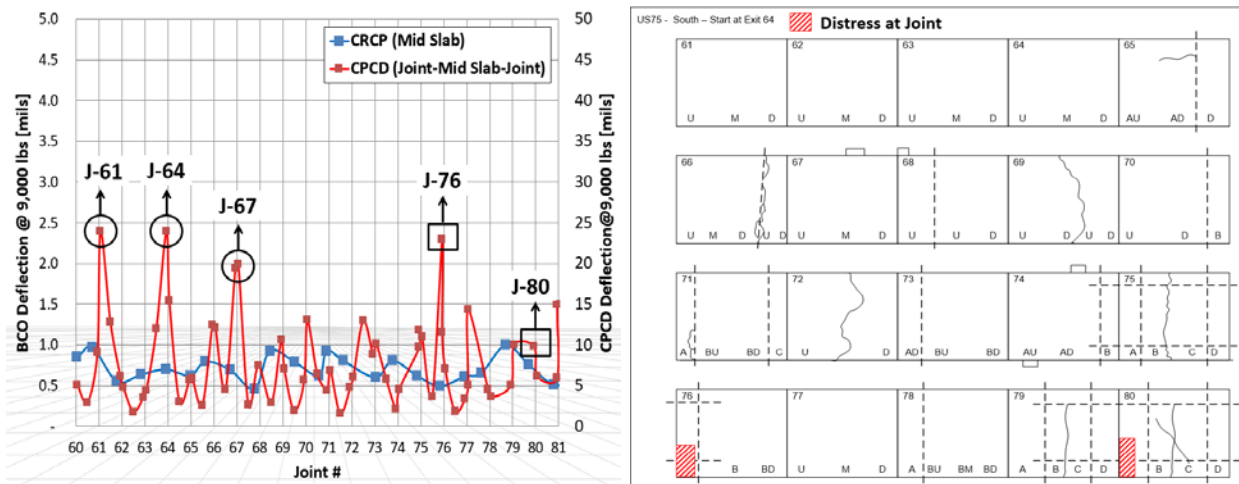


Figure 4.24 FWD deflection and distress map from J-61 to J-80



Figure 4.25 Distress on J-76 and J-80

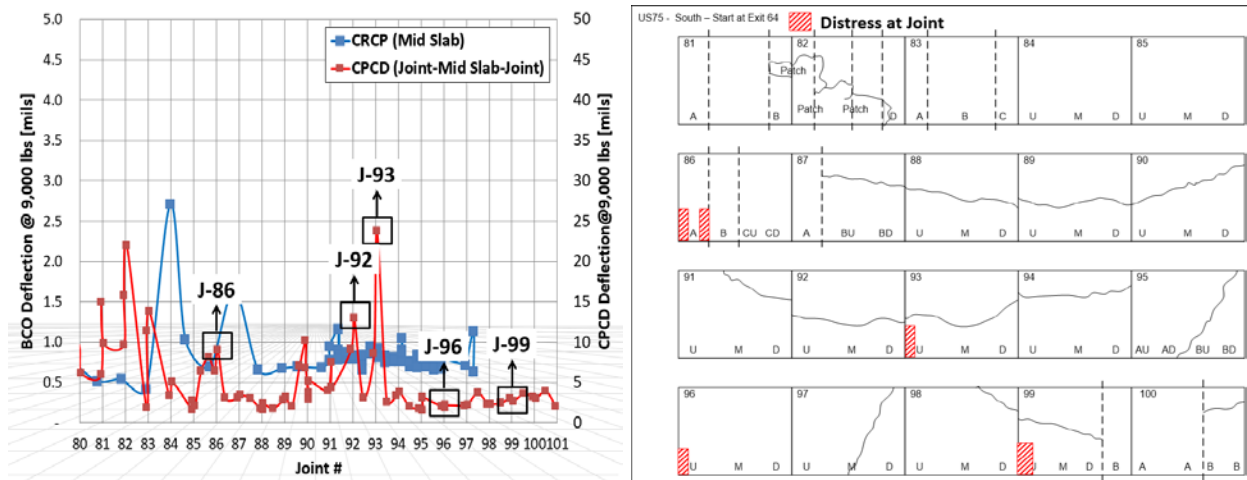


Figure 4.26 FWD deflection and distress map from J-81 to J-100

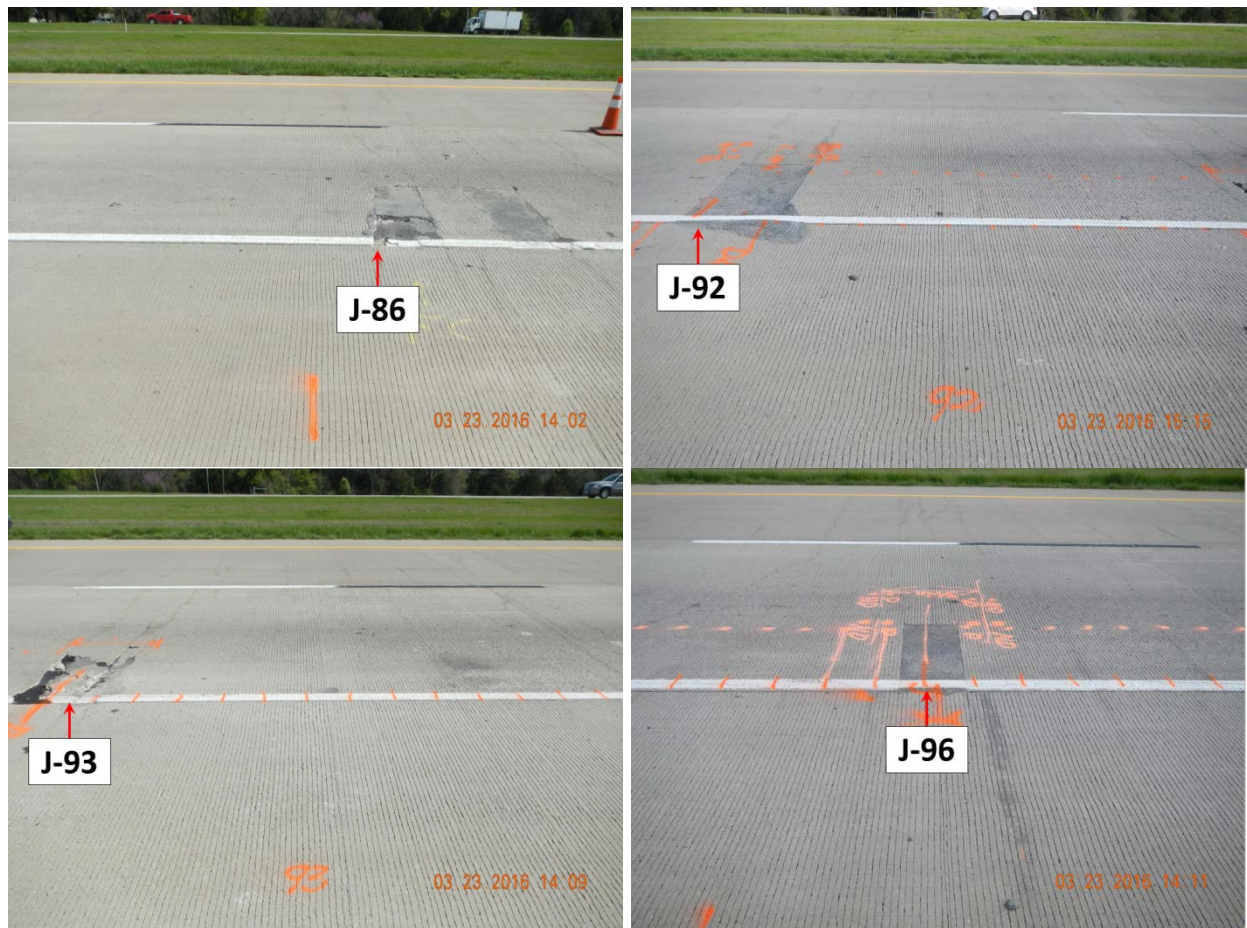


Figure 4.27 Distress on J-86, J-92, J-93, and J-96

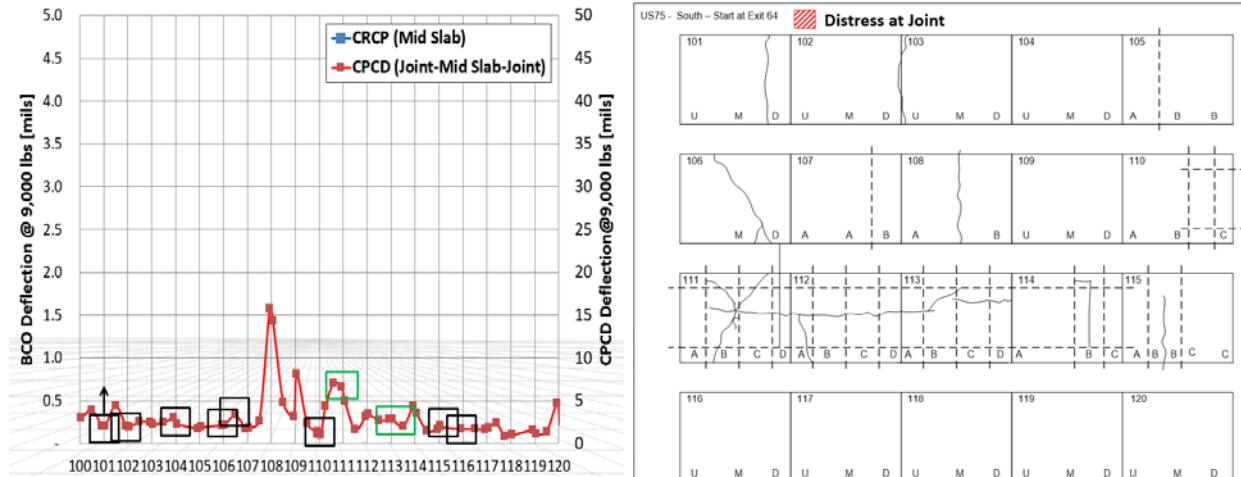


Figure 4.28 FWD deflection and distress map (previous condition) from J-101 to J-120

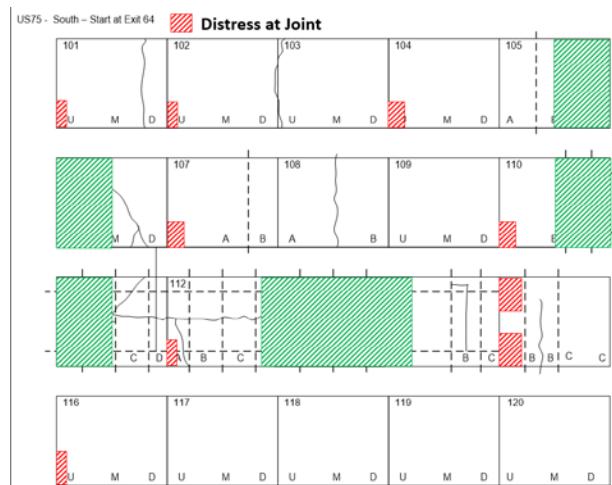


Figure 4.29 Distress map on J-101 and J-120

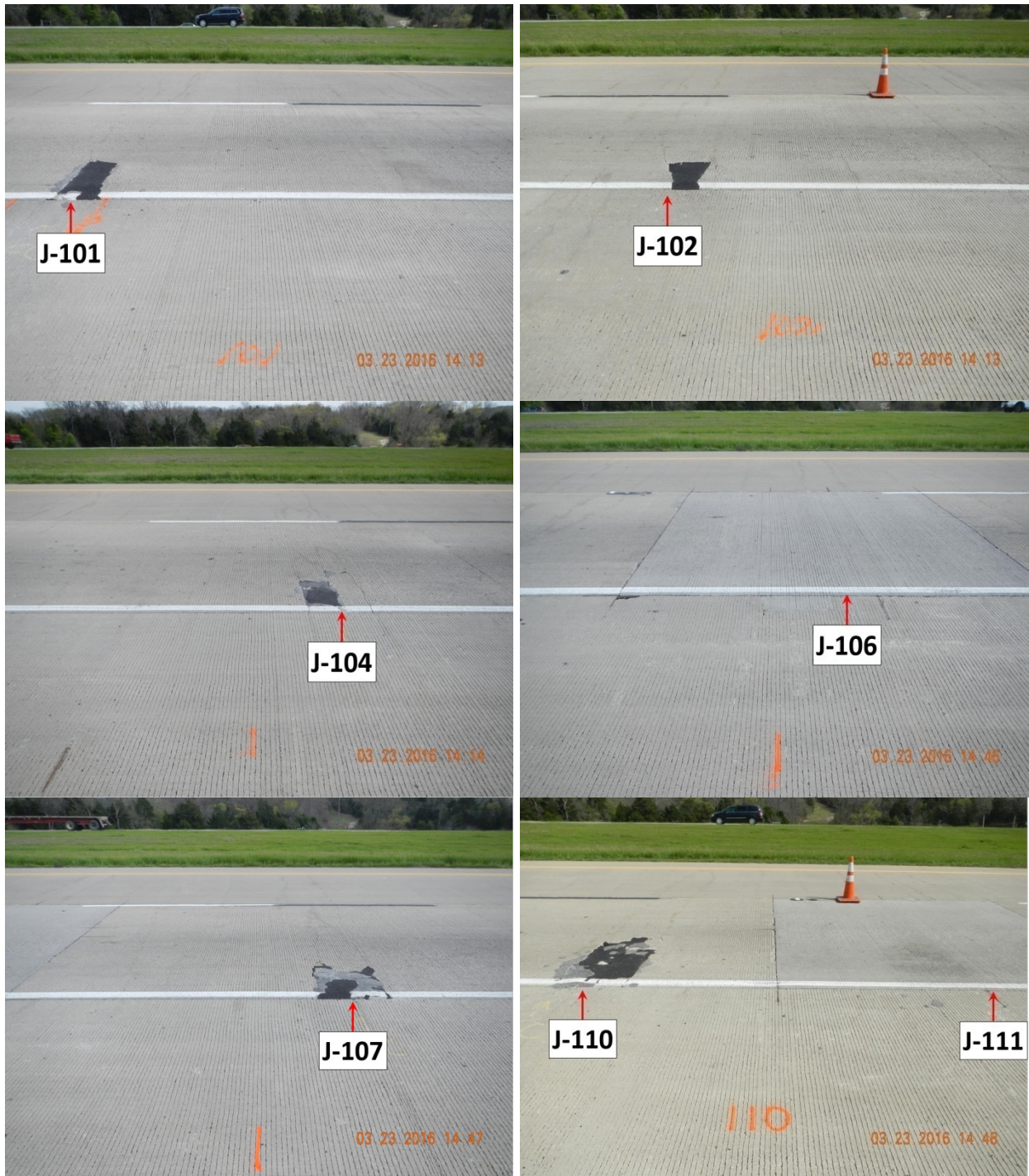


Figure 4.30 Distress on J-101, J-102, J-104, J-106, J-107, J-110, and J-111

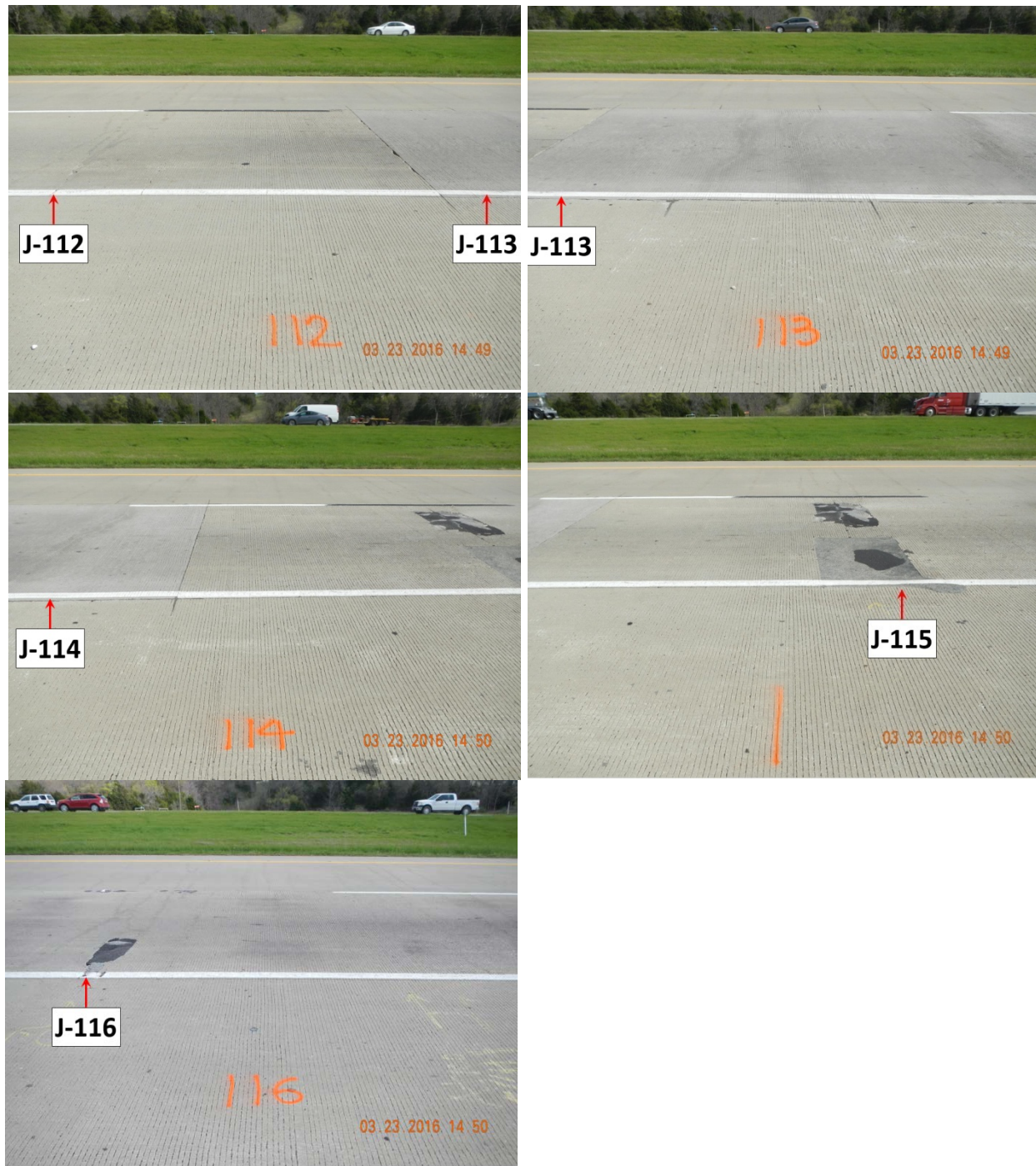


Figure 4.31 Distress on J-112, J-113, J-114, J-115, and J-115

4.2.2.3 Delamination Propagation at Transverse Contraction Joints

As discussed earlier, non-woven fabric was placed at transverse contraction joints on CPCD prior to the concrete placement of BCO, with the objective of delaying reflection cracking and potentially delaying distresses in BCO. The placement of fabric at the interface between existing CPCD and CRCP BCO will break the bond, creating debonding. Although the fabric could delay reflection cracking, debonding could accelerate distress development if debonding extends

substantially beyond the fabric placement area. To evaluate the extent of debonding from the end of the non-woven fabric, MIRA testing was conducted. MIRA testing at one joint location showed that debonding extended by 6-in. beyond the end of non-woven fabric. To validate the MIRA evaluations, cores were taken at delaminated and non-delaminated areas evaluated by MIRA, as shown in Figure 4.32. MIRA evaluations were quite accurate. It is not known when the delamination actually occurred. Considering this section has been under heavy truck traffic for the last 6 years, this rate of delamination propagation is encouraging and could provide good technical evidence of the feasibility of CRCP BCO on CPCD. As discussed in Chapter 3, some early distresses were repaired as early as 2012 by removing both the concrete in the 7-in. BCO and non-woven fabric, followed by placing new concrete. These repairs performed very well, indicating that the use of non-woven fabric was not needed. Encouraged by this finding and the performance of this CRCP overlay on CPCD, TxDOT scheduled another CRCP BCO on CPCD on US 82 in Paris. Deflections on the existing CPCD were measured and almost all the deflections were less than 20 mils, with an average deflection of 6.4 mils. For this scheduled repair, non-woven fabric will not be used, and CRCP overlay will be placed directly on CPCD.

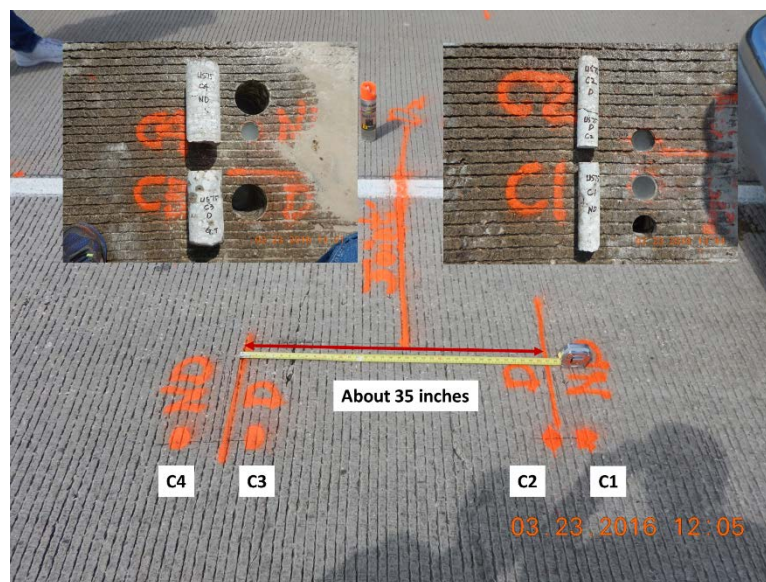


Figure 4.32 Delamination propagation

Figure 4.33 shows that fabric was attached to BCO concrete, which is expected since cement mortar from BCO concrete is absorbed into the fabric, creating mechanical bond. Accordingly, the debonding occurred between the fabric and the top of CPCD.

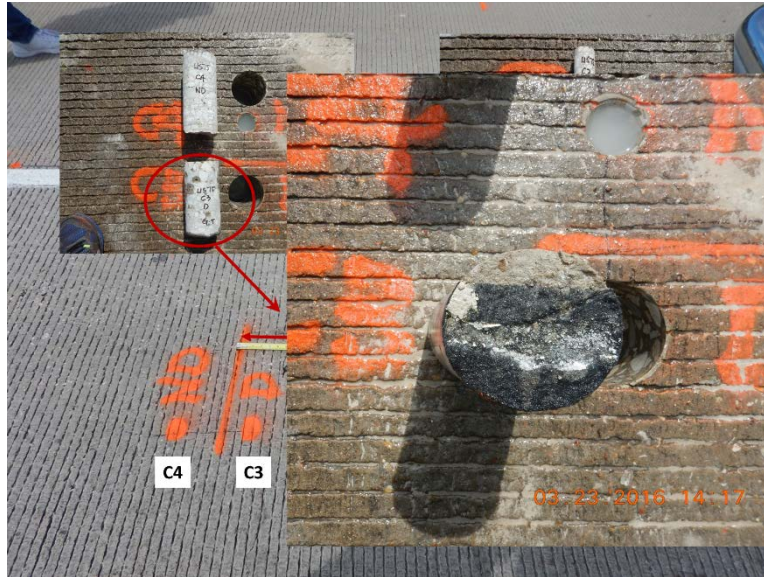


Figure 4.33 Core with an attached non-woven fabric

4.3 UBCO

As discussed in Chapter 3, the performance of two UBCO projects has been excellent, except for distresses in the surface, which have been due to construction-related issues. Also, the deflections in both UBCO projects are extremely small, indicating ample structural capacity of the pavement system. In this chapter, brief discussions are presented on the condition of the UBCO sections first, followed by descriptions of the efforts made to improve UBCO design procedures.

4.3.1 Pavement Evaluation in UBCO Projects

Pavement evaluation was conducted of IH 35 in Denton and IH 35E in Waxahachie, as detailed in Chapter 3. This section will discuss further the findings from the field testing analysis results.

4.3.1.1 Pavement Information and Condition

Field testing was conducted on IH 35 in Denton and IH 35E in Waxahachie. On IH 35 in Denton, a section from reference marker 475+0.69 to 475+0.80 was selected for testing in this research project. The 10-in. existing pavement CPCD was built in 1960 and an 11-in. CPCD UBCO was placed on the top of existing CPCD in 1987, with a 2-in. AC layer in between. Pavement condition survey conducted in 2016 shows excellent performance of this section for the last 29 years with minor surface distresses caused by construction operations.

CPCD UBCO section on IH 35E in Waxahachie consists of 10-in. CPCD UBCO with a 1.6-in. AC layer (165 lbs of AC materials per SY) on 10-in. CPCD. The original 10-in. CPCD was completed in November 1959, and 10-in. CPCD UBCO was placed in October 1990. A section from reference marker 406+0.60 to 406+0.70 was selected for testing in this research project. The pavement performance in this section has been excellent with almost no distresses.

The detailed pavement information for both sections is shown in [Table 4.3](#).

Table 4.3 Pavement information for IH 35 Denton and IH 35E Waxahachie

| Attribute | Information | |
|---------------------------------|--|--|
| | IH 35 Denton | IH 35E Waxahachie |
| CSJ | 0195-02-035 (UBCO) 0195-02-016 (CPCD) | 0048-04-050 (UBCO) 0048-04-024 (CPCD) |
| County | Denton | Ellis |
| TxDOT District | Dallas | Dallas |
| Reference Marker | 475+0.69 – 475+0.8 (0.1 miles) | 406+0.6 – 406+0.7 (0.1 miles) |
| GPS Coordinates | 33.324297, -97.180361 ~ 33.325947, -97.180461 | 33.485486, -96.829769 ~ 32.472033, -96.837739 |
| Construction Year (Existing) | 1960 | 1959 |
| Construction Year (Overlay) | 1987 | 1990 |
| Pavement Type | CPCD UBCO over CPCD | CPCD UBCO over CPCD |
| Slab Thickness | 11-in. CPCD UBCO +2.0-in. HMA+ 10-in. CPCD | 10-in. CPCD UBCO + 1.6-in. HMA+10- in. CPCD |
| Shoulder Type | Tied-Concrete Shoulder | Tied-Concrete Shoulder |
| Base Type | 6-in. Roadbed Treatment (TY-B) | 5.4-in. Asphalt Stabilized Base |
| Subgrade Type | - | 8-in. Lime Treated Subgrade |
| Drainage Type | - | Open Ditch |
| Coarse Aggregate Type | - | - |
| Con. Pavement Details | - | - |

4.3.1.2 Deflection Data Analysis

Detailed FWD testing results were discussed in Chapter 3. Based on the statewide deflection ([Choi et al. 2013](#)), as shown in [Figure 4.34](#), the equivalent slab thicknesses in terms of comparable deflections are 16.2-in. for IH 35E in Waxahachie and 16.9-in. for IH 35 in Denton, if the deflections in “poor” sections are selected.

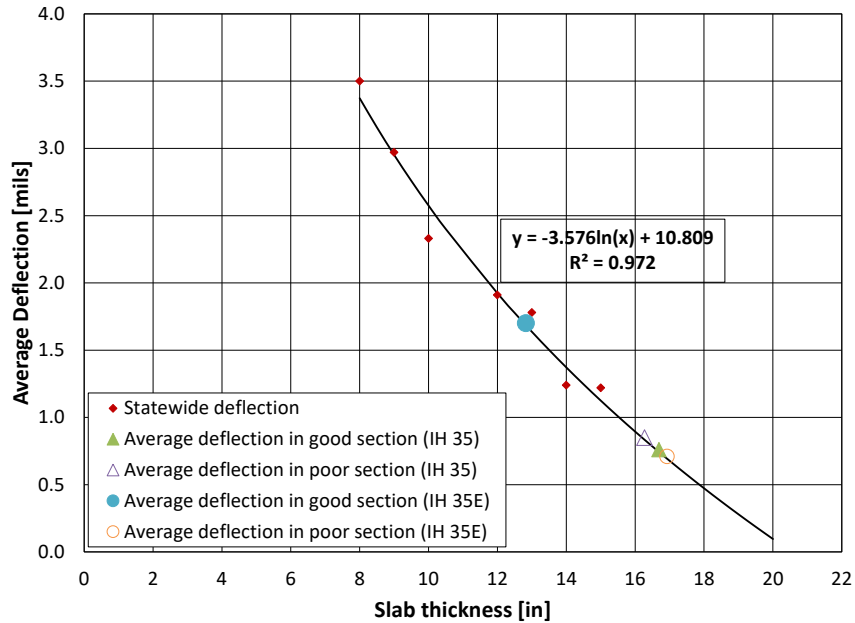


Figure 4.34 Deflection @9,000lbs statewide deflection

On IH 35E in Waxahachie, the average deflection in the “good” section (1.71 mils) is quite a bit larger than that in the “poor” section (0.71 mils), because the selection criteria of “good” and “poor” sections were based on surface distresses that were not related to the structural capacity of the pavement system. Coring at the “good” section revealed a deteriorated asphalt layer, as shown in [Figure 4.35](#). On the other hand, in the “poor” section, the AC interlayer condition was solid, resulting in an average deflection at the mid-slab of 0.71 mils, which is equivalent to a slab thickness of 16.9-in. It should be noted that, despite the lack of structural distresses at this location, the deteriorated asphalt interlayer and resulting larger deflections will ultimately compromise the UBCO performance. It is important to closely monitor the quality of the interlayer during UBCO construction.



Figure 4.35 Deteriorated AC interlayer in a good section of IH 35E

4.3.1.3 Good Pavement Conditions

As discussed earlier, pavement condition surveys of IH 35 in Denton and IH 35E in Waxahachie indicate excellent performance after more than 25 years of UBCO under heavy traffic. Also, equivalent slab thicknesses of more than 16 inches after more than 25 years under heavy traffic indicates the conservative nature of the UBCO designs in these sections.

Efforts were made to evaluate the AASHTO UBCO design method, the most widely used UBCO design procedure, to identify the source of the conservatism.

4.3.2 Evaluation of Current AASHTO UBCO Design Method

It is a general recommendation that when existing PCC pavement condition is poor, BCO is not an appropriate rehabilitation option; instead, UBCO should be considered. The 1993 AASHTO UBCO design method was derived from original work by the COE. For detailed evaluations of the AASHTO UBCO method, a finite element analysis program called DIANA (DISplacement method ANalyzer) was used with the various structural configurations and k-values.

Meanwhile, in the AASHTO 1993 UBCO design procedures, visual condition of the existing pavement is given as one way to estimate the effective slab thicknesses of the existing concrete slab. The visual evaluation approach is subject to several shortcomings, as discussed in Chapter 2, one of which is a poorly defined concept of deteriorated transverse cracks and joints. This report discusses the challenges of determining effective slab thickness.

4.3.2.1 Derivation of the AASHTO UBCO Thickness Design Procedure

Figure 4.36 shows an UBCO system with a slab of thickness h_1 (overlay) on top of the existing slab with a thickness h_2 . The monolithic slab with a thickness h_e is structurally equivalent to the UBCO system with thicknesses of h_1 and h_2 . The bending moments of overlay slab, existing slab, and monolithic slab are M_1 , M_2 , and M_e , respectively.

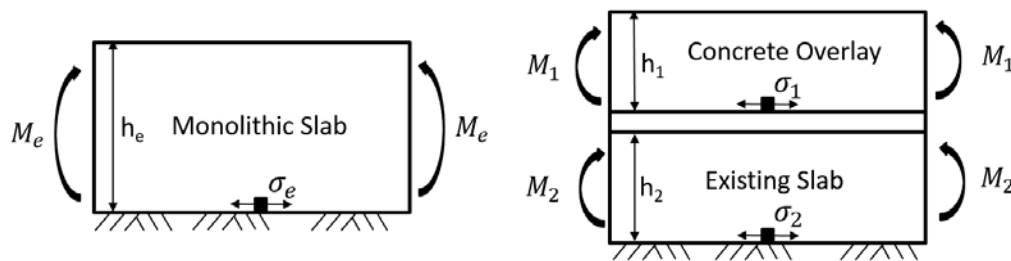


Figure 4.36 Cross section of slabs and their stress under load

In UBCO, it is assumed that the interlayer between the concrete overlay and the existing slab provides frictionless layer between the top and bottom slabs (Chou 1985). The moment in the equivalent slab is the sum of moments in the overlay and existing slabs, as shown in Eqn. 4.2.

$$M_e = M_1 + M_2 \quad (\text{Eqn. 4.2})$$

Based on the relation of $M = \sigma I / y$, Eqn. 4.2 can be rewritten as Eqn. 4.3, where stresses at the bottom of the overlay, existing slab, and monolithic slab are denoted as σ_1 , σ_2 , and σ_e , respectively.

$$\frac{\sigma_e I_e}{\frac{h_e}{2}} = \frac{\sigma_1 I_1}{\frac{h_1}{2}} + \frac{\sigma_2 I_2}{\frac{h_2}{2}} \quad (\text{Eqn. 4.3})$$

I is the moment inertia of the cross section with respect to the neutral axis of the slab and the value of I is equal to $b(h)^3/12$, so Eqn. 4.3 can be rewritten as Eqn. 4.4:

$$\sigma_e h_e^2 = \sigma_1 h_1^2 + \sigma_2 h_2^2 \quad (\text{Eqn. 4.4})$$

If an assumption is made that $\sigma_e = \sigma_1 = \sigma_2$, Eqn. 4.5 can be obtained:

$$h_e^2 = h_1^2 + h_2^2 \quad (\text{Eqn. 4.5})$$

Eqn. 4.5 is the slab thickness design equation for UBCO in the AASHTO design. This equation can be correct only when the condition $\sigma_e = \sigma_1 = \sigma_2$ is true. To verify whether this condition is realistic, a finite element analysis of a UBCO pavement system was conducted to obtain stresses at the bottom of each slab.

4.3.2.2 DIANA Analysis for UBCO

To evaluate the reasonableness of the AASHTO UBCO design methodology, the mechanistic behavior of a UBCO system was analyzed with DIANA. Figure 4.37 shows the geometric configuration of the UBCO system (CPCD over CPCD). The slab size is 15-ft long and 12-ft wide for both UBCO and the existing pavement slab. The FWD loading with a 12-in. diameter was located at center of slab. The thicknesses of overlay and the existing pavement slab are denoted as h_1 and h_2 , with a 2-in. AC interlayer in between. The spring element was used in DIANA to model the modulus of subgrade reaction (k-value) at the bottom of the existing pavement.

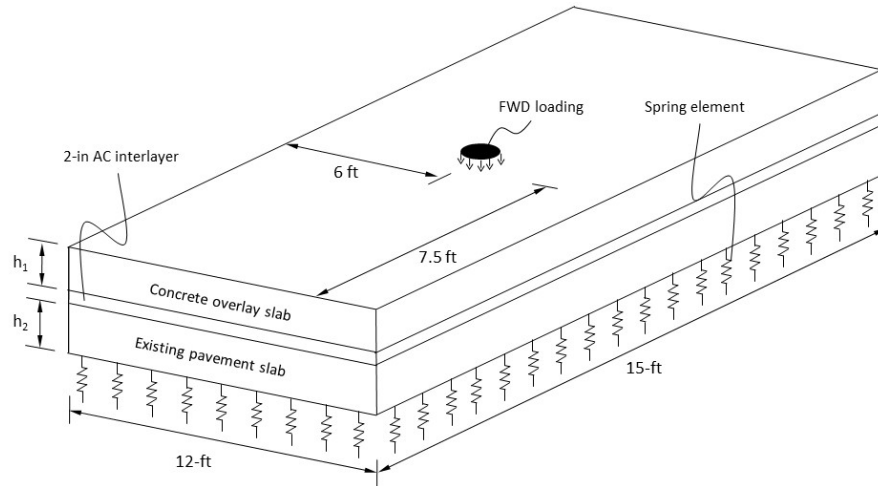


Figure 4.37 Geometric configuration of CPCD UBCO on CPCD

1) Mesh model

Figure 4.38 shows a three-dimensional (3-D) finite element mesh model of UBCO. Twenty-node iso-parametric solid elements were used in the mesh representation of the concrete and asphalt interlayer. To accurately predict the distribution of stress field in the concrete, interface elements were used in the mesh representation of the unbonded condition between the concrete and asphalt interlayer.

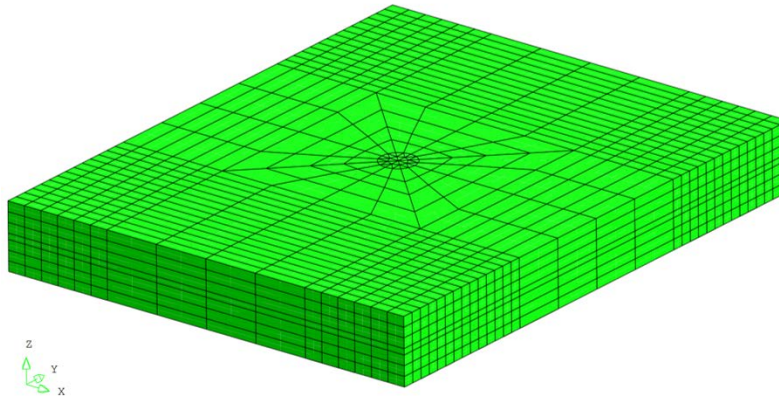


Figure 4.38 3-D finite element mesh model for UBCO pavement system

The interactions between the asphalt interlayer and concrete were analyzed by modeling their contact area using 8+8-node plane quadrilateral interface elements. The interface element, which is equivalent to a series of spring elements, is placed between the faces of concrete and asphalt interlayer. Although the faces of the concrete and asphalt interlayer have the same coordinate values—the interface element has zero-thickness—they separate the faces connected by the interface element. The interface element defines a relation between tractions and relative displacements across the interface. These have normal and shear components. The relation

between shear traction and shear relative displacement describes bond-slip behavior between asphalt interlayer and concrete. The relation between normal traction and normal relative displacement describes unbonded behavior. In this way, the unbonded conditions between asphalt interlayer and concrete can be better modeled.

2) Material properties

In the modeling, the thickness of overlay slab (h_1) varied from 4-in. to 12-in., and the thickness of existing slab (h_2) varied from 4-in. to 13-in., in 1-in. increments. Three levels of modulus of subgrade reaction—100, 200, and 300 psi/in.—were selected. The Poisson's ratio of concrete overlay and the existing concrete was assumed as 0.15, and the elastic modulus of both overlay and the existing slab were 5.0×10^6 psi. For the AC interlayer, 2-in.-thick AC was used in the modeling. The Poisson's ratio and elastic modulus of AC were assumed as 0.3 and 0.4×10^6 psi, respectively. By changing the thickness of overlay slab and the existing pavement slab, the stress (σ_1) at bottom of the overlay slab and stress (σ_2) at the bottom of existing slab can be obtained for the different structure configurations.

3) Analysis results

With various levels of slab thickness and modulus of subgrade reaction, a total of 270 cases were analyzed, as shown in [Table 4.4](#).

Table 4.4 Structure configurations of 3-D UBCO analysis

| | Thickness [inch] | k-value [pci] | Cases |
|---------------|---------------------|------------------|-------|
| Overlay | 4-12 | | 270 |
| Existing Slab | 4-13 | | |
| Base | | 100, 200, 300 | |

In all the cases analyzed, concrete stress at the bottom of overlay slab (σ_1) is always larger than the stress at the bottom of existing slab (σ_2). [Figure 4.39](#) shows the stress ratio of σ_1/σ_2 for various slab thicknesses with a k-value of 100 pci. It shows that the ratio is larger than 1.0 for all the cases, which violates the basic assumption made in the AASHTO UBCO design method, which is $\sigma_e = \sigma_1 = \sigma_2$.

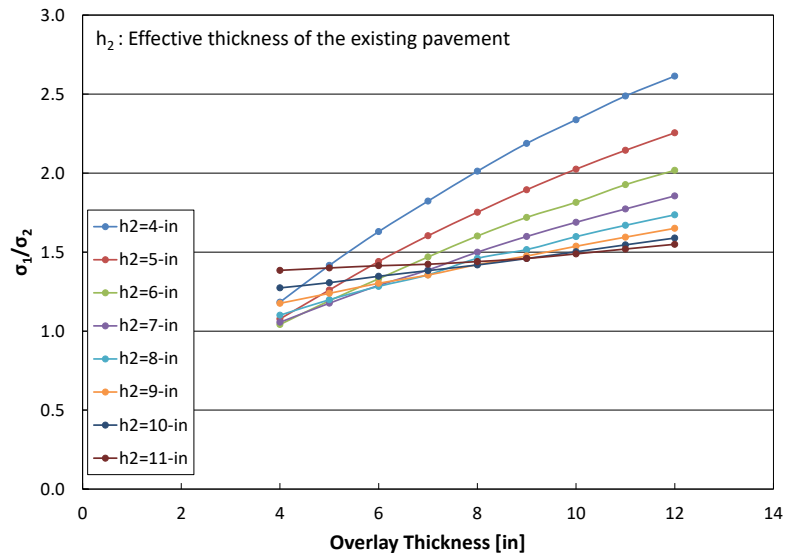


Figure 4.39 The stress ratio of UBCO for the case of k-value = 100 pci

4.3.4 Summary

Field testing was conducted on IH 35 in Denton and IH 35E in Waxahachie and the results show that the performance of those two UBCO sections has been excellent under heavy traffic. Also, deflection analysis shows the conservative nature of the UBCO thickness designs. In-depth evaluations of the AASHTO UBCO design method illustrates unreasonable assumptions in the development of thickness design, which was verified by finite element analysis. Considering the conservative nature of the AASHTO UBCO design led to unreasonable assumptions, as verified by deflection testing and equivalent slab thicknesses, the use of exponent 1.4 instead of 2.0 for UBCO design is recommended, as suggested by the COE for partially bonded overlay. This modification will provide more reasonable UBCO designs, which will encourage more use of UBCOs in Texas.

Chapter 5 Development of CRCP BCO ME Design Program

5.1 Introduction

Valuable information on the structural responses and the performances of PCC pavement overlays were obtained in this research project and presented in Chapter 3 and Chapter 4; however, the inference space is not large and extensive enough to develop generalized and empirical design guidelines solely based on the field performance information. This is the case partly because, thus far, the implementation of PCC overlays has not been extensive in Texas; however, as many miles of PCC pavements in Texas are approaching the end of their design lives, more PCC overlays are expected to be placed in the future. Until an extensive dataset on the field performance of PCC overlays becomes available, mechanistic analyses of the PCC overlay systems should play a bigger role in developing PCC overlay design procedures, with the information obtained in Chapters 3 and 4 providing calibration of the design procedures. Some information in Chapters 3 and 4 is presented in this chapter to facilitate the discussions.

In this chapter, detailed structural analyses were conducted on two overlay structures—(1) CRCP BCO on CRCP and (2) CRCP BCO on CPCD—because no overlay design procedures based on mechanistic principles for those two types of overlays have been developed.

For structural analysis, the finite element program, DIANA, was used. The objective of the modeling and the analysis was to evaluate structural responses of the overlay systems built on existing pavements with varying degrees of structural capacities. Structural responses appropriate for each overlay type were evaluated and slab thickness determined based on existing pavement conditions and future design traffic.

5.2 Distress Mechanisms in CRCP BCO on CRCP

5.2.1 Distress Development due to Delamination Caused by Large Deflections

In general, BCOs are placed where the existing PCC pavement is in a relatively good condition. Here, the word “good” is qualitative and somewhat subjective. Since BCOs are supposed to behave as a monolithic slab throughout the pavement design period, which will ensure lower concrete stresses and deflections, good bond strength at the interface between overlaid and existing pavement slabs is essential. Maintaining a good bond (meaning no debonding at the interface) for the design life of the BCO system, which is 30 years in Texas, requires small slab deflections to accommodate wheel loading applications after the overlay. Large slab deflections would induce substantial shear stresses at the interface, potentially resulting in delamination, which increases tensile stresses at the bottom of the overlaid slab and the probability of slab segmentation. Reduced slab deflections in the overlaid pavement system are achieved when either the slab support condition of the existing pavement system is adequate or larger slab thickness is used for the overlay layer. The latter is not a good option, since it increases construction cost and poses potential geometric compatibility issues, including bridge clearance or drainage issues. A more practical

approach is to place BCO on an existing pavement with relatively low deflections, since such a BCO system will have smaller deflections, even with a thinner overlay slab. Thus, to determine whether existing PCC pavement is a good candidate for BCO or not, criteria on deflections of existing pavement should be developed. Figures 5.1 and 5.2 illustrate typical BCO distresses that occur following the distress mechanism described above.

Developing generalized criteria on the minimum deflections in the existing pavement for BCO feasibility solely from field evaluations of BCO pavement performance is quite difficult. The information required on the behavior of BCO system prior to and after overlay is quite extensive, which includes deflection measurements on existing and overlaid pavements at identical locations and the relationship between deflections on BCO and distresses. In addition, bond strength at the interface and traffic information are also needed. In Texas, there is only one project where all the necessary information was collected, which is the US-287 BCO project in Bowie in TxDOT's Wichita Falls District. Even though the inference space is quite small (only one project), the information obtained in that project is quite extensive, and could provide valuable and useful information in developing deflection criteria. In addition, no publications are available that contain the information on those items, and this is the first project where the effort was made to gather such information. The derivation of deflection criteria to determine whether the existing PCC pavement is a good candidate for BCO or not will be described.



Figure 5.1 Distress due to large deflection in existing CRCP (US 287 in Bowie)



Figure 5.2 Delamination and BCO distress (US 287 in Bowie)

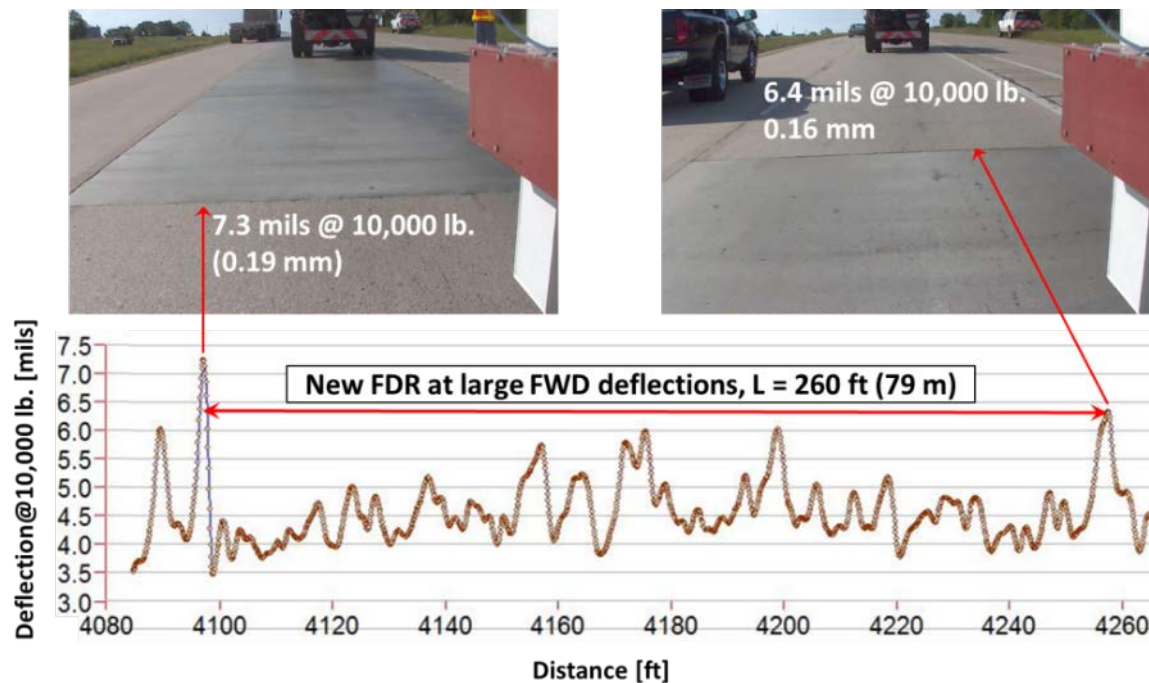
5.2.2 Distress Development along FDR Joints in Existing CRCP

TxDOT conducted a research study to improve the performance of FDR of CRCP (Ryu et al. 2013). The research discovered that the poor FDR practices frequently caused secondary distresses along the repaired joints. Following are some of the major findings from the aforementioned study:

“The primary cause for poor performance of FDR is the failure to restore structural continuity at transverse repair joints. Common characteristics of poorly performing FDRs were large deflections at transverse repair joints. Poor bond between tie bars and the surrounding concrete at repair joints appears to contribute to these large deflections and poor performance.”

“Optimum performance of repairs of CRCP distresses can be achieved only when repair operations are conducted strictly in accordance with the requirements in specifications and design standards. Any deviations could result in less than optimum performance, potentially requiring subsequent repairs of the already-repaired areas. To enhance the efficiency of TxDOT operations on CRCP repairs, periodic training for TxDOT project staff, including maintenance engineers and inspectors, through webinars or other means, on the findings of this study is recommended.”

In the US-287 BCO project in Bowie, distresses were observed on BCO slabs along the repair boundaries in the existing CRCP. As shown in Figure 5.3-(a), large deflections were measured at the FDR repair joints. In April 2012, deflection testing was conducted on existing CRCP with TPAD. Deflection profiles in Figure 5.3-(a) are from the TPAD testing. As a result, the secondary distress occurred again within the FDR slab before the BCO was placed, as illustrated in Figure 5.3-(b). Eventually, the distresses in the FDR areas in the existing CRCP were reflected to the BCO as shown in Figure 5.3-(c). This distress mechanism could be considered as a subset of the distress mechanism discussed earlier (larger deflections of BCO system potentially causing delamination and distress). In other words, large deflections in the existing PCC pavement slabs could be one of the primary distress development mechanisms in BCO.



(a) Deflection profile at FDR slab



(b) Distress within FDR slab

(c) BCO distress

Figure 5.3 Distress at FDR joint (US 287 in Bowie)

5.3 Distress Mechanisms in CRCP BCO on CPCD

CRCP BCO on CPCD has been rarely used, and there are only three projects of this type in the country: two in Georgia and one in Texas. The two projects in Georgia were built in 1970s and, unfortunately, very little documentation was created. In Georgia, the existing pavement was JRC. The Texas project is in Sherman (in TxDOT's Paris District) on US 75 southbound from Exit 64, just north of the City of Sherman. It is a half-mile section built in May (inside lane) and June (outside lane) of 2010. Chapter 4 provides details on this section.

Distress survey results show that there were 22 distresses in the outside lane. Not one distress appeared in the inside lane, which indicated that the effect of heavy truck traffic, among other factors, was a dominant factor affecting distress. It should be noted that tied-concrete shoulders were placed at both inside and outside lanes. All 22 distresses occurred at the locations of transverse contraction joints in the existing CPCD. As discussed in Chapter 4, geotextile was placed on transverse contraction joints to prevent or delay reflection cracking since the deflections at transverse contraction joints prior to the overlay were quite large, primarily due to poor slab support. It is not clear whether the placement of geotextile actually helped lessen the reflection cracking. The distress rate at transverse contraction joints was about 13% of transverse contraction joints (22 divided by a total 170 joints). Considering the large deflections at transverse contraction joints in the existing CPCD and heavy truck traffic, this rate of distress appears not to be excessive.

Figures 5.4 and 5.5 show typical distresses in CRCP BCO on CPCD on US 75. The distresses appear to be confined to the extent of the geotextile. It is not known what type of distresses could have occurred without the geotextile. However, if the deflections at transverse contraction joints in existing CPCD are less than a to-be-developed threshold value, a CRCP overlay without a geotextile could work.

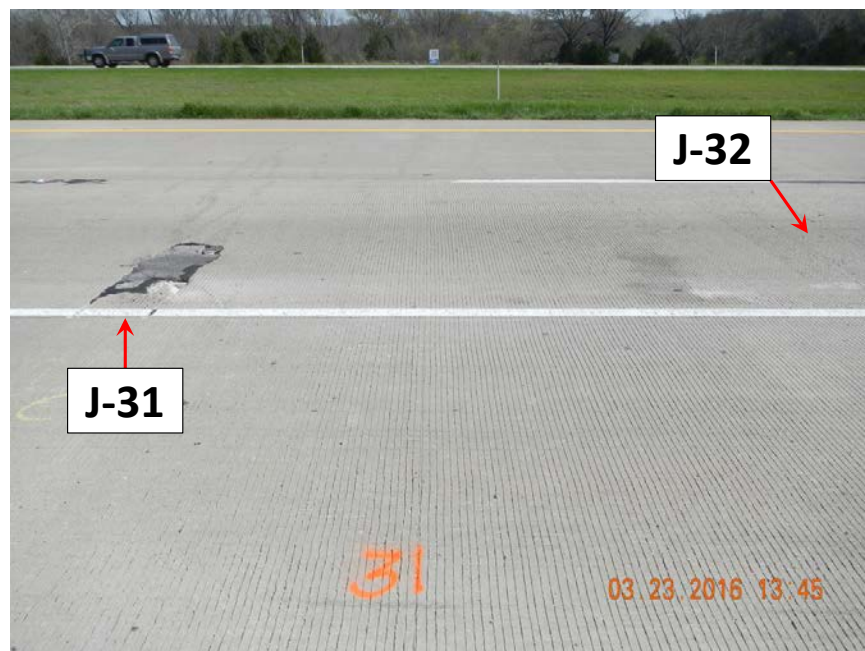


Figure 5.4 Distress in CRCP BCO on CPCD (US 75 in Sherman #1)



Figure 5.5 Distress in CRCP BCO on CPCD (US 75 in Sherman #2)

5.4 Determination of Deflection Threshold Values

5.4.1 CRCP BCO on CRCP

The current methodology for the selection of a proper PCC overlay type is more qualitative and descriptive, which makes it difficult for engineers to determine whether the existing PCC pavement is a good candidate for overlay and, if it is, which overlay type is the most appropriate. There is a need for the development of a methodology that will help engineers make decisions about overlays based on more quantifiable criteria. As discussed earlier, the performance of BCOs appears to depend on the deflections of the pavement system (BCO), which also depends on the structural capacity of the existing pavement. The structural capacity of the pavement system can be best represented by slab deflections. Since TxDOT owns a number of FWDs, one TPAD unit is available for pavement evaluations, and deflection is a good indicator for structural capacity of the pavement system, it would be desirable if a threshold value were developed and used for the determination of overlay feasibility and the selection of a proper overlay type. Developing threshold values for BCOs with different overlay slab thicknesses would require evaluations of a number of BCO projects. Unfortunately, TxDOT did not build BCOs with various overlay slab thicknesses. In addition, FWD testing data prior to the overlay as well as a detailed survey of distresses after the overlay are needed. At this point, there is one BCO project (US 287 in Bowie described earlier) where detailed structural evaluations were conducted prior to the overlay, as well as detailed distress surveys. Prior to the overlay in 2010, a 1,000-ft section was selected and the pavement condition of the 8-in. CRCP was evaluated with FWD and DCP. Statewide deflection testing conducted under the TxDOT rigid pavement database project (0-6274) indicates an average deflection of 3.6 mils for 8-in. CRCP (Choi et al. 2013). However, in the section evaluated,

deflections much larger than the average deflection of 3.6 mils were observed at numerous locations, an indication of poor slab support at those locations. Figure 5.6 indicates that slab support is not uniform within the selected test section. It also shows that larger deflections occurred at locations of wide crack widths and repair boundaries.

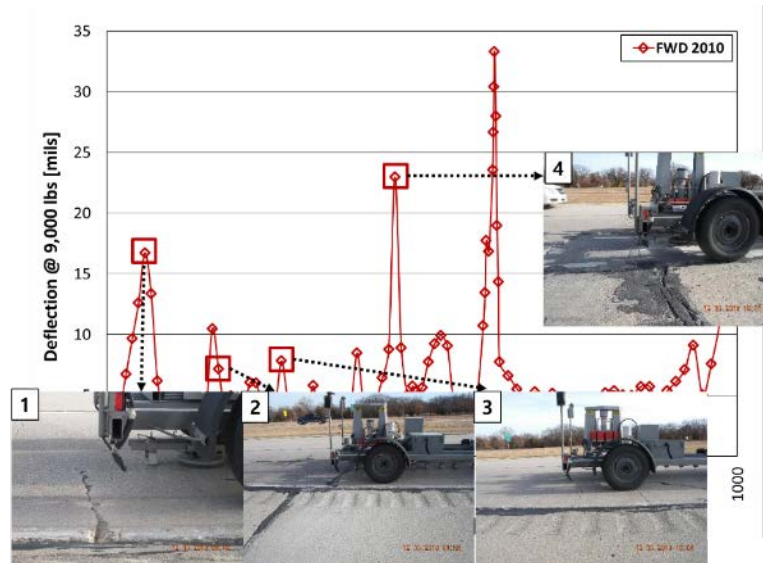


Figure 5.6 FWD deflection with distresses on the existing CRCP

The BCO condition survey was conducted on August 13, 2013, and the pavement condition was compared to the FWD deflections collected on the existing CRCP. At that point, the BCO condition did not meet the traditional definition of “distress,” as there was no segmentation of concrete or severe spalling; however, cracking patterns in the areas of larger deflections in the existing CRCP were not typical cracking in CRCP—cracks were wide and MIRA testing showed delamination at the interface between BCO and existing slab, indicating that distresses were imminent and, as it turned out, distresses developed in those areas. Figure 5.7 shows comparisons between FWD deflections on the existing CRCP and the concrete surface condition on BCO. Figure 5.8 illustrates the relationship between deflections in the existing 8-in. CRCP and the condition of BCO at seven locations. It shows a reasonable relationship between deflections in the existing CRCP measured prior to overlay and BCO condition. It illustrates that BCO condition was good if the deflections in the existing CRCP were less than 4 mils, while delamination occurred where the deflections in the existing CRCP were larger than 7 mils. Although there were no data points for deflections between 4.0 mils and 7.0 mils, 7-mil is recommended as a deflection threshold value at this specific test section—partly because, as discussed in Chapter 4, the bond strength in this section was not adequate. If the bond strength had been adequate, the delamination observed in some locations might not have occurred. This recommended value of 7 mils is applicable only for 4-in. BCO on 8-in. existing CRCP. If the combination of the existing pavement slab thickness and/or overlay thickness is different from this BCO structure (4-in. on 8-in.), the threshold value might be different. However, most of the CRCP sections in Texas that would require BCO in the near future

would have 8-in. or 9-in. slab thickness, at least for a while. Also, as discussed earlier, unless a quite large overlay thickness is used, a small increase in overlay slab thickness might not change the deflection behavior of the BCO system. Also, the threshold value should depend on design traffic. Fortunately, the truck traffic in this section has been quite heavy, even though exact traffic information is not available, and the value derived from this section is considered adequate or somewhat conservative. Accordingly, it is recommended that TxDOT implement this 7-mil threshold value for BCO.

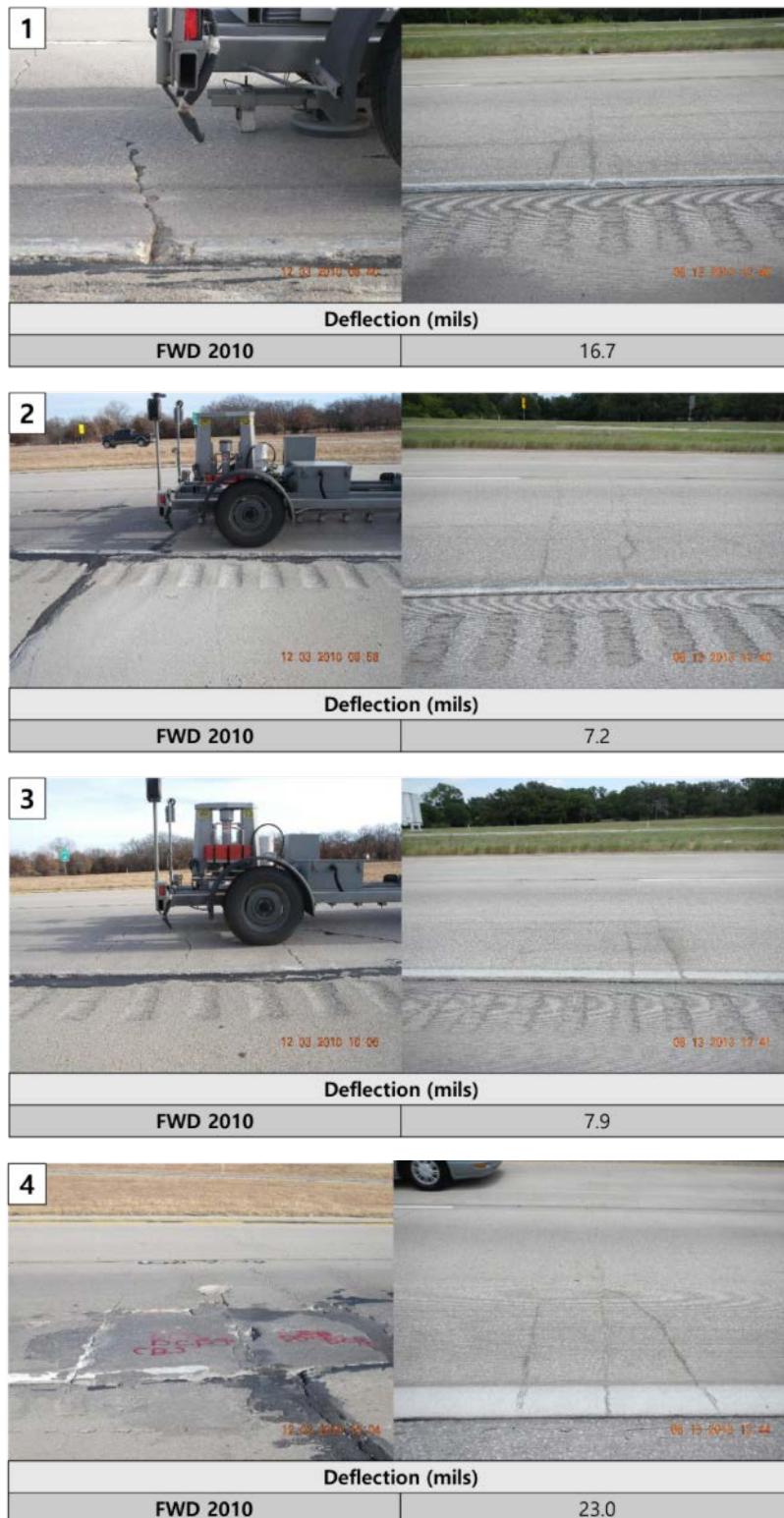


Figure 5.7 Distress comparison between old CRCP and BCO

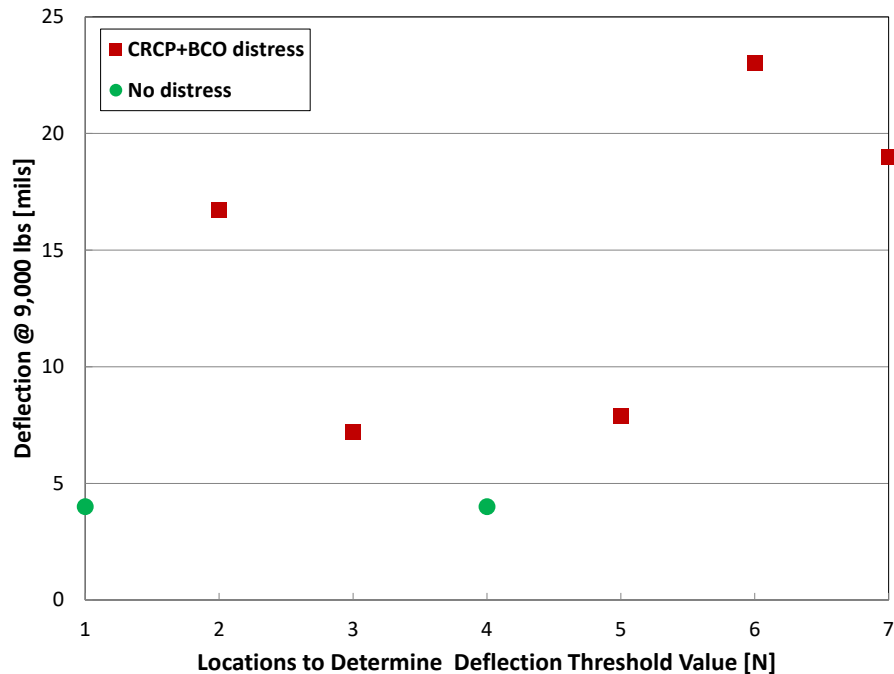


Figure 5.8 FWD deflection with distresses on old CRCP

5.4.2 CRCP BCO on CPCD

As discussed earlier, there is only one CRCP BCO on CPCD in Texas, and the deflection threshold value for CRCP BCO on CPCD was determined from detailed field evaluations and a data analysis of the section (US 75 BCO in Sherman). The performance of US 75 BCO shows quite a unique feature, which is that the majority of the distresses occurred in a section placed on the second day of the outside lane. There were quality control issues during this concrete placement. For example, during placement, some concrete had to be removed and replaced with new concrete due to a difficulty in finishing. **Figure 5.9** shows the condition of BCO, which was removed and replaced. Based on the fact that the majority of the distresses in BCO appeared on the outside lane placed on the second day after the removal of dry concrete, it appears that construction quality issues also contributed to the distress development. It should also be noted that there were numerous distresses in the CPCD in that area even though most of the distresses were repaired prior to BCO construction, which appear to have contributed to the distresses in CRCP BCO.



Figure 5.9 Dry concrete in BCO that was removed and replaced

Figure 5.10 shows a deflection comparison between CPCD and CRCP BCO. BCO distresses and PCCPs to repair distresses in BCO are indicated with black and green hollow squares. This figure indicates a number of distresses and repairs where deflections in CPCD prior to the overlay were actually small (Joints 96 through 120 in Figure 10), which strongly suggests that issues other than structural capacity caused these distresses. Detailed information is not available regarding what actions were taken to prepare the surface of the existing CPCD after the dry concrete had been removed and prior to the placement of new concrete. It is observed that the areas between Joints 122 and 126 had quite large deflections on CPCD, but no distresses in BCO. In that area, there were a number of distresses in CPCD prior to BCO, which explains such large deflections, and those distresses were repaired prior to BCO placement.

Figure 5.11-(a) shows detailed deflection and distress information from Joint #54 to Joint #95. It illustrates six distresses: four distresses occurred where deflections in CPCD were less than 15 mils, while the other two occurred where the deflections in CPCD were more than 20 mils. The four distresses that developed at locations with deflections less than 15 mils appear to be related more with construction quality issues than structural issues. At six locations the deflections are greater than 20 mils; of those, distresses occurred at two locations. Out of 42 transverse contraction joints in the existing CPCD, 36 joints had less than 20 mils of deflection, and out of those 36 joint locations, distresses occurred at 4 locations, which is 11.1% probability of distress—even including the effect of potential quality control issues. On the other hand, there are six joint areas with deflections of more than 20 mils; of those six locations, distresses occurred at two locations, with a 33% probability of distress. Even though no distresses developed at the other four locations, it appears to be reasonable to select 20 mils as a threshold value for CRCP BCO on CPCD. It

should be recognized that this value was developed for 7-in. CRCP BCO; however, the normal range of slab thickness of CRCP BCO on CPCD might not vary from 7-in., and the value of 20 mils is recommended for TxDOT implementation. **Figure 5.11-(b)** illustrates a more detailed plan view description of the conditions of existing CPCD and the locations of distress in CRCP BCO, which shows a strong correlation between distresses in existing CPCD and occurrence of distresses in CRCP BCO.

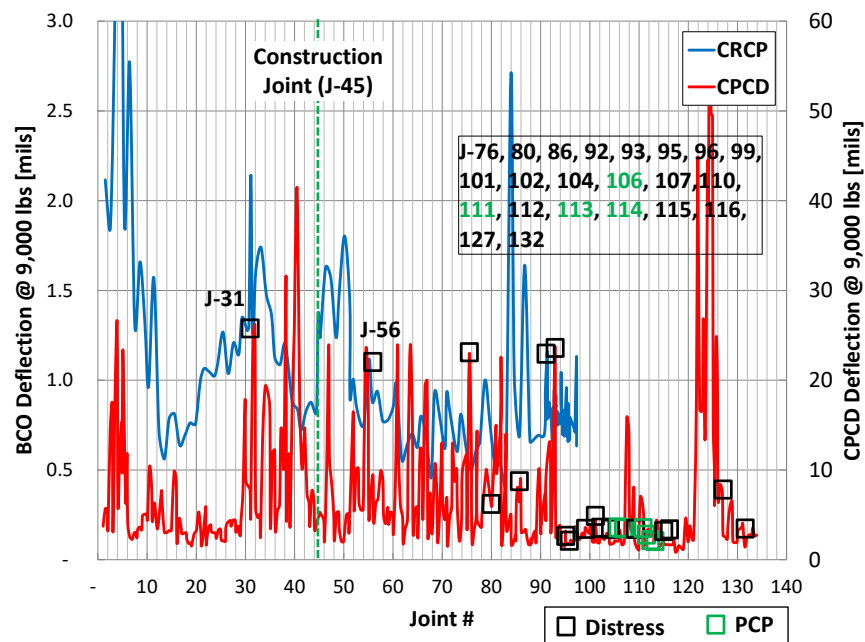
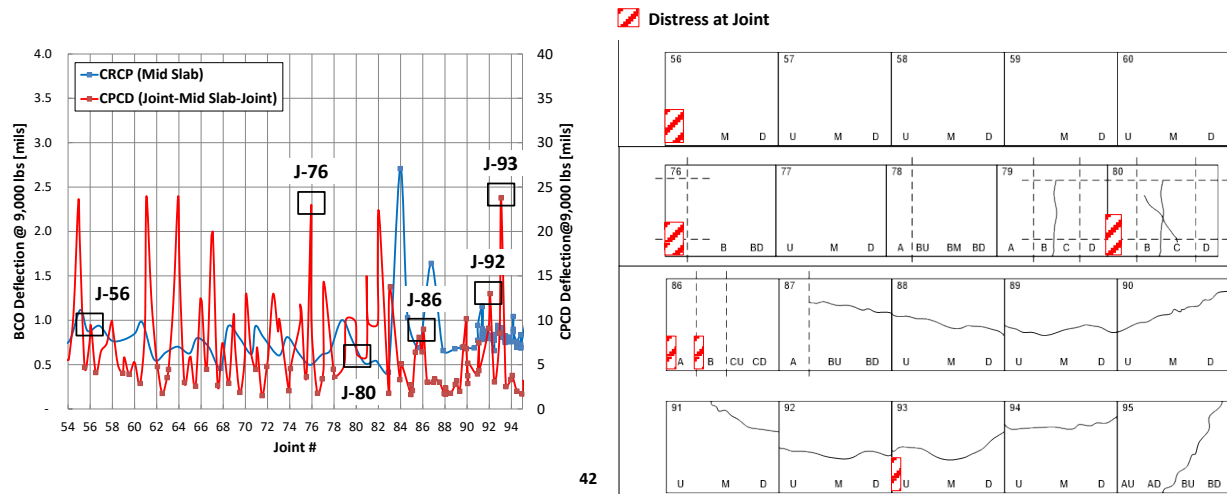


Figure 5.10 Deflection comparison between BCO and CPCD with BCO distresses



a. Deflection vs BCO distress (J-54 to J-94)

b. Distress map

Figure 5.11 Deflection comparison between BCO and CPCD with BCO distresses

5.5 Mechanistic Modeling of CRCP BCO on CRCP

5.5.1 Introduction

This section describes the development of a mechanistic model of debonding failure in CRCP BCO on CRCP and its application to evaluate the effects of certain design parameters on the development of debonding failure. It is essential to understand the exact mechanism of debonding development at the interface between the overlaid concrete and the existing concrete in order to develop an accurate debonding failure prediction model.

Although the number of CRCP BCO projects evaluated in this study are limited, field observations indicate that the heavy traffic loading applications along with deficient slab support in the existing pavement and insufficient bond strength at the interface are the primary causes of debonding failure in CRCP BCO. The US-281 CRCP BCO project in Wichita Falls clearly shows that once a good bonding is provided at the interface, environmental loading itself does not cause debonding in CRCP BCO. However, the traffic volume at this location is relatively smaller than that of the US-287 CRCP BCO site in Bowie. As a result, it is concluded that environmental loading is not a crucial factor affecting debonding failure at later ages in CRCP BCO.

In this section, descriptions of the mechanistic modeling and analysis conducted for debonding failure development are provided first, followed by explanations of how the findings from the mechanistic modeling and analysis were incorporated in the ME CRCP BCO design procedures. The program is called TxBCO-ME.

To validate a probable mechanism of this type of debonding failure, a 3-D mechanistic model was developed and the effects of design parameters on concrete stresses were investigated by

performing a series of analyses with emphasis on evaluating crack spacing on BCO.

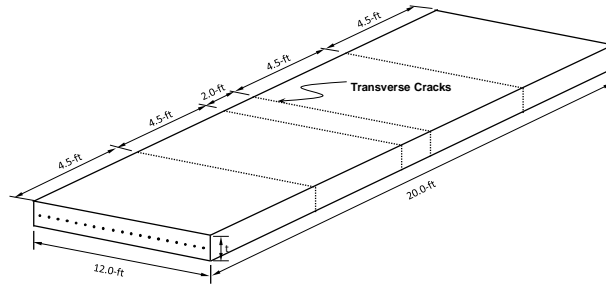
5.5.2 Preliminary Analysis to Determine Geometric Configuration

The geometric configuration of the existing CRCP was employed from the finite element modeling work conducted for the development of TxCRCP-ME program (Ha et al. 2011). The slab is 20-ft long and 12-ft wide. It has transverse cracks spaced 4.5-ft apart except for a spacing of 2-ft in the middle of the slab, as illustrated in Figure 5.12-(a). Two longitudinal ends of the slab were restrained in the longitudinal direction considering the structural characteristics of CRCP. Figures 5.12(a)-(c) show the cases to determine a configuration of BCO causing a critical stress in vertical direction at interface.

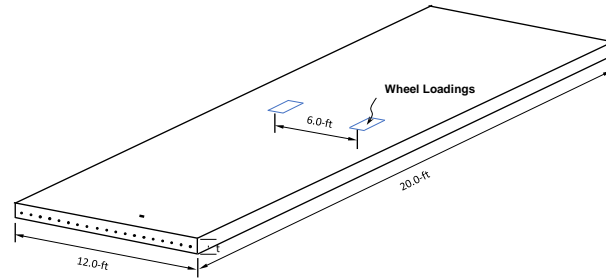
Figure 5.13 shows each modeling and vertical stress analysis results at the interface. The average vertical stresses obtained at the bottom of BCO varied from 99 psi to 103 psi, regardless of BCO geometries. The maximum vertical stresses were also analyzed and they were in a range from 117 psi to 122 psi among four cases. Figure 5.14 presents a vertical stress distribution along the path AA' at the interface with different BCO geometries. The critical stress in the vertical direction occurred at the top of the existing CRCP crack with a range of 1.5 to 2.0-ft away from the center of the wheel path.

Analysis results indicate that a vertical stress at the interface causing debonding failure is highly influenced by the existing CRCP geometry, such as the location of transverse cracking, rather than BCO geometry. A mechanical condition of transverse cracking, called crack stiffness, could also be a crucial factor affecting a critical stress. However, crack stiffness was assumed to be almost zero to simulate severely deteriorated transverse cracks in this analysis. Accordingly, in the existing CRCP, it is assumed that a traffic loading is transferred by longitudinal steel only at transverse cracks. A sensitivity analysis for crack stiffness variation was made for case #1 to provide a reference for the five different levels of crack stiffness, and the results were illustrated in Figure 5.15. As expected, as the crack stiffness decreases, the vertical stress increases. When the crack stiffness exceeds the value of 1.0×10^7 psi/in., transverse cracks appear to behave as mechanically fully-connected condition. In other words, it can be stated that crack stiffness is a critical factor for determining CRCP BCO performance. Also, a large deflection caused by deficient slab support or a low modulus of subgrade reaction along with heavy truck loading applications could cause a large vertical stress at interface, causing delaminations.

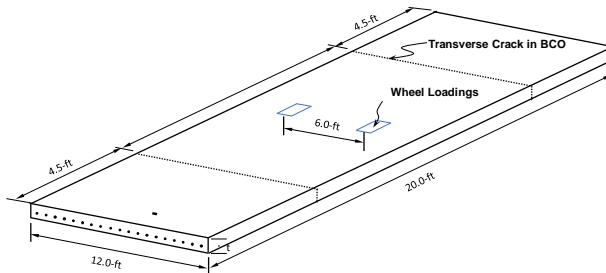
Again, it is noted that 1) a critical stress causing debonding failure at the interface does not vary significantly regardless of BCO geometries and 2) a debonding mechanism in CRCP BCO system is governed by the existing CRCP conditions, such as crack stiffness and the slab support under the existing CRCP.



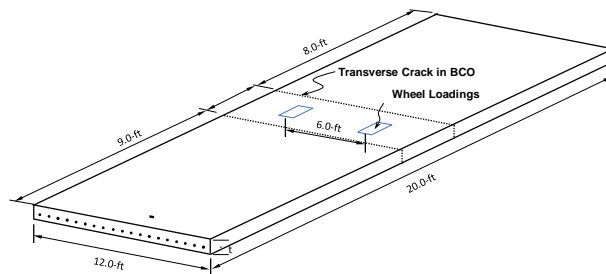
(a) Geometric configuration of the existing CRCP



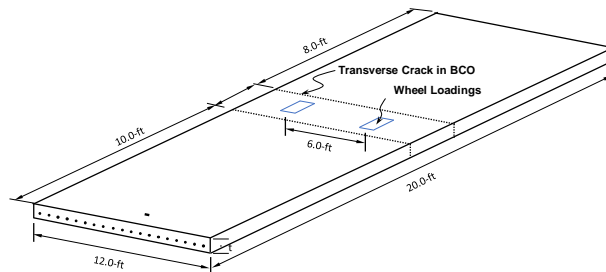
(b) BCO configuration: Case #1 (0-20-0)



(c) BCO configuration: Case #2 (4.5-11-4.5)

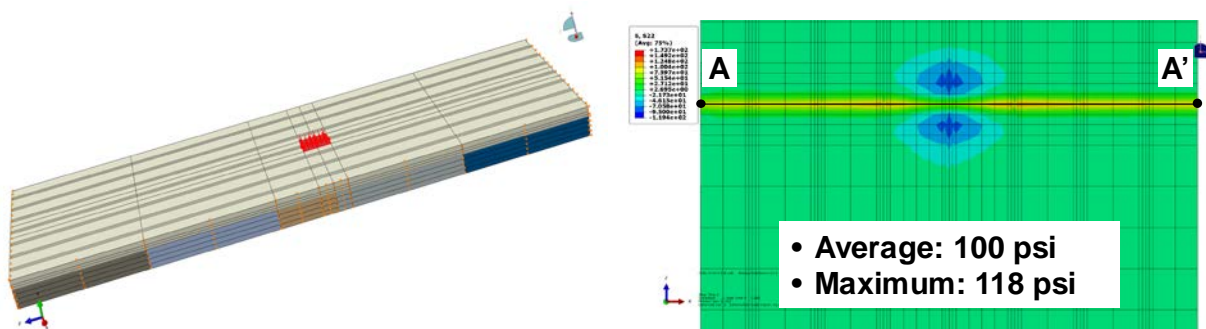


(d) BCO configuration: Case #2 (8-3-9)

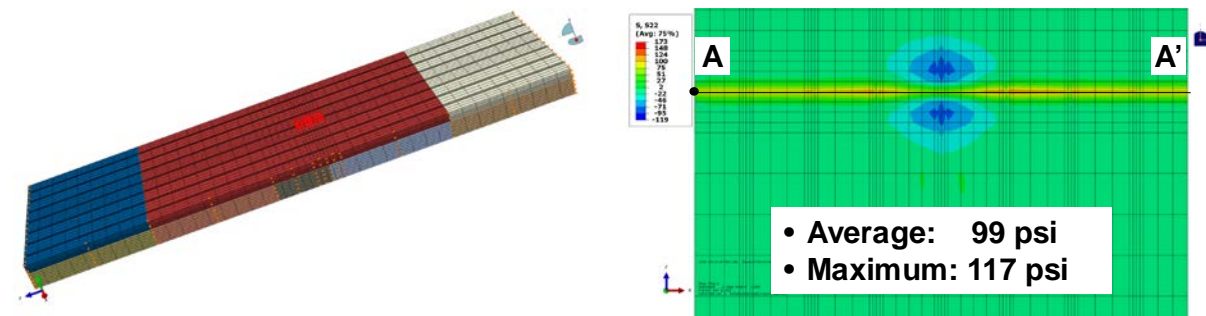


(e) BCO configuration: Case #3 (8-2-10)

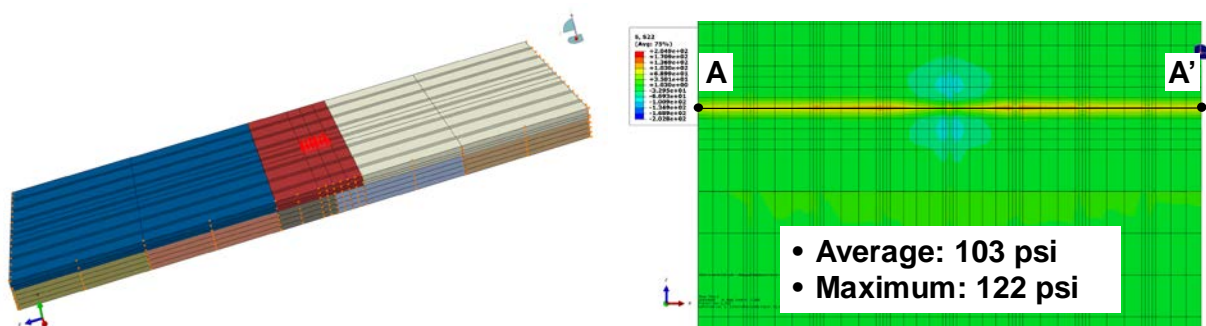
Figure 5.12 Geometric configuration for the existing CRCP and BCOs



(a) Modeling for case #1 (0-20-0), vertical stress at interface



(b) Modeling for case #2 (8-3-9), vertical stress at interface



(c) Modeling for case #3, vertical stress at interface

Figure 5.13 Structural modeling and preliminary analysis results

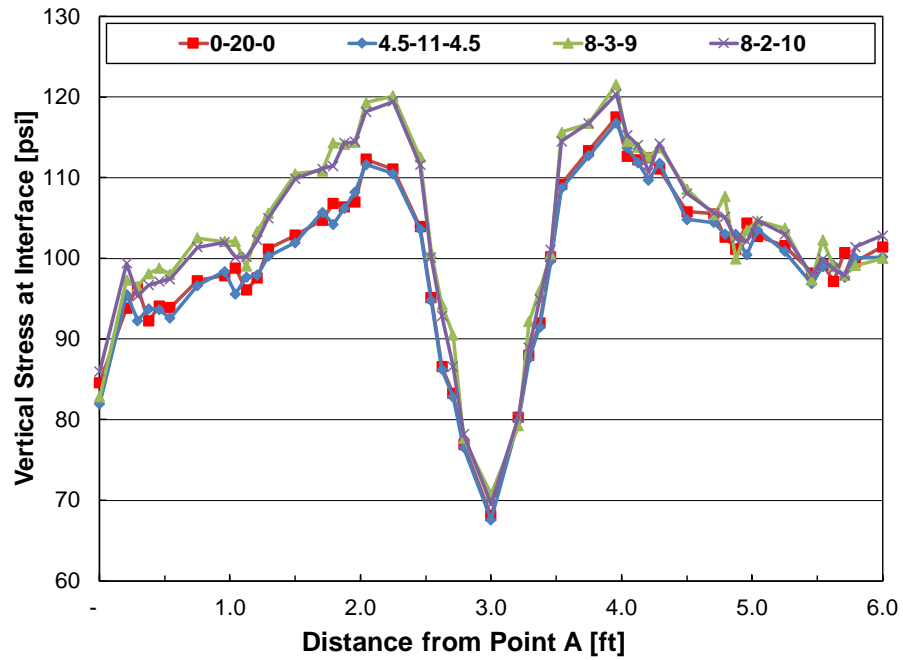


Figure 5.14 Vertical stress distribution along path AA'

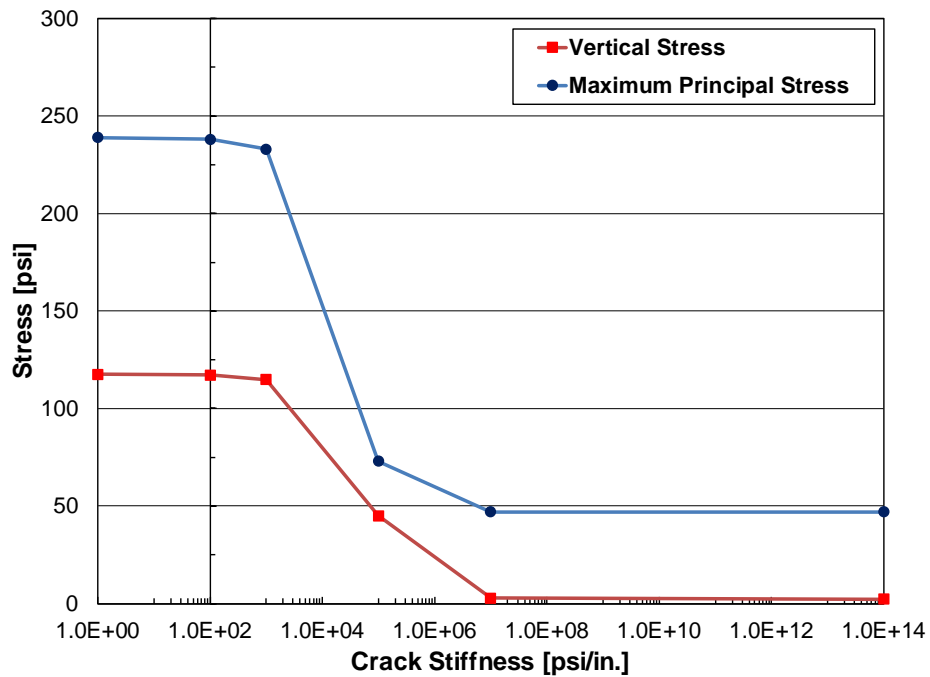


Figure 5.15 Vertical and principal stresses due to crack stiffness variation

5.5.3 Development of Mechanistic Modeling for CRCP BCO on CRCP

5.5.3.1 Finite Element Modeling

As discussed earlier, BCO distress starts from debonding at the interface between existing slab and overlaid slab. **Figure 5.16** shows a selected geometric configuration of CRCP BCO on CRCP from the preliminary analysis.

To modify a bonding condition at the interface between BCO and existing CRCP, surface-to-surface contact (surfaced-based cohesive behavior) of zero thickness was used. The surfaced-based cohesive behavior defines a relation between traction-separation constitutive behavior across the interface. The similarities extend to the linear elastic traction-separation model, damage initiation criteria, and damage evolution laws. Concepts of strain and displacement (used in behavior model formulae for cohesive elements) are reinterpreted as contact separations; contact separations are the relative displacements between the nodes on the slave surface and their corresponding projection points on the master surface along the contact normal and shear directions. Stresses are defined for surface-based cohesive behavior as the cohesive forces acting along the contact normal and shear directions divided by the current area at each contact point. The relation between shear traction and shear relative displacement describes bond-slip behavior. The relation between normal traction and normal relative displacement describes debonding behavior.

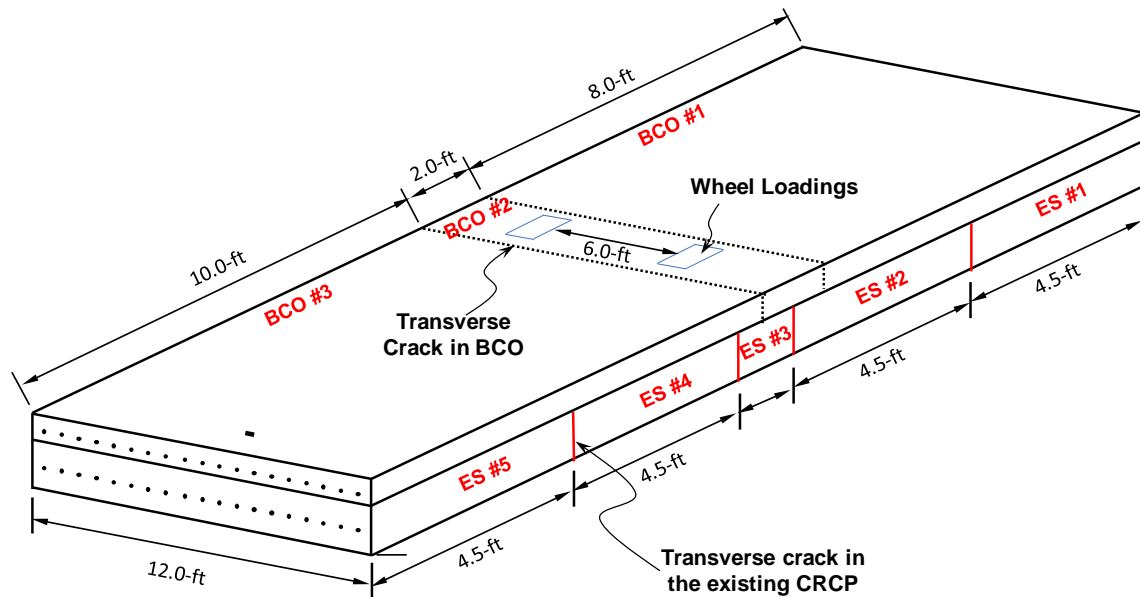


Figure 5.16 CRCP BCO on CRCP configuration

In most 3-D numerical approaches, spring or beam elements have been used to model reinforcing steel as described in **Figure 5.17-(a)** and summarized in the reference (Shoukry et al. 2007). Although these simplified 3-D models are certainly more advanced in comparison with two-dimensional models, their use can only be justified when predicting the overall behavior of cracked

CRCP and/or doweled CPCD. This is because modeling of reinforcing steel with beam elements cannot consider the Poisson effect, and this may cause stress localization problems around the reinforcing steel in the concrete. If the modeling objective includes the examination of concrete stresses developed around the reinforcing steel, detailed 3-D modeling of reinforcing steel using solid elements is essential (Ha et al. 2011). However, this modeling takes more effort and computation time due to the requirement of using very fine meshes. Accordingly, the concrete slab shown in Figure 5.16 was analyzed using a 3-D finite element model that utilizes only solid elements for modeling reinforcing steel as well as the concrete, as illustrated in Figure 5.17-(b).

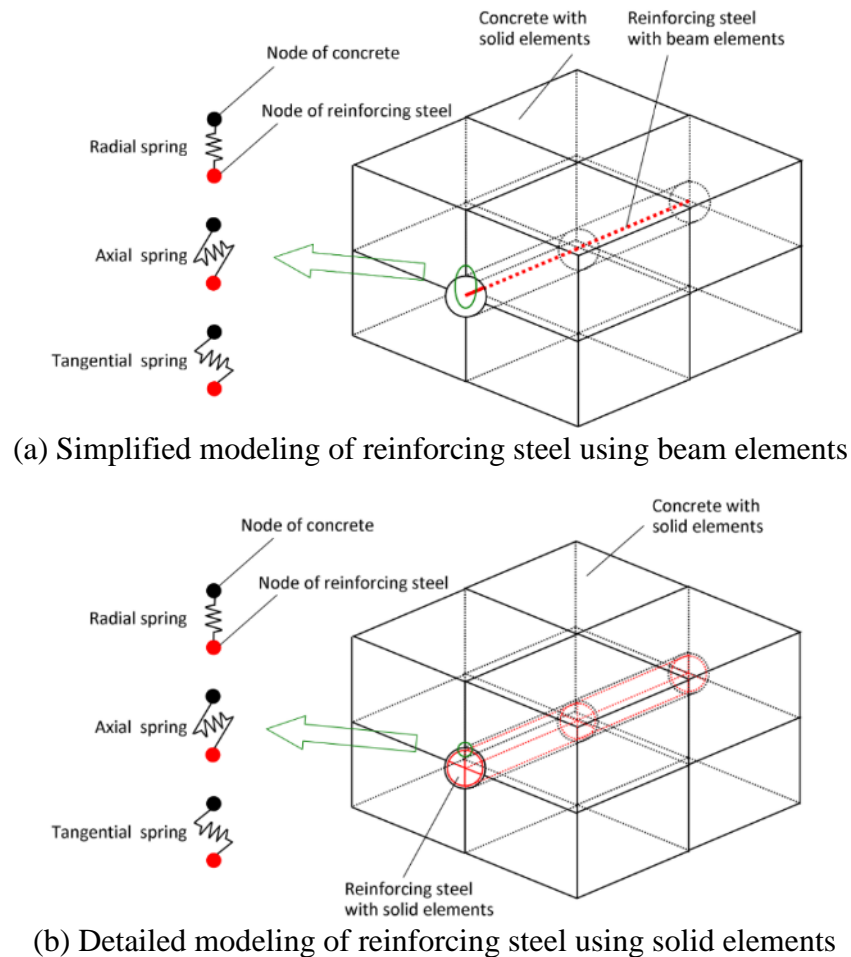
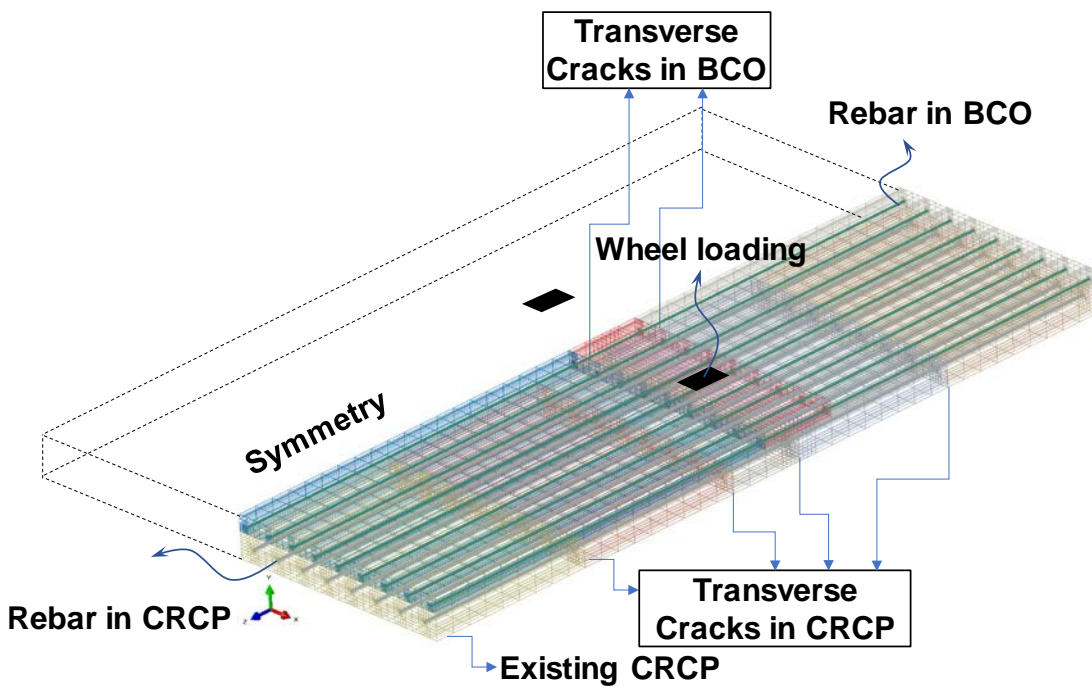


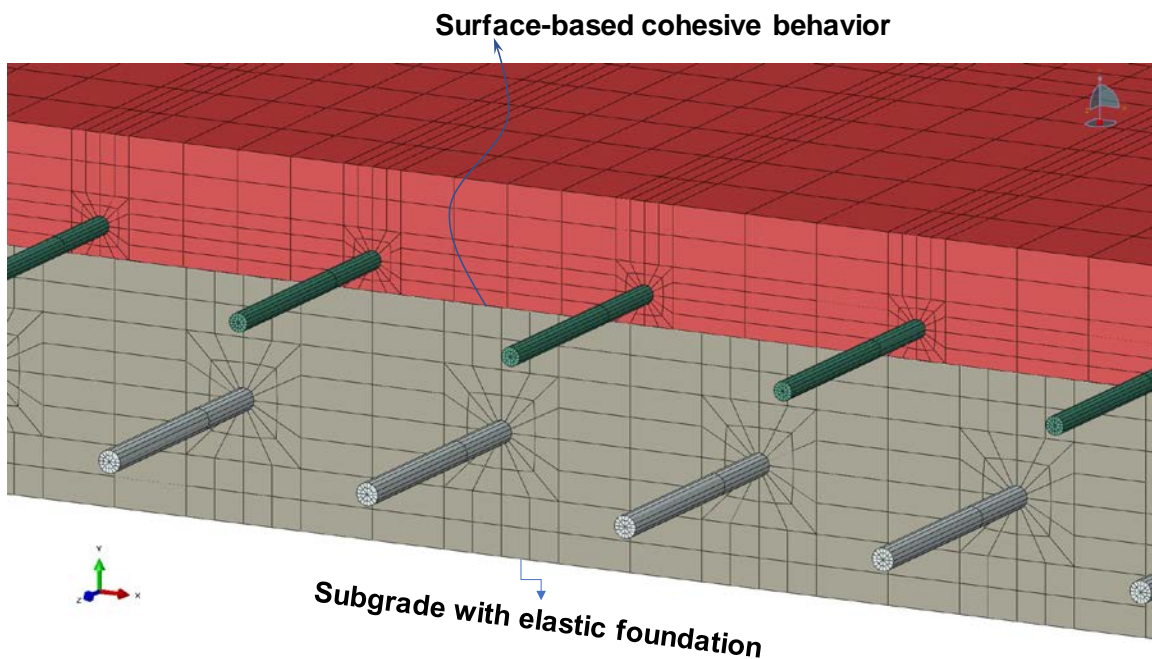
Figure 5.17 Modeling of reinforcing steel and its interface with surrounding concrete

Figure 5.18 shows the finite element mesh model of CRCP BCO on CRCP. A half model of the concrete slab was used to take advantage of symmetry along the transverse axis. The eight-node linear brick elements with incompatible nodes were used in the mesh representation of concrete, rebar, and dowel bar. The interactions between longitudinal steel and surrounding concrete were modeled with surfaced-based cohesive model which is an interaction type of surface-to-surface contact. The surface-to-surface behavior, which is equivalent to a series of spring elements, is

placed between the faces of concrete and longitudinal steel elements. The modulus of subgrade reaction was modeled with an interaction type of elastic foundation.



(a) A half model of the concrete slab



(b) Zoomed-in shaded view

Figure 5.18 Finite element mesh model for CRCP BCO

5.5.3.2 Material Properties and Traffic Loading

The elastic modulus, Poisson's ratio, and the CoTE of concrete were assumed to be 4×10^6 psi, 0.15, and 4.0×10^{-6} /°F, respectively. The elastic modulus, Poisson's ratio, and the CoTE of steel were assumed to be 2.9×10^7 psi, 0.30, and 6.4×10^{-6} /°F, respectively. Longitudinal steel with a diameter of 0.75-in. (#6 bar) was placed at mid-depth for the existing CRCP. In BCO, a diameter of 0.75-in. (#6 bar) rebar was placed at different depths with BCO thickness in accordance with the BCO design standards developed in this research.

Table 5.1 shows the values used for normal stiffness, shear stiffness, and tangential stiffness at each interface. A relatively large normal stiffness was assigned to simulate fully bonded condition at the interface between BCO and the existing CRCP.

The interface between the BCO and existing CRCP was modeled to reflect the surfaced-based cohesive behavior.

As for traffic loading, two 9-kip wheel loadings were applied in the wheel path. They are 6-ft apart and located at the middle of 2-ft BCO slab, which is the position of the transverse crack in the middle of the existing CRCP. Each wheel loading is uniformly distributed over a square that is equal in area to a circle with a radius of 6-in.

Table 5.1 Values for normal stiffness and shear stiffness at each interface

| Type of interface | Normal stiffness (K_{nn}) [psi/in.] | Shear stiffness (K_{ss}) [psi/in.] | Shear stiffness (K_{tt}) [psi/in.] |
|--------------------|---|--|--|
| Concrete and rebar | 1×10^{10} | 7×10^5 | 3×10^5 |
| BCO and CRCP | 1×10^{14} | 1×10^7 | 1×10^7 |
| Transverse crack | 1×10^0 | 1×10^0 | 1×10^0 |

5.5.3.3 Variables Selected for Sensitivity Analysis

The effects of design parameters, material properties, and environmental conditions on the behavior of concrete slabs were analyzed through parametric studies. The evaluations were conducted for different slab thicknesses of the existing CRCP (E_h), different BCO thicknesses (B_h), and the moduli of subgrade reaction (K_v). These influencing factors are illustrated in **Table 5.2**. **Table 5.3** shows analysis cases generated from changes in each influencing factor.

As for thermal loading, third-order nonlinear negative thermal gradients at -1.5°F per inch of slab thickness were assumed (Choi et al. 2009). According to a TxDOT research 0-5832 findings, negative gradients are the critical loading condition with wheel loadings. According to the sensitivity analysis for wheel loading location, critical stress increases when the wheel loading position is closer to the crack. Three levels of the BCO thicknesses—4, 5, and 6 inches—were

analyzed, and three levels of the existing CRCP thicknesses—8, 10, and 12 inches—were also analyzed.

Table 5.2 Variables for sensitivity analysis (CRCP BCO on CRCP)

| Parameters | Values |
|--|-----------------------------------|
| Existing slab thickness (in.) | 8, 10, and 12 |
| Overlay slab thickness in CRCP BCO over CRCP (in.) | 4, 5, and 6 |
| Modulus of subgrade reaction (psi/in.) | 50, 100, 200, 300, 500, and 1,000 |
| Change in concrete temperature | -1.5°F / in. (negative gradient) |

Table 5.3 Analysis cases (CRCP BCO on CRCP)

| Slab Thickness | | CoTE of Concrete α_c , [$\times 10^{-6}/^{\circ}\text{F}$] | Case Number | | | | | |
|--------------------------------|----------------------|--|---|-----|-----|-----|-----|------|
| | | | Modulus of Subgrade Reaction K_v , [psi/in.] | | | | | |
| Existing CRCP E_h , [in.] | BCO B_h , [in.] | | 50 | 100 | 200 | 300 | 500 | 1000 |
| 8 | 4 | 4.0 | 1 | 2 | 3 | 4 | 5 | 6 |
| | 5 | 4.0 | 7 | 8 | 9 | 10 | 11 | 12 |
| | 6 | 4.0 | 13 | 14 | 15 | 16 | 17 | 18 |
| 10 | 4 | 4.0 | 19 | 20 | 21 | 22 | 23 | 24 |
| | 5 | 4.0 | 25 | 26 | 27 | 28 | 29 | 30 |
| | 6 | 4.0 | 31 | 32 | 33 | 34 | 35 | 36 |
| 12 | 4 | 4.0 | 37 | 38 | 39 | 40 | 41 | 42 |
| | 5 | 4.0 | 43 | 44 | 45 | 46 | 47 | 48 |
| | 6 | 4.0 | 49 | 50 | 51 | 52 | 53 | 54 |

5.5.4 Numerical Results for CRCP BCO on CRCP

5.5.4.1 Response to Traffic Loading

For the CRCP BCO on CRCP analysis, 9-kips wheel loading with 79.6 psi tire pressure was applied. The preliminary analysis results revealed that the main causes of critical stress in the vertical direction at the interface are related to a large deformation of the existing CRCP. To simulate the effect of CRCP deformation, five different levels of k -values were analyzed for each case.

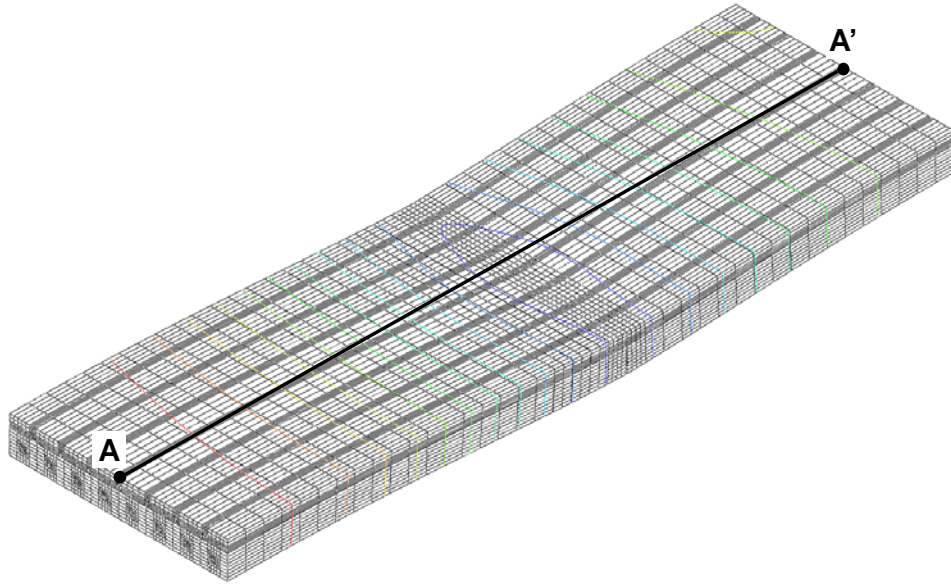
The 8-inch-thick concrete slab was analyzed assuming the modulus of subgrade reaction to be 50 psi/in. (Case 1). **Figure 5.19** shows the deformed shape—magnified by 1,000 times—and deflection along the path AA'. The maximum deflection occurs at the middle of BCO #2, which is at a transverse crack in the existing CRCP. Analysis results show that a deflection increases

significantly as the k-value decreases.

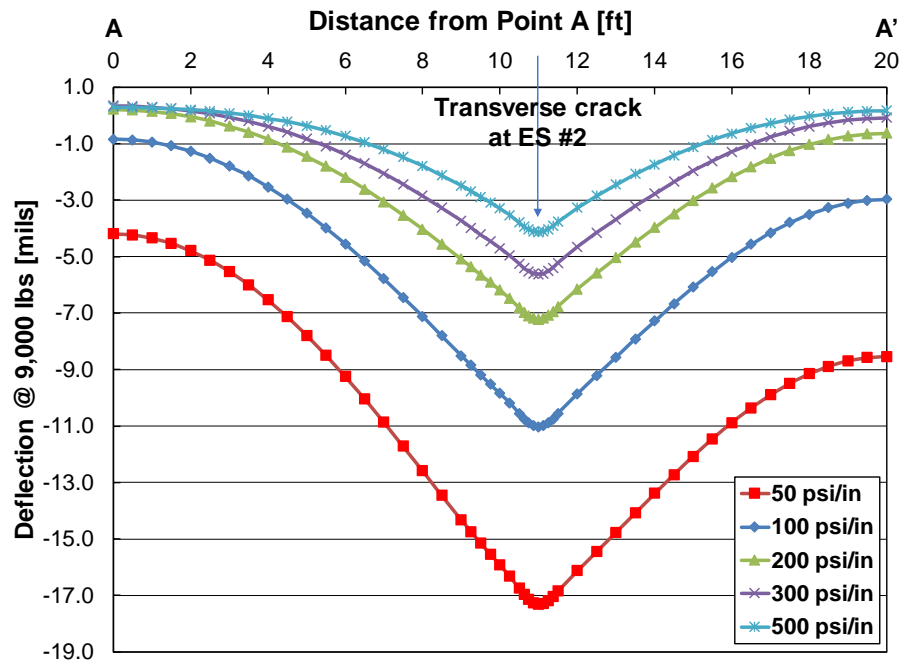
Figure 5.20 shows the distribution of vertical stresses at the middle of BCO #2. A stress contour map clearly shows that the relatively large vertical stresses caused by slab deformation are distributed around the interface and concentrated near the wheel loading location. Accordingly, one of the most effective ways to reduce vertical stress induced by slab deformation can be an increase of BCO thickness. However, from a practical standpoint, an increase of BCO thickness will increase initial construction and potentially cause problems in bridge clearance. Rather, a better way to control an excessive slab deformation could be to limit the deflections in the existing CRCP by specifying a threshold deflection value when evaluating and selecting a rehabilitation option. In this study, the deflection threshold value for a specific project, US 287 in Bowie, is suggested as 7 mils considering field performance.

Since only three CRCP BCO projects are evaluated in this study, where the BCO thicknesses are smaller than or equal to 4-in., the development of a reasonable transfer function may not be feasible that could be employed in design procedures. Once a number of BCOs are placed and evaluated, an accurate transfer function of BCO distress should be developed and included in the design program, as the transfer function has much more significant effect on the accuracy and reasonableness of any ME-based design programs than any other elements.

Figures 5.21-(a) and (b) illustrate vertical stress distributions for the 4-in. BCO over 10-in. and 12-in. existing CRCP systems. The vertical stress due to wheel loading decreases significantly as the slab thickness of the existing CRCP increases, which is due to a decreased slab deformation at interface compared with the 4-in. BCO plus 8-in. CRCP system. They also illustrate the rather large effects of modulus of subgrade reaction on the vertical stresses.

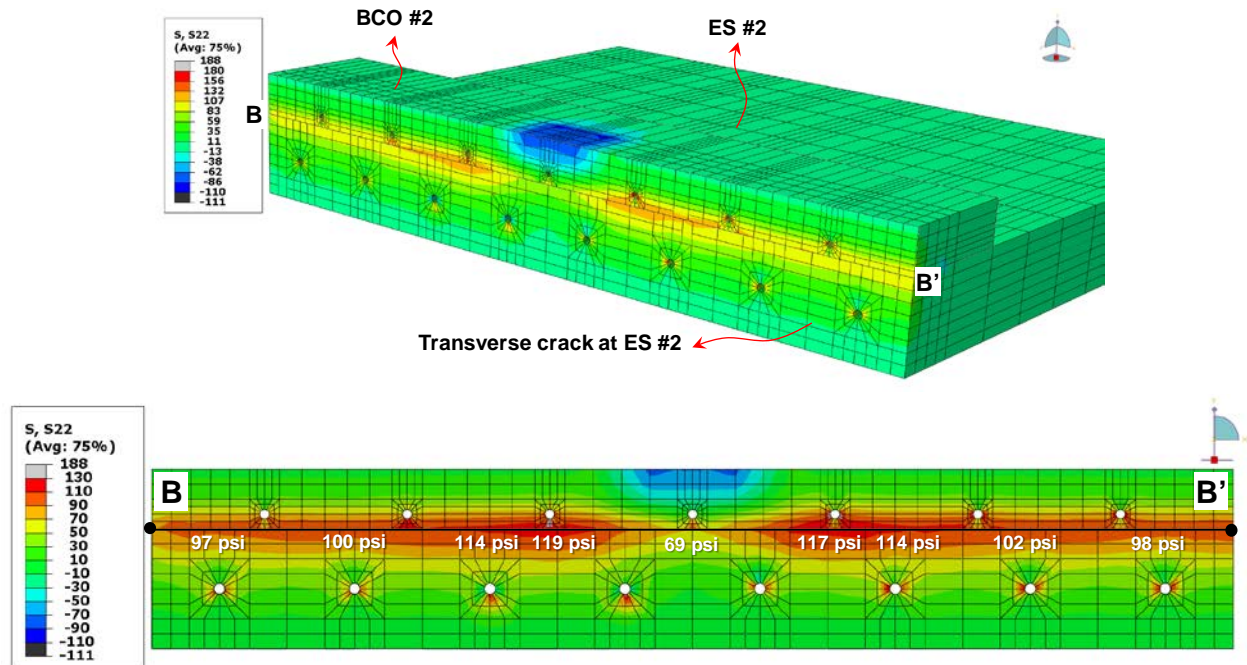


(a) Deformed shape

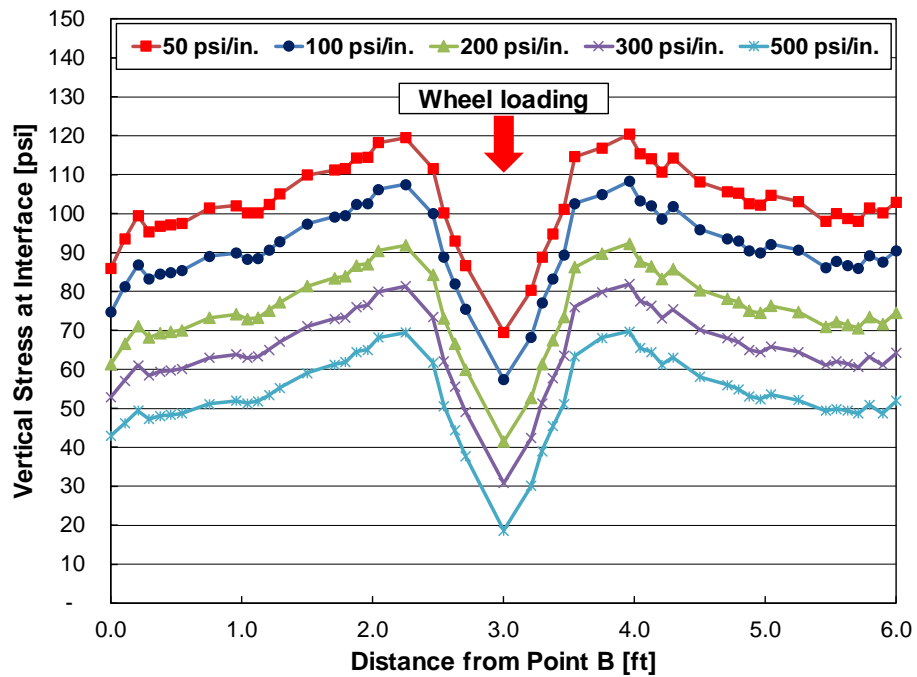


(b) Surface deflection along the path AA'

Figure 5.19 Deformed shape and surface deflection

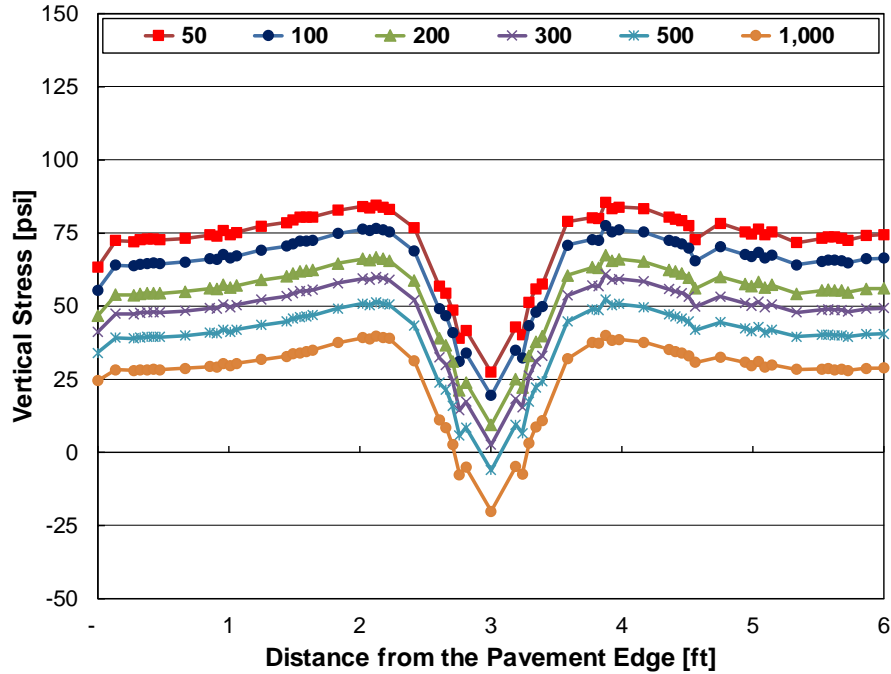


(a) Vertical stress contour (4-in. BCO + 8-in. CRCP: 4B-8E, $k = 50$ psi/in.)

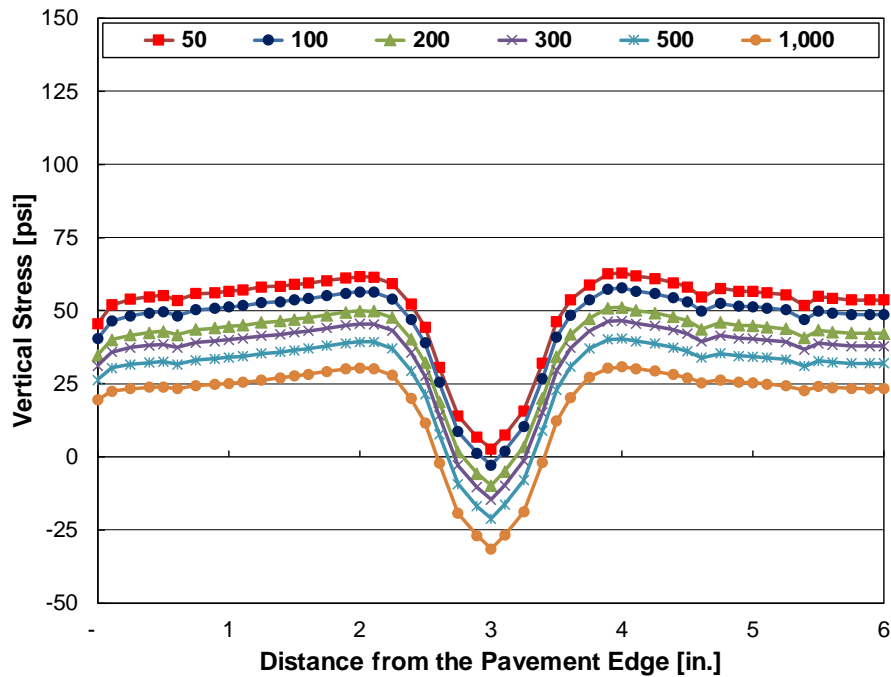


(b) Vertical stress distribution at interface along the path BB' (4B-8E)

Figure 5.20 Vertical stress at interface (4B-8E)



(a) Vertical stress distribution at interface (4-in. BCO + 10-in. CRCP: 4B-E10)



(b) Vertical stress distribution at interface (4-in. BCO + 12-in. CRCP: 4B-12E)

Figure 5.21 Vertical stress at interface (4B-E10 and 4B-12E)

5.5.4.2 Responses to Environmental Loading

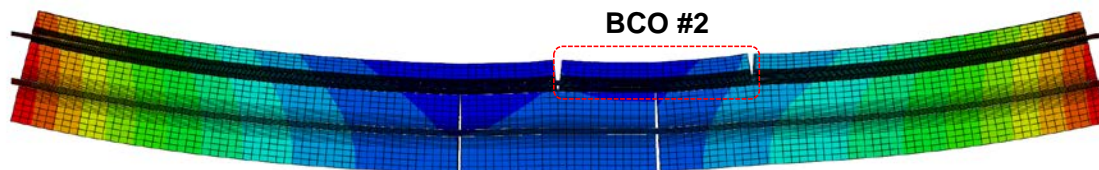
Analysis of wheel loading showed that the vertical stresses in tension were induced at the middle of the bottom of BCO #2 along a transverse crack in CRCP. Stress due to temperature loading was

also evaluated at the same location.

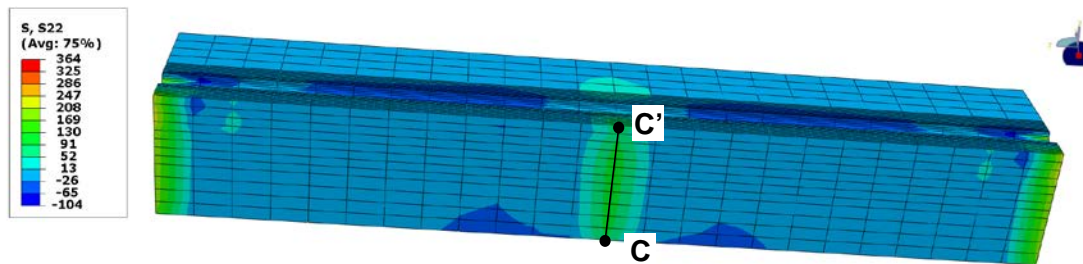
A 4-in. BCO over 10-in. thick CRCP subjected to environmental loading was analyzed by changing the temperature variation along the CRCP slab depth.

Figures 5.22-(a) and (b) show the deformed shape—magnified by 1,000 times—and stress contour at the bottom of BCO #2. The principal stresses were induced in the concrete around longitudinal steel at transverse cracks, and the vertical tensile stresses were also induced at the middle of BCO #2 because of the effect of the existing CRCP deformation.

Figure 5.23 illustrates the effect of the k-value variation on thermal stresses induced by environmental loading with the negative thermal gradient. As shown in Figure 5.23-(b), an increase of the k-value decreases the vertical stresses.

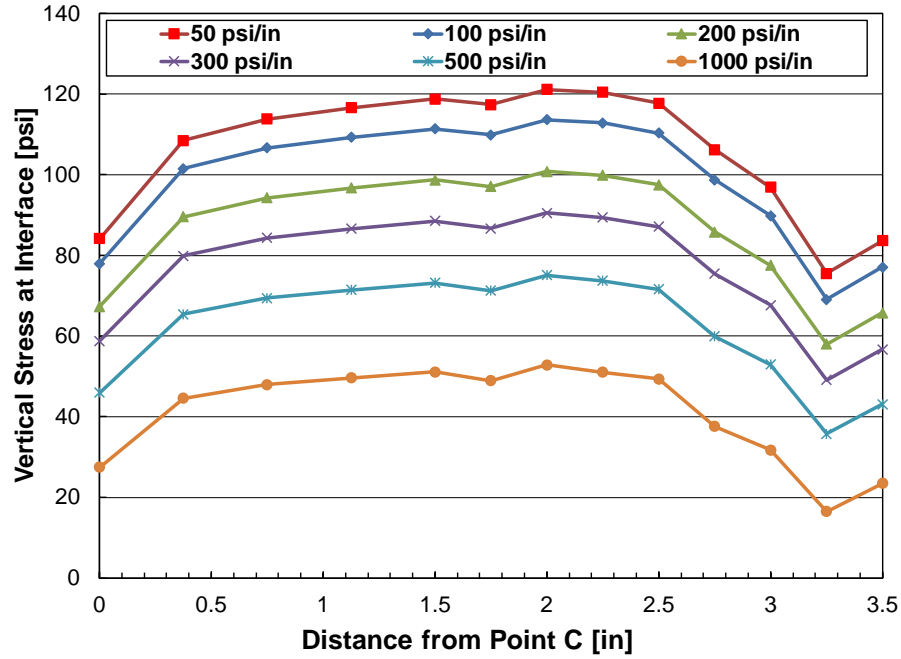


(a) Deformed shape (magnified 1,000 times)

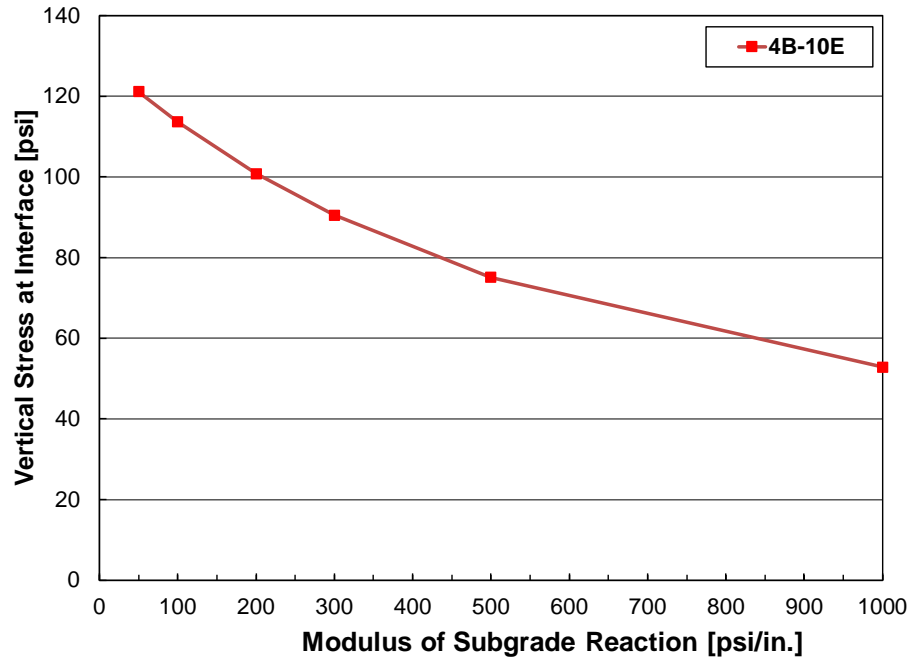


(b) Vertical stress distribution in BCO #2

Figure 5.22 Deformed shape and vertical stress distribution in BCO #2 (4B-10E)



(a) Stress distribution along path CC'



(b) Stresses due to variation of modulus of subgrade reaction

Figure 5.23 Effect of k-value variation on stress induced by the negative temperature loading (3B-10E)

5.6 Mechanistic Modeling of CRCP BCO on CPCD

5.6.1 Development of mechanistic modeling for CRCP BCO on CPCD

5.6.1.1 Finite Element Modeling

Figure 5.24 shows the system of CRCP BCO on CPCD and details such as steel and dowel configuration, spacing, and wheel loading locations.

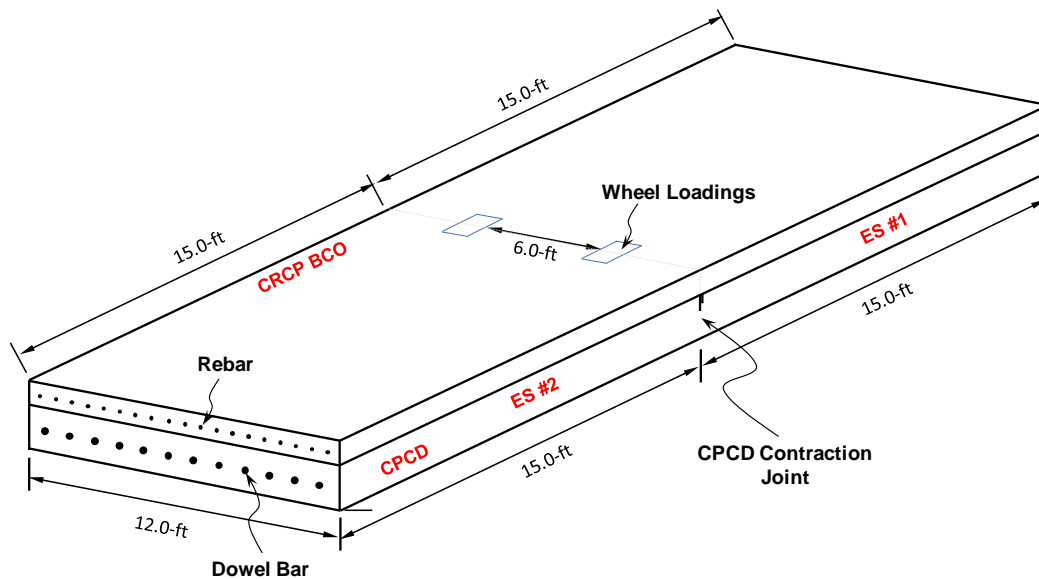
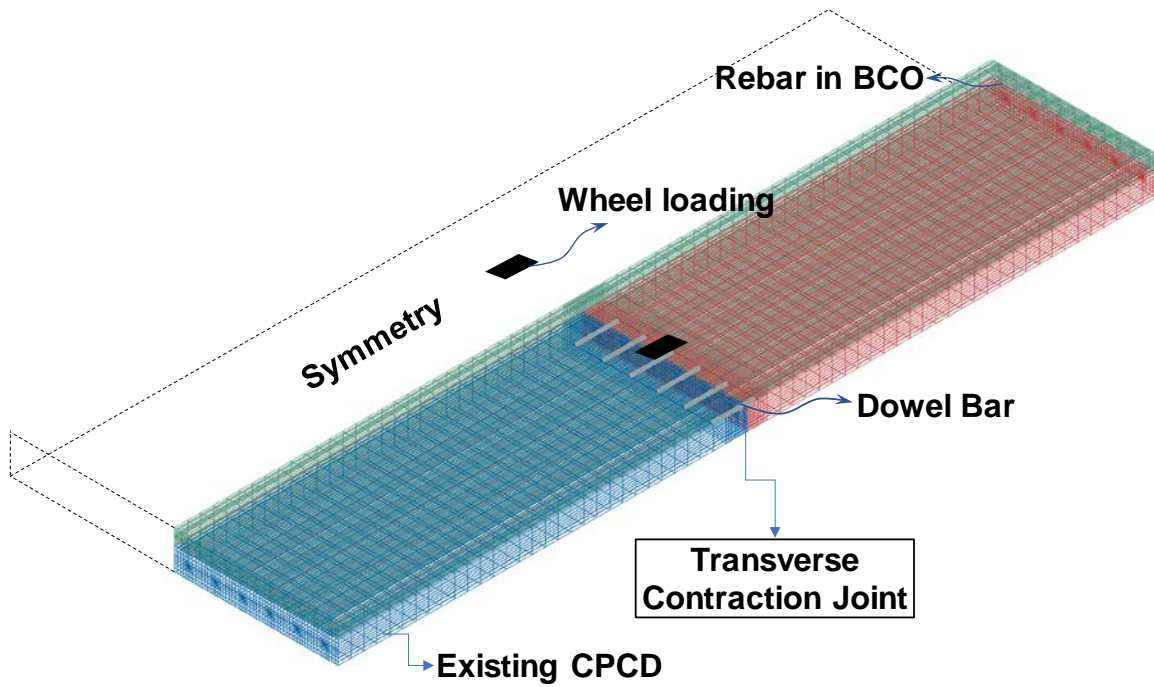


Figure 5.24 CRCP BCO on CPCD configuration

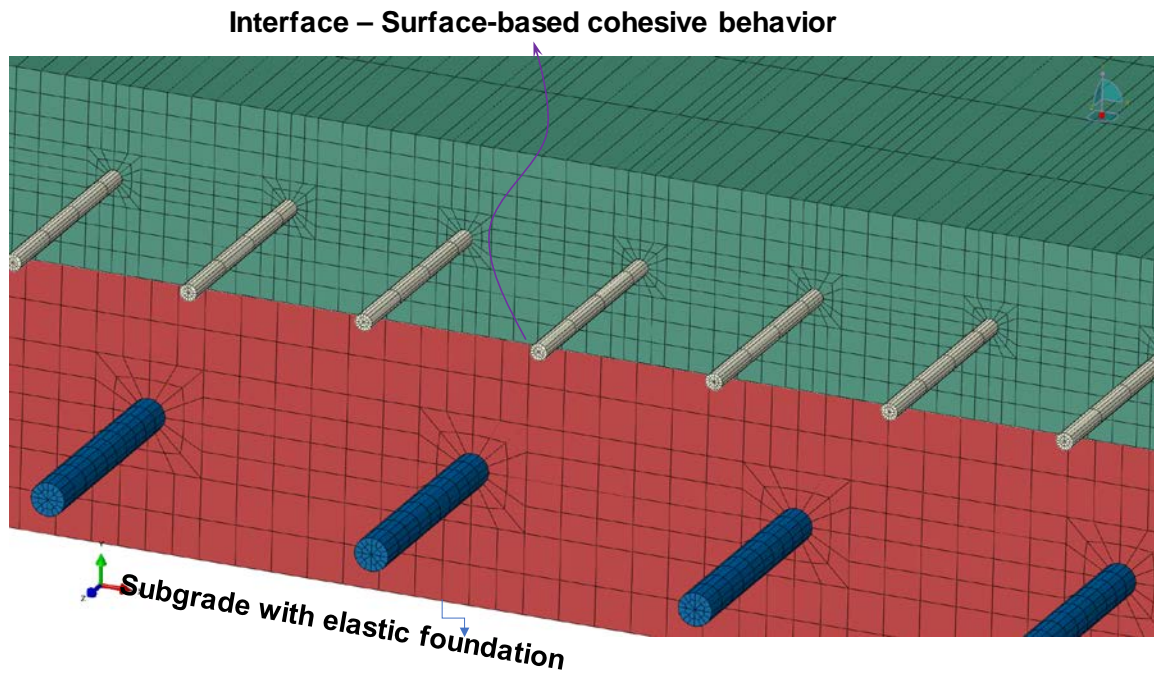
Figure 5.25 shows the finite element mesh model of CRCP BCO on CPCD. A half model of the concrete slab was also used to take advantage of the symmetry along the transverse axis, similar to the modeling of CRCP BCO on CRCP. The eight-node linear brick elements with incompatible modes were used in the mesh representation of concrete, rebar, and dowel bar.

The interactions between longitudinal steel and surrounding concrete were modeled with a surface-based cohesive model, which is an interaction type of surface-to-surface contact. The surface-to-surface behavior, which is equivalent to a series of spring elements, is placed between the faces of concrete and longitudinal steel elements.

The modulus of subgrade reaction was modeled with an interaction type of elastic foundation.



(a) A half model of the concrete slab



(b) Zoomed-in shaded view

Figure 5.25 Finite element mesh model for CRCP BCO on CPCD

5.6.1.2 Material Properties

The material properties used in this modeling and analysis are the same as those with CRCP BCO

on CPCD analysis. The elastic modulus, Poisson's ratio, and the CoTE of dowel bar was also assumed to be 2.9×10^7 psi, 0.30 and $6.4 \times 10^{-6}/^\circ\text{F}$, respectively. A dowel bar with a diameter of 1.0-in. was placed at mid-depth for the existing CPCD. In BCO, a diameter of 0.75-in. rebar (#6 bar) was placed at the mid-depth in BCO.

As for traffic loading, two 9-kip wheel loadings were applied in the wheel path. Each wheel loading is uniformly distributed over a square that is equal in area to a circle with a radius of 6-in.

5.6.1.3 Variables for Sensitivity Analysis

The effects of the k-values and slab thicknesses on the behavior of concrete slabs were analyzed through parametric studies. The evaluations were conducted for different slab thicknesses of the existing CPCDP (E_h), different BCO thicknesses (B_h), and the moduli of subgrade reaction (K_v). These selected factors are shown in Table 5.4. Table 5.5 shows analysis cases generated from changes in the K_v values and slab thicknesses.

As for thermal loading, third-order nonlinear negative thermal gradients at -1.5°F per inch of slab thickness were assumed (Choi et al. 2009). The four levels of the BCO thicknesses and three levels of existing CPCD were selected.

Table 5.4 Variables for sensitivity analysis (CRCP BCO on CPCD)

| Parameters | Values |
|--|---|
| Existing slab thickness (in.) | 10, 11, and 12 |
| Overlay slab thickness in CRCP BCO (in.) | 7, 8, 9, and 10 |
| Modulus of subgrade reaction (psi/in.) | 50, 100, 200, 300, 500, and 1,000 |
| Change in concrete temperature | $-1.5^\circ\text{F} / \text{in.}$ (negative gradient) |

Table 5.5 Analysis cases (CRCP BCO on CPCD)

| Slab Thickness | | CoTE of Concrete $\alpha_c, [\times 10^{-6}/^{\circ}\text{F}]$ | Case Number | | | | | |
|--------------------------------------|----------------------------|---|--|-----|-----|-----|-----|------|
| | | | Modulus of Subgrade Reaction $K_v, [\text{psi}/\text{in.}]$ | | | | | |
| Existing CPCD $E_h, [\text{in.}]$ | BCO $B_h, [\text{in.}]$ | | 50 | 100 | 200 | 300 | 500 | 1000 |
| 10 | 7 | 4.0 | 55 | 56 | 57 | 58 | 59 | 60 |
| | 8 | 4.0 | 61 | 62 | 63 | 64 | 65 | 66 |
| | 9 | 4.0 | 67 | 68 | 69 | 70 | 71 | 72 |
| | 10 | 4.0 | 73 | 74 | 75 | 76 | 77 | 78 |
| 12 | 7 | 4.0 | 79 | 80 | 81 | 82 | 83 | 84 |
| | 8 | 4.0 | 85 | 86 | 87 | 88 | 89 | 90 |
| | 9 | 4.0 | 91 | 92 | 93 | 94 | 95 | 96 |
| | 10 | 4.0 | 97 | 98 | 99 | 100 | 101 | 102 |

5.6.2 Numerical Results for CRCP BCO on CPCD

5.6.2.1 Response to Traffic Loading

In this analysis, the stress causing reflection cracks was analyzed because the first phenomenon of distress for CRCP BCO on CPCD could be initiated from the reflection crack.

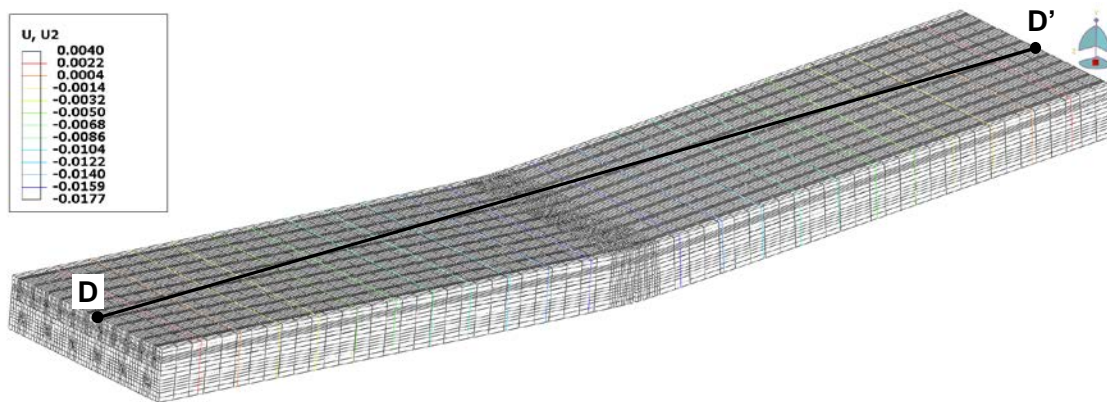
The 7-in.-thick CRCP concrete slab over 10-in. CPCD, which is the same configuration in the US-75 site in Sherman, was analyzed assuming the modulus of subgrade reaction to be 50 psi/in. (Case 55 in Table 5.5). **Figure 5.26** shows the deformed shape—magnified by 1,000 times—and deflection along the path DD'. The maximum deflection occurs at the middle of BCO, which is transverse contraction joint in the existing CPCD. As shown in **Figure 5.26-(b)**, the slab deflection is highly influenced by changes in the modulus of subgrade reaction in CRCP BCO on CPCD system.

The FDR joints could be considered as the same condition with transverse contraction joint in finite element method analysis. The causes for several distresses on US 75 in FDR slabs could be due to a large deflection, resulting in a large tensile stress on top of FDR joints. Both deflections and principal stresses causing the reflection crack development increase linearly with traffic loading as shown in **Figure 5.27**. The principal stress under 18-kips of wheel loading application was 706 psi when the modulus of subgrade reaction is 50 psi/in.

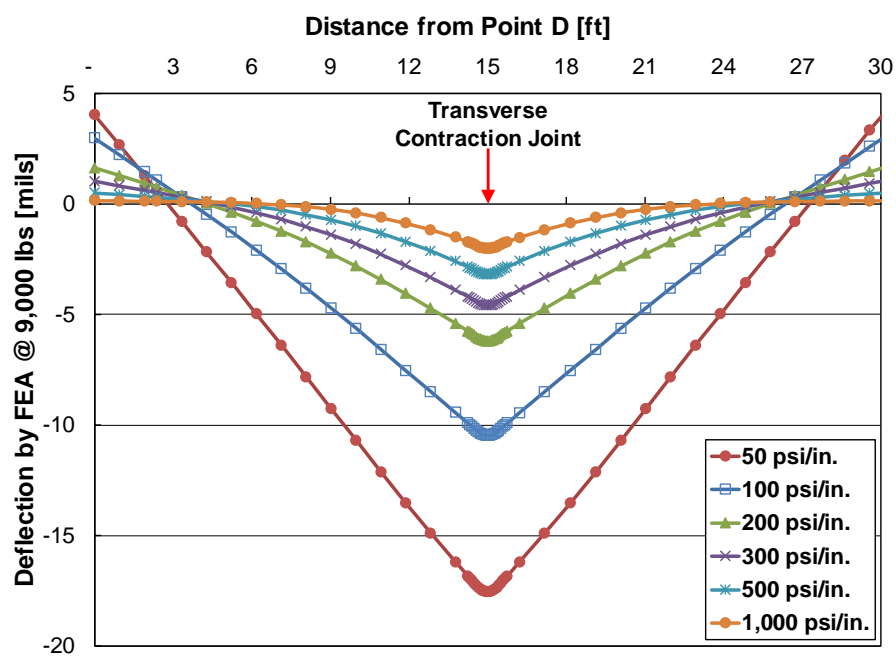
Figure 5.28 shows a side view of principal stresses distribution—magnified by 300 times—around a transverse contraction joint.

Figure 5.29-(a) presents a cross section view at a transverse contraction joint that includes principal

stresses. As illustrated in [Figure 5.29-\(b\)](#), the maximum principal stress was induced at the interface under the center of the wheel loading location. When the moduli of subgrade reactions are lower than 100 psi/in., the maximum principal stresses are larger than 230 psi, and the overall principal stresses are also larger than 200 psi. Note that the slab support condition at US 75 in Sherman was quite poor due to inferior flexible base materials with high PIs and poor drainage condition. Even though it is a little premature to determine a reliable threshold value as per the pavement support condition regarding whether the project is suitable for BCO, it appears that CPCDs with deficient slab support conditions may not be good candidates for the CRCP BCO because the existing slab deformations due to traffic loading affect the principle stress significantly, resulting in a possible BCO distresses. Also, field performance evaluation data need to be continuously collected and then compared with theoretical analysis results to develop a reliable design program. Since the traffic loading is a crucial factor affecting the reflection crack in BCO system, a historical traffic information also needs to be collected and reviewed prior to the BCO design.



(a) Deformed shape



(b) Surface deflection along the path DD'

Figure 5.26 Deformed shape and surface deflection

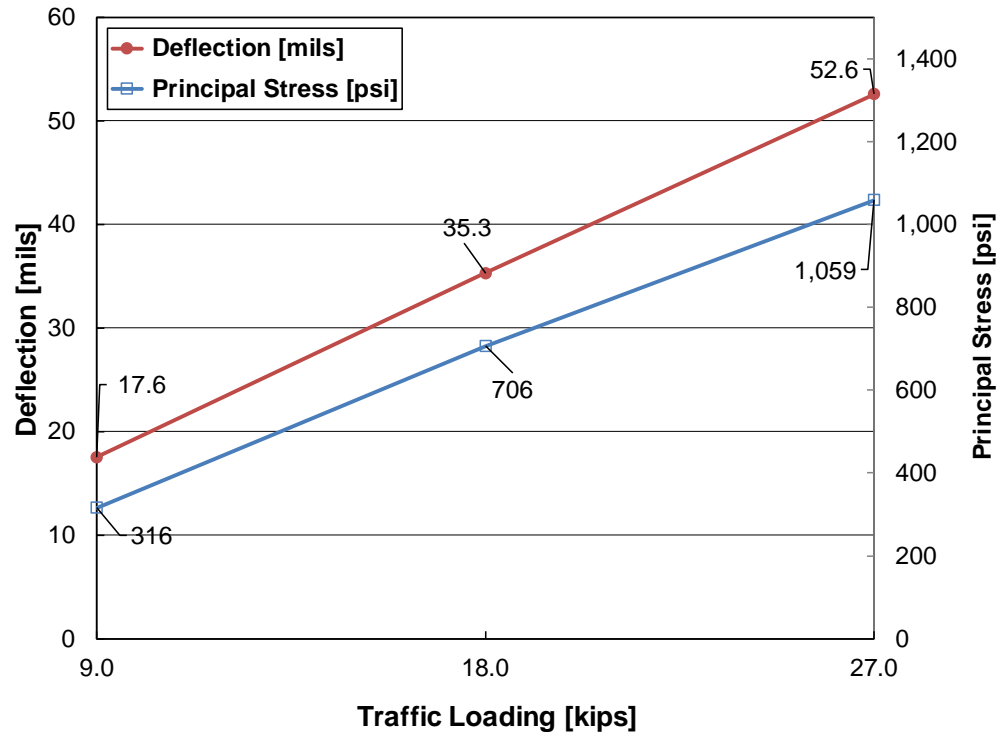


Figure 5.27 Effect of traffic loading on vertical stress at interface

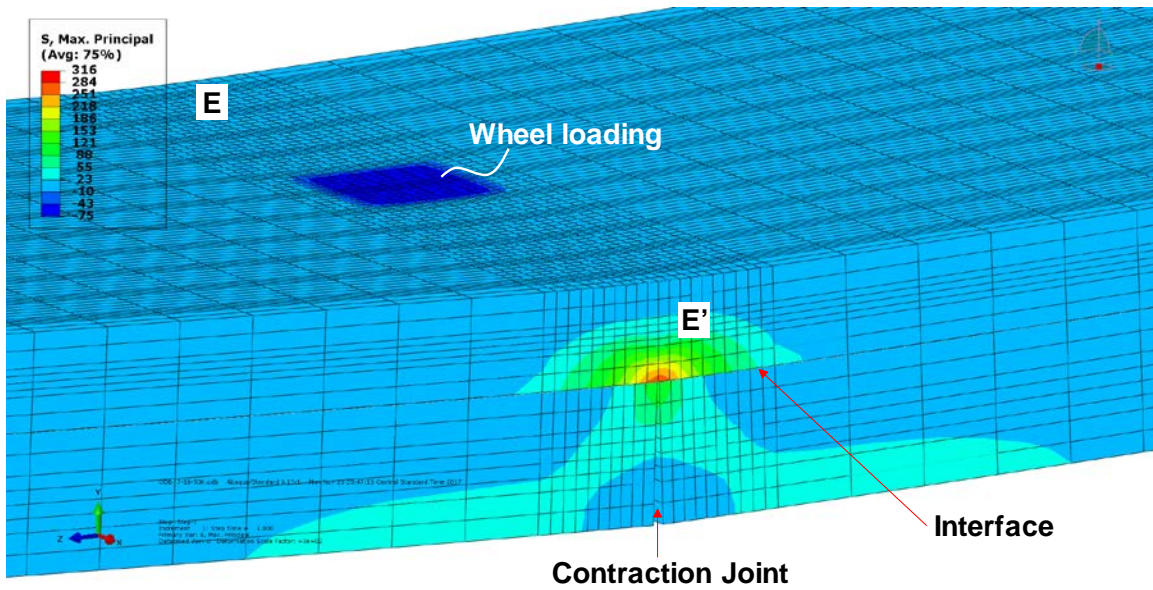
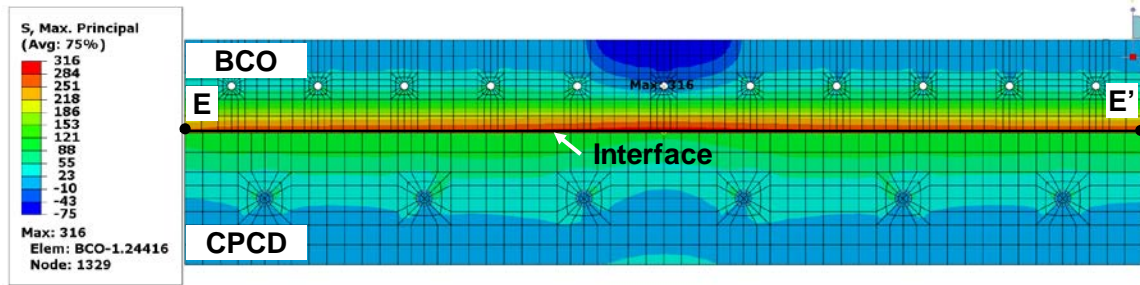
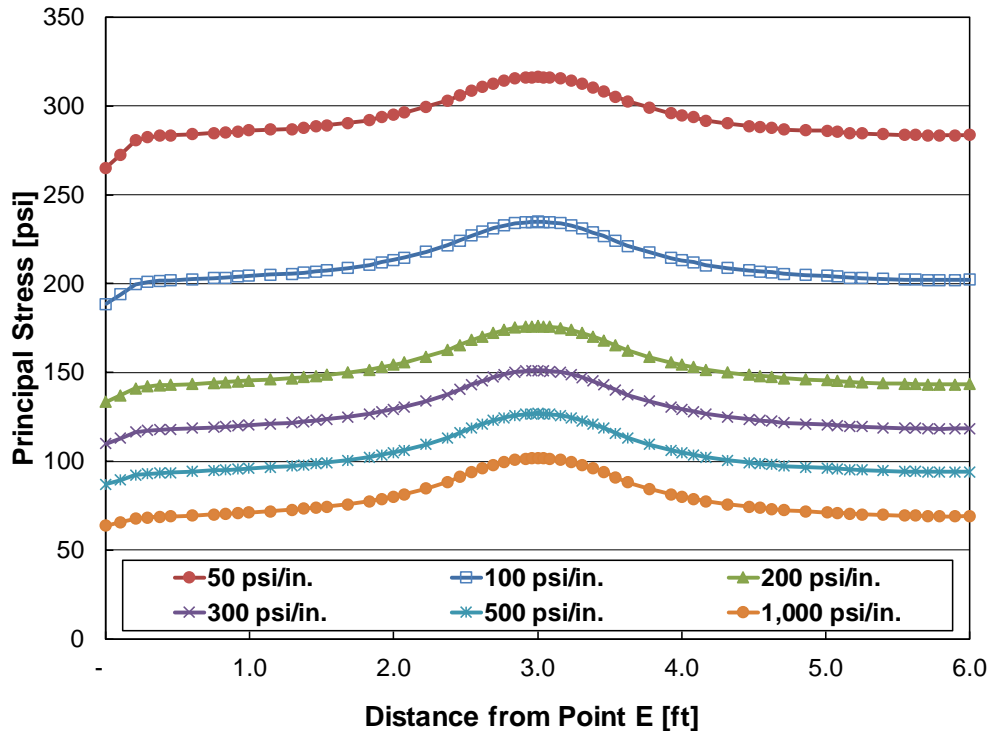


Figure 5.28 Principal stress distribution (7-in. BCO+10-in. CPCD: 7B-10C)



(a) Cross-section view at transverse contraction joint (principal stress)

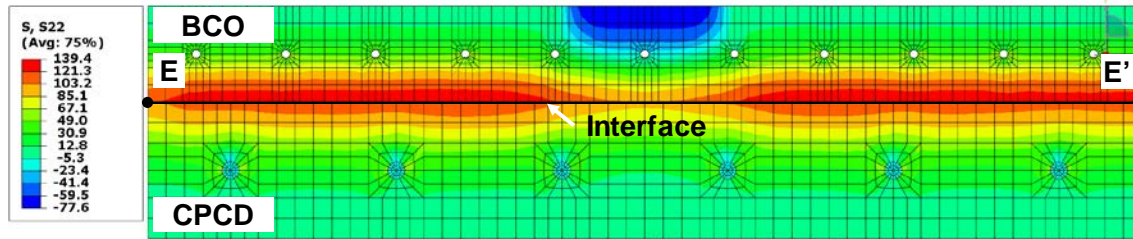


(b) Principal stress distribution along path DD' (7B-10C)

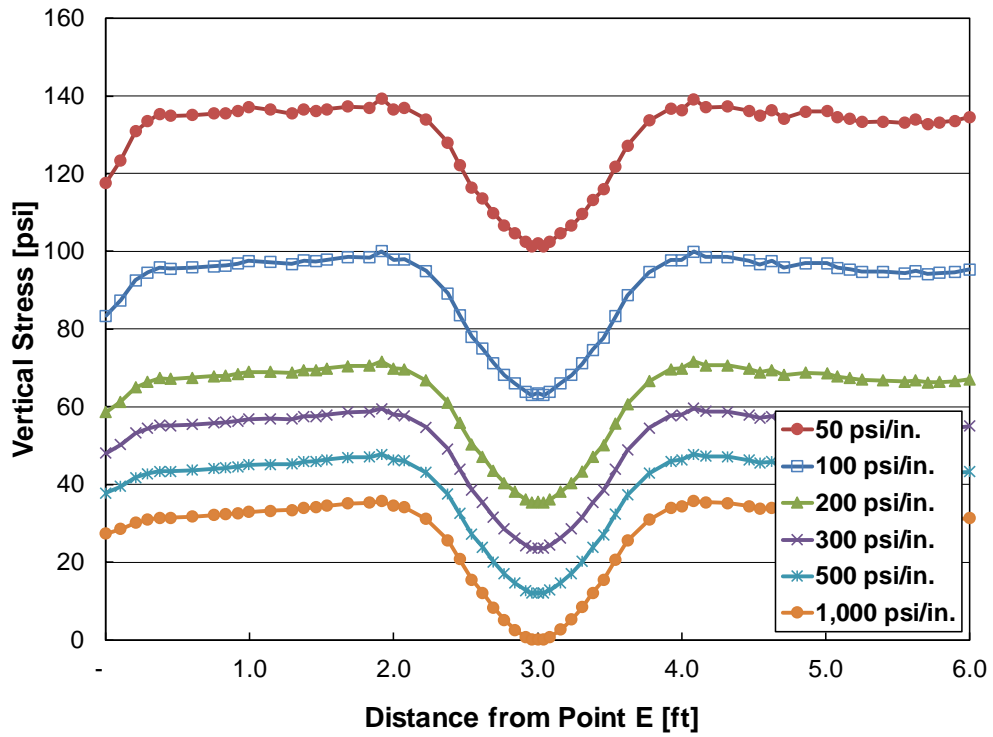
Figure 5.29 Principal stress distribution at interface

Figure 5.30-(a) presents a cross section view at a transverse contraction joint that includes the vertical stresses. Figure 5.30-(b) shows the vertical stresses distribution along the path EE' on interface. As with the maximum principal stresses, the vertical stresses increase significantly as the moduli of subgrade reaction decrease.

The maximum principal stresses related to the development of reflection cracks are summarized in Table 5.6.



(a) Cross-section view at transverse contraction joint (vertical stress)



(b) Vertical stress distribution along path EE' (7-B-10C)

Figure 5.30 Vertical stress distribution at interface (7B-10C)

Table 5.6 Vertical stresses table at interface (CRCP BCO on CPCD)

| Slab Thickness | | CoTE of Concrete $\alpha_c, [\times 10^{-6}/^{\circ}\text{F}]$ | Principal Stress [psi] | | | | | |
|--------------------------------------|----------------------------|---|--|-----|-----|-----|-----|------|
| | | | Modulus of Subgrade Reaction $K_v, [\text{psi}/\text{in.}]$ | | | | | |
| Existing CPCD $E_h, [\text{in.}]$ | BCO $B_h, [\text{in.}]$ | | 50 | 100 | 200 | 300 | 500 | 1000 |
| 10 | 7 | 4.0 | 353 | 265 | 196 | 164 | 137 | 112 |
| | 8 | 4.0 | 305 | 230 | 173 | 148 | 124 | 100 |
| | 9 | 4.0 | 277 | 212 | 160 | 137 | 114 | 92 |
| | 10 | 4.0 | 242 | 188 | 143 | 122 | 102 | 82 |
| 12 | 7 | 4.0 | 320 | 246 | 189 | 160 | 131 | 99 |
| | 8 | 4.0 | 301 | 231 | 170 | 143 | 117 | 92 |
| | 9 | 4.0 | 282 | 215 | 159 | 134 | 109 | 86 |
| | 10 | 4.0 | 246 | 191 | 143 | 120 | 98 | 77 |

5.7 CRCP BCO Mechanistic Empirical Design Program

5.7.1 Development of TxBCO-ME program

In the previous sections, mechanistic modeling and analysis were conducted to identify the maximum principle stresses causing delamination at the interface in CRCP BCO on CRCP and reflective cracking in CRCP BCO on CPCD.

In CRCP BCO on CRCP, the analysis results show that a vertical stress at the interface causing delamination increases as the BCO thickness becomes smaller. Observed distresses on US 287 at Bowie support the findings from these analysis results. As of now, since a transfer function for CRCP BCO on CRCP cannot be developed because of the small number of BCO projects, the transfer function developed and used in the TxCRCP ME (Ha, et al 2011) has been utilized in the CRCP BCO on CRCP ME design program. To develop more accurate CRCP BCO designs, a transfer function for CRCP BCO should be developed with a more extensive dataset. For the damage calculations, the same fatigue equation used in the TxCRCP ME was also utilized. The main differences for CRCP BCO on CPCD program are the deflection threshold value and distress type.

The overall algorithm of the design program is similar to the TxCRCP ME program, as shown in [Figure 5.31](#). There are five modules, which are the input module, stress analysis module, damage estimation module, delamination prediction module, and output presentation module. For the TxBCO-ME design program, stresses by wheel and temperature loading are calculated by the numerical modelling as discussed in this section. The calculated stresses are organized in the table embedded in the program associated with the combination of three input variables of overlay and existing concrete thickness and modulus of subgrade reaction.

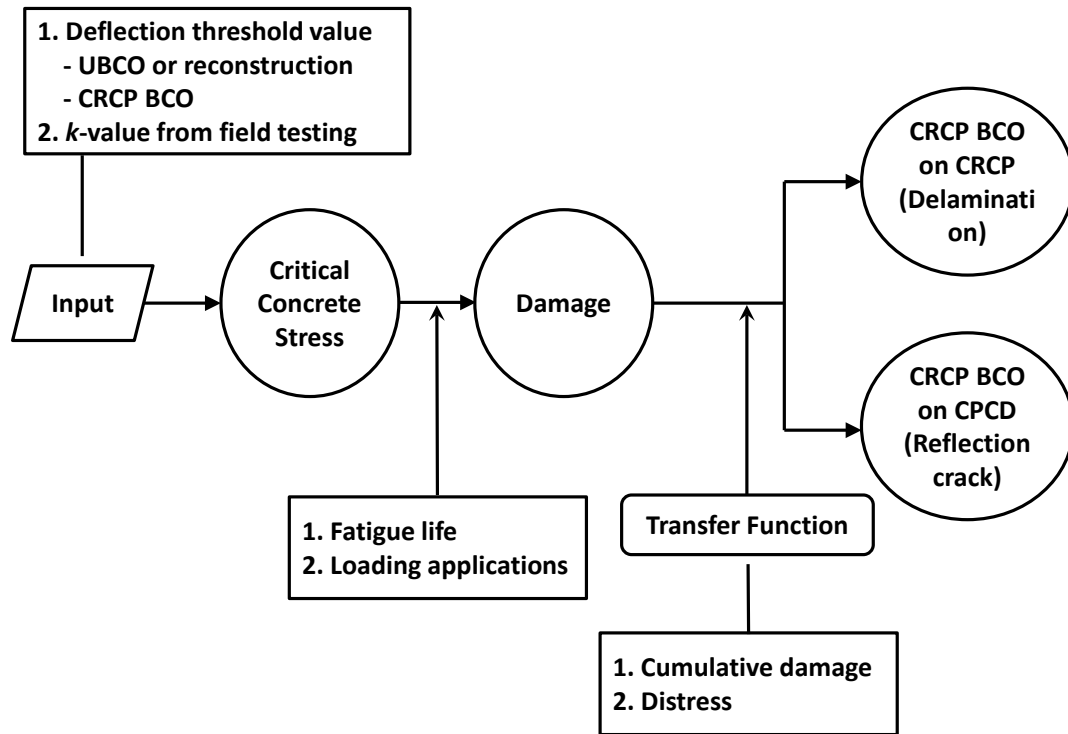


Figure 5.31 Overall algorithm of ME CRCP BCO design program

The TxBCO-ME design program interface comprises one main window and seven sub-windows for inputs and analysis, which open by clicking buttons in the main window, as shown in [Figure 5.32](#).

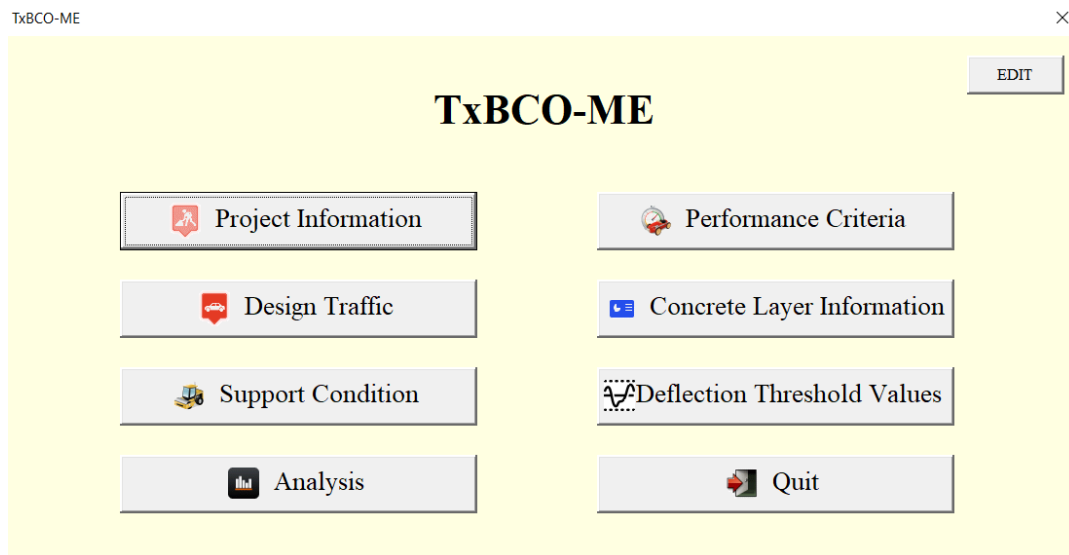


Figure 5.32 The interface of the CRCP BCO design program

5.7.2 General Inputs

The CRCP BCO design program has six categories of the inputs: project information, performance

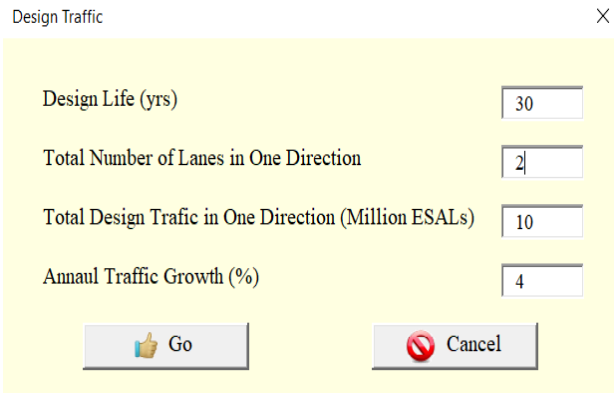
criteria, design traffic, concrete layer information, support condition, and deflection threshold values. Each category has several input variables as shown blow.

- 1) Project Information
 - a. TxDOT District
 - b. County
 - c. Highway
 - d. CSJ
 - e. Direction
 - f. Station (Begin)
 - g. Station (End)
- 2) Performance Criteria
 - a. Number of Distresses per Mile
- 3) Design Traffic
 - a. Design Life (yrs)
 - b. Total Number of Lanes in One Direction
 - c. Total Design Traffic in One Direction (Million ESALs)
 - d. Annual Traffic Growth (%)
- 4) Concrete Layer Information
 - a. Overlay Thickness (in.)
 - b. Existing Concrete Thickness (in.)
 - c. 28-day Modulus of Rupture (psi)
 - d. 28-day Modulus of Elasticity (ksi)
 - e. BCO System Type
- 5) Support Condition
 - a. Composite k (psi/in.)
- 6) Deflection Threshold Values
 - a. Deflection on CRCP
 - b. Deflection on CPCD

5.7.3 Program Execution

To execute the program, all required input variables should be estimated and inserted into the specific sub-screens as illustrated in **Figure 5.33**. Clicking “OK” would complete the submission

of the input values into the program.



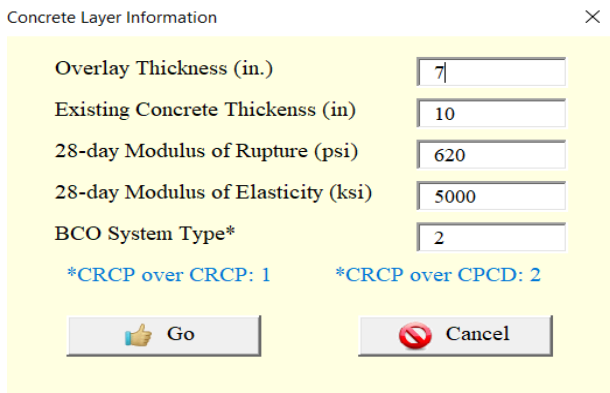
Design Traffic

Design Life (yrs)

Total Number of Lanes in One Direction

Total Design Traffic in One Direction (Million ESALs)

Annual Traffic Growth (%)



Concrete Layer Information

Overlay Thickness (in.)

Existing Concrete Thickness (in)

28-day Modulus of Rupture (psi)

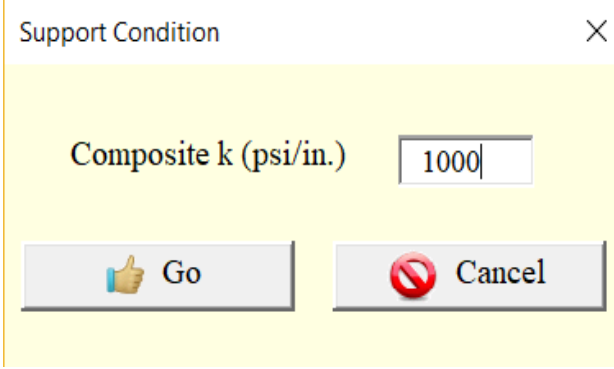
28-day Modulus of Elasticity (ksi)

BCO System Type*

*CRCP over CRCP: 1 *CRCP over CPCD: 2

a. Design Traffic

b. Concrete Layer Information



Support Condition

Composite k (psi/in.)

c. Concrete Layer Information

Figure 5.33 The sub-windows of the interface for required inputs

After inserting all of the input values, clicking “Analysis” in the screen, as shown in [Figure 5.32](#), will generate another sub-screen, presenting the total number of distresses per mile as shown in [Figure 5.34](#). If the predicted number of distresses is not acceptable, then changes in the input values are made and the program is run, until the number of distresses becomes acceptable. However, at this point, it is not known what would be the acceptable number of distresses in the BCO for design. Further efforts will be needed to determine a reasonable number of distresses acceptable for BCO design.

Even though a BCO design program was developed based on M-E principles, the number of data points that could reliably validate the reasonableness of the designs is quite limited. It is recommended that, until more extensive datasets become available, the implementation of this program is not recommended; rather, it is suggested that the application of the threshold deflection values be adopted for the feasibility investigation of the overlay. At this point, for the slab thickness design for BCO, the 1993 AASHTO design procedure is recommended.

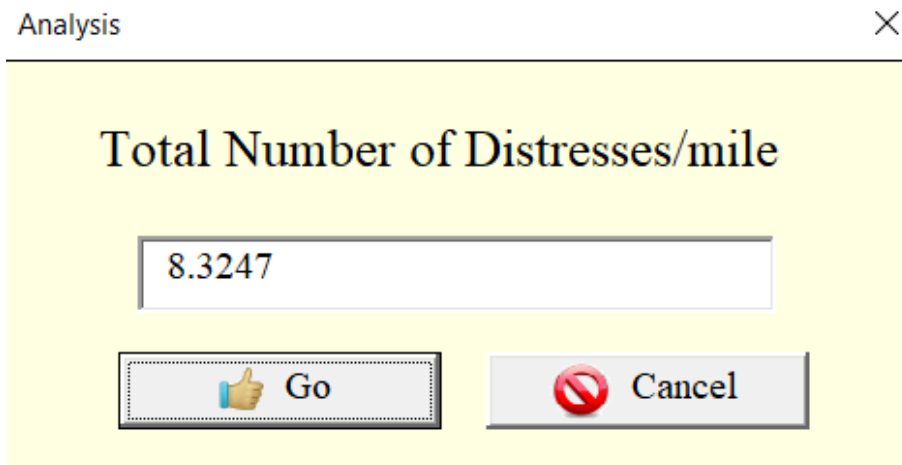


Figure 5.34 Program result screen

Chapter 6 Development of PCC Overlay Design Standards and Specifications

6.1 Introduction

As segments of TxDOT's vast PCC pavement network are approaching the end of their design lives, guidelines for the selection of proper rehabilitation methods, including specifications and design standards for rehabilitations, will be needed. Up to this point, TxDOT has not had guidelines on the selection of proper rehabilitation of PCC pavements; rather, the selection is left to the district pavement engineers or other district staff engineers. Also, no design standards have been developed for concrete overlays, except for whitetopping. The final products of this research project include guidelines, specifications, and design standards for PCC overlays. This chapter addresses specifications and design standards for concrete overlays.

Unlike new PCC pavement construction, the construction of PCC overlays, especially BCOs, requires a higher level of construction and material quality control, due to BCO's behavior and performance (which is that the overlaid layer and existing concrete layer will behave monolithically). If this assumption is not incorporated in designs, the performance of BCO could be seriously compromised. As for the UBCO, the existing pavement is assumed to behave as a part of a slab support system, which is easily achieved with an AC layer of approximately 2-in. placed on top of the existing concrete layer. In other words, the factors involved in the performance and the construction of UBCO are quite similar to new PCC pavement construction, and no new special specifications are needed to be developed.

In general, required slab thicknesses for UBCO are comparable to those needed for new PCC pavements. Also, the construction practices of UBCO are quite similar to those of new PCC pavement, and there is no need for separate design standards or specifications for UBCO. Instead, the existing design standards for CRCP and CPCD could be used for UBCO, except for minor revisions for transition areas. Accordingly, in this study, design standards and specifications for BCO only were developed. Before the specifications and design standards for BCO developed in this study are outlined, brief discussions are presented on the findings in this study that led to the development of specifications and design standards for BCO.

6.2 BCO

BCO could present one of the most efficient ways to rehabilitate aged PCC pavements. Because of the way BCO pavement system is supposed to behave, which is a monolithic behavior of the combined overlaid and existing slabs, two important benefits are achieved: (1) a smaller slab thickness needed for overlay and (2) resulting lower rehabilitation cost. On the other hand, this assumption of a monolithic behavior requires that the existing pavement must be in a relatively good condition and that any distresses that could impede the monolithic behavior after overlay should be properly repaired. In addition, a solid bond needs to be achieved between existing and overlaid slabs. What constitutes "good condition" of existing PCC pavement is quite qualitative

and somewhat subjective, and discussions were presented in Chapter 5 regarding more quantitative criteria on “good condition” of the existing PCC pavement appropriate for BCO. This section discusses repair needs that must be addressed in the existing PCC pavement to ensure good performance of BCO.

6.2.1 Distress Repairs in the Existing Pavement

Section 4 – Bonded Concrete Overlay of Chapter 10 – Rigid Pavement Rehabilitation in the TxDOT Pavement Manual describes the needed repairs in the existing pavement for BCO as follows:

“All the major distresses present in the existing pavement should be repaired prior to the overlay placement. The main guideline to follow when performing this work is to assess whether the distress is likely to affect the performance of the overlay within a few years. If that is the case, the distress has to be repaired before the BCO is built.

Deep spalling, delaminations, punchouts, and deteriorated patches must be repaired. Existing asphalt concrete (AC) patches should be removed and replaced with PCC patches so the existing pavement is made structurally sound. Concrete repairs should be performed in accordance with Sections 2 and 3. Working longitudinal cracks may be repaired by stitching, as described in Section 6, “Stitching.”

It is common practice to remove and replace the large deteriorated areas when structural distresses are extensive. When the distress is caused by a localized foundation weakness, it is necessary to ensure that the weak base layer materials are removed and the remaining base is well compacted during FDR, as detailed in Section 2. When voids are detected under existing slabs, grout should be injected to stabilize the pavement.

When constructing a BCO over a CPCD section, it is necessary to ensure that the sections have adequate load transfer efficiency. CPCD sections built without dowels will need to have dowel bar retrofits done prior to constructing the overlay. Section 7, “Dowel Bar Retrofit,” details these requirements.”

According to the findings from the BCO site on US 287 in Bowie, 7.0 mils is recommended as a deflection threshold value of this specific test section for BCO. The analysis of field performance shows a reasonable relationship between deflections in the existing CRCP evaluated prior to overlay and BCO performance.

At the US-287 BCO site in Bowie, distresses developed in BCO slabs within a year, and most of the distresses were at repair joint areas in the existing CRCP. As discussed earlier, it appears that these distresses were due to large deflections along the perimeters of the FDR areas in the existing CRCP. The large deflections along the perimeters of FDR areas are due to (1) loss or inadequacy of structural continuity at repair joints and/or (2) inadequate slab support along repair boundaries. Both issues have been properly addressed by revision of Item 361 in 2014 TxDOT specifications. In addition, to address large deflections caused by localized inadequate slab support, the Pavement Manual suggests that the weak base layer materials should be removed and the remaining base should also be well compacted during FDR. Although the issues related to proper repairs of PCC distresses are addressed in Item 361 and TxDOT’s Pavement Manual, it is believed that BCO

specifications should also address those issues directly or indirectly. The specifications developed in this study address those issues directly, since addressing those issues in the BCO specifications will attract better attention from contractors.

6.2.2 Construction Variables related to Interface Bond

In the US-281 BCO project built in June 2002 in Wichita Falls, surface preparation on the existing CRCP was done with a shot-blasting machine as shown in Figure 6.1-(a) to provide a clean surface as well as a rough texture. The lower and upper parts of Figure 6.1-(b) illustrate the close-up view of the surface condition after and before the shot-blasting, respectively. Bond strength testing was conducted, in accordance with ASTM C 1583, on March 22, 2016 at nine locations that included near and away from a transverse crack as shown in Figure 6.2. In Figure 6.2, three cores shown in the upper part of the figure, which were taken few feet away from the markings G1, G2 and C1/C2, reveal solid bonding between existing and overlaid concretes. Figure 6.3 shows the failure planes after bond strength testing at those four locations shown in Figure 6.2. Out of four locations, two failed within the existing concrete slab and the other two failed within the overlaid slab. The difference in concrete tensile strengths in the existing slab and overlaid slab was not large. Also, the bond (tensile) strengths near and away from a transverse crack were comparable, indicating little effect, if any, that a transverse crack has on bond (tensile) strength. Figure 6.4 shows a condition of a transverse crack in this location. First, a solid bond at the interface is observed. Next, the depth of the transverse crack is limited to about 2 inches from the surface. In other words, the crack was developed to relieve stresses caused by temperature and moisture variations in the overlaid slab, not due to stresses from wheel loading applications. The warping and curling behavior of the overlaid slab in this area was not severe enough to cause the transverse crack to extend through the overlaid slab. If the transverse crack had extended to the interface, the interface bond condition could have been compromised, resulting in bond failure at the interface and potential distresses in this location. From a theoretical standpoint, warping and curling stresses depend, to a large extent, on the slab thickness—the greater the slab thickness, the lower the warping/curling stress. This result arises because warping/curling stress depends on the ratio of the distance between the free slab edges to the radius of relative stiffness, and the radius of relative stiffness is proportional to the three-fourths power of slab thickness. What happened here is that bond strength was adequate, which made the effective slab thickness 12-in. If the surface preparation had been poor quality, tensile stresses at the interface might have exceeded bond strength and there might have been delamination and distresses.

As discussed in the previous chapters, in all nine locations evaluated for bond strength at the US-281 site in Wichita Falls, failure planes in concrete were all either within the existing or overlaid slabs, but none at the interface. In other words, bond strengths at the interface were greater than the tensile strengths of concrete in the existing slab or overlaid slab in all those locations. The average bond strength obtained was 197 psi. This value is somewhat lower than the expected tensile strength of concrete in both the existing or overlaid slabs. However, this result indicates that the bond strength at this location was adequate to provide monolithic behavior of the overlaid

pavement system.

The general condition of US 281 in Wichita Falls is shown in **Figure 6.9**. Transverse cracks are so tight that it was not easy to identify them. It is believed that good bond has been responsible for keeping transverse cracks quite tight and achieving good BCO performance.



(a) Shot-blasting operation of the concrete surface



(b) Close-up view of surface texture before and after shot-blasting

Figure 6.1 Surface preparation of existing CRCP on the US-281 BCO project in Wichita Falls



Figure 6.2 Bond strength testing and concrete cores on US 281

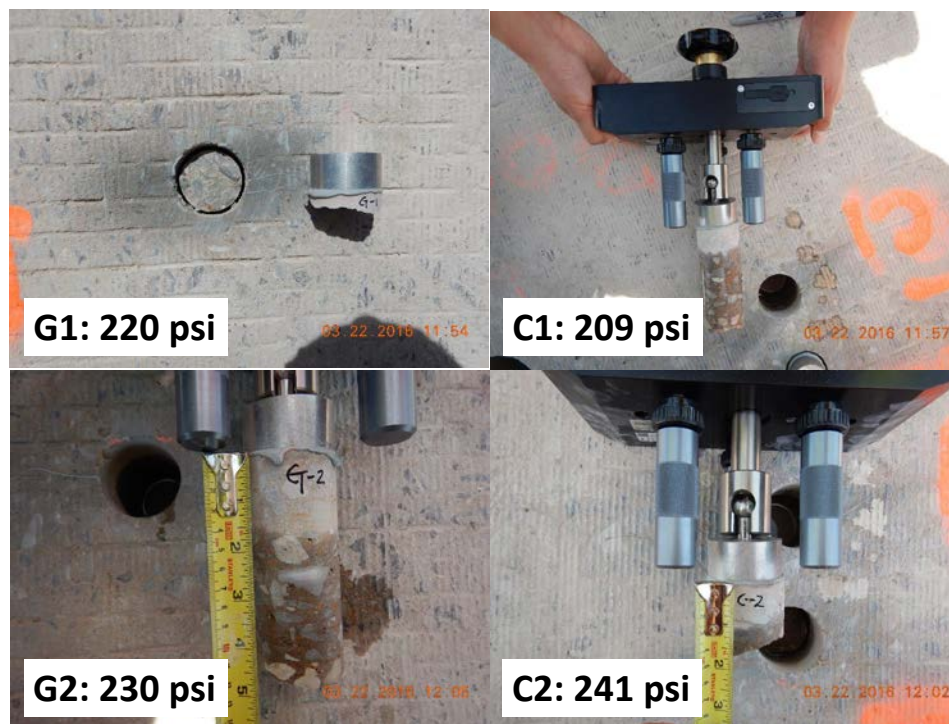


Figure 6.3 Bond strength testing and failure mode on US 281 in Wichita Falls



Figure 6.4 Close-up view of concrete core taken at transverse crack



Figure 6.5 Overall BCO condition on US 281 in Wichita Falls

In the US-287 BCO project in Bowie, the surface of the existing CRCP was prepared by the same method applied to US 281 in Wichita Falls. **Figure 6.6** shows the surface texture after the shot blasting. Compared with the surface texture prepared in US 281 project, as shown in Figure 6.1-(b), the surface texture shown in Figure 6.6 appears to be not as rough. Unfortunately, measurements were not made on surface texture characteristics on both projects, and direct comparison of the surface textures in both projects is not possible. As discussed earlier, bond

strength in the US-287 project in Bowie was quite low and all the failures in bond testing were at the interface. More specifically, bond strength testing was conducted at 14 locations on November 15, 2012, 9 or 10 days after BCO placement. Bond testing showed that failures occurred at the interface at 11 locations, as illustrated in [Figure 6.6](#). At the other three locations, the concrete in overlaid layer became loose during coring, and pull-out bond testing was not even feasible. It appeared that almost no bonding existed at those three locations. Bond strength varied from 117 psi to 241 psi at the remaining 11 testing locations, with an average value of 186 psi. If the three locations where bonding did not exist are included, the average bond strength would be 146 psi, which is much lower than the value obtained in US 281 in Wichita Falls, even though the age of bond strength testing in US 287 in Bowie was only 9 or 10 days. It should be recalled that the bond strength of US 287 in Bowie was obtained prior to the opening of the pavement to the traffic, while the bond strength in US 281 in Wichita Falls was obtained after 14 years of traffic applications. It should also be recalled that the failure planes in US 281 in Wichita Falls were not at the interface, while those in US 287 in Bowie were all at the interface. Even though large deflections in the existing CRCP appear to be responsible for early-age distresses and poor performance of the BCO on US 287 in Bowie, what could have happened if the bonding at the interface had been good remains unknown. Considering the significant effect of good bonding on BCO performance, including bonding requirements, such as bond strength, in the specifications may be needed; the bond strength requirements were incorporated in the draft specifications developed in this study. However, the bond strength requirements might increase the BCO cost, since contractors see them as added uncertainty and raise the bid price. Since these bond strength requirements are new, providing a bonus for good bond strength might be a good incentive, until the PCC paving industry becomes knowledgeable on how to achieve good bond strength and comfortable with those requirements.



Figure 6.6 Close-up view of surface texture after shot-blasting, US 287 BCO in Bowie

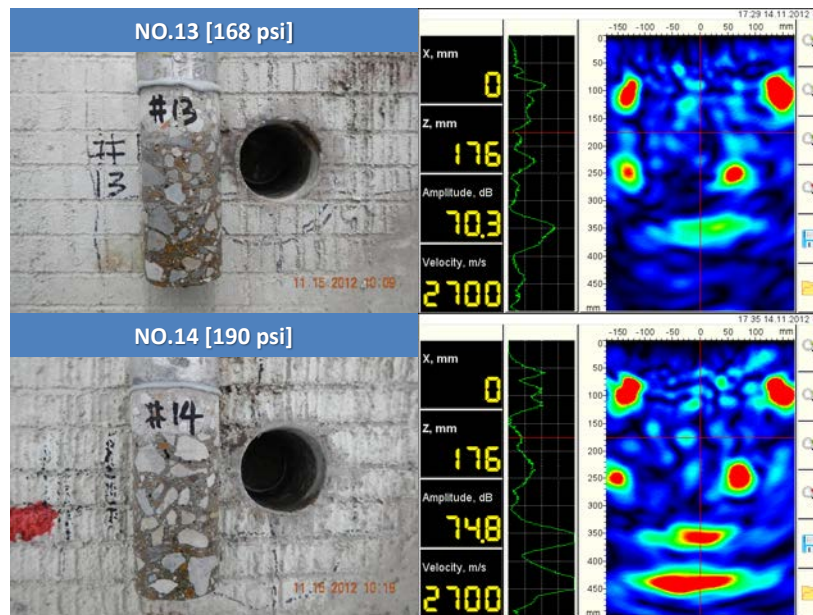


Figure 6.7 Bond strength and MIRA testing (interface failure)

6.2.3 Longitudinal Reinforcement Design

Figures 6.8 and 6.9 show steel placements in 4-in. BCO projects on US 281 in Wichita Falls and US 287 in Bowie, respectively. In both projects, longitudinal steel was placed on top of transverse steel, which was placed on top of the existing PCC pavement. The longitudinal steel was placed near the bottom of BCO layer because the concrete volume changes near the interface could be

minimized by longitudinal steel, which could improve bond strength. As discussed earlier, this steel placement worked well for US 281 in Wichita Falls, while bond strength and BCO performance were rather poor at US 287 in Bowie. However, it is believed that, when BCO thickness is 4-in., the placement of longitudinal steel near the bottom of BCO is a good practice. **Table 6.1** illustrates the recommended reinforcing steel percentage and steel depths in BCO in TxDOT Pavement Manual.

6.2.4 Recommended Design Standards and Specifications

Based on the above discussions, draft special specifications and design standards were developed for BCO. Draft special specifications are in Appendix A, and draft design standards are in Appendix B.



Figure 6.8 Longitudinal rebar placement on US 281 in Wichita Falls



Figure 6.9 Longitudinal rebar placement on US 287 in Bowie

Table 6.1 Reinforcement requirements (TxDOT)

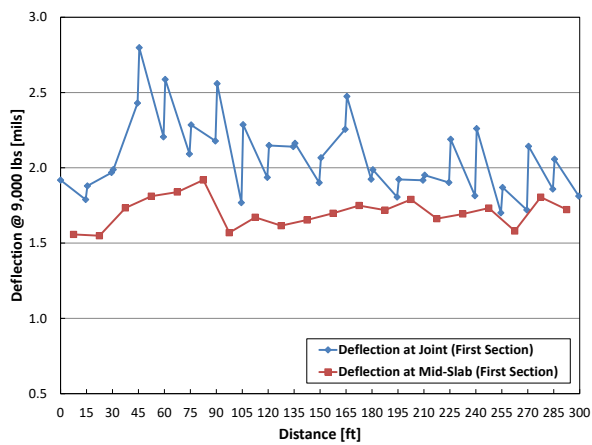
| BCO Thickness | Longitudinal Steel (%) | Vertical Location | Fibers |
|---------------|------------------------|-------------------|--------|
| ≤ 3 in. | N/A | N/A | Yes |
| ≤ 5 in. | 0.6% | Bottom of BCO | No |
| > 5 in. | 0.6% | Middle of BCO | No |

6.3 UBCO

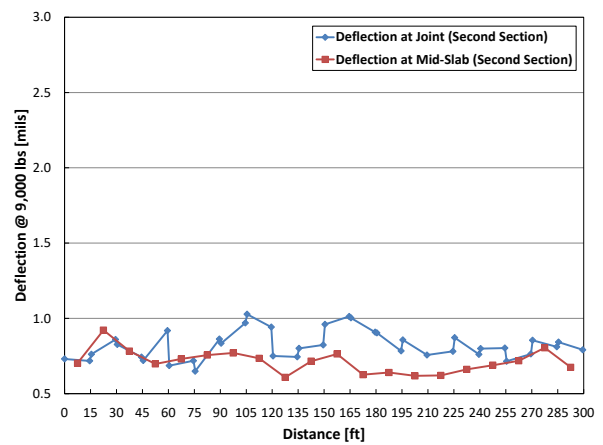
6.3.1 Quality of HMA Interlayer

As discussed in Chapters 3 and 4, at the IH 35E UBCO site in Waxahachie, the condition of UBCO was excellent, with quite small deflections and practically no distresses, except for a small crack near a transverse contraction joint, which will be discussed in the next section. For field evaluation purposes, the project was divided into two sections: good and poor. A section with the area containing a small crack was classified as a *poor* section, and the rest a *good* section. Deflections were measured at both sections and they were larger in the good section than in the poor section, as shown in [Figure 6.10](#). Coring was conducted in both sections to obtain concrete cores for material evaluations as well as the condition of the hot mix asphalt (HMA) interlayer. The HMA interlayer in the good section was deteriorated while that in the poor section was in a good condition, as shown in [Figure 6.11](#). It appears that the poor condition of the HMA interlayer in the good section resulted in larger deflections, while the good condition of the HMA interlayer in the poor section yielded smaller deflections. Even though the UBCO condition in both good and poor sections is quite excellent at this point, the long-term structural performance of the good section might be not as good as that of the poor section. This indicates that, for UBCO design and

construction, close attention should be paid to the materials selection and placement of the HMA interlayer.



(a) Good section



(b) Poor section

Figure 6.10 Deflection comparison between joint and mid-slab on IH 35E in Ellis County



(a) Good section, G-1



(b) Good section, G-3



(c) Poor section, C-1



(d) Poor section, C-3

Figure 6.11 Deteriorated AC interlayer in good and poor sections, IH 35E

6.3.2 Joint Mismatch

While field testing was conducted on IH 35E in Waxahachie, a narrow transverse crack was observed near a transverse contraction joint of the UBCO CPCD, which was not typical in CPCD. As discussed previously, this crack led to the selection of this area as a “poor” section. To investigate the cause(s) of the crack, a concrete core, which included existing and overlaid concrete slabs as well as the interlayer, was taken at the crack. The coring indicated that the crack was on top of the transverse contraction joint in the existing slab, as shown in [Figure 6.12](#), which shows not only a transverse crack, but delamination as well in the overlaid layer. It indicates that the transverse contraction joint in UBCO was not on top of the transverse contraction joint in the existing slab, with an offset of approximately 6-in. This “mismatch” of transverse contraction joints in the existing and overlaid slabs could cause transverse cracks and delamination as observed in this location. Recall that HMA interlayer in this section was in good condition, and still a transverse crack and delamination occurred. Eventually, the combination of a transverse crack and

delamination would result in spalling in this area. Accordingly, this joint mismatch could be a serious issue. Chapter 5 of the Iowa DOT Pavement Design Manual recommends that joints are typically mismatched to maximize load transfer from the underlying existing concrete pavement. Also, the ME-Design Guide states that “the transverse joints in UBCO are nearly deliberately mismatched with those in the underlying pavement. A minimum offset distance of 3 ft between the joints in the overlay and the underlying joints or cracks is usually recommended. By placing the joint in the overlay after the joint in the underlying pavement, a sleeper slab effect is provided that further improves load transfer across the joints.”

In the two UBCO projects evaluated in this study, load transfer at transverse contraction joints in UBCO was excellent, as discussed in Chapter 3, even though transverse contraction joints in UBCO were installed at the locations of the transverse contraction joints in the existing slabs. It appears that, as long as current TxDOT CPCD design standards are followed for UBCO, which means dowels are used in overlay concrete slab, matching transverse contraction joints in the existing and UBCO could be a good option. On the other hand, mismatching transverse contraction joints might work well as recommended by the Iowa DOT and MEPDG. Since TxDOT never tried mismatching transverse contraction joints in CPCD UBCO, no recommendations could be made on this.



Figure 6.12 Delamination and crack due to joint mismatch between existing CPCD and overlaid CPCD

Chapter 7 Conclusions and Recommendations

Extensive field evaluations were conducted of the performance of various types of PCC overlays in Texas. Also, theoretical analyses were conducted to identify distress mechanisms as well as to develop ME design procedures for BCOs. The findings from the extensive field evaluations and mechanistic analyses of PCC overlay projects and data analyses are summarized as follows:

- The performance of CRCP BCO on CRCP varied quite substantially, with some projects providing excellent performance under heavy traffic for more than 30 years, while some projects failed within a few years, requiring additional rehabilitation. In general, a positive correlation has been observed between overlay thickness and long-term performance, even though there are exceptions.
- The performance of CPCD UBCO on CPCD has been excellent, with almost no distresses observed after more than 25 years of heavy truck traffic. Part of the reason for the excellent performance is that the pavement was over-designed (overlay slab thicknesses of 10-in. and 11-in.). The quality of the asphaltic concrete interlayer material and construction is also important, since the deterioration of the interlayer material increased slab deflections. Another important finding is that the transverse contraction joints in the overlay should match the locations of the transverse contraction joints in the existing slab.
- Bond strength testing conducted in BCO projects indicated a positive correlation between bond strength and BCO performance. However, what is more significant is the correlation between the bond failure planes during bond testing and BCO performance. In projects with an excellent performance, the bond failure planes during bond testing were not found at the interface; rather, they were all either within the existing slab or in the overlay. On the other hand, in one project with poor performance, all the failure planes were at the interface.
- The satisfactory performance of CRCP BCO on CPCD showed this pavement system has a good potential for the rehabilitation of deteriorated CPCD.
- Assumptions made in the 1993 AASHTO design methods for UBCO are not reasonable and result in over-design of slab thicknesses. More specifically, the assumption of identical concrete stresses due to wheel loading at the bottom of the overlay, existing slab, and equivalent slab is technically erroneous. The exponent value derived from this assumption, which is 2, is not reasonable, and the value should be reduced to 1.4.
- For the selection of an optimum overlay type, accurate evaluation of the structural condition of existing pavement is important. Slab deflection was determined as the best indicator of the structural condition of the existing pavement for the feasibility of BCO. Based on the field performance, 7 mils was selected as a threshold value for 4-in. or

thicker CRCP BCO on 8-in. CRCP.

For a satisfactory performance of CRCP BCO on 8-in. CRCP, (1) the structural condition of the existing pavement should be such that the maximum deflection should not exceed 7 mils, (2) good interfacial bond strength should be achieved, (3) adequate overlay slab thickness should be selected, and (4) the quality of the construction and materials should be adequate. To ensure good bond strength is achieved during BCO construction, bond strength testing was included as a job control testing in the proposed special specifications for BCO.

Although a BCO design program was developed based on M-E principles, the number of data points that could reliably validate the reasonableness of the designs is quite limited. It is recommended that, until more extensive datasets become available, the implementation of this program is not recommended; rather, it is suggested that the application of the threshold deflection values be adopted for the feasibility investigation of the overlay. At this point, for the slab thickness design for BCO, the 1993 AASHTO design procedure is recommended.

References

- AASHTO (1993). *AASHTO Guide for Design of Pavement Structures*, American Association of State Highway and Transportation Officials, Washington, D.C.
- ACPA (1990). *Guidelines for Bonded Concrete Overlay*, Technical bulletin TB 007-P, American Concrete Pavement Association.
- ARUP (2014). *Guidelines on the Depth of Overlay to be used on Rural Regional and Local Roads*. Department of Transport, Tourism and Sport, Ireland.
- Bagate, M., McCullough, B. F., & Fowler, D. W. (1987). *A Mechanistic Design for Thin-Bonded Concrete Overlay Pavements* (No. FHWA/TX-88+457-3). Center for Transportation Research, The University of Texas at Austin.
- Bagate, M., McCullough, B. F., Fowler, D. W., & Muthu, M. (1985). *An Experimental Thin-Bonded Concrete Overlay Pavement* (No. FHWA/TX-87/63+357-2F). Center for Transportation Research, The University of Texas at Austin.
- Ballarini, R., & Liao, M. (2012). *Mechanistic Modeling of Unbonded Concrete Overlay Pavements* (No. MN/RC 2012-02). Department of Civil Engineering, University of Minnesota.
- Bissonnette, B., Courard, L., Fowler, D. W., & Granju, J. L. (Eds.). (2011). *Bonded Cement-based Material Overlays for the Repair, the Lining or the Strengthening of Slabs or Pavements: State-of-the-art Report of the RILEM Technical Committee 193-RLS* (Vol. 3). Springer Science & Business Media.
- Cable, J. K., Fanous, F. S., Ceylan, H., Wood, D., Frentress, D., Tabbert, T. R., ... & Gopalakrishnan, K. (2005). *Design and Construction Procedures for Concrete Overlay and Widening of Existing Pavements*. Center for Portland Cement Concrete Pavement Technology, Iowa State University.
- Choi, P., Ryu, S., Zhou, W., Saraf, S., Yeon, J., Ha, S., & Won, M. (2013). *Project level performance database for rigid pavements in Texas, II* (No. FHWA/TX-14-0-6274-2). Center for Multidisciplinary Research in Transportation, Texas Tech University.
- Choi, S., Won, M. C., Sudoi, E., & Nasrazadani, S. (2009). *Horizontal cracking mechanism in CRCP* (No. FHWA/TX-09/0-5549-2). Center for Transportation Research, The University of Texas at Austin.
- Chojnacki, T. (2000). *Evaluation of fiber-reinforced unbonded overlay* (No. RI97-05). Missouri Department of Transportation, Research, Development and Technology.
- Chou, Y. T. (1983). *Investigation of the FAA Overlay Design Procedures for Rigid Pavements*. Geotechnical Laboratory, US Army Engineer Waterways Experiment Station.
- Chou, Y. T. (1985). *Equation for Nonbonded Concrete Overlays*. Geotechnical Laboratory, US Army Engineer Waterways Experiment Station.
- Circular, A. (2009). *Airport Pavement Design and Evaluation*. U.S Department of Transportation, Federal Aviation Administration.
- Daleiden, J. F., Rauhut, J. B., Killingsworth, B., Antwi, E. O., Darter, M. I., & Ahmad, R. (1994).

- Evaluation of the AASHTO design equations and recommended improvements* (No. SHRP-P-394). Strategic Highway Research Program.
- Darter, M. I., Hall, K. T., & Kuo, C. M. (1995). *Support under Portland Cement Concrete Pavements* (NCHRP 372. Appendix A). National Research Council, Transportation Research Board.
- Delatte Jr., N. J., Fowler, D. W., McCullough, B. F., & Gräter, S. F. (1998). Investigating performance of bonded concrete overlays. *Journal of Performance of Constructed Facilities*, 12(2), 62-70. American Society of Civil Engineers
- Delatte, N., & Sehdev, A. (2003). Mechanical Properties and Durability of Bonded-Concrete Overlays and Ultrathin Whitetopping Concrete. *Transportation Research Record*, 1834(1), 16-23.
- Delatte, N. J. (2014). *Concrete Pavement Design, Construction, and Performance*, CRC Press.
- Delatte, N. J., Gräter, S., Treviño, M., Fowler, D., & McCullough, B. F. (1996). *Partial Construction Report of a Bonded Concrete Overlay on IH-10, El Paso, and Guide for Expedited Bonded Concrete Overlay Design and Construction*. (No. FHWA/TX-97/2911-5F). Center for Transportation Research, the University of Texas at Austin.
- Eagleson, B., Heisey, S., Hudson, W. R., Meyer, A. H., & Stokoe, K. H. (1982). *Comparison of the Falling Weight Deflectometer and the Dynaflect for Pavement Evaluation* (No. FHWA/TX-82/33+ 256-1 Intrm Rpt.). Center for Transportation Research, University of Texas at Austin.
- Eichhorn, C. L., Hicks, R. G., Noble, R., & Zhou, H. (1986). *Development of an Improved Overlay Design Procedure for Oregon* (No. FHWA-OR-RD-88-03A). Oregon Department of Transportation.
- Felt, E. J. (1956). Resurfacing and Patching Concrete Pavements with Bonded Concrete. In *Highway Research Board Proceedings* (Vol. 35).
- Fick, G. J., & Harrington, D. S. (2012). *Concrete Overlay Field Application Program: Final Report: Volume I*. National Concrete Pavement Technology Center, Institute for Transportation, Iowa State University.
- Fick, G., & Harrington, D. S. (2015 (Revised Feb 2016)). *Guide Specification for Concrete Overlays*. National Concrete Pavement Technology Center, Institute for Transportation, Iowa State University.
- Gillette, R. W. (1965). A 10-Year Report on Performance of Bonded Concrete Resurfacing. *Highway Research Record*, 94.
- Ha, S., Yeon, J., Choi, B., Jung, Y., Zollinger, D. G., Wimsatt, A., & Won, M. C. (2011). *Develop Mechanistic-Empirical Design for CRCP* (No. FHWA/TX-11-0-5832-1). Center for Multidisciplinary Research in Transportation, Texas Tech University.
- Hall, K. T., Correa, C. E., Carpenter, S. H., & Elliot, R. P. (2001). Rehabilitation Strategies for Highway Pavements. *National Cooperative Highway Research Program*, Web Document, 35.
- Harrington, D., Fick, G., & Taylor, P. (2014). *Preservation and Rehabilitation of Urban Concrete*

- Pavements Using Thin Concrete Overlays: Solutions for Joint Deterioration in Cold Weather States* (No. InTrans Project 09-361). National Concrete Pavement Technology Center, Institute for Transportation, Iowa State University.
- Huang, Y. H. (1993). *Pavement analysis and design*. Pearson Education.
- Jameson, G. (2008). *Technical basis of Austroads guide to pavement technology, part 2: pavement structural design* (No. AP-T98/08). Austroads.
- JHRF (1995). *Design and Execution Manual for Bonded Concrete Overlays*, Japan Highway Research Foundation, Japan.
- Jundhare, D. R., Khare, K. C., & Jain, R. K. (2012). Ultra-Thin Whitetopping in India: State-of-Practice. *International Journal on Transportation and Urban Development*, 2(1)
- Lahitou, L. A., Choi, S. C., & Won, M. C. (2008). *Debonding in Bonded Concrete Overlays Over Continuously Reinforced Concrete Pavements* (No. FHWA/TX-09/0-4893). Center for Transportation Research, The University of Texas at Austin.
- Lance Huddleston, J., & Fowler, W. (1995). *Effects of Early Traffic Loading on a Bonded Concrete Overlay* (No. TX - 96/2911-3). Center for Transportation Research, The University of Texas at Austin.
- Lee, S. W., Park, J. Y., Kim, Y. K., & Jeong, J. H. (2014). Comparison of Performance of Overlay Pavements Constructed on Deteriorated Concrete Pavements using LTPP Database. *KSCE Journal of Civil Engineering*, 18(5), 1380-1388.
- Li, J., Uhlmeier, J. S., Mahoney, J. P., & Muench, S. T. (2011). *Use of the 1993 AASHTO Guide, MEPDG and Historical Performance to Update the WSDOT Pavement Design Catalog* (No. WA-RD 779.1). Washington State Department of Transportation.
- Lundy, J. R., McCullough, B. F., and Fowler, D. W. (1991). *Delamination of Bonded Concrete Overlays at Early Ages* (No. FHWA/TX-91+1205-2). Center for Transportation Research, The University of Texas at Austin.
- McCullough, B. F., & Fowler, D. W. (1994). *Bonded Concrete Overlay (BCO) Project Selection, Design, and Construction* (No. TX-95-920-6F). Center for Transportation Research, The University of Texas at Austin.
- McCullough, B. F., & Rasmussen, R. O. (1999). *Fast-track Paving: Concrete Temperature Control and Traffic Opening Criteria for Bonded Concrete Overlays, Volume I* (No. FHWA-RD-98-167). U.S Department of Transportation, Federal Highway Administration.
- McGhee, K. H. (1994). *Portland Cement Concrete Resurfacing* (Vol. 204). Transportation Research Board.
- Medina-Chavez, C. I., Choi, S., & Won, M. C. (2008). Concrete pavement overlays and failure mechanisms (No. FHWA/TX-09/0-4893-2). Center for Transportation Research, The University of Texas at Austin.
- Molenaar, A. A. A. (1983). *Structural Performance And Design of Flexible Road Constructions and Asphalt Concrete Overlays*. Delft University of Technology, Netherlands.
- Mu, F., & Vandenbossche, J. M. (2011). *Development of Design Guide for Thin and Ultra-Thin*

- Concrete Overlays of Existing Asphalt Pavements, Task 2: Review and Selection of Structural Response and Performance Models* (No. MN/RC 2011-25). Department of Civil and Environmental Engineering, University of Pittsburgh.
- O'Flaherty AM, C., & Hughes, D. (2015). *Highways: The Location, Design, Construction And Maintenance of Road Pavements*. ICE Publishing.
- Packard, R. G. (1973). *Design of Concrete Airport Pavement* (No. EB050. 03P). Portland Cement Association.
- Rasmussen, R. O., Rogers, R., and Ferragut, T. R. (2011). *Continuously Reinforced Concrete Pavement Design and Construction Guideline*. U.S Department of Transportation, Federal Highway Administration.
- Ray, G. K. (1967). *Design of Concrete Overlays for Pavements*. *Journal of American Concrete Institute*, 64(8), 470-474. American Concrete Institute
- Roesler, J. R., & Hiller, J. E. (2013). *Continuously Reinforced Concrete Pavement: Design Using the AASHTOWare Pavement ME Design Procedure* (No. FHWA-HIF-13-025). U.S Department of Transportation, Federal Highway Administration.
- Rollings, R. S. (1988). *Design of Overlays for Rigid Airport Pavements*. Federal Aviation Administration Washington DC.
- Ryu, S. W., Choi, P., Choi, S., & Won, M. C. (2013). *Improvements of Full-Depth Repair Practices for Distresses in Continuously Reinforced Concrete Pavement*. *Transportation Research Record*, 2368(1), 102-113.
- Ryu, S., Won, H., & Won, M. C. (2011). *Continuously Reinforced Bonded Concrete Overlay of Distressed Jointed Concrete Pavements* (No. FHWA/TX-11-5-4893-01-1). Center for Multidisciplinary Research in Transportation, Texas Tech University.
- Shoukry, S. N., Fahmy, M., Prucz, J., & William, G. (2007). *Validation of 3DFE Analysis of Rigid Pavement Dynamic Response to Moving Traffic and Nonlinear Temperature Gradient Effects*. *International Journal of Geomechanics*, 7(1), 16-24.
- Smith, K. D., Yu, H. T., & Peshkin, D. G. (2002). *Portland Cement Concrete Overlays: State of the Technology Synthesis* (No. FHWA-IF-02-045). U.S Department of Transportation, Federal Highway Administration.
- Tayabji, S., Gisi, A., Blomberg, J., & DeGraaf, D. (2009). *New Applications for Thin Concrete Overlays: Three Case Studies*. *National Conference on Preservation, Repair, and Rehabilitation of Concrete Pavements*, 87-99.
- Tayabji, S. D., & Okamoto, P. A. (1985). *Thickness Design of Concrete Resurfacing*. *Third International Conference on Concrete Pavement Design and Rehabilitation*, 367-379.
- The U.S. Army Corps of Engineers (1984). *Engineering and Design Airfield Rigid Pavement Mobilization Construction*. Office of the Chief of Engineers, Department of the Army Corps of Engineers.
- Treviño, M., McCullough, B. F., & Krauss, T. (2000). *Full-Scale Bonded Concrete Overlay on IH-30 in Ft. Worth, Texas* (No. 9-572-1). Center for Transportation Research, The University of Texas at Austin.

Voigt, G. F., Carpenter, S. H., & Darter, M. I. (1989). *Rehabilitation of Concrete Pavements; Volume II: Overlay Rehabilitation Techniques* (No. FHWA/RD-88-072). Federal Highway Administration, US Department of Transportation.

Zealand, T. N. (2000). *New Zealand Supplement to the Document, Pavement Design—A Guide to the Structural Design of Road Pavements*. Austroads Publication No. AP-17.

Appendix A. SPECIAL SPECIFICATIONS FOR BCO

Special Specification XXXX

Bonded Concrete Pavement Overlay



1. DESCRIPTION

Construct bonded concrete pavement overlay in accordance with the typical sections shown on the plans. This specification references and incorporates current special provisions to the following items.

- Item 354, "Planning and Texturing Pavement,"
- Item 360, "Concrete Pavement,"
- Item 361, "Repair of Concrete Pavement,"
- Item 421, "Hydraulic Cement Concrete," and
- Item 422, "Concrete Superstructures."

2. MATERIALS

Furnish materials in accordance with Item 360, "Concrete Pavement," and Item 421, "Hydraulic Cement Concrete," unless otherwise noted in this Specification.

- 2.1. **Hydraulic Cement Concrete.** Provide Class P or K concrete as shown on the plans, in accordance with Item 421, "Hydraulic Cement Concrete." Design Class K to meet a minimum average compressive strength of 2,600 psi in 12 hr., unless other early strength and time requirements are shown on the plans or are allowed. The maximum water to cementitious ratio for Class K concrete is increased to 0.45. Use coarse with a maximum normal size not to exceed 1/3 of the slab thickness that will produce concrete with a rated coefficient of thermal expansion (CoTE) value of 5.5×10^{-6} in./in./F or less as listed in the Concrete Rated Source Quality Catalog.
- 2.2. **Curing Materials.** Provide Type 2 membrane curing compound conforming to DMS-4650, "Hydraulic Cement Concrete Curing Materials and Evaporation Retardants." Provide cotton mats in accordance with Section 422.2.7, "Curing Materials."

3. EQUIPMENT

Provide equipment in accordance with Item 360, "Concrete Pavement." Provide enough concrete mixing, delivery, and paving equipment to meet the requirements of this Specification. Equipment is supplemented by the following:

- 3.1. **Existing Concrete Pavement Surface Preparation Equipment.** Provide power-operated water blasting or shot blasting equipment capable of removing dirt, oil, paint, membrane curing compound, and other foreign material, as well as any laitance or loose concrete from the surface receiving the new concrete. Provide self-contained, portable vacuum unit to dispose of waste generated from these operations.

4. CONSTRUCTION

Construct thin bonded concrete pavement overlay with thicknesses shown on the plans.

Adequately light the active work areas for all nighttime operations. Provide and maintain tools and materials to perform testing.

4.1. **Paving and Quality Control Plan.** Submit a paving and quality control plan for approval before beginning pavement construction operations. Include details of all operations in the concrete paving process, including longitudinal construction joint layout, sequencing, curing, lighting, early opening, leave-outs, sawing, inspection, testing, construction methods, other details, and description of all equipment. List certified personnel performing the testing. Submit revisions to the paving and quality control plan for approval.

4.2. **Job-Control Testing.** Perform all fresh and hardened concrete job-control testing at the specified frequency unless otherwise shown on the plans. Provide job-control testing personnel meeting the requirements of Item 421, "Hydraulic Cement Concrete." Provide and maintain testing equipment, including strength testing equipment at a location acceptable to the Engineer. Use of a commercial laboratory is acceptable. Maintain all testing equipment calibrated in accordance with pertinent test methods. Make strength-testing equipment available to the Engineer for verification testing.

Provide the Engineer the opportunity to witness all tests. The Engineer may require a retest if not given the opportunity to witness. Furnish a copy of all test results to the Engineer daily. Check the first few concrete loads for slump and temperature to verify concrete conformance and consistency on start-up production days. Sample and prepare strength-test specimens (2 specimens per test) on the first day of production and for each 3,000-sq. yd. or fraction thereof of concrete pavement thereafter. Prepare at least 1 set of strength-test specimens for each production day. Perform slump and temperature tests each time strength specimens are made. Monitor concrete temperature to ensure that concrete is consistently within the temperature requirements. The Engineer will direct random job-control sampling and testing. Immediately investigate and take corrective action as approved if any Contractor test result, including tests performed for verification purposes, does not meet specification requirements.

The Engineer will perform job-control testing when the testing by the Contractor is waived by the plans; however, this does not waive the Contractor's responsibility for providing materials and work in accordance with this Item.

4.2.1. **Job-Control Strength.** Use 2,600 psi at 12-hr. for Class K concrete or use 3,200 psi for Class P concrete job-control concrete strength in accordance with Tex-418-A unless otherwise shown on the plans or permitted. Investigate the strength test procedures, the quality of materials, the concrete production operations, and other possible problem areas to determine the cause when a job-control concrete strength test value falls below the required job-control strength. Take necessary action to correct the problem, including redesign of the concrete mix if needed. The Engineer may suspend concrete paving if the Contractor is unable to identify, document, and correct the cause of low-strength test values in a timely manner. The Engineer will evaluate the structural adequacy of the pavements if any job-control strength is more than 15% below the required job-control strength. Remove and replace pavements found to be structurally inadequate at no additional cost when directed.

Perform bond strength testing in accordance with ASTM C1583 "Standard Test Method for Tensile Strength of Concrete Surfaces and Bond Strength or Tensile Strength of Concrete Repair and Overlay Materials by Direct Tension (Pull-off Method)," at 7 days of overlay concrete and 2 tests daily – one in the morning and the other in the afternoon placements. The locations of the testing shall be a minimum 3-ft away from free edges. If a daily average value falls below 180 psi, investigate the causes of the low strength and make necessary changes to achieve an average strength of 180 psi.

4.2.2. **Split-Sample Verification Testing.** Perform split-sample verification testing with the Engineer on random samples taken and split by the Engineer at a rate of at least 1 for every 10 job-control samples. The Engineer will evaluate the results of split-sample verification testing. Immediately investigate and take corrective action as approved when results of split-sample verification testing differ more than the allowable differences shown in Table 1, "Verification Testing Limits," or the average of 10 job-control strength results and the Engineer's split-sample strength result differ by more than 10%.

Table 1
Verification Testing Limits

| Test Method | Allowable Differences |
|---|-----------------------|
| Temperature, Tex-422-A | 2°F |
| Compressive strength, Tex-418-A | 10% |

- 4.3. **Repair Distresses in Existing Pavement.** Repair distresses in the existing pavement in accordance with Item 361, "Repair of Concrete Pavement." Pay particular attention to the installation of tie bars at repair joints in accordance with the requirements in Item 361 so that structural continuity will be restored. Once distressed concrete and base materials are completely removed, install reinforcing steel per CRCP Design Standards and place concrete in accordance with Item 360.
- 4.4. **Prepare Surface of Existing Pavement.** Prepare the existing concrete surface to provide adequate surface texture for bonded overlay.
- 4.4.1. **Surface Preparation.** Provide rough texture of the existing pavement surface by shot-blasting, sand-blasting and/or milling. If milling is used for providing rough texture, remove concrete damaged during milling by shot-blasting or high-pressure water blasting at no additional cost to the Department.
- 4.4.2. **Clean Concrete Surface Prior to Paving.** Remove all dirt, oil, paint, laitance and loose concrete by shotblasting or hydrocleaning the entire concrete pavement surface to be overlaid. Begin concrete placement within 8 hr. following cleaning operation unless otherwise directed by the Engineer. Re-clean the surface if it becomes contaminated. Vacuum the waste generated from this operation. Do not push, shove, or drag the waste material over the cleaned surfaces.
- 4.5. **Joints.** Install joints as shown on the plans. Clean and seal joints in accordance with Item 438, "Cleaning and Sealing Joints." Repair excessive spalling of the joint saw groove using an approved method before installing the sealant. Seal all joints before opening the pavement to all traffic.
- Install a rigid transverse bulkhead shaped accurately to the cross-section of the pavement when placing of concrete is stopped.
- 4.6. **Concrete Delivery.** Clean delivery equipment as necessary to prevent accumulation of old concrete before loading fresh concrete. Use agitated delivery equipment for concrete designed to have a slump of more than 5- in. Segregated concrete is subject to rejection.
- Begin the discharge of concrete delivered in agitated delivery equipment conforming to the requirements of Item 421, "Hydraulic Cement Concrete." Place non-agitated concrete within 45 min. after batching. Reduce times as directed when hot weather or other conditions cause quick setting of the concrete.
- 4.7. **Concrete Placement.** Ensure that the surface of the existing concrete pavement is in damp condition with no free water on the surface when placing the new concrete overlay. Place the concrete as near as possible to its final location, and minimize segregation and rehandling. Distribute concrete using shovels where hand spreading is necessary. Do not use rakes or vibrators to distribute concrete.
- 4.7.1. **Consolidation.** Consolidate all concrete by approved mechanical vibrators operated on the front of the paving equipment. Use immersion-type vibrators that simultaneously consolidate the full width of the placement when machine finishing. Keep vibrators from dislodging reinforcement. Use hand-operated vibrators to consolidate concrete along forms, at all joints and in areas not accessible to the machine-mounted vibrators. Do not operate machine-mounted vibrators while the paving equipment is stationary. Vibrator operations are subject to review.
- 4.7.2. **Temperature Restrictions.** Place concrete that is between 40°F and 95°F when measured in accordance with [Tex-422-A](#) at the time of discharge, except that concrete may be used if it was already in transit when the temperature was found to exceed the allowable maximum. Take immediate corrective action or cease concrete production when the concrete temperature exceeds 95°F.

Do not place concrete when the ambient temperature in the shade is below 40°F and falling unless approved. Concrete may be placed when the ambient temperature in the shade is above 35°F and rising or above 40°F. Protect the pavement with an approved insulating material capable of protecting the concrete for the specified curing period when temperatures warrant protection against freezing. Submit for approval proposed measures to protect the concrete from anticipated freezing weather for the first 72 hr. after placement. Repair or replace all concrete damaged by freezing.

Do not place concrete when the anticipated 24-hr. ambient temperature is expected to change by more than 25°F from the ambient temperature at the time the first load of concrete is placed.

- 4.8. **Spreading and Finishing.** Spread and finish the final concrete surface to the depth, width, grade, and cross-slope as shown on the plans. Finish all concrete pavement with approved self-propelled equipment. Use power-driven spreaders, power-driven vibrators, power-driven strike-off, screed, or approved alternate equipment. Use the transverse finishing equipment to compact and strike-off the concrete to the required section and grade without surface voids. Use float equipment for final finishing. Use concrete with a consistency that allows completion of all finishing operations without addition of water to the surface. Use the minimal amount of water fog mist necessary to maintain a moist surface. Reduce fogging if float or straightedge operations result in excess slurry.

- 4.8.1. **Finished Surface.** Perform sufficient checks with long-handled 10-ft. and 15-ft. straightedges on the plastic concrete to ensure the final surface is within the tolerances specified in Surface Test A in Item 585, "Ride Quality for Pavement Surfaces." Check with the straightedge parallel to the centerline.

- 4.8.2. **Maintenance of Surface Moisture.** Prevent surface drying of the pavement before application of the curing system by means that may include water fogging, the use of wind screens, and the use of evaporation retardants. Apply evaporation retardant at the manufacturer's recommended rate. Reapply the evaporation retardant as needed to maintain the concrete surface in a moist condition until curing system is applied. Do not use evaporation retardant as a finishing aid. Failure to take acceptable precautions to prevent surface drying of the pavement will be cause for shutdown of pavement operations.

- 4.8.3. **Surface Texturing.** Complete final texturing before the concrete has attained its initial set. Drag the carpet longitudinally along the pavement surface with the carpet contact surface area adjusted to provide a satisfactory coarsely textured surface. Prevent the carpet from getting plugged with grout. Do not perform carpet dragging operations while there is excessive bleed water.

A metal-tine texture finish is required unless otherwise shown on the plans. Provide longitudinal tining unless otherwise shown on the plans. Immediately following the carpet drag, apply a single coat of evaporation retardant, if needed, at the rate recommended by the manufacturer. Provide the metal-tine finish immediately after the concrete surface has set enough for consistent tining. Operate the metal-tine device to obtain grooves approximately 3/16-in. deep, with a minimum depth of 1/8-in., and approximately 1/12- in. wide. Do not overlap a previously tined area. Use manual methods to achieve similar results on ramps, small or irregular areas, and narrow width sections of pavements. Repair damage to the edge of the slab and joints immediately after texturing.

Target a carpet drag texture of 0.04- in., as measured by [Tex-436-A](#), when carpet drag is the only surface texture required on the plans. Ensure adequate and consistent macro-texture is achieved by applying enough weight to the carpet and by keeping the carpet from getting plugged with grout. Correct any location with a texture less than 0.03- in. by diamond grinding or shot blasting. The Engineer will determine the test locations at points located transversely to the direction of traffic in the outside wheel path.

- 4.8.4. **Small, Irregular Area, or Narrow Width Placements.** Use hand equipment and procedures that produce a consolidated and finished pavement section to the line and grade where machine placements and finishing of concrete pavement are not practical.

- 4.8.5. **Emergency Procedures.** Use hand-operated equipment for applying texture, evaporation retardant, and cure in the event of equipment breakdown.

- 4.9. **Curing.** Keep the concrete pavement surface from drying as described in Section 3054.4.8.2., "Maintenance of Surface Moisture," until the curing material has been applied. Maintain and promptly repair damage to curing materials on exposed surfaces of concrete pavement continuously for at least 3 curing days or until pavement is opened to traffic. A curing day is defined as a 24-hr. period when either the temperature taken in the shade away from artificial heat is above 50°F for at least 19 hr. or the surface temperature of the concrete is maintained above 40°F for 24 hr. Curing begins when the concrete curing system has been applied. Stop concrete paving if curing compound is not being applied promptly and maintained adequately. Other methods of curing in accordance with Item 422, "Concrete Superstructures," may be used when specified or approved.
- 4.9.1. **Membrane Curing.** Spray the concrete surface uniformly with 2 coats of membrane curing compound at an individual application rate of no more than 180- sq. ft. per gallon. Apply the curing compound before allowing the concrete surface to dry.
- Manage finishing and texturing operations to ensure placement of curing compound on a moist concrete surface, relatively free of bleed water, to prevent any plastic shrinkage cracking. Time the application of curing compound to prevent plastic shrinkage cracking.
- Maintain curing compounds in a uniformly agitated condition, free of settlement before and during application. Do not thin or dilute the curing compound.
- Apply additional compound at the same rate of coverage to correct damage where the coating shows discontinuities or other defects or if rain falls on the newly coated surface before the film has dried enough to resist damage. Ensure that the curing compound coats the sides of the tining grooves.
- 4.9.2. **Curing Class K Concrete.** Provide membrane curing in accordance with Section 3054.4.9.1, "Membrane Curing," for all Class K concrete pavement. When shown on the plans, promptly follow by wet mat curing in accordance with Section 422.4.8., "Final Curing," until opening strength is achieved but not less than 12 hours.
- 4.10. **Sawing Joints.** Saw joints to the depth shown on the plans as soon as sawing can be accomplished without damage to the pavement regardless of time of day or weather conditions. Some minor raveling of the saw-cut is acceptable. Use a chalk line, string line, sawing template, or other approved method to provide a true joint alignment. Provide enough saws to match the paving production rate to ensure sawing completion at the earliest possible time to avoid uncontrolled cracking. Reduce paving production if necessary to ensure timely sawing of joints. Promptly restore membrane cure damaged within the first 72 hours. of curing or until opening to traffic.
- 4.11. **Protection of Pavement and Opening to Traffic.** Testing for early opening is the responsibility of the Contractor regardless of job-control testing responsibilities unless otherwise shown on the plans or as directed. Testing result interpretation for opening to traffic is subject to approval.
- 4.11.1. **Protection of Pavement.** Erect and maintain barricades and other standard and approved devices that will exclude all vehicles and equipment from the newly placed pavement for the periods specified. Protect the pavement from damage due to crossings using approved methods before opening to traffic. Where a detour is not readily available or economically feasible, an occasional crossing of the roadway with overweight equipment may be permitted for relocating equipment only but not for hauling material. When an occasional crossing of overweight equipment is permitted, temporary matting or other approved methods may be required.
- Maintain an adequate supply of sheeting or other material to cover and protect fresh concrete surface from weather damage. Apply as needed to protect the pavement surface from weather.
- 4.11.2. **Opening Pavement to All Traffic.** Do not open the pavement to traffic, including vehicles of the Contractor, until the last concrete placed is at least 12 hr. old and meets a minimum compressive strength of 2,600 psi.

Such opening, however, in no manner relieves the Contractor of his/her responsibility for the work in accordance with Item 7, "Legal Relations and Responsibilities."

Before opening sections of the pavement to traffic, seal the joints and clean the pavement.

- 4.11.2.1. **Strength Testing.** Test concrete specimens cured under the same conditions as the portion of the pavement involved.
- 4.12. **Pavement Thickness.** The Engineer will check the thickness in accordance with [Tex-423-A](#) unless other methods are shown on the plans. The Engineer will perform 1 thickness test consisting of 1 reading at approximately the center of the paving equipment every 500- ft. or fraction thereof.
- 4.13. **Ride Quality.** Measure ride quality in accordance with Item 585, "Ride Quality for Pavement Surfaces," unless otherwise shown on the plans.

5. MEASUREMENT

This item will be measured as follows:

- 5.1. **Bonded Concrete Pavement Overlay.** The bonded concrete pavement overlay will be measured by the square yard of surface area in place.

6. PAYMENT

- 6.1. **Bonded Concrete Pavement Overlay.** The work performed and materials furnished in accordance with this Specification and measured as provided under "Measurement" will be paid for at the unit price for "Bonded Concrete Pavement Overlay" of the depth specified. This price is full compensation for surface preparation of the existing concrete pavement, furnishing materials for sealing joints; for mixing, placing, finishing, curing, and sawing concrete; for cleaning and sealing concrete joints; and for manipulations, labor, tools, equipment, and incidentals necessary to complete the work.

DATE: _____
FILE: _____

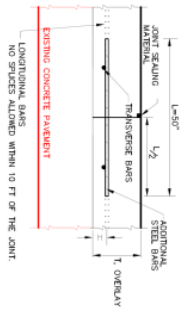
DISCLAIMER:
The use of this standard is governed by the "Texas Engineering Practice Act". No warranty of any kind is made by TxDOT for any purpose whatsoever. TxDOT assumes no responsibility for the conversion of this standard to other formats or for incorrect results or damages resulting from its use.

TABLE NO.1 LONGITUDINAL STEEL

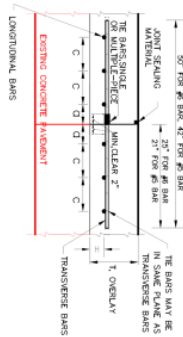
| SLAB THICKNESS | TABLE NO. 1. LONGITUDINAL STEEL | | | | | | | | | |
|----------------|---------------------------------|--------------|------------------------------|---------------|--|---------------|---|--------------|------------------|--------------|
| | REGULAR BARS | | REGULAR BARS WITH STIFFENING | | FIRST SPACING BARS AT TRANSVERSE JOINT | | ADDITIONAL STEEL BARS AT TRANSVERSE JOINT | | TRANSVERSE STEEL | |
| BAR SIZE | BAR SIZE | HEIGHT (in.) | SPACING (in.) | SPACING (in.) | SPACING (in.) | SPACING (in.) | SPACING (in.) | LENGTH (in.) | LENGTH (in.) | LENGTH (in.) |
| 4.0 | #5 | 1.0 | 9.5 | 3 to 4 | 19 | 50 | 50 | 50 | 50 | 50 |
| 4.5 | #5 | 1.0 | 9.0 | 3 to 4 | 18 | 50 | 50 | 50 | 50 | 50 |
| 5.0 | #5 | 1.5 | 8.5 | 3 to 4 | 17 | 50 | 50 | 50 | 50 | 50 |
| 5.5 | #5 | 2.0 | 8.0 | 3 to 4 | 16 | 50 | 50 | 50 | 50 | 50 |
| 6.0 | #5 | 2.5 | 7.5 | 3 to 4 | 15 | 50 | 50 | 50 | 50 | 50 |
| 6.5 | #5 | 3.0 | 7.0 | 3 to 4 | 14 | 50 | 50 | 50 | 50 | 50 |
| 7.0 | #5 | 3.5 | 6.5 | 3 to 4 | 13 | 50 | 50 | 50 | 50 | 50 |
| 7.5 | #5 | 3.7 | 6.0 | 3 to 4 | 12 | 50 | 50 | 50 | 50 | 50 |
| 8.0 | #6 | 4.0 | 5.0 | 3 to 4 | 16 | 50 | 50 | 50 | 50 | 50 |
| 8.5 | #6 | 4.2 | 4.5 | 3 to 4 | 15 | 50 | 50 | 50 | 50 | 50 |
| 9.0 | #6 | 4.5 | 4.0 | 3 to 4 | 14 | 50 | 50 | 50 | 50 | 50 |
| 9.5 | #7 | 4.7 | 3.5 | 3 to 4 | 13 | 50 | 50 | 50 | 50 | 50 |
| 10.0 | #7 | 5.0 | 3.0 | 3 to 4 | 12 | 50 | 50 | 50 | 50 | 50 |

TABLE NO.2 TRANSVERSE STEEL AND THE BARS

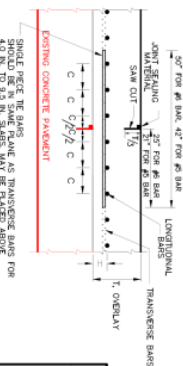
| TABLE NO.2 | | TRANSVERSE STEEL | | THE BARS | |
|---------------------|----|---------------------------------|----|---------------------------------|----|
| SLAB THICKNESS (IN) | | TRANSVERSE STEEL | | CONCRETE STRENGTH (SECTION 2-2) | |
| BAR SPACING | | CONCRETE STRENGTH (SECTION 2-2) | | CONCRETE STRENGTH (SECTION 2-2) | |
| 40 - 75 | #5 | 48 | #5 | 24 | 24 |
| 80 - 100 | #5 | 48 | #5 | 24 | 24 |



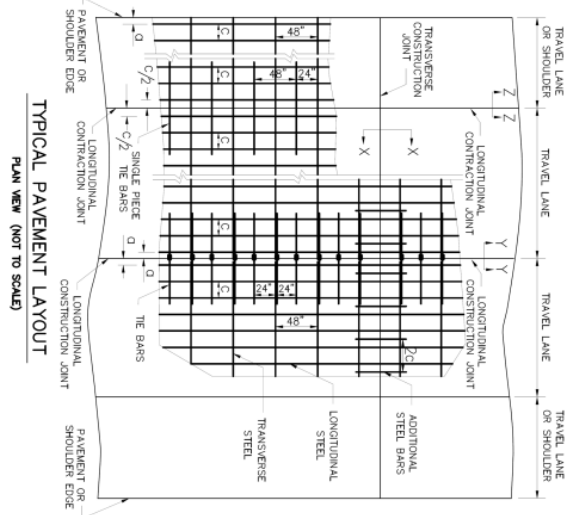
SECTION X - X



SECTION Y - Y



SECTION Z - Z



GENERAL NOTES

- [illegible]

SHEET 1 OF 1

| | |
|--|---|
| Texas Department of Transportation | Region 5 Station Standards |
|--|---|

**BONDED
CONTINUOUSLY REINFORCED
CONCRETE OVERLAY**
T - 4 to 10 INCHES
CRCP BCO-18

| FILE | ORIGINAL | DATE | TIME | FILE |
|-------|----------|------|------|-------|
| 10001 | 10001 | 100 | 100 | 10001 |
| 10002 | 10002 | 100 | 100 | 10002 |
| 10003 | 10003 | 100 | 100 | 10003 |
| 10004 | 10004 | 100 | 100 | 10004 |
| 10005 | 10005 | 100 | 100 | 10005 |
| 10006 | 10006 | 100 | 100 | 10006 |
| 10007 | 10007 | 100 | 100 | 10007 |
| 10008 | 10008 | 100 | 100 | 10008 |
| 10009 | 10009 | 100 | 100 | 10009 |
| 10010 | 10010 | 100 | 100 | 10010 |
| 10011 | 10011 | 100 | 100 | 10011 |
| 10012 | 10012 | 100 | 100 | 10012 |
| 10013 | 10013 | 100 | 100 | 10013 |
| 10014 | 10014 | 100 | 100 | 10014 |
| 10015 | 10015 | 100 | 100 | 10015 |
| 10016 | 10016 | 100 | 100 | 10016 |
| 10017 | 10017 | 100 | 100 | 10017 |
| 10018 | 10018 | 100 | 100 | 10018 |
| 10019 | 10019 | 100 | 100 | 10019 |
| 10020 | 10020 | 100 | 100 | 10020 |
| 10021 | 10021 | 100 | 100 | 10021 |
| 10022 | 10022 | 100 | 100 | 10022 |
| 10023 | 10023 | 100 | 100 | 10023 |
| 10024 | 10024 | 100 | 100 | 10024 |
| 10025 | 10025 | 100 | 100 | 10025 |
| 10026 | 10026 | 100 | 100 | 10026 |
| 10027 | 10027 | 100 | 100 | 10027 |
| 10028 | 10028 | 100 | 100 | 10028 |
| 10029 | 10029 | 100 | 100 | 10029 |
| 10030 | 10030 | 100 | 100 | 10030 |
| 10031 | 10031 | 100 | 100 | 10031 |
| 10032 | 10032 | 100 | 100 | 10032 |
| 10033 | 10033 | 100 | 100 | 10033 |
| 10034 | 10034 | 100 | 100 | 10034 |
| 10035 | 10035 | 100 | 100 | 10035 |
| 10036 | 10036 | 100 | 100 | 10036 |
| 10037 | 10037 | 100 | 100 | 10037 |
| 10038 | 10038 | 100 | 100 | 10038 |
| 10039 | 10039 | 100 | 100 | 10039 |
| 10040 | 10040 | 100 | 100 | 10040 |
| 10041 | 10041 | 100 | 100 | 10041 |
| 10042 | 10042 | 100 | 100 | 10042 |
| 10043 | 10043 | 100 | 100 | 10043 |
| 10044 | 10044 | 100 | 100 | 10044 |
| 10045 | 10045 | 100 | 100 | 10045 |
| 10046 | 10046 | 100 | 100 | 10046 |
| 10047 | 10047 | 100 | 100 | 10047 |
| 10048 | 10048 | 100 | 100 | 10048 |
| 10049 | 10049 | 100 | 100 | 10049 |
| 10050 | 10050 | 100 | 100 | 10050 |
| 10051 | 10051 | 100 | 100 | 10051 |
| 10052 | 10052 | 100 | 100 | 10052 |
| 10053 | 10053 | 100 | 100 | 10053 |
| 10054 | 10054 | 100 | 100 | 10054 |
| 10055 | 10055 | 100 | 100 | 10055 |
| 10056 | 10056 | 100 | 100 | 10056 |
| 10057 | 10057 | 100 | 100 | 10057 |
| 10058 | 10058 | 100 | 100 | 10058 |
| 10059 | 10059 | 100 | 100 | 10059 |
| 10060 | 10060 | 100 | 100 | 10060 |
| 10061 | 10061 | 100 | 100 | 10061 |
| 10062 | 10062 | 100 | 100 | 10062 |
| 10063 | 10063 | 100 | 100 | 10063 |
| 10064 | 10064 | 100 | 100 | 10064 |
| 10065 | 10065 | 100 | 100 | 10065 |
| 10066 | 10066 | 100 | 100 | 10066 |
| 10067 | 10067 | 100 | 100 | 10067 |
| 10068 | 10068 | 100 | 100 | 10068 |
| 10069 | 10069 | 100 | 100 | 10069 |
| 10070 | 10070 | 100 | | |